4^{th} EuFN and FIT4NANO Joint Workshop / Meeting

Vienna, September 27^{th}–30^{th}, 2021

Supported by:

Scientific Committee

EuFN

Guillaume Audoit	CEA-LETI, Grenoble, France
Petr Bábor	CEITEC, Brno, Czech Republic
Joakim Reuteler	ETH, Zürich, Switzerland
Philip Moll	EPFL, Lausanne, Switzerland

FIT4NANO

Gregor Hlawacek	Helmholtz-Zentrum Dresden-Rossendorf e.V., Germany
Gerhard Hobler	Technische Universität Wien, Austria
Katja Höflich	Ferdinand Braun Insitute, Germany
Tom Wirtz	Luxembourg Institute of Science and Technology, Luxembourg

EuFN Workshop Committee

Guillaume Audoit	CEA-LETI, Grenoble, France
Philip Moll	EPFL, Lausanne, Switzerland
Frank Altmann	Fraunhofer IMWS, Halle, Germany
Petr Bábor	CEITEC, Brno, Czech Republic
Gregor Hlawacek	Helmholtz-Zentrum Dresden-Rossendorf e.V., Germany
Joakim Reuteler	ETH, Zürich, Switzerland
Robert Winkler	Technische Universität Graz, Austria

Local Organisation

Gerhard Hobler	Technische Universität Wien, Austria

Book of Abstracts

Nico Klingner	Helmholtz-Zentrum Dresden-Rossendorf e.V., Germany

Impressum / Imprint

Medieninhaber /	Publisher:	G. Hlawacek, N. Klingner, G. Hobler
Verlagsort /	Place of publication:	Vienna, Austria
Hersteller /	Printer:	druck.at Druck- und Handelsgesellschaft mbH
Herstellungsort /	Printed at:	Leobersdorf, Austria

	Monday		Page
G. Hlawacek	FIT4NANO Core group meeting (on invitation only)	08:00	
G. Hlawacek	FIT4NANO MC meeting (on invitation only)	10:00	
	Registration	12:00	
	Welcome	13:30	
P. Rack	Understanding Focused Ion Beam Sputtering and Gas-Assisted Etching via the EnvizION Monte Carlo Simulation	13:45	16
K. Höflich	Focused electron beam induced deposition of metals and insight gained from surface deposition techniques	14:15	18
H. Plank	3D-Nanoprinting via Focused Particle Beams	14:30	20
D. Kuhness	3D Nano-Printing of Plasmonically Active Gold-Nanoantennas	14:45	22
A. Fernandez-Pacheco	Investigation of novel effects in three-dimensional magnetic nanostructures fabricated by focused electron beam induced deposition	15:00	24
	Break/Posters	15:15	
A. J. Smith	in-situ toolkit for SEM or FIB/SEM: From Life Science FIB applications to micro-/ nanomachining and GIS systems - micromanipulators and add-ons for addressing a multitude of tasks	15:45	26
J. Lindsay	Rapid FIB preparation of thin films for TKD analysis	16:05	28
Jany B.	Local Phase Identification at Nanoscale of Different Titanium Oxides by EBSD Dictionary Based Indexing Approach	16:20	30
A. Krasheninnikov	Production of Defects in Two-Dimensional Materials under Ion Irradiation: Insights from First-Principles and Analytical Potential Molecular Dynamics Simulations	16:35	32
F. Liu	Graphene nanomesh for electron and phonon engineering	16:50	34
	Reception/Posters	17:05	
	End	19:30	

	Tuesday		
	Get together	08:15	
K. Modic	Scaling down thermodynamic techniques for quantum materials	08:30	38
C. Guo	Focused-ion-beam as a topological edge-mode writer in higher-order topological insulator Bismuth	09:00	40
T. Richter	VELION - A Novel FIB-SEM Nanofabrication Instrument Concept and its Applications in Nanoscale Science and Engineering	09:15	42
I. Ortlepp	Tip- and Laser-based 3D-Nanofabrication up to Ø100 mm	09:35	44
A. B. Mosberg	The Virtual FIB: Simulating FIB Degrees Of Freedom To More Effectively Explore And Communicate Advanced FIB Workflows	09:50	46
	Break/Posters	10:05	
J. Schwiedrzik	Investigating structure-property relationships of hierarchical materials at the microscale	10:35	48
H. Noad	Stress-Strain Relation in a Micromachined Quantum Material	11:05	50
V. Deinhart	Automated nanofabrication of two-dimensional materials with focused helium ions	11:20	52
S. G. Robson	Single Ion Detection with a keV Focussed Ion Beam for Quantum Computing Applications	11:35	54
D. Spemann	FIB Meets EBIS: Development of Deterministic Ion Implantation Based on Image Charge Detection	11:50	56
	Lunch/Posters	12:05	
J. M. De Teresa	Using a palette of FIB-based processes to create functional nanomaterials and devices	13:30	58
I. Szymańska	Potential FEBID/FIBID precursors of groups 10 and 11 with O- and N-donor ligands	14:00	60
G. Goupil	Effect of the stage temperature on sample preparation and surface chemistry in FIBIP and FEBIP	14:15	62
M. Madajska	Carboxylate, amidinate and imidoylamidinate ligand in copper complexes and their influence on volatility and electron sensitivity	14:30	64
P. Philipp	Influence of contaminations on the sputtering of silicon with low energy argon ions	14:45	66
	Break/Posters	15:00	
V. Hegrova	Correlative Probe and Electron Microscopy technology using AFM in SEM	15:30	68
O. de Castro	The npSCOPE: a New Multimodal Instrument for the In-Situ Correlative Analysis of Nanoparticles	15:50	70
S. Lohmann	Contrast Modes in Transmission Experiments using Broad and Focussed keV Ion Beams	16:05	72
F. Perez-Willard	New Protocols for the Fabrication of TEM and APT Specimens with LaserFIBs	16:20	74
	Break/Posters	16:40	
S. Mayr	Xe Plasma Focused Ion Beam Milling for Fabricating Soft X-ray Transparent Sample Windows	17:00	76
P. Mazarov	Using of light and heavy ion beams in modern FIBs	17:15	78
A. Maćkoxz	Fabrication of micro and nanostructures from crystals of topological insulators	17:30	80
L. Bischoff	Investigation of Boron Liquid Metal Alloy Ion Sources for Focused Ion Beam Applications	17:45	82
	End	18:00	
	Dinner	19:30	

	Wednesday		Page
	Get together	08:15	
F. Perez-Murano	Ion beam based fabrication of nanoelectronic and nanomechanical devices	08:30	86
H. J. Engelmann	Challenges to TEM sample preparation of stacked Si/SiO2/Si nanopillars for SETs using Focused Ion Beam	09:00	88
M. Slama	Advanced TEM Lamella Preparation in FIB-SEM by Taking Advantage of Innovative Lift-out Methods	09:15	90
B. Winiarski	3D Correlative Tomography and Microscopy	09:35	92
C. Burkhardt	Rapid prototyping of probes for surface enhanced Raman scattering (SERS) with focused ion beams	09:50	94
	Break/Posters	10:05	
T. Wirtz	Multimodal characterisation on FIB instruments combining nano-scale SIMS and SE imaging	10:35	96
J. Almoric	Development of an O-TOFSIMS integrated on a UHV FIB/SEM workstation: challenges and innovative approaches for in depth correlated nano-analyzes and high-resolution imaging	10:50	98
J. Jurczyk	Focused Electron Beam Induced Mass Spectrometry – new, versa-tile method of in-situ analysis of nanomaterials	11:05	100
L. Pillatsch	fibTOF: The use of secondary ion mass spectrometry capabilities for material characterization on a FIB-SEM microscope	11:20	102
A. Priebe	Review of fluorine gas-assisted FIB-TOF-SIMS for enhanced 3D chemical characterization of materials in nanoscale	11:40	104
K. Wieczerzak	Challenges and benefits of fluorine gas coinjection during FIB-TOF-SIMS analysis	11:55	106
	Lunch / Posters	12:10	
F. Allen	Defect Engineering, Ion Implantation and Nanofabrication using the Helium Ion Microscope	13:30	108
N. Klingner	Transformation of tin spheres into hollow cubes by He+ irradiation	14:00	110
M .Schmidt	How hot does it get? Heat-Generation under the He+-Ion Beam and Implications for Imaging and Milling of Biological Objects	14:15	112
M. S. Anwar	Magneto-structural phase transition in Fe60V40 alloy thin films	14:30	114
	Break/Posters	14:45	
D. Phifer	Achieving Near “Damage-free” (S)TEM Sample Preparation by Low-energy Argon from Focused Multi-ion Plasma FIB	15:15	116
L. McElwee-White	Mechanism-Based Design of Precursors for FEBID and FIBID	15:35	118
A. Weitzer	The Battle for the last few Nanometers - Refining 3D Nanoprinting of Closed Structures via FEBID	15:50	120
R. Winkler	FEBID 3D-Nanoprinting at Low Substrate Temperatures: Pushing the Speed While Keeping the Quality	16:05	122
	Break/Posters	16:20	
M. Manoccio	Compact Chiral Nano Helix Arrays as Femtomolar Biosensing Tool	16:45	124
A. Tsarapkin	Direct writing of chiral and nonlinear plasmonic devices	17:00	126
L. M. Seewald	Adding the Design Possibility of Variable Diameters via Blurred Electron Beams during 3D Nanoprinting via FEBID	17:15	128
G. Audoit	Closing	17:30	
	End	17:45	

	Thursday	
T.Wirtz, G.Hobler, K.Höflich, A.Gandy	WG1/2/3/4 meeting (open to all, parallel sessions)	08:00
G. Hlawacek	FIT4NANO Action meeting (open to all, all WGs, MC, CG)	11:00
	End	12:00

4th EuFN and FIT4NANO
Joint Workshop

Exhibitors

September 27th - 30th, 2021
Vienna, Austria

Helium Ion Microscopy Images of Aerosols trapped in filters
HZDR

NenoVision

AFM for SEM LiteScope™

LiteScope™ is a unique Atomic Force Microscope (AFM) designed for „plug & play“ integration into the Scanning Electron Microscopes (SEMs).

This connection enables to merge the strengths of both techniques, resulting in effective workflow and possibilities of complex sample analysis that is difficult or readily impossible by conventional, separate AFM and SEM instrumentation.

Thanks to the unique technology of Correlative Probe and Electron Microscopy, shortly CPEM, it allows for nanometer precise in-flight AFM and SEM data correlation.

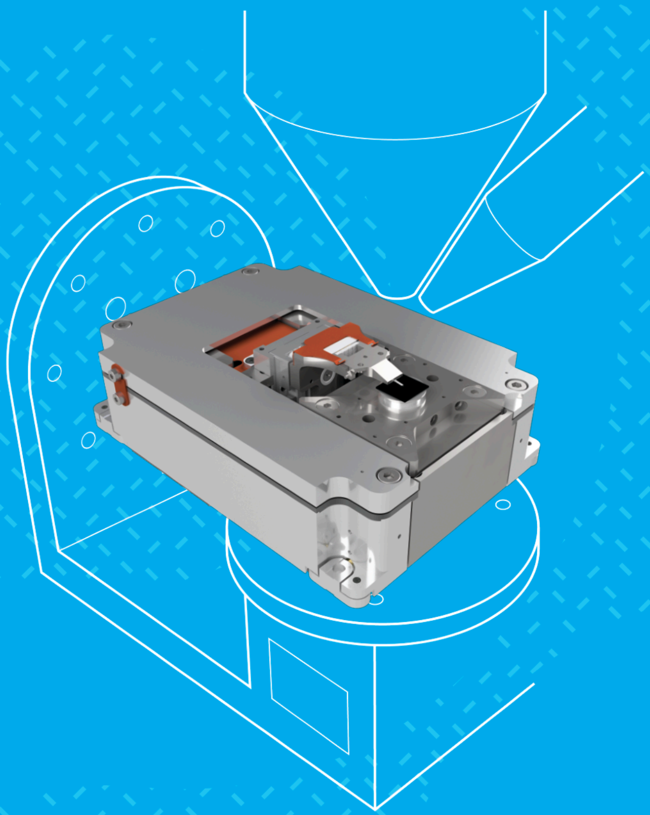

LiteScope 2.0

Product values

- **Material Science:** 1D/2D materials, Steel & metal alloys, Batteries, Ceramics, Polymers
- **Nanostructures:** Modified surfaces FIB/GIS, Quantum dots, Nano-patterning
- **Semicondutors:** Solar cells, Integrated circuits, Failure analysis
- **Life Science:** Cell biology, Protein technology

Measurement modes

- **Imaging modes:** Topography and surface roughness
- **Mechanical modes:** Energy dissipation (tapping mode), FMM (contact mode), F-z curves, nanoindentation
- **Electrical modes:** C-AFM, C-CPEM, KPFM, PFM, I-V spectroscopy, STM
- **Magnetic modes:** MFM

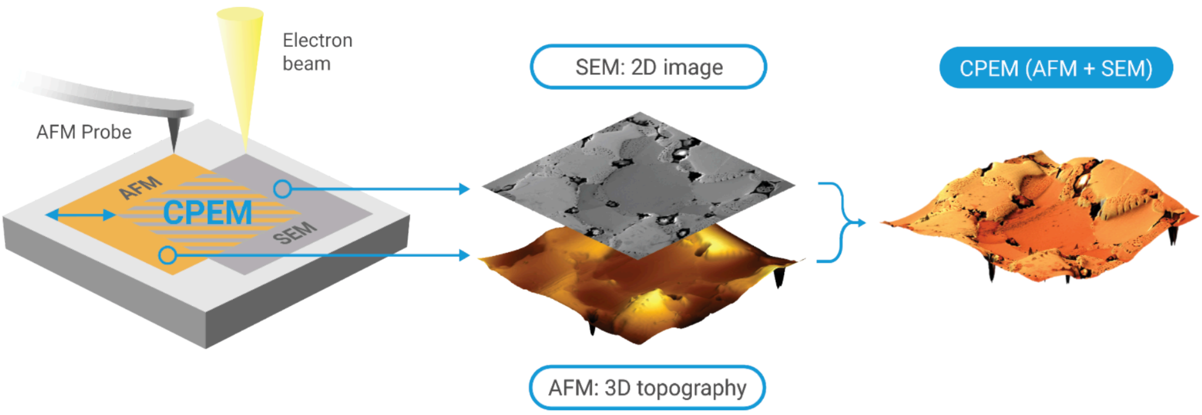

NenoVision s.r.o.
Purkyňova 649/127
612 00 Brno, Czech Republic

info@nenovision.com
+420 605 287 732

www.nenovision.com

kleindiek
nanotechnik

TESCAN

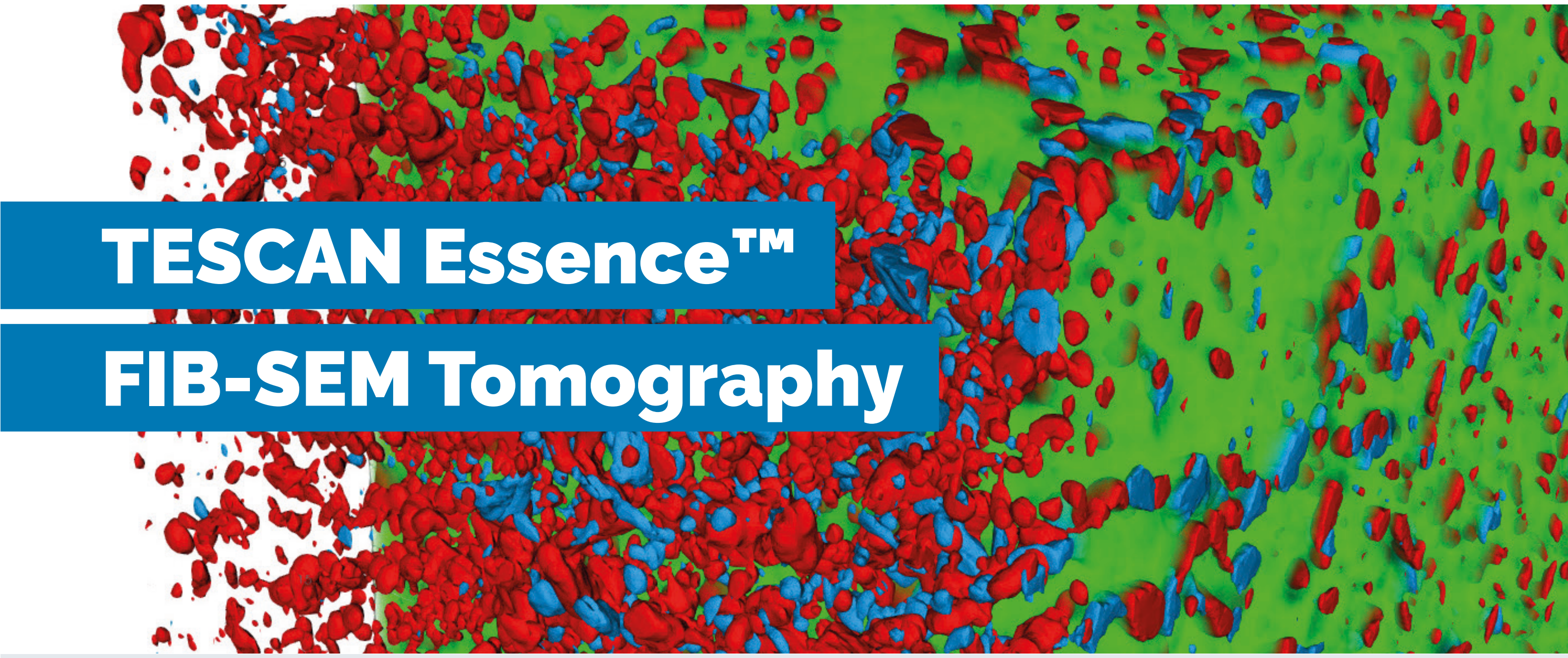

TESCAN Essence™ FIB-SEM Tomography

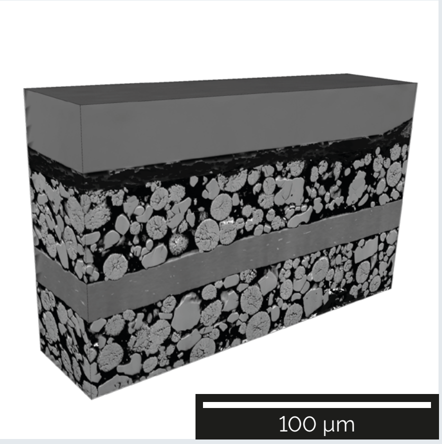

▲ FIB-SEM tomography of a Li-ion battery, 200x50x100 µm @ 100 nm voxel resolution

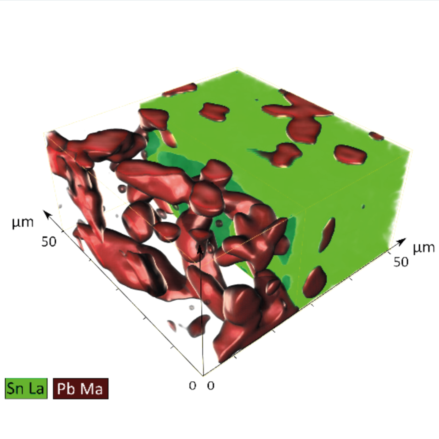

▲ 3D EDS elemental analysis of a solder microstructure

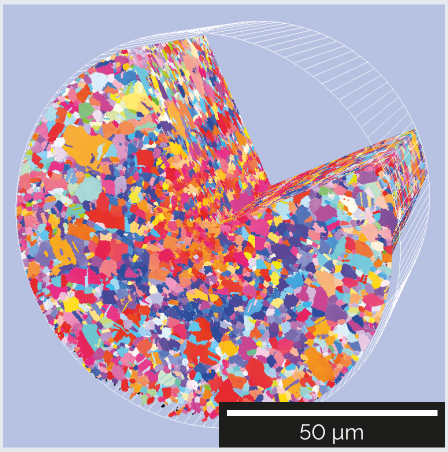

▲ 3D EBSD analysis of a cold-drawn, 90 µm diameter Copper wire

Key Benefits:

- ✓ **Obtain high quality data with ease using the step-by-step guided workflows to set-up acquisition parameters**
- ✓ **Execute tomography jobs with greater efficiency using the familiar, intuitive control interface** with full integration within the FIB-SEM control software
- ✓ **Acquire large datasets reliably with the support of automatic adjustments procedures** that assure system stability
- ✓ **Save time by using automated volume preparation routines** for unattended sample processing
- ✓ **Acquire multi-scale and multi-modal 3D data** with up to 8 imaging detectors extended by 3D EDS and 3D EBSD microanalysis
- ✓ **Achieve tomographic results faster using Plasma FIB-SEM** with the added support for TESCAN's Rocking Stage in the tomography workflow for high performance milling

For more information visit

www.tescan.com

Helio 5 DualBeam family delivers exceptional performance

Building on the high-resolution, low volatage advantages in Gallium DualBeam, extending the range of (S)TEM sample prep automation

Helios 5 PFIB

60kV high-resolution STEM (HRSTEM) image of a high-quality, ultra-thin lamella (<100> $SrTiO_3$) produced with a Helios 5 UX DualBeam.

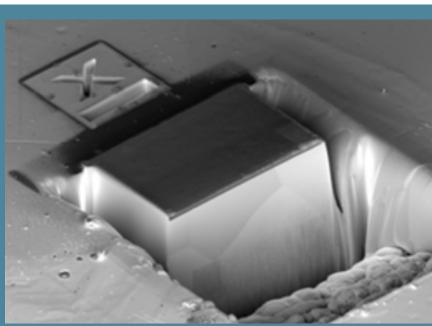

Sample surface prepared for 3D data acquisition using a Helios DualBeam and Auto Slice & View 4 (AS&V4).

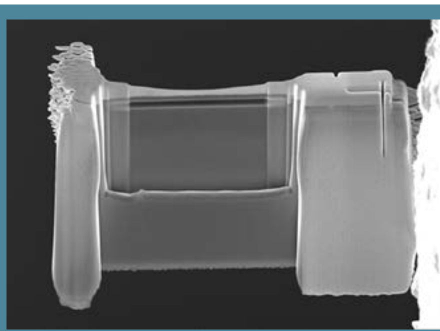

High-quality TEM lamella produced with a Helios DualBeam in less than one hour using AutoTEM 5 Software, which offers the easiest, most automated TEM sample preparation workflow.

- High throughput Xe Plasma FIB with high-resolution, sub-nanometer SEM imaging and analysis
- Uniform large area deprocessing
- Deep structure characterization, fast large sample (cube, pillar or wedge) extraction, 3D serial slicing

Helios 5 Hydra

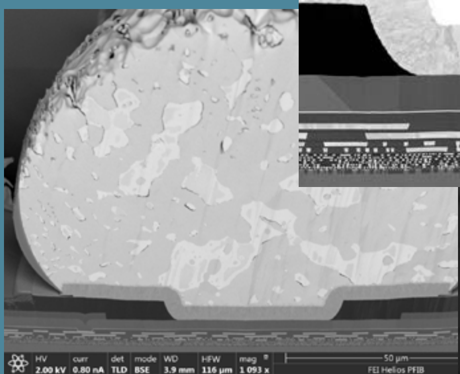

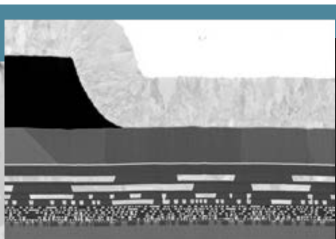

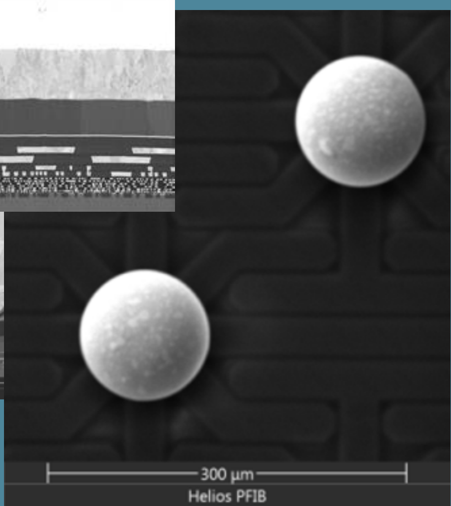

Soldier bump cross-section (160x75 µm) is ready for high-resolution imaging in just 15 minutes.

High-resolution STEM image of a hig-quality GaAs lamella prepared with a Helios Hydra UX DualBeam using Ar FIB for the fianl polishing.

- On-the-fly switchable ion species (Xe, Ar, O, N) for optimized PFIB processing
- Oxygenions for faster and more uniform removal of carbon-based materials
- Focused 500V Arions for thinning (S)TEM lamella with the lowest damage

Find out more at **thermofisher.com/dualbeam**

ThermoFisher SCIENTIFIC

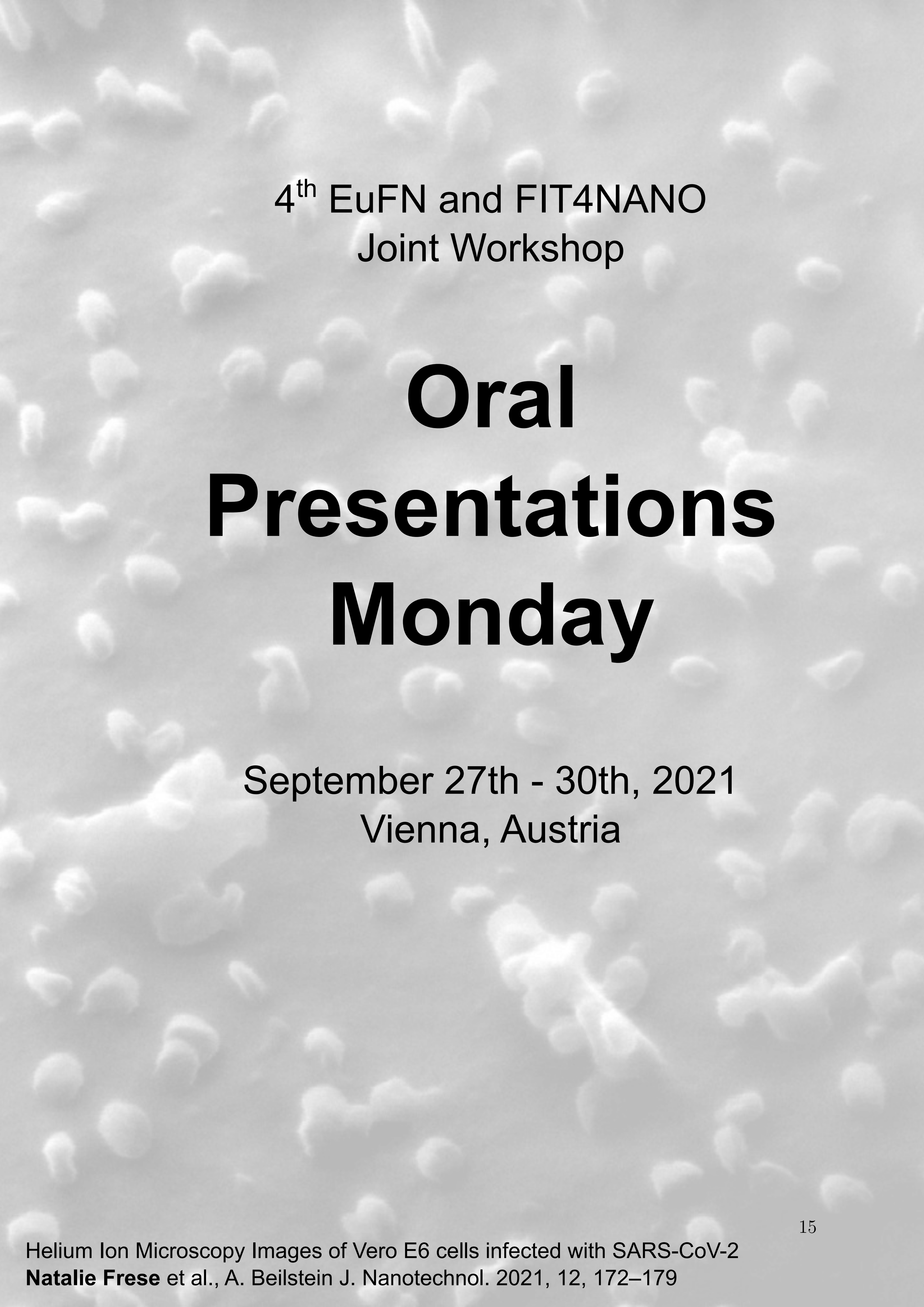

4th EuFN and FIT4NANO
Joint Workshop

Oral Presentations Monday

September 27th - 30th, 2021
Vienna, Austria

Helium Ion Microscopy Images of Vero E6 cells infected with SARS-CoV-2
Natalie Frese et al., A. Beilstein J. Nanotechnol. 2021, 12, 172–179

Understanding Focused Ion Beam Sputtering and Gas-Assisted Etching via the EnvizION Monte Carlo Simulation

Philip Rack[1,2,*] Kyle Mahady[1], Shida Tan[3], Yuval Greenzweig[4], Amir Raveh[4]
[1] 1University of Tennessee, Department of Materials Science and Engineering, Knoxville, Tennessee 37996, USA

[2]Oak Ridge National Laboratory, Center for Nanophase Materials Science, Oak Ridge, Tennessee 37830, USA

[3]Intel Corporation, Santa Clara, California 95054, USA

[4]Intel Israel, Haifa 31015, Israelffiliation 1 (Calibri 8, full affiliation)

[*] corresponding author email: prack@utk.edu

In this talk, we will overview the attributes of our EnvizION Monte Carlo Simulation which at its core consists of ion-solid interactions [1] based on SRIM/TRIM, but has a dynamic voxelized substrate matrix. We have also added a secondary electron routine [2] to emulate imaging as well as end-point detection during nanoscale processing. Most recently, we have written a routine to model adsorbed precursor gas and model ion- and electron-induced chemical reactions to emulate gas-assisted focused ion beam etching. In this talk, we describe simulations using our simulation code EnvizION, which simulates both the physical sputtering [3] and monolayer adsorption of XeF2 to a SiO2 substrate, and the reactions between adsorbed gas and surface atoms which lead to volatilization and material removal [4]. We first compare pure SiO2 sputtering results and then study the effect of gas-assisted etching on the resolution of etched nanoscale vias, and the influence of ion species such as Ne+ and Ga+, to characterize the underlying limitations on etching resolution. Simulations are compared against experimental results, for validation and to understand experimentally observed features.

[1] K.T. Mahady, P.D Rack, S. Tan, Y. Greenzweig, R. Livengood, A. Raveh, *Monte Carlo simulations of nanoscale Ne+ ion beam sputtering: Investigating the influence of surface effects, interstitial formation, and the nanostructural evolution*, Nanotechnology vol. 28 no. 4 pp. 045305 (1-14) (January 2017).

[2] K.T. Mahady, S. Tan, Y. Greenzweig, R. Livengood, A. Raveh, J.D. Fowlkes, P.D Rack, *Monte Carlo Simulations of Secondary Electron Emission Due to Ion Beam Milling*, Journal of Vacuum Science and Technology B, vol. 35 no. 4 041805 (1-12) (August 2017)

[3] K.T. Mahady, S. Tan, Y. Greenzweig, R. Livengood, A. Raveh, P.D Rack, *Simulating Advanced Focused Ion Beam Nanomachining: a quantitative comparison of experimental and simulation results*, Nanotechnology vol. 29 no. 49 pp495301(1-13) (December 2018).

[4] K.T. Mahady, S. Tan, Y. Greenzweig, A. Raveh, P.D Rack, *Monte Carlo Simulation of Nanoscale Material Focused Ion Beam Gas-Assisted Etching: Ga+ and Ne+ Etching of SiO2 in the Presence of a XeF2 Precursor Gas*, Nanoscale Advances vol. 1 no. 9 pp. 3584-3596 (September 2019).

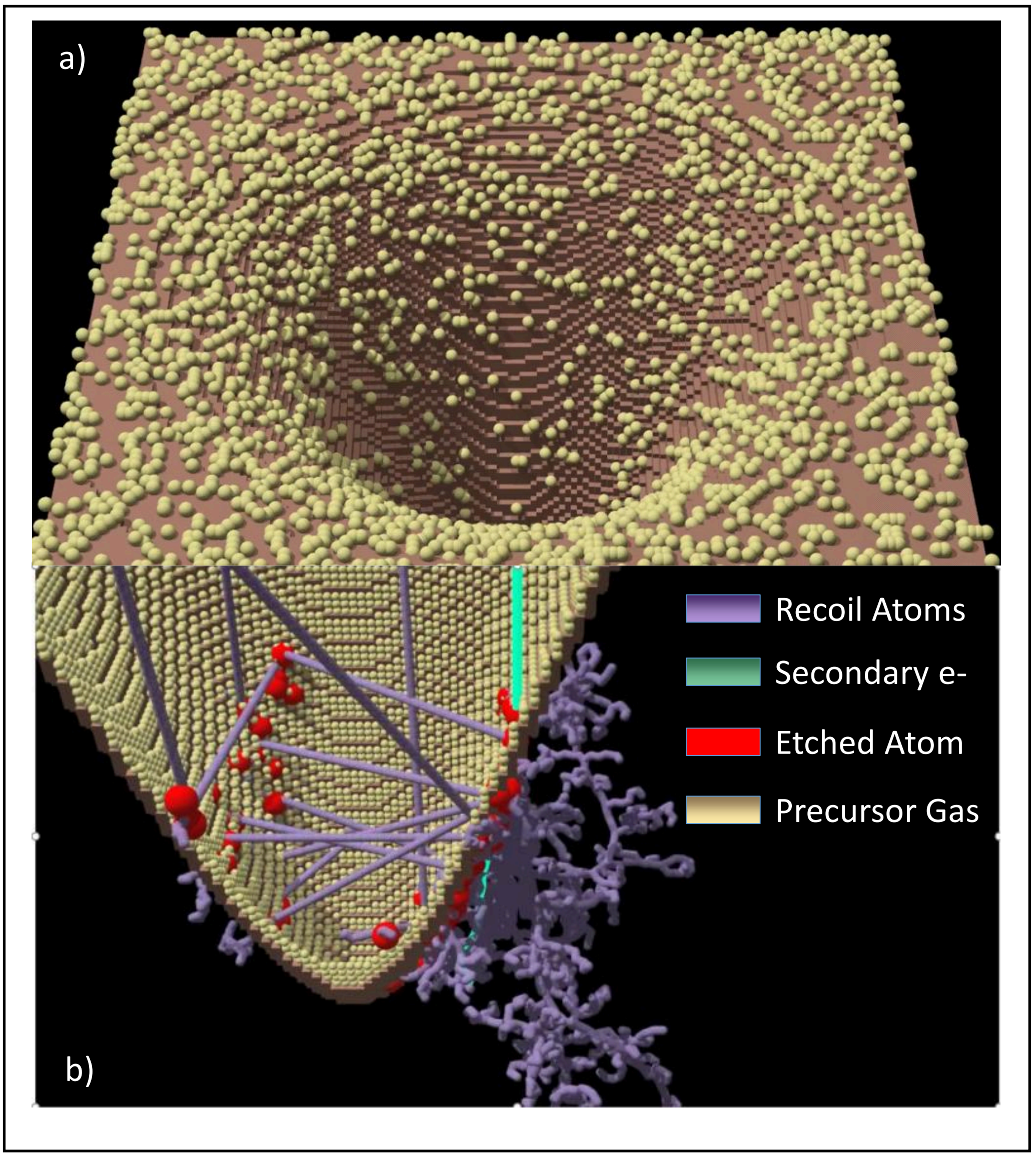

Fig. 1: a) Schematic illustrating a milled via structure in EnvizION with reactive precursor gas coverage of ~ 75% on the top surface. b) Visualization of a single ion strike on the via sidewall that produces a recoil atom cascades (purple), secondary electron emission (green) and in the presence of precursor reactive gas (yellow), generates reactive ion etching events (red).

Focused electron beam induced deposition of metals and insight gained from surface deposition techniques

I. Utke[1,*], P. Swiderek[2,*], K. Höflich[3,4,*], K. Madajska[5], J. Jurczyk[1,5], P. Martinović[2], I.B. Szymańska[6,*]

[1] Empa - Swiss Federal Laboratories for Materials Science and Technology, 3602 Thun, Switzerland
[2] Institute for Applied and Physical Chemistry (IAPC), University of Bremen, 28359 Bremen, Germany
[3] Ferdinand-Braun-Institut gGmbH, Leibniz-Institut für Höchstfrequenztechnik, 12489 Berlin, Germany
[4] Helmholtz-Zentrum Berlin für Materialien und Energie, 14109 Berlin, Germany
[5] AGH University of Science and Technology Kraków, 30-059 Kraków, Poland
[6] Nicolaus Copernicus University in Torun´, Faculty of Chemistry, 87-100 Toruń, Poland

[*] ivo.utke@empa.ch, swiderek@uni-bremen.de, katja.hoeflich@fbh-berlin.de, pola@umk.pl

Nanostructured materials made from group 10 (Ni, Pd, Pt) and group 11 (Cu, Ag, Au) elements have outstanding technological relevance in microelectronics, nano-optics, catalysis, and energy conversion. Processes that allow for the easy and reliable fabrication of such nanostructures are heavily sought after. Focused electron beam induced deposition (FEBID) is the only direct-write technique that can fabricate nanostructures with arbitrary shape and dimensions down to the sub-10 nm regime. However, the complex chemistry of FEBID involving electron-induced dissociation processes of metalorganic precursors molecules, surface kinetics, and thermal effects is poorly understood and far from being optimized.

Here, we review in a comparative manner the performance and the underlying chemical reactions of surface deposition processes, namely, chemical vapour deposition (CVD), atomic layer deposition (ALD), and FEBID itself [1]. The knowledge gained in CVD and ALD as related surface deposition techniques will help us to understand the spatially selective chemistry occurring in FEBID. Fundamental surface and gas-phase studies provide insight to electron-induced chemistry and desorption of precursor fragments. Specific emphasis is put on the type of the ligands and their different behaviour under thermal, surface-related, and electron-induced processes.

The comprehensive overview includes reactive environments and purification approaches as these may provide valuable information on the design of novel precursors. The evaluation of the precursor and process performance is extended to include W, Co, Fe, Ru, Rh, and Ir to represent a general guide towards future developments in FEBID, cf. Fig. 1. These may not only rely on the design novel compounds but also on optimized deposition strategies inspired by ALD and CVD.

[1] I. Utke, et al.: Coordination and organometallic precursors of group 10 and 11: Focused electron beam induced deposition of metals and insight gained from chemical vapour deposition, atomic layer deposition, and fundamental surface and gas phase studies; Coord. Chem. Reviews 445 (**2021**), 213851

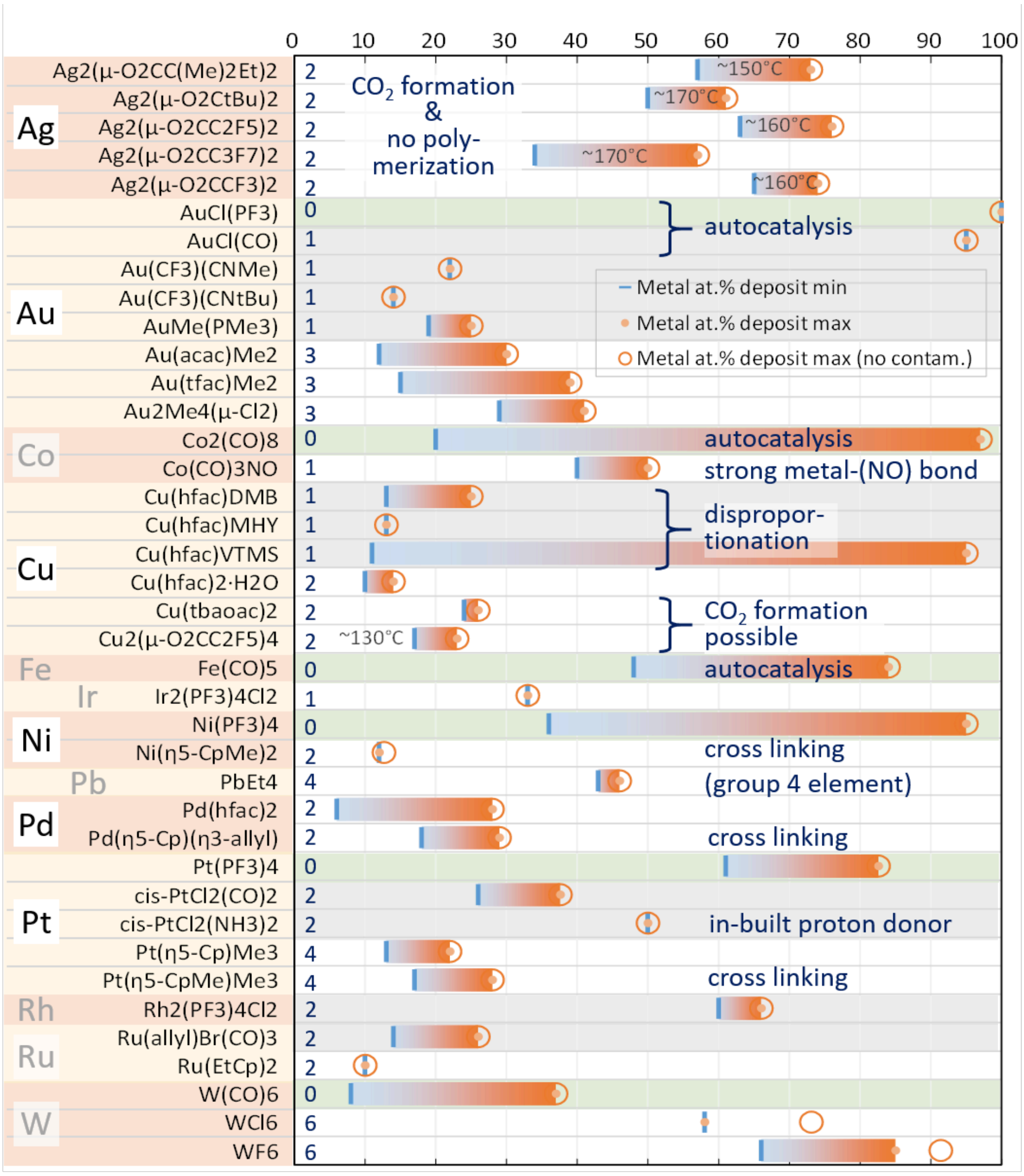

Fig. 1: FEBID precursors summarized according to the central metal atom with their metal content range (blue-orange bars). The metal oxidation state is noted vertically next to the precursor names. Precursors are highlighted with ligands being all neutral (light green bars), mixed neutral + ionic (grey bars), or fully ionic (white). Specific FEBID conditions and precursor ligand peculiarities are noted. Note that the large ranges of FEBID metal content for the individual precursors found in literature point to the dominant role temperature and residual gas conditions can have in FEBID [1].

3D-Nanoprinting via Focused Particle Beams

H. Plank[1,2,3,*] , R. Winkler[1], D. Kuhness[1], L. Seewald[1], J. Sattelkow[1], A. Weitzer[2], V. Reisecker[2], J. Hinum-Wagner[1], M. Brugger-Hatzl[1], G. Kothleitner[2,3]

[1] Christian Doppler Laboratory - DEFINE, Graz University of Technology, 8010 Graz, Austria
[2] Institute of Electron Microscopy and Nanoanalysis, Graz University of Technology, 8010 Graz, Austria
[3] Graz Centre for Electron Microscopy, 8010 Graz, Austria

[*] corresponding author email: harald.plank@felmi-zfe.at

Additive, direct-write manufacturing has become an essential part in research and development during the last decade. While methods down to the microscale have meanwhile entered industrial fabrication, the meso- and in particular the nanoscale are far more challenging with respect to resolution, spatial precision, predictability and reliability. Within the small pool of additive, direct-write technologies for nanoscale fabrication, focused particle beam induced deposition via both, ions and electrons, have proven their powerful capabilities. That technology class relies on the highly localized nano-synthesis of surface adsorbed precursor molecules, which are introduced in the vacuum chamber by a gas injection system. Hence, there are only little demands on substrate materials (vacuum and certain beam compatibility) and surface morphologies (accessible by the beam), making them true direct-write methods. As a currently unique possibility, both techniques allow for the fabrication of even complex, freestanding 3D nano-objects (Fig. 1a,b) by the controlled movement of the particle beam. Together with constantly improving software packages for a reliable upfront design, both technologies are ready to take on a unique cutting-edge role in the area of direct-write, additive manufacturing.
In this presentation, we shed light on recent progress of Focused Electron Beam Induced Deposition (FEBID) with emphasis on current fabrication and tuning possibilities in 3D space. That starts with a view on meshed objects, consisting of individually arranged and interconnected nano-wires, and then turns towards closed designs (Fig. 1c), where new effects become relevant. We then turn briefly into materials, their structural and chemical composition and discuss post-processing approaches, which tune or even entirely change the material properties. Finally, we comment on current activities towards multi-material objects and its challenges during fabrication and post-processing (Fig. 1d). The contribution is complemented by application examples to give an idea, how morphological and functional aspects in 3D space can lead to new application concepts, which are complicated or even impossible with alternative approaches.

[1] M. Huth, L. Keller, H. Plank, R. Winkler; *Kleingedrucktes mit großem Effekt*. Physik in unserer Zeit (**2020**), 51, 2, 64.

[2] R. Winkler, J.D. Fowlkes, P.D. Rack, H. Plank; *3D Nanoprinting via Focused Electron Beams*. J. Appl. Phys. 125 (**2019**), 210901.

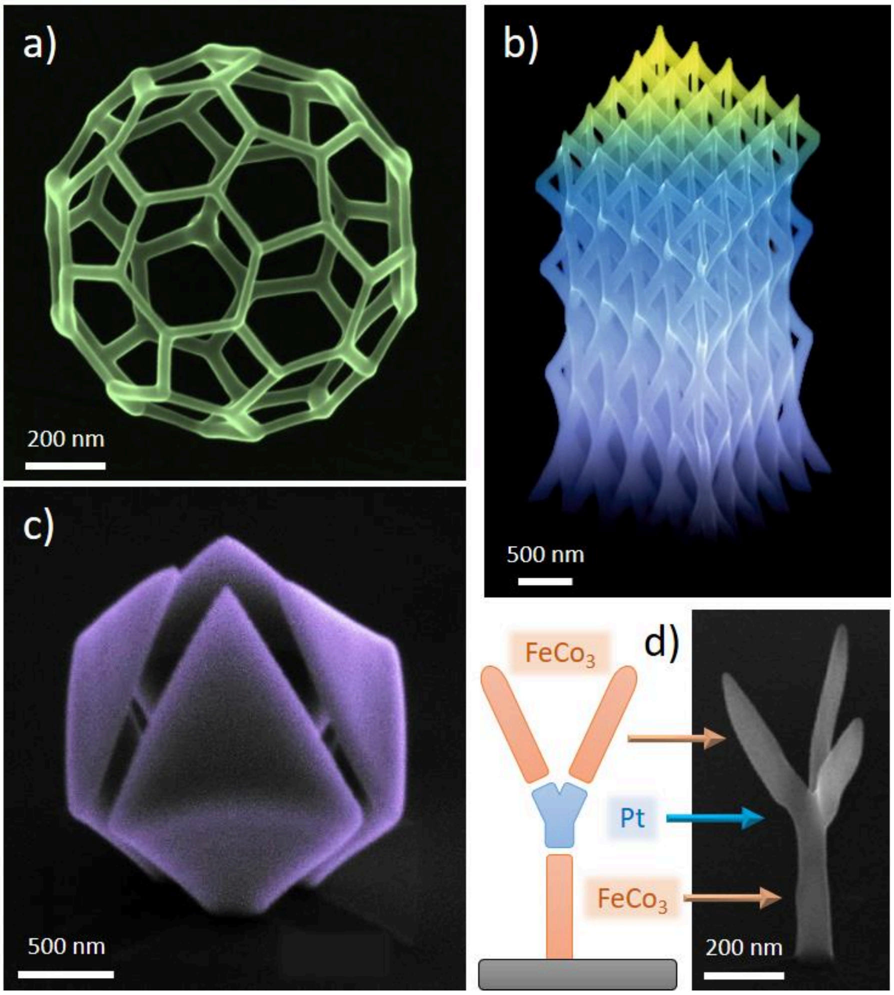

Fig. 1: 3D nanoprinting via Focused Particle Beam Induced Deposition from the gas phase. While (a) shows the resolution capabilities with individual branches in the sub-50 nm regime, (b) gives an example of a larger 3D structure with branch diameter and apex radii in the sub-100 nm and sub-10 nm regime, respectively, both fabricated in a single step. (c) shows a semi-closed 3D structure, which not only reveal additional challenges during fabrication but in particular open up new application possibilities due to added design flexibility. To expand the latter even further, multi-material 3D fabrication becomes relevant, as representatively shown in (d) by a Pt – FeCo3 multi-material structure. Figure is adapted from reference [1].

3D Nano-Printing of Plasmonically Active Gold-Nanoantennas

D. Kuhness[1], D. Knez[2], G. Haberfehlner[2], A. Gruber[1], H. Fitzek[3], R. Winkler[1], G. Kothleitner[2,3], H. Plank[1,2,3,*]

[1] Christian Doppler Laboratory - DEFINE, Graz University of Technology, 8010 Graz, Austria
[2] Institute of Electron Microscopy and Nanoanalysis, Graz University of Technology, 8010 Graz, Austria
[3] Graz Centre for Electron Microscopy, 8010 Graz, Austria

[*] corresponding author email: harald.plank@felmi-zfe.at

The area of nano-plasmonics is still interesting in the context of real applications, such as direct nano-emitters or high-performance sensors. However, for spatially precise and flexible fabrication of such nanoscale devices, versatile methods are in demand. Although traditional methods, like e-beam lithography, are very powerful, well established and highly reliable, they are somehow limited in their applicability (e.g. flat surfaces). In such situations, additive direct-write manufacturing can be a solution, although techniques for reliable sub-100 nm fabrication are only a few. In that respect, focused particle beam induced deposition from the gas phase is a promising technology pool, which not only meets resolution requirements but also allows true 3D nano-printing on a large number of materials and surface morphologies. While both, ion (FIBID) and electron beams (FEBID) can be used for that kind of nanofabrication, we here focus on the latter. While powerful in many aspects, FEBID materials notoriously suffer from high carbon contents, which is particularly dramatic when aiming on plasmonic applications. Fortunately, there are chemical post-growth treatments, which can transfer original materials in pure metals. However, that approach has mostly disruptive character when working with fragile 3D nano-architectures. Following that challenge, we have dissected FEBID growth characteristics of AuC_x nanostructures and combine individual advantages via advanced patterning approaches. That allows direct-write fabrication of high-fidelity shapes with nanoscale features in the sub-10 nm range. Such structures are then transferred into pure Au nano-antennas with minimal morphological disruption due the new design and optimized purification protocols (Fig. 1). The plasmonic activity is not only experimentally confirmed via Raman and STEM-EELS measurements but in particular in good agreement with simulations (Fig. 2). By that, the latter turns into an upfront design tool, which underlines the value of 3D-FEBID as fabrication tool for 3D nano-plasmonic concepts in the future.

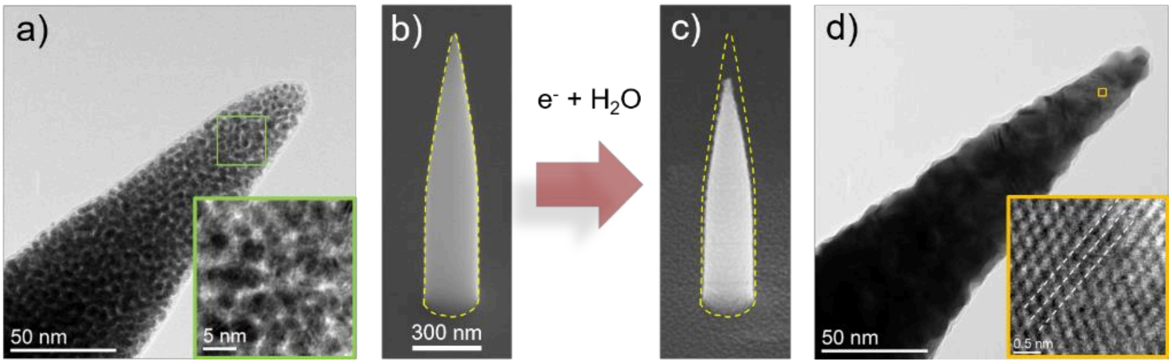

Fig. 1: Transfer of AuC_x FEBID nanopillars into pure Au nano-antennas. Transmission electron microscopy (TEM; a,d) and scanning electron microscopy (SEM; b,c) images of an AuC_x FEBID nanopillar after deposition (a,b) and after purification (c,d), using a scanning electron beam in low pressure H_2O atmospheres. The volume loss during purification becomes clearly evident by the dashed yellow lines in (c), which indicate the original shape from (b). The TEM images (a) and (d) nicely show the structural change from individual, isolated Au grains into compact Au materials (see indicated crystal planes).

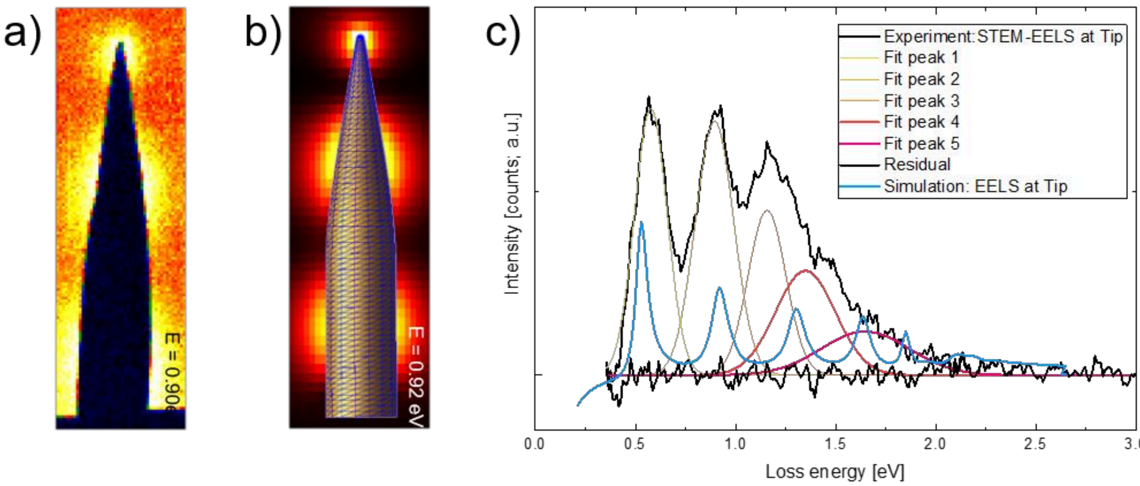

Fig. 2: Plasmonic activity of FEBID-based Au nanoantennas. (a) scanning TEM (STEM) based electron energy loss spectroscopy (EELS) map at a plasmon loss energy of 0.90 eV, which reveals laterally resolved information about plasmonic activities. (b) EELS map simulation, based on the real morphology taken from (a), which reveals very good agreement to real data (a). (c) shows a direct comparison of experimental (black) and simulated STEM-EELS spectrum data (see legend) taken from the tip region of the Au nanoantenna, revealing again good agreement, which is in particular remarkable as the simulation model did not use any additional scaling / fit parameter / functions.

Investigation of novel effects in three-dimensional magnetic nanostructures fabricated by focused electron beam induced deposition

A. Fernández-Pacheco[1,2*], L. Skoric[2], C. Donnelly[2], D. Sanz-Hernández[2], F. Meng[2], M.A. Cascales-Sandoval[1], A. Hierro-Rodríguez[2,3], C. Abert[4], D. Suess[4]
[1] SUPA, School of Physics & Astronomy, University of Glasgow, Glasgow G12 8QQ , UK
[2]Cavendish Laboratory, University of Cambridge, JJ Thomson Ave, Cambridge CB3 0HE, UK
[3]Physics Department, University of Oviedo, 33007 Oviedo, Spain
[4]Faculty of Physics, University of Vienna, Vienna, Austria

[*] corresponding author email: amalio.fernandez-pacheco@glasgow.ac.uk

The expansion of nanomagnetism to three dimensions provides exciting opportunities to explore new physical phenomena, and at the same opens fascinating prospects to create 3D magnetic devices which could be exploited in future technologies [1].

Focused Electron Beam Induced Deposition (FEBID) is a powerful tool to realize complex 3D magnetic nanostructures, opening up an exciting route to prototype 3D spintronic devices [2]. In this contribution, I will present a selection of recent works where we have been investigating new effects in 3D magnetic nanostructures with complex geometries patterned by FEBID.

First, I will introduce a new computational framework for the 3D printing of complex-shaped nanostructures using focused electron beam induced deposition [3]. Second, I will show how the control achieved over 3D nanofabrication can be exploited to create artificial chiral nanostructures where the combination of tunable geometrical chirality and magnetic interactions allows us to imprint non-trivial chiral spin textures and topological defects at precise locations [4]. Finally, I will show how the magnetoelectrical response of a 3D spintronic nanowire device differs from traditional planar devices [5]. Specifically, the non-trivial 3D geometry leads naturally to a strong anomalous magnonic contribution to the total magnetoresistance signal, result of the non-collinear configuration of magnetic states and electrical currents.

[1] A. Fernández-Pacheco et al; *Three dimensional nanomagnetism*, Nature Communications 8, (2017), 1.

[2] L. Skoric et al; *Layer-by-Layer Growth of Complex-Shaped Three-Dimensional Nanostructures with Focused Electron Beams,* Nano Letters 20, (202), 184.

[3] A. Fernández-Pacheco et al, Materials 13, (2020), 3774.

[4] D. Sanz-Hernández et al; *Artificial Double-Helix for Geometrical Control of Magnetic Chirality*, ACS Nano 14, (2020), 8084.

[5] F. Meng et al; *Non-Planar Geometrical Effects on the Magnetoelectrical Signal in a Three-Dimensional Nanomagnetic Circuit*, ACS Nano 15, (2021), 6765

in situ toolkit for SEM or FIB/SEM: From Life Science FIB applications to micro-/nanomachining and GIS systems - micromanipulators and add-ons for addressing a multitude of tasks

A. J. Smith[1,*], A. Rummel[1], K. Schock[1], S. Strähle[1], S. Kleindiek[1]

[1] Kleindiek Nanotechnik, Aspenhaustr. 25, 72770 Reutlingen, Germany
[*] corresponding author email: andrew.smith@kleindiek.com

SEM and FIB/SEM microscopes are used in a wide variety of settings for many different applications. Integrating micromanipulators allows operators to enhance their microscopes' functionality even further. Giving microscopes "hands" yields the ability to touch, characterize, and manipulate samples in novel and exciting ways. Furthermore, by adding specialized plug-ins or additional dedicated tools to the setup, advanced applications are accessible.

Micromanipulators can be equipped with plug-ins that provide low-noise electrical leads for electrical measurements, dedicated force sensors for material characterization, or microgrippers for handling small objects such as TEM lamella or other micro-objects.

A specialized version of the microgripper plug-in, suitable for working under cryo (LN2) conditions, allows handling frozen TEM lamella prepared in cryo-FIB (Fig. 1). Being able to reliably retrieve FIB-processed lamella from frozen bulk samples and move them to suitable receptacles for cryo-TEM investigation is one of many crucial steps in obtaining data from biological materials [1].

Adding a compact and flexible Gas Injection System (GIS) is another way in which a microscope can be modified in order to address more applications. Using a flexible gas injection system (Fig. 2) provides the means for operators to experiment with various precursor substances/chemistries. Other use cases include injecting water vapor or air (or N2) for charge compensation. Similarly, oxygen gas, hydrogen gas, or other reactive gases can be introduced into the microscope chamber.

Another very specialized tool that can enhance a FIB/SEMs capability is a dedicated concentric rotation drive. This tool can be used to center the desired Region Of Interest (ROI) on top of the axis of rotation. Rotation can be continuous so that the FIB can be used to sharpen or reshape samples as desired (Fig. 3). Potential applications for this are (pre-)processing samples for Atom Probe Tomography (APT) or flat punch experiments. A novel use for such a rotation drive is in-SEM X-Ray Diffraction (XRD). Here, an x-ray target material is positioned under the SEM's beam. The target is irradiated by the electron beam, thus generating x-rays. The sample is mounted to the dedicated, separate rotation drive. An X-ray detector mounted to the SEM chamber records a diffraction pattern each time the sample is rotated by a small amount while remaining stationary in X,Y, and Z.

Oftentimes, researchers need to work with beam-sensitive materials. Reducing damage induced by the electron beam (during imaging) or artefacts from ion beam milling can be achieved by cooling the sample (Fig. 4). To that end, a compact and waterless Peltier cooling stage is introduced. Before/after examples of SEM imaging and FIB milling experiments will be shown.

[1] M. Schaffer, et al., A cryo-FIB lift-out technique enables molecular-resolution cryo-ET within native Caenorhabditis elegans tissue, Nature Methods 16 (2019), 757

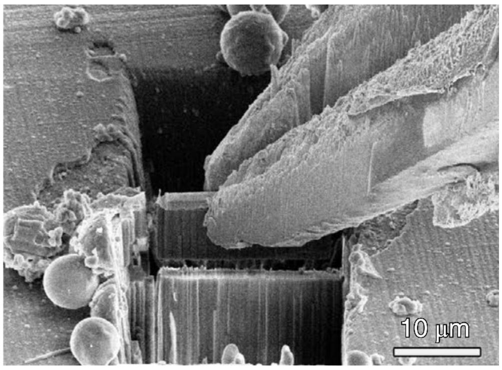

Fig. 1: A cooled gripper is used to retrieve a frozen TEM lamella milled in cryo FIB.

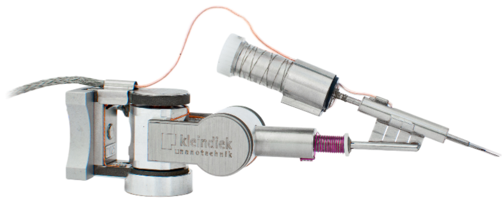

Fig. 2: GIS plug-in module. The reservoir can be filled with a wide variety of materials.

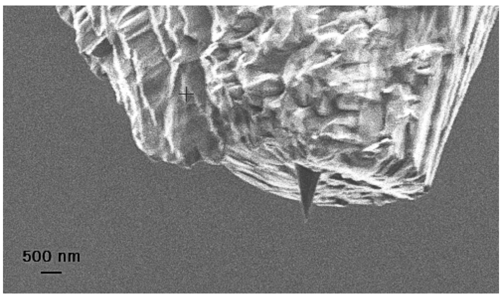

Fig. 3: sharp tip milled using a box milling pattern and concentric sample rotation.

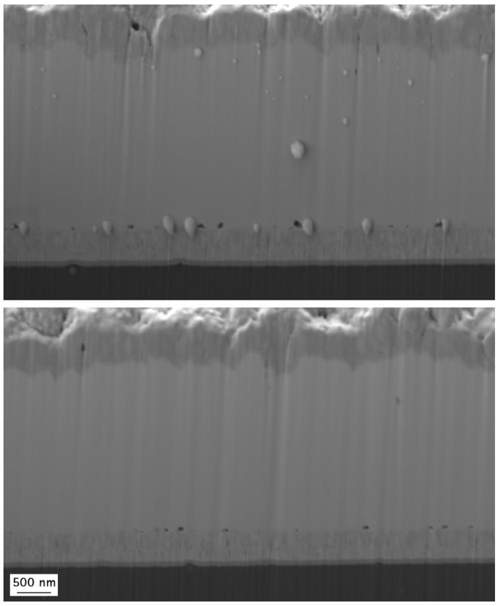

Fig. 4: CIGS solar cell cross section. Top: room temperature. Bottom: sample cooled to –60°C.

Rapid FIB preparation of thin films for TKD analysis

J. Lindsay[1], P. Trimby[1], I. Anderson[1]

[1.] Oxford Instruments NanoAnalysis, Halifax Road, High Wycombe, HP12 3SE, UK
[*] corresponding author email: john.lindsay@oxinst.com

Transmission Kikuchi diffraction (TKD) has proven to be an effective extension to conventional electron backscatter diffraction (EBSD), enabling routine characterization of nanocrystalline materials [1-3]. However, TKD necessitates electron transparent samples and, due to the use of relatively low electron beam energies compared to conventional transmission electron microscopy (TEM), ideal sample thicknesses are usually in the range of 50-100 nm. This makes sample preparation for TKD as challenging as TEM, typically involving electropolishing, Ar ion milling, or standard focused ion beam scanning electron microscope (FIB-SEM) lift out techniques. For the analysis of surface thin films, preparation of a cross section through the film and underlying substrate is relatively simple using FIB lift out but, in comparison, it is very difficult to prepare good TEM samples from the 2D plane of the thin film (published approaches usually involve significant wedge milling and can take many hours to complete – e.g. [4]).

Here we introduce a simple and novel approach to TKD sample preparation of surface layers, utilizing a FIB-SEM without requiring lift out or significant sample surface cleaning. Our technique can prepare suitably thin samples for off-axis TKD measurements within 30 minutes. This approach enables effective TKD analyses of nanostructured surface films and has the added benefit of allowing simple correlation with additional surface analysis techniques, either within the SEM (e.g. energy dispersive X-ray spectrometry (EDS), conventional EBSD or electron imaging) or separately (e.g. atomic force microscopy - AFM).

We will demonstrate this TKD preparation technique on nanocrystalline metals and thin films using Ga FIB.   Large area TKD samples will also be shown, prepared using femtosecond laser milling and Xe FIB thinning.

References

1. R. R. Keller and R. H. Geiss, J. Microscopy 245 (2012) 245–51.
2. P. W. Trimby, Ultramicroscopy 120 (2012) 16-24
3. P. W. Trimby et al., Acta Materialia 62 (2014) 69–80
4. C. Li et al., Ultramicroscopy 184 (2018) 310–317

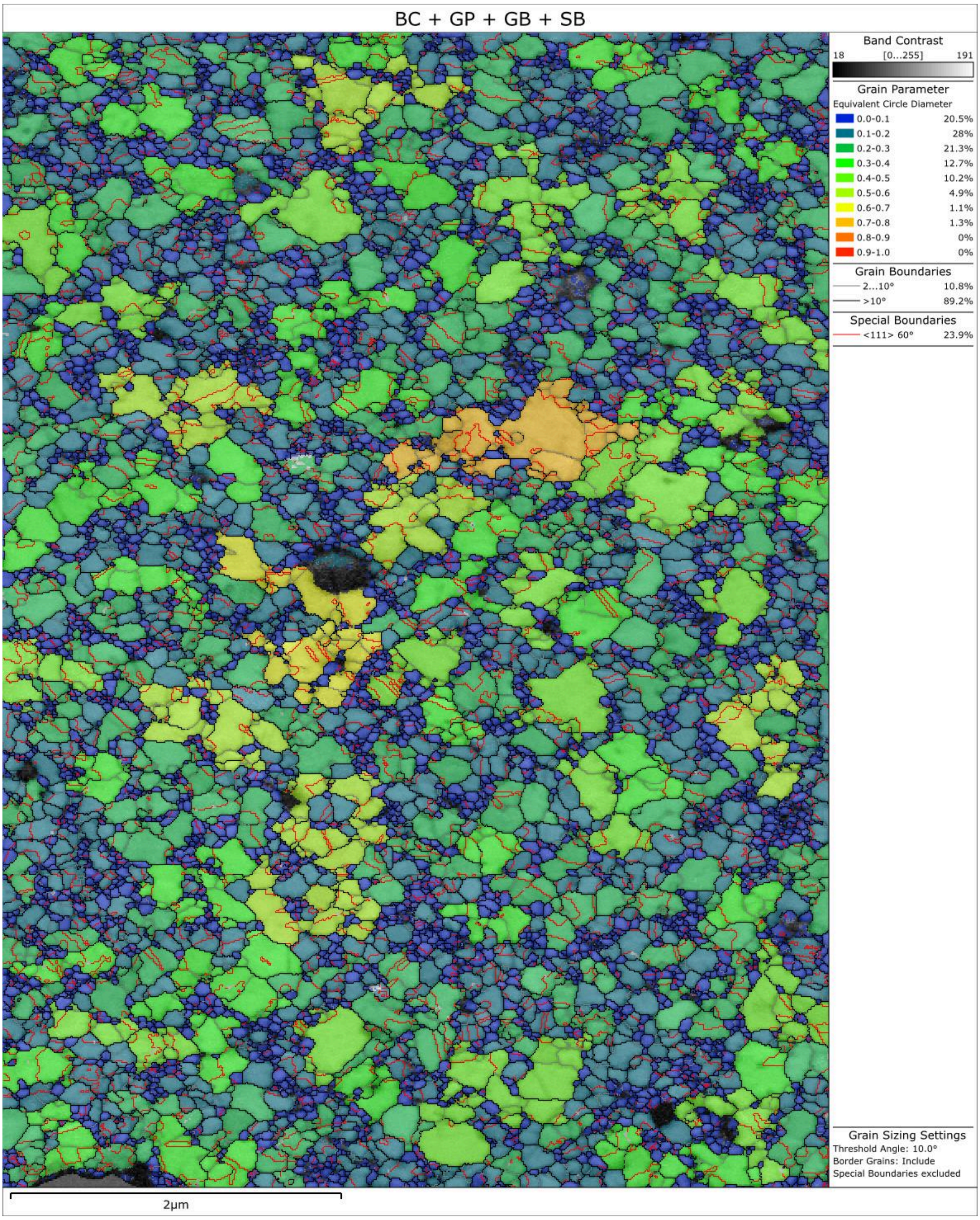

Fig 1 TKD map acquired from an Au film, film thickness is approximately 20 nm and the sample was prepared in less than 30 minutes.

Local Phase Identification at Nanoscale of Different Titanium Oxides by EBSD Dictionary Based Indexing Approach

B.R. Jany[1*], K. Cieslik[1], A. Kryshtal[2], A. Kruk[2], and F. Krok[1]
[1] The Marian Smoluchowski Institute of Physics, Jagiellonian University, Lojasiewicza 11, 30-348 Krakow, Poland
[2] Faculty of Metals Engineering and Industrial Computer Science and the International Centre of Electron Microscopy for Materials Science, AGH University of Science and Technology, 30-059 Krakow, Poland
[*] corresponding author email: benedykt.jany@uj.edu.pl

Local phase identification at nanoscale is a challenging task which employs usually combination of different time consuming and expensive TEM techniques (diffraction, EDX/EELS spectroscopy, etc.). Only small sample areas present in the prepared cross-sectional thin foil could be examined. Here we present results on EBSD dictionary based phase ID from crystalline titanium oxide nanowires prepared on SrTiO3(001) surface using extremely low oxygen partial pressure ELOP method [1]. Many titanium oxide phases could be formed by changing ELOP conditions, having various tailored applications for use in photocatalysis and nanoelectronics. The SEM EBSD data were collected from different nanowires at 5keV beam energy in the form of 4D data i.e. for each x,y position full EBSD diffraction was recorded. The diffraction data were next indexed using dictionary based approach. Different titanium oxide phases (~15 different phases) were calculated using dynamic EBSD simulation [3] as implemented in EDAX OIM Matrix software. Later, the dictionaries resulted from dynamic simulations were compared with experimental data by comparing cross correlation coefficient as used in Kikuchipy software [4]. This resulted in successful nanowires phase identification. The obtained results were confirmed by STEM ELNES (energy loss near edge structure) analysis of titanium and oxygen edges of nanowires cross sections, which act as a fingerprint of titanium oxides.

Our results show that by using EBSD dictionary based indexing approach one can successfully identify locally at nanoscale different titanium oxides phases from relatively large areas using simple and achievable SEM EBSD measurements.

[1] D. Wrana, C. Rodenbücher, B.R. Jany, A.P. Kryshtal, G. Cempura, A. Kruk, P. Indyka, K. Szot, F. Krok, Bottom-up process of self-formation of highly conductive titanium oxide (TiO) nanowires on reduced SrTiO3, Nanoscale 11, 89-97 (2019).

[2] Y.H. Chen, S.U. Park, D. Wei, G. Newstadt, M.A. Jackson, J.P. Simmons, M. De Graef and A.O. Hero (2015) "A dictionary approach to electron backscatter diffraction indexing", Microscopy and Microanalysis 21: 739-752 (2015).

[3] P. G. Callahan and Marc De Graef, Microsc. Microanal. 19, 1255–1265 (2013).

[4] Håkon Wiik Ånes, Ole Natlandsmyr, Tina Bergh, & Lars Lervik. pyxem/kikuchipy: kikuchipy. Zenodo https://doi.org/10.5281/zenodo.3597646 (2021).

Production of Defects in Two-Dimensional Materials under Ion Irradiation: Insights from First-Principles and Analytical Potential Molecular Dynamics Simulations

A. V. Krasheninnikov[1*]

[1] Institute of Ion Beam Physics and Materials Research, Helmholtz-Zentrum Dresden-Rossendorf, 01328 Dresden, Germany
[*] Corresponding author email: a.krasheninnikov@hzdr.de

Ion irradiation has successfully been used for introducing impurities and creating defects in two-dimensional (2D) materials in a controllable manner. Moreover, focused ion beams, especially when combined with in-situ or post-irradiation chemical treatments, can be employed for patterning and even cutting 2D systems with a high spatial resolution. The optimization of this process requires the complete microscopic understanding of the interaction of energetic ions with the low-dimensional targets. In my presentation, I will dwell upon the multi-scale atomistic computer simulations of the impacts of ions onto free-standing (e.g., suspended on a TEM grid) and supported (deposited on various substrates) 2D materials, including graphene, hexagonal boron-nitride (h-BN) and transition metal dichalcogenides (TMDs), such as MoS_2 and WS_2. The theoretical results will be augmented by the experimental data obtained by the coworkers. I will first overview the general trends in defect production [1] then touch upon our recent work on irradiation-induced defects in h-BN [2,3] which are interesting in the context of single-photon quantum emitters. Finally, I will present the results of density-functional-theory-based molecular dynamics (DFT-MD) simulations of the low-energy ion impacts onto 2D materials [4] aimed at assessing the ion energy required to displace the atom and demonstrate that the widely-used binary collision formula is not applicable in this case. I will also discuss fundamental limitations and pitfalls in using DFT-MD in simulations of effects of irradiation on solids.

[1] A. V. Krasheninnikov, Nanoscale Horizons, 5 (2020) 1447.

[2] M. Fischer, J.M. Caridad, A. Sajid, S. Ghaderzadeh, M. Ghorbani-Asl, L. Gammelgaard, P. Bøggild, K. S. Thygesen, A. V. Krasheninnikov, S. Xiao, M. Wubs, and N. Stenger, Sci. Adv. 7 (2021) eabe7138.

[3] S. Ghaderzadeh, S. Kretschmer, M. Ghorbani-Asl, G. Hlawacek and A. V. Krasheninnikov, Nanomaterials 11 (2021) 1214.

[4] S. Kretschmer, S. Ghaderzadeh, S. Facsko, and A. V. Krasheninnikov, (2021) submitted for publication.

Graphene nanomesh for electron and phonon engineering

F. Liu[1*], J. Guo[1], S. Ogawa[2], Y. Morita[2], M. Schmidt[1], M. Muruganathan[1], and H. Mizuta[1*]

[1] Japan Advanced Institute of Science and Technology (JAIST), Nomi, Japan
[2] National Institute of Advanced Industrial Science and Technology (AIST), Tsukuba, Japan.
*Corresponding author email: mizuta@jaist.ac.jp, fayong@jaist.ac.jp

Graphene nanomesh (GNM) is a new artificial nanostructure in which the periodic nanopores are patterned on monolayer graphene. Profiting from its configurable structure, it has significant potential for applications in electron and phonon engineering beyond the normal graphene [1]. Recently, with the help of high-speed helium ion beam milling (HIBM) technology, the ultrafine patterning of GNM has been actively explored [2]. The focused He+ beam has two main advantages over the conventional focused Ga+ beam, which are higher precision and lower damage. Carving suspended graphene into sub-10 nm structures is getting particularly interested for various advanced applications such as bandgap engineering [3] and nanoscale phonon engineering [4]. In this talk, we discuss our recent achievements in fabricating suspended GNM with sub-10 nm diameter periodic nanopores by HIBM technology and the practical applications for activation energy tuning, quantum dot formation and nanoscale thermal rectification. By ultrafine controlling the pitch (nanopore center to center) of GNM from 15 nm to 50 nm with 6 nm pore diameter, the exponential relationship between the thermal activation energy and porosity was observed [5], which provides a new approach to build potential barriers for quantum dot formation [6]. We also patterned asymmetric GNM structure on a half area of suspended graphene for seeking thermal rectification phenomena. By developing a new thermal bridge method, we observed a substantial difference in nanoscale thermal transport via the asymmetric GNM structure in the forward (*J+*) and reverse (*J-*) directions in contrast to symmetrical electron transport [7].

Reference:

[1] J. Bai et al.; *Nat. Nanotechnol.* 5(**2010**), 190. [2] M. E. Schmidt *et al*; *ACS Appl. Mater. Interfaces.* 10(**2018**), 10362. [3] M. E. Schmidt *et al*; *Small*, 15(**2019**), 1903025. [4] A. Arora *et al*; *Phys. Rev. B* 96(**2017**), 165419. [5] F. Liu *et al*; *Micromachines* 11(**2020**), 387. [6] F. Liu *et al*; *EDTM2021*, **2021**, Chengdu, China. [7] F. Liu *et al*; *SSDM2020*, **2020**, Toyama, Japan.

Acknowledgment:

The authors acknowledge T. Iijima and H. Ota for the usage of the HIM at the AIST SCR station for the helium ion irradiations. This work was supported by the Grant-in-Aid for Scientific Research No. 18H03861, 19H05520 from the Japan Society for the Promotion of Science (JSPS).

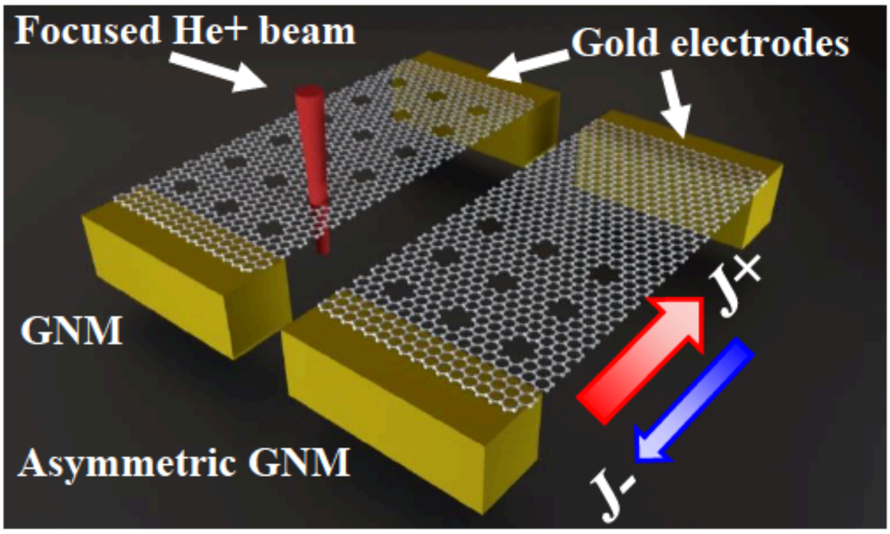

Fig. 1: Schematic illustration of GNM device (left) and asymmetric GNM device (right) patterned by HIBM on suspended graphene.

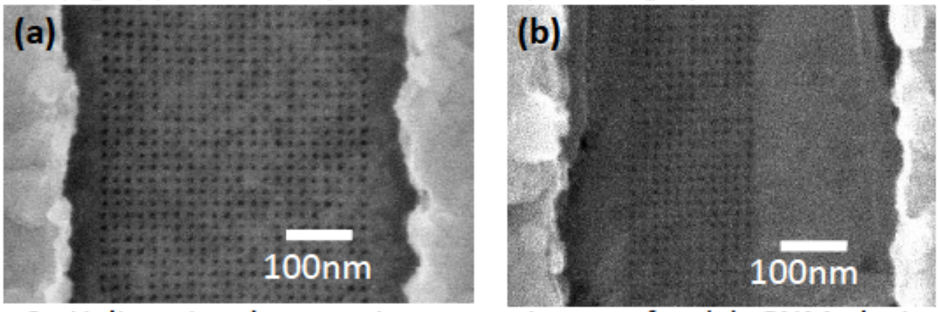

Fig. 2: Helium ion beam microscopy images for (a) GNM device (b) asymmetric GNM device. The average of nanopore diameter can be identified as 6 nm approximately.

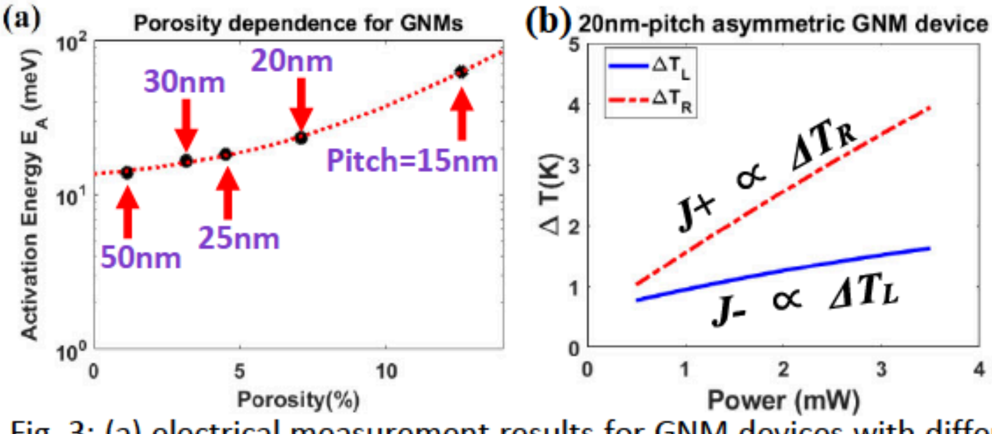

Fig. 3: (a) electrical measurement results for GNM devices with different pitches. (b) thermal measurement results for asymmetric GNM device by "differential thermal leakage method" at 150 K environmental temperature. The value of ΔT_R is related to $J+$ and the value of ΔT_L is related to $J-$.

4th EuFN and FIT4NANO
Joint Workshop

Oral Presentations Tuesday

September 27th - 30th, 2021
Vienna, Austria

Helium Ion Microscopy Images of Aerosols trapped in filters
HZDR

Scaling down thermodynamic techniques for quantum materials

S. Thadathil[1], V. Zambra[1], S. Safari[1], M. Nauman[1], L. Shafeek[1], S. Fritze[1], K.A. Modic[1*]

[1] Institute of Science and Technology Austria, Am Campus 1, 3400 Klosterneuburg, Austria

[*] corresponding author email: kimberly.modic@ist.ac.at

The focused ion beam (FIB) has revolutionized electrical transport measurements in 3D quantum materials by allowing access to the microscale[1,2]: electrical contacts can now accurately be placed on micron-sized single crystals that were impossible to contact by hand. However, thermodynamic techniques like heat capacity and magnetometry typically call for large millimeter-sized single crystals. We will discuss how the FIB is being used to develop and modernize thermodynamic methods by miniaturizing calorimeters, cantilevers[3], and transducers. This talk places a special emphasis on the motivation and challenges associated with determining the anisotropic properties of quantum materials. Thus, we focus on several recent in-situ advances made to the FIB system that are paving the way for the sensitive detection of such properties.

[1] Maja D. Bachmann, *et. al.*; *Spatial control of heavy-fermion superconductivity in CeIrIn$_5$;* Science **366**, 6462, (**2019**), 221.

[2] F. Ronning, *et. al.*; *Electronic in-plane symmetry breaking at field-tuned quantum criticality in CeIrIn$_5$;* Nature **548**, 313-317, (**2017**).

[3] K.A. Modic, *et. al.*; *Resonant torsion magnetometry in anisotropic quantum materials;* Nature Communications **9**, 3975, (**2018**).

Focused-ion-beam as a topological edge-mode writer in higher-order topological insulator Bismuth

Chunyu Guo[1], Xiangwei Huang[1], Carsten Putzke[1] and **Philip J. W. Moll**[1*]

[1] Laboratory of Quantum Materials (QMAT), Institute of Materials (IMX), Ecole Polytechnique Fédérale de Lausanne (EPFL), CH-1015 Lausanne, Switzerland.
[*] corresponding author email: philip.moll@epfl.ch

With increasing number of materials habor topological phases, band topology and its influence on electronic properties draw major attentions in recent years. Typically, a three-dimensional topological insulator features the so-called surface-bulk correspondence: an insulating bulk covered with a gapless surface state. Recent development highlights the exploration of higher order topology. This means that instead of a topological surface state, the gapless state only forms on the edge of a higher order topological insulator (HOTI). Bismuth was theoretically predicted to be an example of HOTI, and the existence of edge state was later confirmed by scanning tunneling microscope (STM) experiments [1]. Motivated by this observation, the possibility of artificially writing topological conduction channel using focused-ion beam technique is explored. A strain-free membrane device [Fig. 1(a)] was fabricated for the systematic study of electronic transport properties of Bismuth down to low temperature and high magnetic field. By adding FIB-induced lines on the device surface, a clear change of conductivity is observed. Detailed analysis reveals a direct relation between the number of FIB-induced lines and the conductivity increasement, each line approximately corresponds to two conductance quantum [Fig. 1(b)]. This correspondence is a direct indication of FIB-induced one-dimensional gapless edge state. These findings not only shed new light on exploring the quantum transport properties of HOTI, but also open a new avenue for future application of artificial topological conduction channel encoder via FIB technique.

[1] Frank Schindler, Zhijun Wang et al., *Higher-Order Topology in Bismuth;* Nature Physics 14 (**2018**), 918.

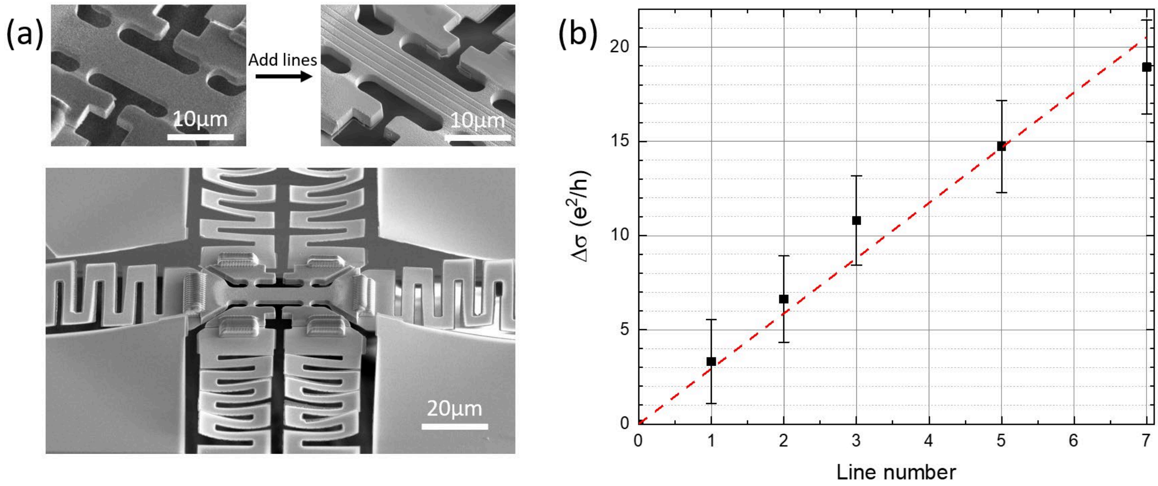

Fig. 1: (a) Scanning electron microscope image of FIB-structured membrane device in µm-scale. (b) Consistent relation between the number of FIB-induced lines and the conductivity increasement due to that, the conductance unit e^2/h is a half conductance quantum.

VELION - A Novel FIB-SEM Nanofabrication Instrument Concept and its Applications in Nanoscale Science and Engineering

T. Richter[1] and P. Mazarov[1]

[1] Raith GmbH, Konrad Adenauer Allee 8, 44263 Dortmund, Germany

[*] Corresponding author email: torsten.richter@raith.de

Raith has advanced FIB instrumentation over the last fifteen years with the vision that nanofabrication has special requirements that should drive the development of FIB technology.

The plasmonics and nanophotonics community has clearly demonstrated that there are applications whereby FIB-Lithography has its advantages in first delivering the answers to important questions in nanoscale science and engineering. One important motivation for using FIB nanofabrication is the relative simplification of the overall process, especially for the direct processing at the nanometer scale of novel materials (Fig. 1). With a FIB-centric setup where the ion beam is always perpendicular to the sample plane and the use of a laser interferometer stage at nm accuracy more sophisticated application become possible (Fig. 2). The VELION takes advantage of stability, large and fully corrected fields-of-view, and laser interferometer stages, which are essential components for sophisticated nanofabrication instrumentation. These are mandatory for plasmonics and nanophotonics, which often require high resolution nanolithography with tight dimensional control over areas much larger than a single field-of-view.

With the appreciation that the ion's properties can have dramatic consequences on the physical and chemical nature of the resulting nanostructures, we also discuss the motivations behind applications employing either Gallium or non-Gallium species, such as Silicon, Gold, Germanium, Lithium, Bismuth and clusters (Fig. 3).

We report on applications that reveal the potential of the VELION in terms of complex nanofabrication utilizing universal ion sources incl. light and heavy ions.

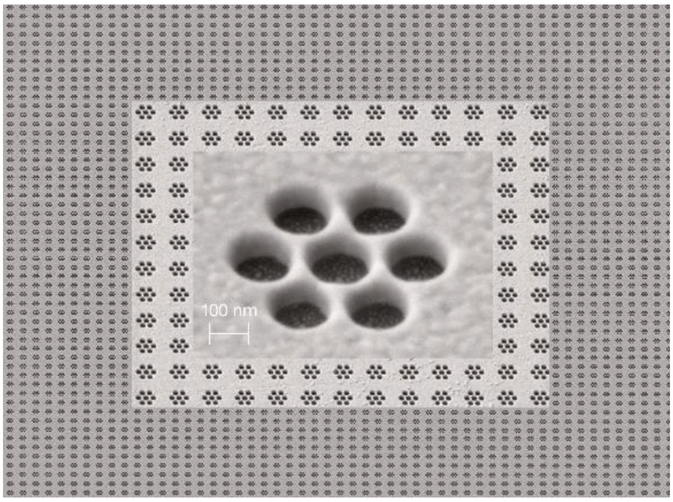

Fig. 1: Plasmonic device of oligomer array fabricated into Au film

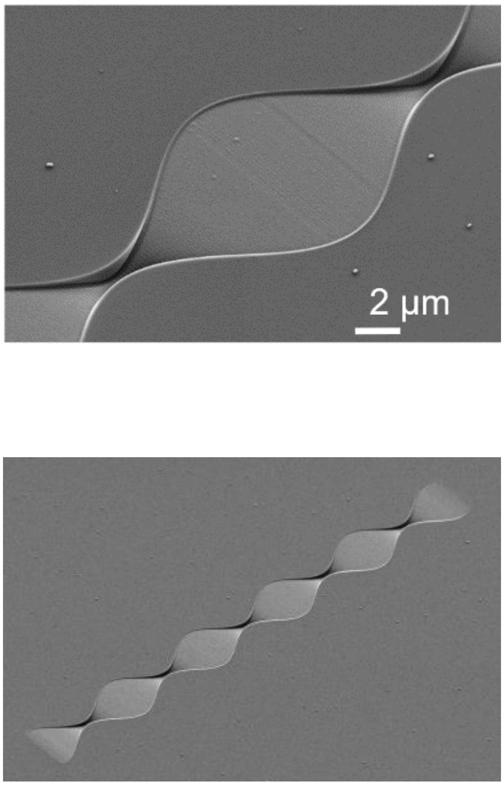

Fig. 2: Microfluidic mixer

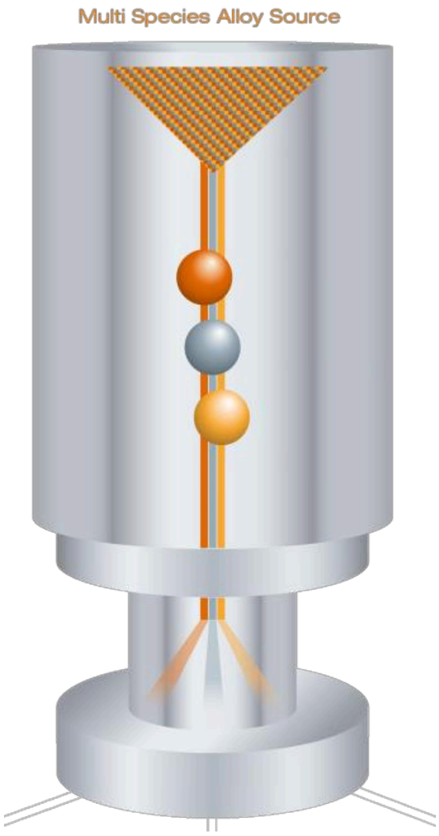

Fig. 3: Ion select. Multi species configuration

Tip- and Laser-based 3D-Nanofabrication up to ∅100 mm

I. Ortlepp[1*], J. Stauffenberg[1] and E. Manske[1]

[1] Technische Universität Ilmenau, Institute of Process Measurement and Sensor Technology, 98693 Ilmenau, Germany

[*] corresponding author email: ingo.ortlepp@tu-ilmenau.de

The field of optical lithography is subject to intense research and has gained enormous improvement. However, the effort necessary for creating structures in the size of 20 nm and below is considerable using conventional technologies. For that reason, enormous effort is directed to the development of alternative fabrication technologies. However, new and promising technologies are only demonstrated as a proof of concept on a labscale of several square micrometres and for their implementation, there is a lack of adequate measuring and positioning techniques that span the scale from subnanometres to the wafer size. [1,2] In recent years, nanopositioning and nanometrology have experienced an enormous progression at the Technische Universität Ilmenau, especially regarding the further development of 3D precision measurement technology [3]. Consequently, the aim is to combine the latest micro- and nanofabrication processes with the enormous advantages of nanopositioning and nanometrology. For that purpose, nanopositioning and nanomeasuring machines (NPM machines, fig. 1), developed at the Technische Universität Ilmenau, are available, which have been proving their capability for nanomeasuring tasks since several years [4]. When combining the advantages of advanced structuring processes with the positioning capabilities of NPM machines, there is the potential to push the limits of patternability, with sub-nanometre performance, across scales up to ∅100 mm. Based on this combination, 3D nanofabrication and nanostructuring of 3D surfaces (e.g. aspheres) is getting within reach. To achieve this, (AFM-) tip-based techniques (fig. 2) in the sub-10 nm range, techniques for laser-based nanofabrication (fig. 3) at the physical limits of optical technologies and new solutions of nanofabrication on free-form surfaces are combined with different NPMs and investigated in our project.

[1] Tseng, A. et al. “Recent Developments in Tip-Based Nanofabrication and Its Roadmap”. In: Journal of Nanoscience and Nanotechnology 8.5 (May 2008), pp. 2167–2186. doi: 10.1166/jnn.2008.243.

[2] Seo, J.-H., et al. “Nanopatterning by Laser Interference Lithography: Applications to Optical Devices”. In: Journal of Nanoscience and Nanotechnology 14.2 (2014), pp. 1521–1532. doi: 10.1166/jnn.2014.9199.

[3] Manske, E., et al. “Recent developments and challenges of nanopositioning and nanomeasuring technology”. In: Measurement Science and Technology 23.7 (2012), p. 074001. doi:10.1088/0957-0233/23/7/074001.

[4] Jäger, G., et al. “Nanopositioning and nanomeasuring machine NPMM-200—a new powerful tool for large-range micro- and nanotechnology”. In: Surface Topography: Metrology and Properties 4.3 (July 2016), p. 034004. doi: 10.1088/2051-672x/4/3/034004.

[5] Ortlepp, I., et al. "Tip- and Laser-based 3D-Nanofabrication in Extended Macroscopic Working Areas". In: Nanomanufacturing and Metrology (accepted for publication).

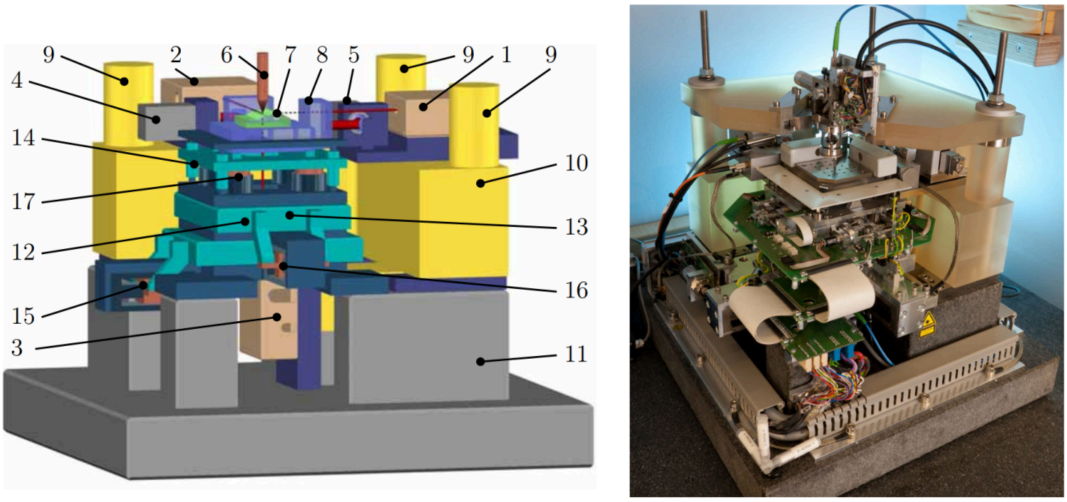

Fig. 1: Basic mechanical and optical design of the NMM-1. 1: x-Interferometer, 2: y-Interferometer, 3: z-Interferometer, 4: Roll and yaw angle sensor, 5: Pitch and yaw angle sensor, 6: Probe, 7: Sample, 8: Corner mirror, 9: Zerodur pillar, 10: Metrology frame (Zerodur©), 11: Base, Guides of the 12: x-axis, 13: y-axis, 14: z-axis and Drives of the 15: x-axis, 16: y-axis, 17: z-axis. [5]

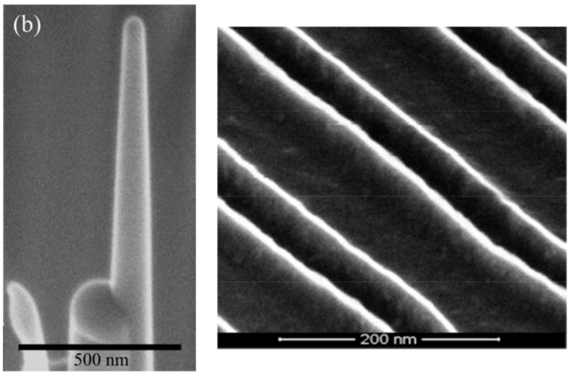

Fig. 2: Left: Diamond tip for FESPL after micromachining using a focused gallium ion beam. Right: SEM image of double line features, structured with the described FESPL technique. A fully etched trench between the two parallel lines is observed and the line distance is 30 nm. [5]

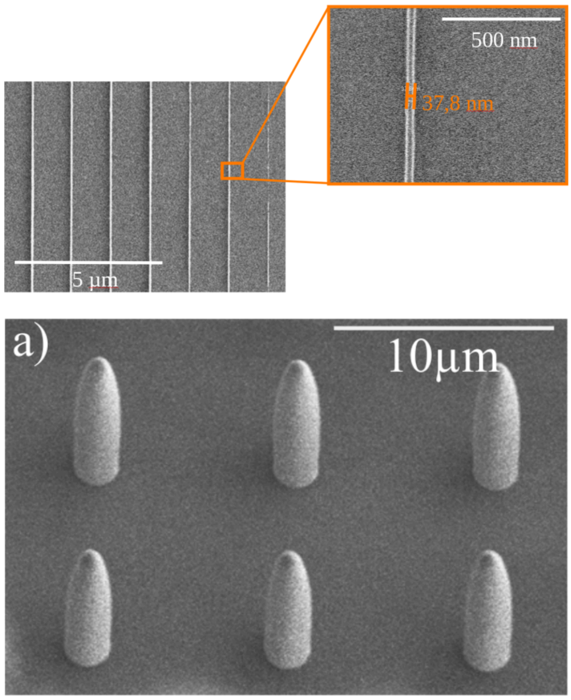

Fig. 3: Structuring results with the described setup. Top: Smallest line widths of 37.8 nm could be achieved. Bottom: Demonstration of the capability for 3D writing. [5]

The Virtual FIB: Simulating FIB Degrees Of Freedom To More Effectively Explore And Communicate Advanced FIB Workflows

A. B. Mosberg[1*]

[1] SuperSTEM, STFC Daresbury Laboratories, Keckwick Lane, Warrington WA4 4AD, UK
[*] corresponding author email: abmosberg@superstem.org

The most ubiquitous FIB system configuration is the two-beam FIB-SEM with its complementary electron and ion beams allowing for both observation and manipulation of samples [1]. These systems are generally equipped with a 5-axis stage (Figure 1a) which enable operators to tilt to either beam, and the ease of moving between beams is a cornerstone of the flexibility that makes FIB so useful.More recently, the emergence of new instrumentation such as lift-out needles with accurate motorized rotation [2] and triple-beam configurations [3,4] have the potential to add significant new capabilities to FIB systems, but the process of developing workflows for these situations is currently straining against the capabilities of 5-axis stages which are optimized for the two-beam configuration.

A tool to help predict and rapidly experiment with advanced rotational degrees of freedom in FIB would thus be useful. Simulating a FIB chamber in 3D makes it easier to develop an intuition for how to make maximal use of these new systems, and this work presents an open-source tool to tackle this. By simulating and visualizing the different degrees of freedom available in a FIB it provides operators with a way explore new protocols and fully understand the results of rotation operations on their process, as well as a way to effectively communicate complex FIB protocols.

Being open-source and built as an application template to the much larger and actively developed 3D modeling software Blender (www.blender.org) also ensures wide compatibility, easy installation and significant customization potential for advanced users. Simultaneously, a core goal of the project is to make a simplified and intuitive interface with FIB-relevant controls (Figure 2), easily accessible and suitable for current or prospective FIB users at every skill level.

[1] L. A. Giannuzzi, F. A. Stevie (eds.), "Introduction to Focused Ion Beams: Instrumentation, Theory, Techniques, and Practice" (Springer, New York).

[2] A. B. Mosberg *et al.*, *FIB lift-out of conducting ferroelectric domain walls in hexagonal manganites, Appl*. Phys. Lett. 115 (**2019**), p.122901.

[3] M. P. Echlin *et al.*, *A new TriBeam system for three-dimensional multimodal analysis, Rev*. Sci. Instrum. 83, (**2012**), p.023701.

[4] T. Sato *et al.*, *High quality lamella preparation of gallium nitride compound semiconductor using Triple Beam™ system,* J. Phys. Conf. Ser. 902, (**2017**), p.012019.

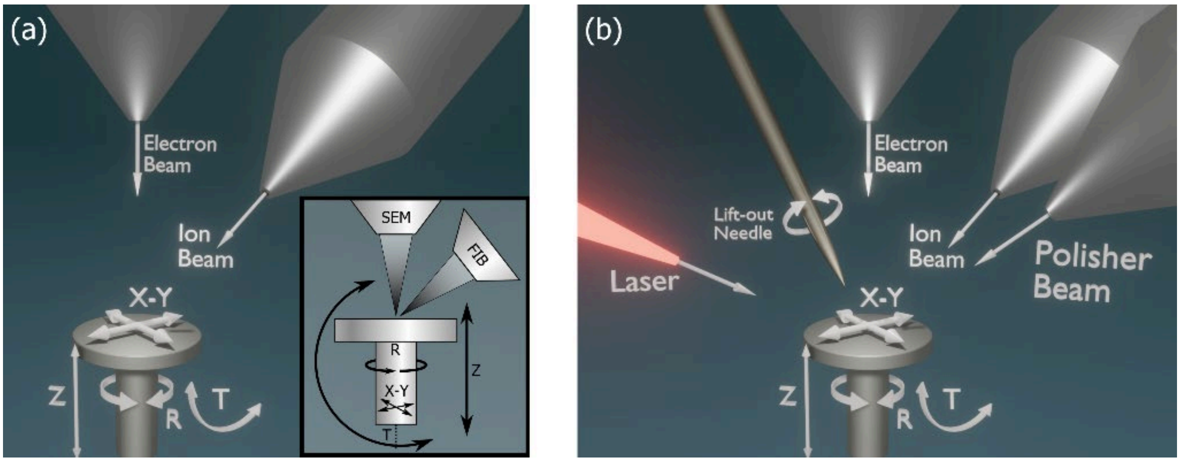

Fig. 1: Representation of new challenges to 5-axis stage movements. (a) 3D representation of 5-axis stage degrees of freedom in two-beam system. Inset: 2D representation describing same degrees of freedom. (b) Examples of different new capabilities challenging the 5-axis stage: Lift-out needle rotation axes and third beams coming in from different angles complicate the navigation.

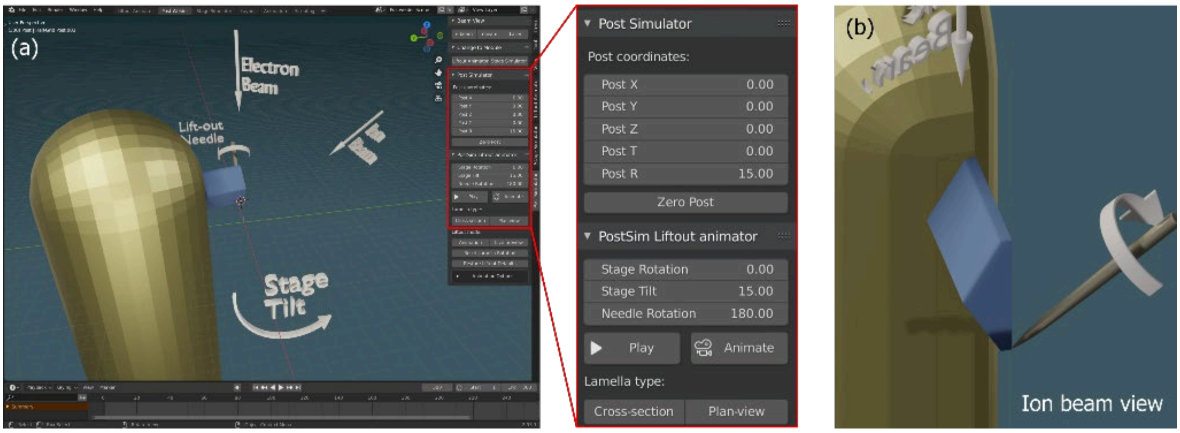

Fig. 2: Virtual FIB user interface: (a) Screenshot of simulated lift-out welding of cross-section lamella to post, demonstrating a potential workflow for cross-section lift-out. Highlight: FIB-relevant controls, reproducing degrees of freedom from FIB. (b) View from the ion beam, demonstrating that the lamella can be welded to the post in this configuration.

Investigating Structure-Property Relationships of Hierarchical Materials at the Microscale

J.J. Schwiedrzik[1*]

[1] Empa Swiss Federal Laboratories for Materials Science and Technology, Laboratory for Mechanics of Materials and Nanostructures, CH-3602 Thun, Switzerland
[*] corresponding author email: jakob.schwiedrzik@empa.ch

Mineralized tissues feature hierarchical architectures that combine stiffness, toughness, and strength with a low specific weight. To better understand the mechanisms leading to this advantageous combination of attributes, their mechanical properties have to be investigated at all length scales.

The development of focused ion beam (FIB) technology has provided a tool for preparing micromechanical specimens with high precision. Novel testing techniques, such as micropillar compression or microtensile testing allow measuring post-yield mechanical properties at the length scale of micrometers. We develop instrumentation, novel specimen geometries, and experimental methods for performing microscale experiments under tightly controlled boundary and environmental conditions as well as sensor concepts allowing to probe materials at high strain rates representative of an impact or fracture.

The development of novel instruments and methods makes a careful characterization and validation necessary to achieve a high level of accuracy and reliability. We tackle this problem using detailed finite element modelling of the experimental setup as well as calibration and validation experiments on well-characterized materials. This allows us to push the boundaries of experimental micromechanics using FIB-prepared specimens while retaining a high level of confidence in our results. Application to osteonal bone has demonstrated a significant scale effect and allowed insights into microscale deformation mechanisms, anisotropy, tension-compression asymmetry, and hydration.

Significant issues in experimental micromechanics of mineralized tissues are the long time needed for specimen preparation, the variation in the underlying microstructure, and the resulting scatter that complicates the data analysis. Therefore, efforts are undertaken to speed up specimen preparation, standardize and automate experimental protocols and data analysis, and combine mechanical experiments with site-matched microstructural analysis using Raman spectroscopy or STEM imaging to identify microscale structure-property relationships, which can be used to develop and validate multiscale models of bone fracture.

Stress-Strain Relation in a Micromachined Quantum Material

H. M. L. Noad[1*], J. Schmalian[2,3], M. Garst[3,4], N. Kikugawa[5], D. A. Sokolov[1], A. P. Mackenzie[1,6] and C. W. Hicks[1,7*]

[1] Max-Planck-Institut für Chemische Physik fester Stoffe, Nöthnitzer Str. 40, 01187 Dresden, Germany
[2] Institut für Theorie der Kondensierten Materie, Karlsruher Institut für Technologie, 76131 Karlsruhe, Germany
[3] Institut für Quantenmaterialien und Technologien, Karlsruher Institut für Technologie, 76131 Karlsruhe, Germany
[4] Institut für Theoretische Festkörperphysik, Karlsruher Institut für Technologie, 76131 Karlsruhe, Germany
[5] National Institute for Materials Science, Tsukuba, Ibaraki 305-0003, Japan
[6] Scottish Universities Physics Alliance, School of Physics and Astronomy, University of St Andrews, St Andrews KY16 9SS, United Kingdom
[7] School of Physics and Astronomy, University of Birmingham, Birmingham B15 2TT, United Kingdom
[*] corresponding author email: noad@cpfs.mpg.de, C.Hicks.1@bham.ac.uk

Stress-strain measurements are well established in materials science and engineering for characterizing the elastic properties of structural materials and are promising for the study of quantum materials. Until now, they have not been applied to quantum materials because the measurement conditions are more difficult: samples are small and often brittle, temperatures are usually cryogenic, and space is limited. Through focused ion beam micromachining of mm-scale samples and using a new cryo-compatible uniaxial pressure cell [1], we have developed a method to do these measurements accurately and reliably under the required conditions. Applying this technique to Sr_2RuO_4, we clearly resolve signatures of a uniaxial-pressure-tuned electronic transition [2] and quantitatively reconstruct the Young's modulus as a function of strain. The combination of FIB micromachining and cryogenic stress-strain measurements will be useful in a wide variety of quantum materials.

[1] M. E. Barber, A. Steppke, A. P. Mackenzie, C. W. Hicks; *Piezoelectric-based uniaxial pressure cell with integrated force and displacement sensors*; Review of Scientific Instruments 90 (**2019**), 023904.

[2] V. Sunko, E. Abarca Morales, I. Marković, M. E. Barber, D. Milosavljević, F. Mazzola, D. A. Sokolov, N. Kikugawa, C. Cacho, P. Dudin, H. Rosner, C. W. Hicks, P. D. C. King, A. P. Mackenzie; *Direct observation of a uniaxial stress-driven Lifshitz transition in Sr_2RuO_4*; npj Quantum Materials 4 (**2019**), 1.

Automated nanofabrication of two-dimensional materials with focused helium ions

V. Deinhart[1,2*], L.-M. Kern[2], J. N. Kirchhof[3], S. Jürgensen[3], D. Iagodkin[3], J. Richter[3], E. Krauss[4], T. Feichtner[5], D. Engel[2], S. Kovalchuk[3], B. Hecht[4], K. Bolotin[3], B. Pfau[2], S. Reich[3] and K. Höflich[1]

[1] Ferdinand-Braun-Institut für Höchstfrequenztechnik, 12489 Berlin, Germany
[2] Max Born Institute for Nonlinear Optics and Short Pulse Spectroscopy, 12489 Berlin, Germany
[3] Freie Universität Berlin, Department of Physics, 14195 Berlin, Germany
[4] Physics Institute, University of Würzburg, 97074 Würzburg, Germany
[5] Dipartimento di Fisica, Politecnico di Milano, 20133 Milano, Italy
[*] corresponding author email: victor.deinhart@fbh-berlin.de

Helium ion microscopes (HIMs) represent ideal platforms for patterning of two-dimensional (2d) material systems. In a HIM, a tightly focused beam of Helium (He) ions is created via a potential applied to an atomically sharp tip consisting of three atoms resulting in virtual spot sizes below 3 Å [1]. Even though, He has a large interaction volume in bulk materials due to its small mass, this is negligible for 2d and very thin bulk materials. Therefore, focused He ion beams are especially suited to process 2d materials with a very high spatial resolution achieving sub 5 nm resolution [2]. This can be used for milling nanostructures or for creation of spatially localized defects. He ion patterning comes with its own technical difficulties which highly depend on the used material system and desired patterning results. For example, to obtain sub 5 nm milling resolution, special scanning strategies may be chosen adjusted to the pattern geometry. In particular for defect creation, it may be mandatory to prevent any unintended ion beam irradiation of the sample (e.g. imaging of the sample). Lastly, depending on the used ion doses, patterning can take long times. Hence, an automation of the process itself is beneficial. To mitigate these difficulties, we created the Python-based toolbox *fib-o-mat* [2], which will be presented herein. This toolbox allows to create optimized ion beam patterns for a variety of applications (e.g. arbitrary shaped and geometry adapted beam paths, automated creation of large area patterns) and allows to circumvent some of the challenges that where introduced above. To highlight the advantages of *fib-o-mat* for He ion patterning, we present the processing of several different material systems demonstrating different features implemented in the package (c.f. Fig. 1). Additionally, we showcase some other *fib-o-mat* based tools streamlining the patterning process of ion sensitive materials.

[1] G. Hlawacek et al.; Helium Ion Microscopy; J. Vac. Sci. Technol. B 32 (**2014**), 020801

[2] V. Deinhart et al.; The patterning toolbox FIB-o-mat: Exploiting the full potential of focused helium ions for nanofabrication; Beilstein J. Nanotechnol. 12 (**2021**), 304.

[3] J. N. Kirchhof et al.; Tunable Graphene Phononic Crystal; Nano Lett. 21 (**2021**), 2174

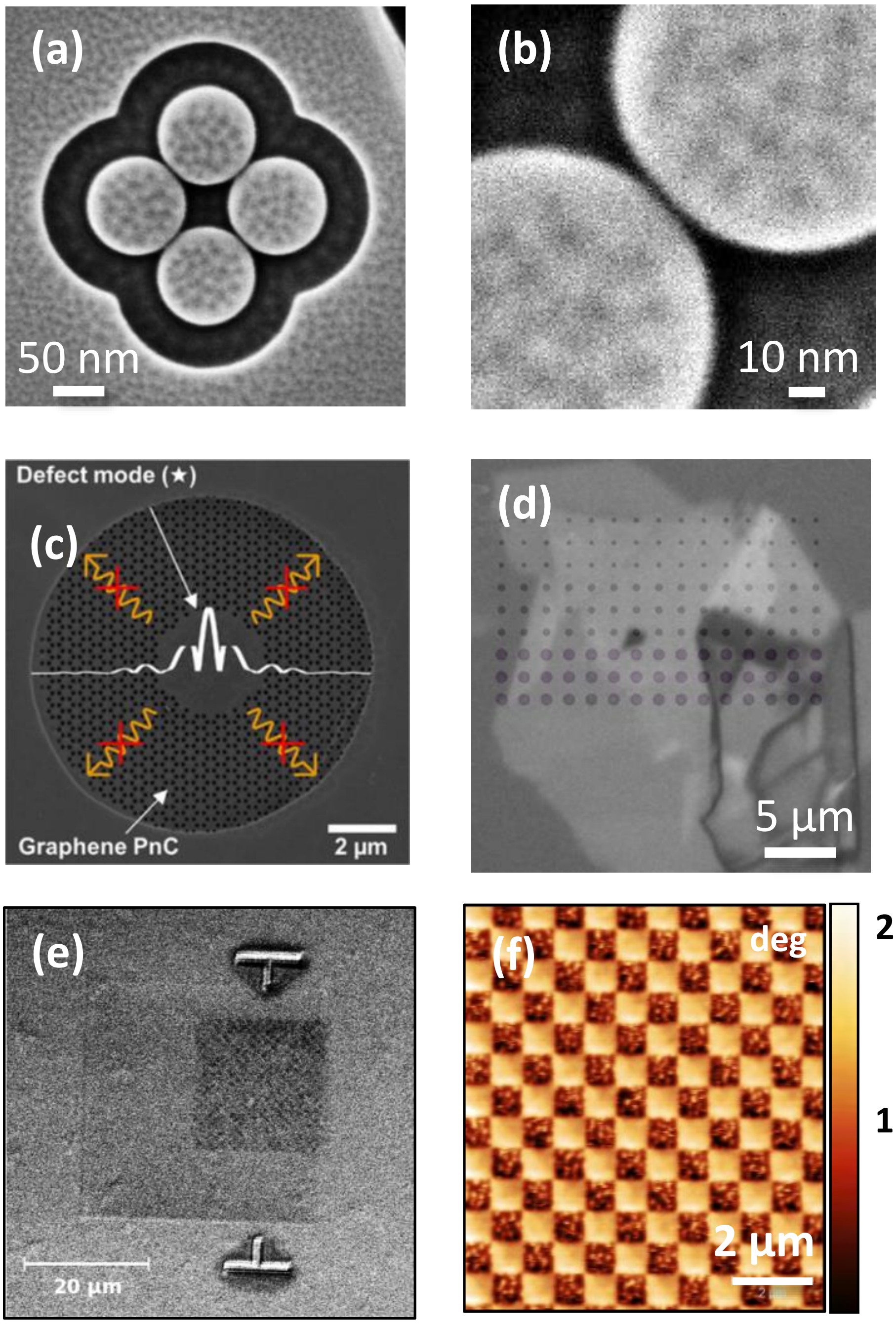

Fig. 1: (a) Secondary electron (SE) HIM image of a gold quadrumer. (b) Zoomed inset of the quadrumer showing the gap between two monomers (3 nm gap width). (c) SE HIM image of He milled graphene phononic crystal [3]. (d) Optical image of MoS_2/hBN flake overlayed with a He-FIB pattern for aligning the He microscope's field of view and the FIB pattern with the flake. (e) and (f) Kerr and magnetic force microscopy images of a checkerboard pattern on a 25 nm thick Co/Pt multilayer deposited on a 150 nm thick SiN membrane. The He-FIB patterns for all samples shown in the figure are generated with *fib-o-mat* [1].

Single Ion Detection with a keV Focussed Ion Beam for Quantum Computing Applications

S. G. Robson[1*], P. Räcke[2,3], A. M. Jakob[1], N. Collins[1], H. R. Firgau[4], V. Schmitt[4], A. Morello[4], D. Spemann[2,3], D. N. Jamieson[1]

[1] Centre for Quantum Computation and Communication Technology, School of Physics, University of Melbourne, Parkville VIC 3010, Australia
[2] Leibniz Institute of Surface Engineering (IOM), Permoserstr. 15, D-04318 Leipzig, Germany
[3] Leibniz Joint Lab "Single Ion Implantation", Permoserstr. 15, D-04318 Leipzig, Germany
[4] Centre for Quantum Computation and Communication Technology, School of Electrical Engineering and Telecommunications, UNSW Sydney, Sydney NSW 2052, Australia
[*] corresponding author email: simonr1@student.unimelb.edu.au

The realisation of a quantum computer based on donors in silicon grows tantalisingly closer [1]. However, deterministic fabrication of large-scale donor-qubit arrays is still yet to be demonstrated. Qubit integration via single ion implantation into an active detection substrate is a promising technique [2], but persistent challenges remain. Namely, device-to-device variations due to intrinsic defects or sample contamination act to lower the ion detection efficiency. A careful ion detector fabrication strategy with feedback at each stage of the development process is therefore critical.

Here, we present a new method to both characterise single ion detectors and perform counted ion implantation, based on the ion beam induced charge (IBIC) principle [3]. Using a modified focussed ion beam setup, equipped with an electron beam ion source [4] and on-chip ultra-low noise detection electronics [5], we measure the detector's IBIC response as a function of beam position. A sub-500 nm spot size together with a range of ion species and kinetic energies from 10—100 keV allow high-resolution maps of the underlying detector electrical landscape to be acquired. These aid in understanding the role interface and bulk defects play in the IBIC response, as well as providing further insight of the physics of ion-solid interactions.

In addition, the setup also functions as a promising method for achieving mask-less directed ion implantation. We demonstrate the ability to perform 2000 12 keV Ar^+ and H_2^+ counted implants into ~50 μm^2 with >99% fidelity, whilst keeping the current of the focussed ion beam constant at <1 ion/s. With upcoming future upgrades to the system, we aim to establish an attractive technique for the rapid mask-free engineering of scalable shallow donor nano-arrays [5].

[1] G. Tosi et al*; Silicon quantum processor with robust long-distance qubit couplings.* Nat. Commun. 8 (**2017**), 450

[2] J. van Donkelaar et al; *Single atom devices by ion implantation.* J. Physics: Condens. Matter 27 (**2015**), 154204

[3] M. B. H. Breese, P. J. C. King, G. W. Grim, & F. Watt; *Microcircuit imaging using an ion-beam-induced charge.* J. Appl. Phys. 72 (**1992**), 2097

[4] P. Räcke et al; *Nanoscale ion implantation using focussed highly charged ions*. New J. Phys. 22 (**2020**), 083028

[5] A. M. Jakob et al; *Deterministic Single Ion Implantation with 99.85% Detection Confidence for Donor Arrays in Silicon.* arXiv preprint arXiv:2009:02892 (**2020**)

FIB Meets EBIS: Development of Deterministic Ion Implantation Based on Image Charge Detection

Paul Räcke[1,2], Jürgen W. Gerlach[1,2], Jan Meijer[2,3] and Daniel Spemann[1,2*]

[1] Leibniz Institute of Surface Engineering (IOM), 04318 Leipzig, Germany
[2] Leibniz Joint-Lab „Single Ion Implantation", 04318 Leipzig, Germany
[3] Felix Bloch Institute for Solid State Physics, Universität Leipzig, 04103 Leipzig, Germany
*corresponding author email: daniel.spemann@iom-leipzig.de

At the Leibniz Joint Lab "Single Ion Implantation" deterministic ion implantation, i.e. the implantation of counted single ions, a key technology for solid state quantum technology applications, is currently under development. We present the experimental setup that is based on a Focused Ion Beam (FIB) system equipped with an Electron Beam Ion Source (EBIS), report on the present state of the development and address some challenges ahead.

Deterministic ion implantation for applications in quantum technologies requires (i) detecting each ion delivered to the sample with confidences close to 100% and (ii) delivering the ion to the implant site with nanoscale precision. For the ion detection, a pre-detection approach has been chosen that is based on the image charge created in an array of electrodes as the individual ion passes through. As the detection signal is proportional to the ion charge [1,2], highly charged ions significantly enhance the detection sensitivity. Hence, a focussed beam of highly charged ions is necessary for our approach to fulfill both conditions above. Therefore, a FIB based ion implanter equipped with an EBIS was set up [3]. The ion optical system was optimised and characterised via secondary electron imaging of a Chessy test sample. The smallest measured ion beam foci are well below 200 nm, showing that nanoscale ion implantation using an EBIS is feasible. Prototypes of image charge detectors were characterized using ion bunches in a test setup. The results indicate that single ion detection can be achieved with this approach when using highly charged ions. In addition, this new ion implanter offers kinetic ion energies from a few to several hundred keV in a comparably compact set-up by exploiting the high charge states of the ions provided by the EBIS.

[1] P. Räcke, D. Spemann, J. W. Gerlach, B. Rauschenbach, J. Meijer; *Detection of small bunches of ions using image charges*; Sci. Rep. 8 (**2018**) 9781.
[2] P. Räcke, R. Staacke, J. W. Gerlach, J. Meijer, D. Spemann; *Image charge detection statistics relevant for deterministic ion implantation*; J. Phys. D: Appl. Phys. 52 (**2019**) 305103
[3] P. Räcke, R. Wunderlich, J. W. Gerlach, J. Meijer, D. Spemann; *Nanoscale ion implantation using focussed highly charged ions*; New J. Phys. 22 (**2020**) 083028

Using a palette of FIB-based processes to create functional nanomaterials and devices

J. M. De Teresa [1,2*]

[1] Instituto de Nanociencia y Materiales de Aragón (INMA), Univerdad de Zaragoza-CSIC, 50009 Zaragoza, Spain
[2] Laboratorio de Microscopías Avanzadas (LMA), Universidad de Zaragoza, 50018 Zaragoza, Spain
[*] corresponding author email: deteresa@unizar.es

Today, nanolithography is a key enabling technology in various research and application fields[1]. Focused Ion Beam (FIB) equipment is a relevant tool in nanolithography to directly pattern materials and build devices. In my talk, I will discuss some applications based on FIB processing, which are summarized in Fig. 1. After introducing different FIB-based approaches and their potential applications, I will focus the attention towards Focused Ion Beam Induced Deposition (FIBID), where the FIB decomposes precursor molecules in order to grow deposits. In our lab, we use FIBID to grow nanomaterials with metallic[2], magnetic[3] or superconducting[4] functionality. Special attention will be drawn to the use of FIBID under cryogenic conditions (Cryo-FIBID), a new technique based on the formation of a condensed layer of the precursor material via substrate cooling. We have applied Cryo-FIBID to grow W-C[5], Pt-C[6] and Co-C[7] deposits, observing a-few-hundred-times enhancement in the growth speed when compared to standard room-temperature FIBID. In addition, Cryo-FIBID entails a minimized ion-induced damage. The perspectives opened by Cryo-FIBID processing will be discussed.

[1] Book *Nanofabrication: nanolithography techniques and their applications*, J. M. De Teresa (editor), Institute of Physics (IOP), Bristol, U. K., 2020.

[2] N. Marcano et al.; Appl. Phys. Lett. 96, 082110 (2010) ; C. I. Hiley et al., Phys. Rev. B 92, 104413 (2015)

[3] C. Sanz, C. Magén , J. M. De Teresa; Nanomaterials 9, 1715 (2019)

[4] R. Córdoba et al., Nano Letters 19 (2019) 8597; P. Orús, R. Córdoba, G. Hlawacek, J. M. De Teresa, Nanotechnology 32 (2021) 085301

[5] R. Córdoba, P. Orús, S. Strohauer, T.E. Torres, J. M. De Teresa; Scientific Reports 9, 14076 (2019); J. M. De Teresa, P. Orús, R. Córdoba, P. Philipp, Micromachines 10, 799 (2019)

[6] A. Salvador-Porroche, S. Sangiao, P. Philipp, P. Cea, J. M De Teresa; Nanomaterials 10, 1906 (2020)

[7] A. Salvador-Porroche et al., submitted manuscript

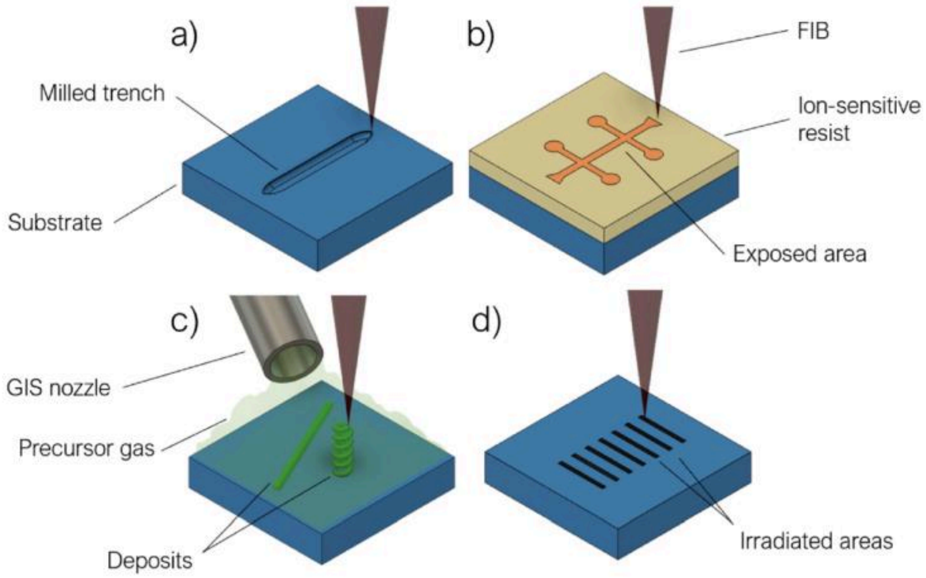

Fig. 1: Some applications of FIB equipment: (a) FIB milling; (b) FIB lithography; (c) FIB induced deposition (FIBID); (d) FIB irradiation. This image has been reproduced from chapter 5 in the book *Nanofabrication: nanolithography techniques and their applications*, J. M. De Teresa (editor), Institute of Physics (IOP), Bristol, U. K., 2020.

Potential FEBID/FIBID precursors of groups 10 and 11 with O- and N-donor ligands

K. Madajska[1], A. Butrymowicz[1], and I. B. Szymańska[1*]

[1] Nicolaus Copernicus University in Toruń, Faculty of Chemistry, Gagarina 7, 87-100 Toruń, Poland
[*] corresponding author email: pola@umk.pl

Volatile metal coordination compounds are used in the vapour deposition methods as the so-called metal source precursors. The choice of the volatile and sensitive to the electron or ion beam precursor is crucial for nanostructure growth success: its chemical nature and dissociation behavior determine the composition of the deposit [1].

In our research, we focus on obtaining new, volatile and electron/ion-sensitive metal complexes group 10 and 11 that can be used in CVD or FEBID/FIBID methods. Therefore, the research aims to study of electrons and ions interactions with potential precursors: new nickel(II), palladium(II), copper(I), copper(II), and silver(I) complexes with perfluorinated or bulky amidinates and carboxylates of the general formula $(NH)_2CR^-$ or RCO_2^-, where R = C_nF_{2n+1}, ^{t}Bu and heteroligand compounds containing carboxylates and amidines with general formula $[M_x(NH_2NHCR)_y(O_2CR')_z]$, where R' = CF_3, C_2F_5 [2]. Investigating the interactions of compounds with electrons/ions will allow for the future mechanism-based design of precursors for FEBID/FIBID. It is advisable to study compounds that contain the same ligand but different metals such, as Ni(II), Pd(II), Cu(I), Cu(II), and Ag(I) in the coordination centre.

Acknowledgments: The studies were supported by Nicolaus Copernicus University in Toruń PDB No. 103.
The A.B. and K.M wish to acknowledge the Nicolaus Copernicus University in Toruń for a grant: „Grants4NCUStudents" – IDUB project: 4101.00000070.

[1] I. Utke, P. Swiderek, K. Höflich, K. Madajska, J. Jurczyk, P. Martinović, I. B. Szymańska; *Coordination and organometallic precursors of group 10 and 11: Focused electron beam induced deposition of metals and insight gained from chemical vapour deposition, atomic layer deposition, and fundamental surface and gas phase studies*; Coord Chem Rev. **(2021)**, 10.1016/j.ccr.2021.213851.

[2] K. Madajska, I. B. Szymańska; *New Volatile Perfluorinated Amidine–Carboxylate Copper(II) Complexes as Promising Precursors in CVD and FEBID Methods;* Materials (**2021**), 14, 3145A.

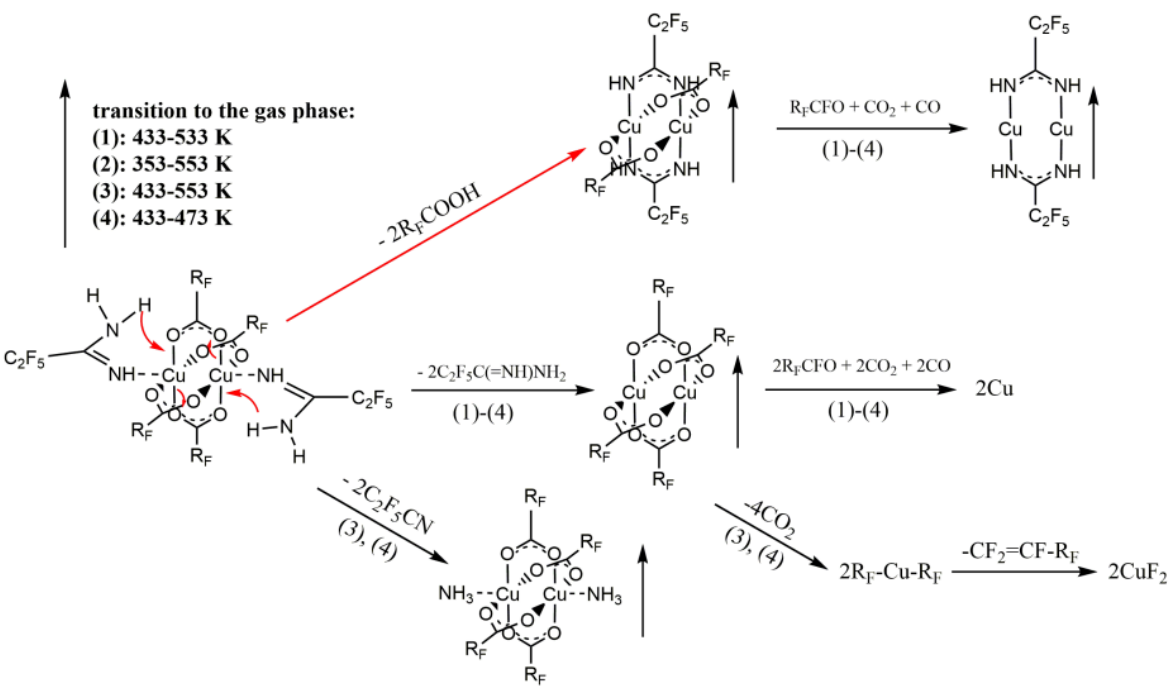

Fig. 1: Proposed mechanism of $[Cu_2(AMDH)_2(\mu\text{-}O_2CR_F)_4]$ thermal decomposition based on VT IR and EI MS studies. [2]

Effect of the stage temperature on sample preparation and surface chemistry in FIBIP and FEBIP

G. Goupil[1*], *J. Silvent*[1] *and A.Delobbe*[1]

[1] Orsay Physics, Fuveau, France

[*] corresponding author email: gregory.goupil@orsayphysics.com

Cryogenic stage impact was studied on samples presenting challenges in their preparation steps for visualization. Even if optimization of time processing using ultra-fast methods to increase the deposition speed of metal using FIBs was already presented by [1], the conditions used required a dedicated cryo system to reach the temperatures tested. In this study, a simpler system based on a Peltier temperature stage controlled was used to check its impact on sample preparation.

Two aspects of the advantage of such stage were checked. The first one is when coupling the chemistry to the stage temperature. Several parameters have to be taken into account to assess a good deposition.

The second one is the milling control. Due to interactions with the as-constitutive element of the FIB such as Ga or due to heat effect induced by scanning the region of interest, some samples can be very tricky to be cut and the final preparation may not be suitable for further analysis or observation. Coupled with the diminution of the processing time described in [1] for the initial steps of deposition, this simple stage addon had shown some interesting results on sensitive samples by avoiding local surface artifacts. For example, for localization purposes, it is generally necessary to realize a first image of the sample using the FIB. For accurate positioning, the best is to realize this image with the same FIB parameter used after and for big cuts, the current use is generally important causing surface modification such as flakes or melted zones. These surface artifacts deteriorate the final quality of the milled walls. It is also known that the milling of some materials are difficult using the Ga FIB due to their low melting temperature (as indium or gallium). Using the cryo Peltier stage to perform cross section or tem lamella preparation allows to avoid the artifacts due to the beam. After optimization, this process can be then transferred to packaged semiconductors covered with polymers, really difficult to be cut properly when milled without surface covering or only with low currents.

As presented on figure 1, the impact of cooling down the temperature of wax during the cross sectioning step show significant results. By decreasing the stage temperature from RT to -20°C the surface modification due to the beam exposition is reduced and the final quality of the wall is improved.

A selection of different samples will be presented to assess the effect of this addon on preparation using FIBs.

[1] Córdoba, R., Orús, P., Strohauer, S. et al. Ultra-fast direct growth of metallic micro- and nano-structures by focused ion beam irradiation. Sci Rep 9, 14076 (2019).

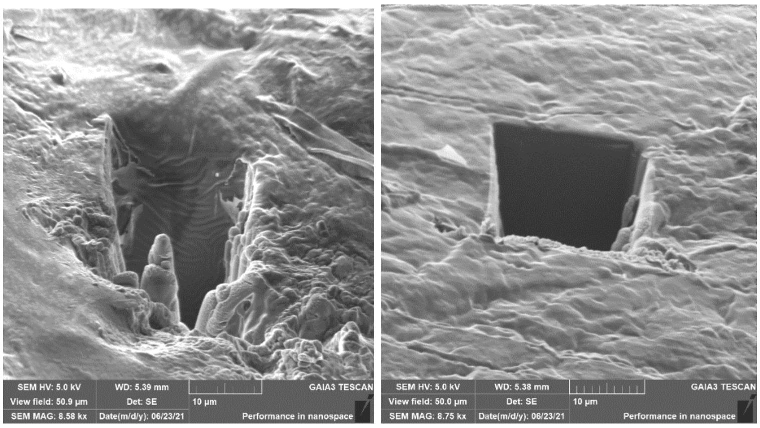

Fig. 1: Image of a cross sections done on wax covering a sample at 10 nA by a Ga FIB. On the left, the stage was at room temperature and on the right it was set at -20°C.

Carboxylate, amidinate and imidoylamidinate ligand in copper complexes and their influence on volatility and electron sensitivity

K. Madajska[1], I. B. Szymańska[1]

[1] Faculty of Chemistry, Nicolaus Copernicus University in Toruń, Gagarina 7, 87-100 Toruń, Poland
[*] corresponding author email: 502533@doktorant.umk.pl

Focused electron beam induced deposition (FEBID) is a direct maskless nanolithography technique based on the local dissociation of adsorbates upon the irradiation with an electron beam. It is used for making 2D and 3D nanostructures.[1][2] The choice of precursor is crucial for the success of FEBID. [3] So far, both fluorinated and branched-chain silver carboxylates have been used in the FEBID process, obtaining structures with a purity of 59-76 at.% Ag. Using copper(II) carboxylate $[Cu_2(O_2CC_2F_5)_4]$, a purity of 23 at.% Cu was achieved.[4] This fact shows that research is still needed to understand the interaction of compounds with electrons to find the appropriate ligands for FEBID precursors.

Here we report on our study of new perfluorinated complexes: heteroleptic copper(II) amidine–carboxylate $[Cu_2(NH_2(NH{=})CC_2F_5)_2(\mu\text{–}O_2CC_2F_5)_4]$ (Figure 1a), copper(I) amidinate $[Cu_2((NH)_2CC_2F_5)_2]$ (Figure 1b), and copper(II) imidoylamidinate $[Cu\{NHC(C_2F_5)NC(CH_3)NH\}_2]$ (Figure 1c). The sublimation experiment carried out for $[Cu_2(NH_2(NH{=})CC_2F_5)_2(\mu\text{–}O_2CC_2F_5)_4]$ showed that it goes into the gas phase at 90^{o}C without decomposition. In turn, $[Cu_2((NH)_2CC_2F_5)_2]$ and $[Cu\{NHC(C_2F_5)NC(CH_3)NH\}_2]$ sublimed at 100^{o}C. Observations using the transmission electron microscope (TEM) revealed that the heteroleptic copper(II) amidine–carboxylate compound is most sensitive to interaction with electrons (Figure 2). Under the influence of the beam, it immediately decomposed with the formation of copper(II) fluoride crystals. This is also evidenced by the spectra of mass spectrometry with electron ionization in the gas phase. For this compound, no molecular ion was detected, opposite to the other two tested compounds.

Acknowledgements: The financing of this work was by Nicolaus Copernicus University in Torun (PDB no.103).

[1] I. Utke and A. Gölzhäuser, Small, Minimally Invasive, Direct: Electrons Induce Local Reactions of Adsorbed Functional Molecules on the Nanoscale, *Angewandte Chemie Int. Ed.* 49 (**2010**), 9328.

[2] D. Belić, M. M. Shawrav, E. Bertagnolli, H. D. Wanzenboeck, Direct writing of gold nanostructures with an electron beam: On the way to pure nanostructures by combining optimized deposition with oxygen-plasma treatment, *Beilnstein J. Nanotechnol*. 8 (**2017**), 2530.

[3] I. Utke, P. Hoffmann, J. Melngailis, Gas-assisted focused electron beam and ion beam processing and fabrication, *J. Vac. Sci. Technol. B* 26 (**2008**), 1197.

[4] I. Utke, P. Swiderek, K. Höflich, K. Madajska, J. Jurczyk, P. Martinović, I. B. Szymańska, Coordination and organometallic precursors of group 10 and 11: Focused electron beam induced deposition of metals and insight gained from chemical vapour deposition, atomic layer deposition, and fundamental surface and gas phase studies Coordination Chemistry Reviews, In press, https://doi.org/10.1016/j.ccr.2021.213851.

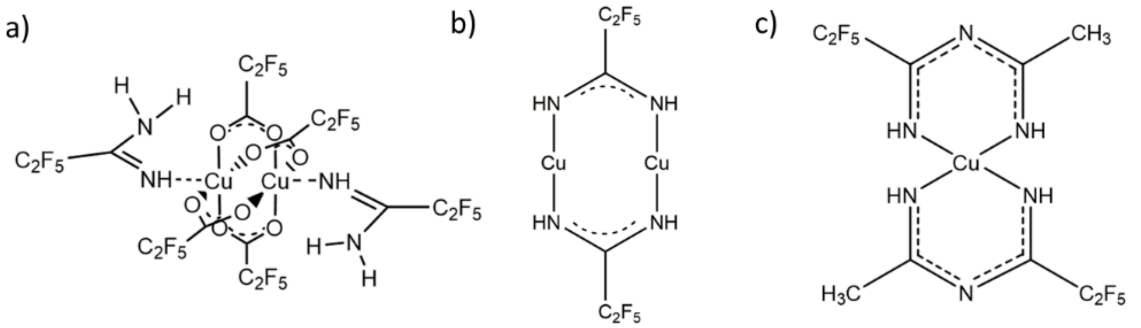

Fig. 1: Structures of the studied complexes: a) $[Cu_2(NH_2(NH{=})CC_2F_5)_2(\mu{-}O_2CC_2F_5)_4]$, b) $[Cu_2((NH)_2CC_2F_5)_2]$, c) $[Cu\{NHC(C_2F_5)NC(CH_3)NH\}_2]$.

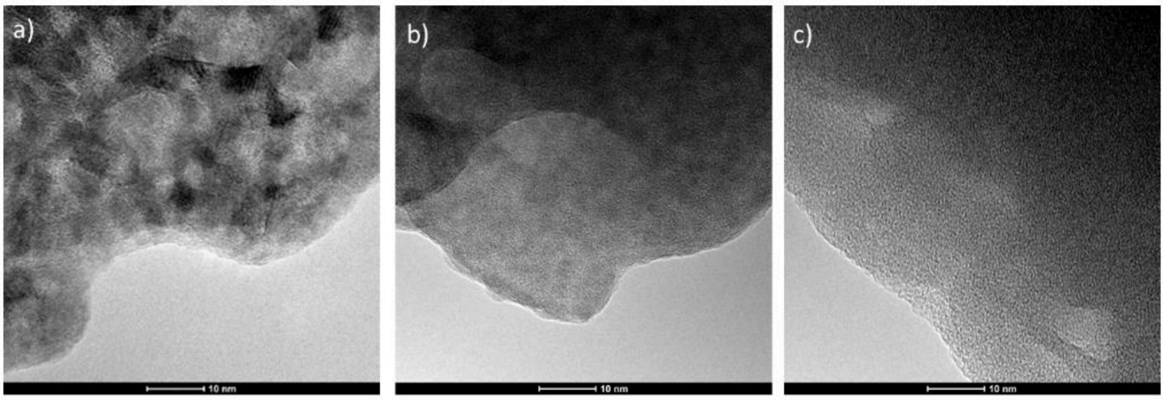

Fig. 2: TEM observations: a) $[Cu_2(NH_2(NH{=})CC_2F_5)_2(\mu{-}O_2CC_2F_5)_4]$, b) $[Cu_2((NH)_2CC_2F_5)_2]$, c) $[Cu\{NHC(C_2F_5)NC(CH_3)NH\}_2]$.

Influence of contaminations on the sputtering of silicon with low energy argon ions

A Grégoire Defoort[1], Alan Bahm[2], Patrick Philipp[1*]

[1] Advanced Instrumentation for Nano-Analytics (AINA), Materials Research and Technology Department, Luxembourg Institute of Science and Technology, L-4422 Belvaux, Luxembourg
[2] Materials & Structure Analysis, Thermo Fisher Scientific, 97124 Hillsboro, Oregon, United States of America
[*] corresponding author email: patrick.phillipp@list.lu

FIB-based techniques play an important role in materials science and technology, ranging from sample preparation and characterisation to nanopatterning and nanofabrication. The shrinking of device sizes goes along with the need for a better control and understanding of the ion beam processes. Residual gas molecules in the instrument chambers, with a typical vacuum in the 10^{-6} to 10^{-7} mbar range, are one parameter that can affect ion beam processes, yet their contribution has not been investigated thoroughly.

In this presentation we are going to show how the adsorption of water molecules on the sample surface affects the sputtering of silicon by low energy argon ions (e.g. 50 – 200 eV). Molecular Dynamics simulations making use of the LAMMPS package [1] and the ReaxFF force field [2,3] have been carried out for the indicated energy range and incidence angles between 0 and 85° with respect to the surface normal to compare sputtering and damage formation for pristine silicon and silicon covered with a water layer. The focus will be on the implantation and irradiation-induced diffusion of argon atoms and the mixing of oxygen and hydrogen atoms in the silicon substrate.

References:

[1] S. Plimpton, *Fast Parallel Algorithms for Short-Range Molecular Dynamics*, Journal of Computational Physics.

[2] D. A. Newsome, D. Sengupta, H. Foroutan, M. F. Russo, and A. C. T. Van Duin, *Oxidation of Silicon Carbide by O 2 and H 2O: A ReaxFF Reactive Molecular Dynamics Study, Part I*, J. Phys. Chem. C **116**, 16111 (2012).

[3] A. D. Kulkarni, D. G. Truhlar, S. Goverapet Srinivasan, A. C. T. Van Duin, P. Norman, and T. E. Schwartzentruber, *Oxygen Interactions with Silica Surfaces: Coupled Cluster and Density Functional Investigation and the Development of a New ReaxFF Potential*, J. Phys. Chem. C **117**, 258 (2013).

Correlative Probe and Electron Microscopy technology using AFM in SEM

Veronika Hegrova[1*], Radek Dao[1], Michal Pavera[1], Jan Neuman[1]

[1]NenoVision s.r.o., Purkynova 649/127, 61200, Brno, Czech Republic
[*]Corresponding author: conference@nenovision.com

Scanning electron microscopy (SEM) and atomic force microscopy (AFM) are two of the most used, complementary techniques for surface analysis at the nanoscale. Thus, when a compact AFM is integrated into SEM, it brings novel possibilities for true correlative microscopy and advanced multi-modal sample characterization. It is beneficial in various fields, such as Material science, Nanotechnology, Semiconductors, or Life science.

Correlative Probe and Electron Microscopy (CPEM) represents a hardware correlative technology, enabling simultaneous acquisition of SEM and AFM data and seamless correlation. The strength lies in combining AFM modes (3D topography, electrical, mechanical, and magnetic measurements) with SEM capabilities (fast imaging, chemical analysis, surface modification). This technique can be applied using LiteScope 2.0, produced by NenoVision, ensuring the data are collected in the same coordinate system and with identical pixel size resulting in 3D complex multi-channel sample characterization.

The advantages mentioned above are demonstrated on magnetic nanopatterning of metastable iron-nickel thin film in Fig. 1. The sample is fabricated using focused ion beam (FIB) irradiation under different angles. AFM in FIB/SEM promptly characterizes the transformed surface topography, magnetic properties, and material contrast by detecting secondary and back-scattered electrons. Since the thin film is prone to immediate oxidation, the in-situ approach is crucial to prevent the surface from air exposure and simultaneously detect different techniques under the same conditions.

As we can see, the AFM-in-SEM strategy benefits from the complementarity of both techniques alongside significant savings both in time and resources. In-situ analysis and CPEM technology open doors to new possibilities for advanced data correlation and measurements in many areas of both research and industry.

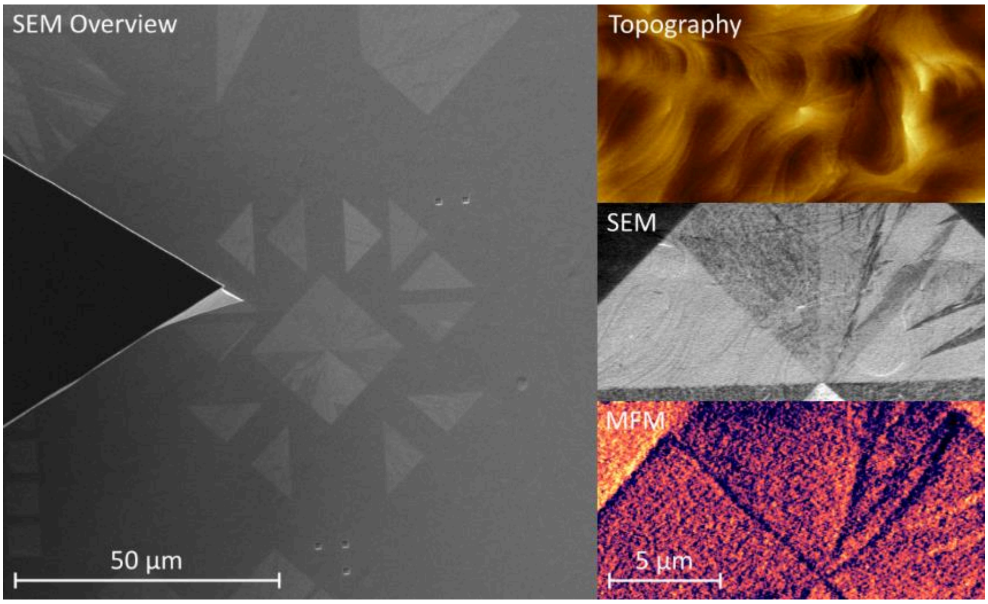

Fig. 1: Characterization of metastable iron-nickel thin film. SEM overview shows tip of the AFM probe above the FIB milled structure, on the right side are simultaneously acquired channels (AFM topography, SEM and magnetic signal).

The npSCOPE: a New Multimodal Instrument for the In-Situ Correlative Analysis of Nanoparticles

Olivier De Castro[1*], Antje Biesemeier[1], Eduardo Serralta[4], Olivier Bouton[2], Rachid Barrahma[2], Quang Hung Hoang[1], Sebastien Cambier[3], Tatjana Taubitz[1], Nico Klingner[4], Gregor Hlawacek[4], Serge Duarte Pinto[5], Peter Gnauck[6], Falk Lucas[7], Cecilia Bebeacua[7] and Tom Wirtz[1]

[1]Advanced Instrumentation for Nano-Analytics (AINA), MRT Department, Luxembourg Institute of Science and Technology, 41 rue du Brill, L-4422 Belvaux, Luxembourg;
[2]Prototyping, MRT Department, Luxembourg Institute of Science and Technology, 41 rue du Brill, L-4422 Belvaux, Luxembourg;
[3]Environmental Health, ERIN Department, Luxembourg Institute of Science and Technology, 41 rue du Brill, L-4422 Belvaux, Luxembourg;
[4]Institute of Ion Beam Physics and Materials Research, Helmholtz-Zentrum Dresden-Rossendorf e.V., Bautzner Landstr. 400, 01328 Dresden, Germany;
[5]Photonis Netherlands B.V., Dwazziewegen 2, 9301 ZR Roden, The Netherlands;
[6]Carl Zeiss Microscopy GmbH, ZEISS Group, Rudolf-Eber-Straße 2, D-73447 Oberkochen, Germany;
[7]ETH Zurich, ScopeM, Otto-Stern-Weg 3, 8093 Zurich, Switzerland.
[*] corresponding author email: olivier.decastro@list.lu

Nano-sized materials or objects are nowadays the subject of interest in various scientific fields, ranging from features in solid material based devices (e.g. solar cell materials' grain boundaries [1]), to interactions of nanomaterials with biological systems (e.g. processes for drug delivery to the human organism [2]). A common demand across these different scientific fields is to analyze structural, morphological, and chemical composition at nanoscale. The focused ion beam (FIB) technique, based on the high brightness gas field ion source (GFIS) providing He and Ne primary ion beams, has been proven to be a promising tool for imaging and chemical analysis at nanoscale [3][4]. Over the last years, we have been developing a new instrument, the npSCOPE, based on the use of the GFIS as key enabling element in combination with several analytical techniques for correlative investigations at the nanoscale, including: I) secondary electron (SE) microscopy, providing high lateral resolution (< 1 nm); II) scanning transmission ion microscopy (STIM) [5], providing 3D volume information; III) secondary ion mass spectrometry (SIMS) [4], providing highly spatially resolved chemical information with excellent sensitivity. The instrument furthermore incorporates cryo-capabilities to analyze samples at low temperatures (< -140 °C). This enables investigations of biological samples close to their natural states under cryo-conditions. Moreover, this is also extremely useful for studying beam sensitive samples such as polymer, battery or OLED materials.
Here, we will present the instrument, its performance and a number of applications results related to nanoparticle research, i.e. nanoparticles contained within biological model systems.

[1] P. Schöppe, S. Schönherr, R., Wuerz, W. Wisniewski, G. Martínez-Criado, M. Ritzer, K. Ritter, C. Ronning, C. S. Schnohr; *Rubidium Segregation at Random Grain Boundaries in Cu(In,Ga)Se2 Absorbers*. Nano Energy 42 **(2017)**, p. 307.

[2] N. Tureli, A. E. Tureli, M. Schneider; *Inhalable Antibiotic Nanoformulations for the Treatment of Pseudomonas Aeruginosa Infection in Cystic Fibrosis – A Review*. Drug Deliv. Lett. 4 (3) **(2014)**, p. 193.

[3] J. Morgan, J. Notte, R. Hill, B. Ward; *An Introduction to the Helium Ion Microscope*. Micros. Today 14 (4) **(2006)**, p. 24.

[4] T. Wirtz, O. De Castro, J. N. Audinot, P. Philipp; *Imaging and Analytics on the Helium Ion Microscope*. Annu. Rev. Anal. Chem. 12 **(2019)**, p. 523.

[5] E. Serralta, N. Klingner, O. De Castro, M. Mousley, S. Eswara, S. Duarte Pinto, T. Wirtz, G. Hlawacek; *Scanning Transmission Imaging in the Helium Ion Microscope Using a Microchannel Plate with a Delay Line Detector*. Beilstein J. Nanotechnol. 11 **(2020)**, p. 1854.

Contrast Modes in Transmission Experiments using Broad and Focussed keV Ion Beams

G. Hlawacek[1], R. Holeňák[2], N. Klingner[1], S. Lohmann[1,2*], D. Primetzhofer[2] and E. Serralta[1,3]

[1] Helmholtz-Zentrum Dresden-Rossendorf, Institute of Ion Beam Physics and Materials Research, Dresden, Germany
[2] Uppsala University, Department of Physics and Astronomy, Uppsala, Sweden
[3] Technische Universität Dresden, Germany
[*] corresponding author email: s.lohmann@hzdr.de

The helium ion microscope (HIM) is an instrument for high-resolution imaging, composition analysis, and materials modification at the nanometre scale [1]. Transmission experiments could further improve the analytical capabilities of this technique, and multiple contrast modes are possible. We have explored these possibilities at keV energies using a HIM in a scanning transmission approach and a broad beam in a time-of-flight medium-energy ion scattering (ToF-MEIS) set-up.
In the ToF-MEIS system, we simultaneously detect flight times and angular distributions of particles exiting thin self-supporting foil targets as shown in Fig. 1. We have found a strong trajectory-dependence of the specific energy loss for all ions heavier than protons that can be attributed to charge-exchange events in close collisions [3,4]. Thus, channelling and blocking of transmitted ions does not only allow for mapping of intensity but also of different energy loss moments [2].

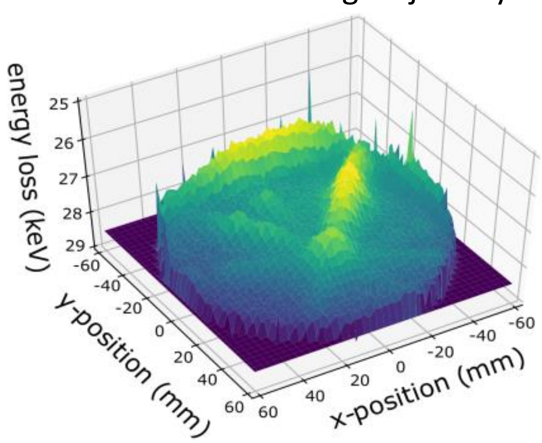

Figure 1: 3D surface map of the mean energy loss of 50 keV He transmitted through a 200 nm single-crystalline silicon foil [2].

A position- and time-sensitive detector comprising of an MCP and a delay line was developed and installed in two HIM prototype instruments [5]. The system allows for analysis of selected scattering directions, and contrasts due to orientation of thallium chloride nanocrystals, channelling in single-crystalline silicon and material contrast for layered films have been demonstrated.

[1] G. Hlawacek et al. J. Vac. Sci. Technol. B 32 (**2014**), 20801.
[2] R. Holeňák et al. Ultramicroscopy 217 (**2020**), 113051.
[3] S. Lohmann and D. Primetzhofer, Phys. Rev. Lett. 124 (**2020**), 096601.
[4] S. Lohmann et al., Phys. Rev. A 102 (**2020**), 062803.
[5] E. Serralta et al. Beilstein J. Nanotechnol. 11 (**2020**), 1854.

New Protocols for the Fabrication of TEM and APT Specimens with LaserFIBs

F. Pérez-Willard[1*] and T. Volkenandt[1]

[1] Carl Zeiss Microscopy GmbH, D-73447 Oberkochen, Germany
[*] corresponding author email: fabian.perez-willard@zeiss.com

Transmission electron microscopy (TEM) and atom probe tomography (APT) are essential techniques for the analysis of today's and future materials and devices.

Today, sample preparation for TEM and APT is often done by FIB-SEM, especially if it needs to be site-specific. Highly precise FIB machining, often at low FIB energies, is required to form a 20-100 nm thick lamella containing the region of interest (ROI) for TEM, or a sharp needle with an end radius of around 50 nm for APT. In both cases, the lamella or the needle-shaped specimen need to be isolated from the rest of the sample. This is achieved either by a FIB lift-out method or in the APT case, alternatively by clearing a large area of hundreds of microns in diameter around the tip ("moat" preparation).

In this talk, we will present new protocols for the fabrication of TEM and APT specimens that combine precise FIB shaping and massive laser material removal in so-called LaserFIBs. This new class of instruments enables the preparation of ROIs deeply buried below the sample surface (Fig. 1) [1] or highest-throughput APT sample preparation [2]. The presentation will also address questions like: Is there any sample or instrument damage created by the laser? Which type of materials can be machined? What is the biggest TEM sample I can prepare? When does it make sense to prepare such large lamellas? And, how site-specific is the laser preparation?

[1] F. Pérez-Willard, T. Volkenandt, *Exploring Laser-Assisted TEM Sample Preparation with ZEISS Crossbeam laser*, ZEISS Application Note (2020), available online: https://zeiss.widen.net/s/vtscqtwvjt/en_wp_crossbeam-laser-for-tem-prep

[2] T. Volkenandt, S. Hiller, C. Stebler, F. Pérez-Willard, *Targeted Sample Preparation with ZEISS Crossbeam laser*, ZEISS Technical Note (2021), available online: https://zeiss.widen.net/s/d87jfkslmc/en_wp_crossbeam_laser_registration

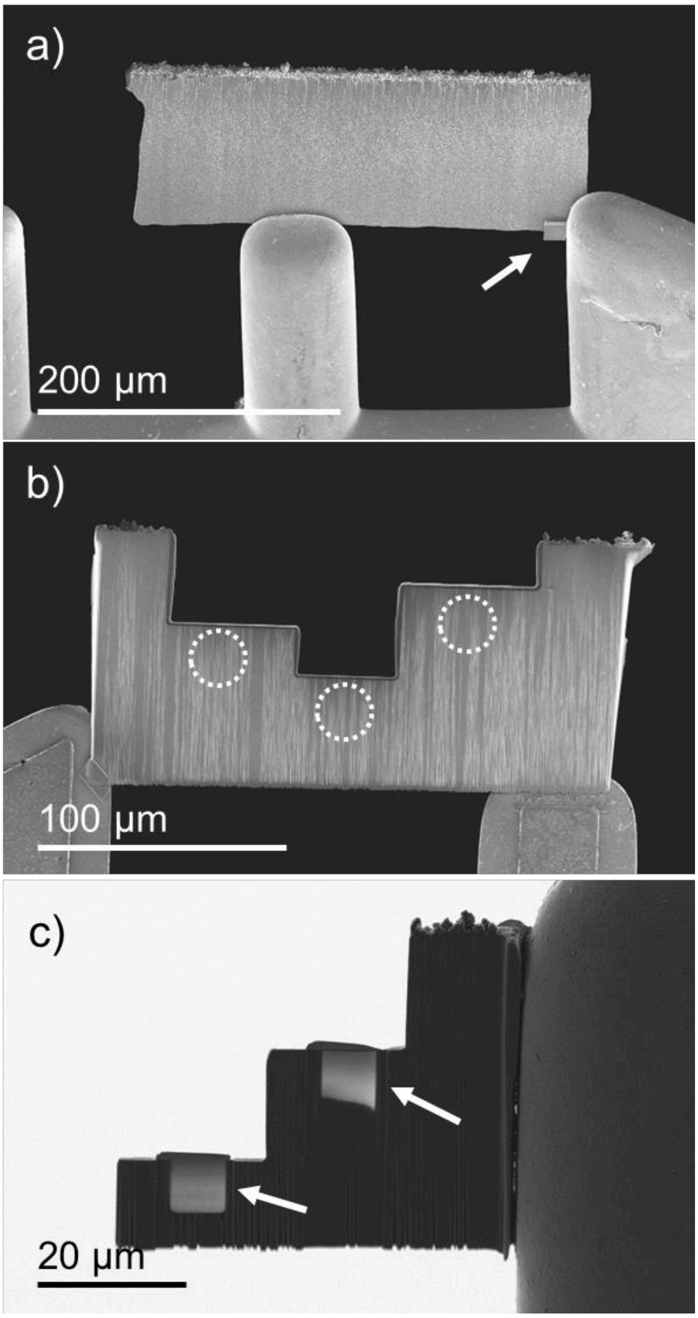

Fig. 1: Three large laser-processed lamellas. The laser preparation was followed by standard in-situ lift out, FIB shaping to access deeply buried ROIs (b), and thinning (c). (a) The lamella is 300 × 140 µm² in size. For comparison, the arrow points towards a standard FIB lamella (15 x 14 µm²). (b) This 220 × 104 µm² lamella was shaped by FIB to make ROIs 45, 65, and 25 µm below the surface (dotted circles) accessible. (c) Third lamella after final thinning of two ROIs (white arrows).

Xe Plasma Focused Ion Beam Milling for Fabricating Soft X-ray Transparent Sample Windows

S. Mayr[1,2]*, S. Finizio[1], J. Reuteler[3], S. Stutz[1], C. Dubs[4], M. Weigand[5], A. Hrabec[1,2,6], J. Raabe[1] and S. Wintz[1,7]

[1] Paul Scherrer Institut, 5232 Villigen PSI, Switzerland
[2] Laboratory for Mesoscopic Systems, Department of Materials, ETH Zurich, 8093 Zurich, Switzerland
[3] Scientific Center for Optical and Electron Microscopy, ETH Zurich, 8093 Zurich, Switzerland
[4] INNOVENT e.V. Technologieentwicklung Jena, 07745 Jena, Germany
[5] Helmholtz-Zentrum Berlin, 14109 Berlin, Germany
[6] Laboratory for Magnetism and Interface Physics, Department of Materials, ETH Zurich, 8093 Zurich, Switzerland
[7] Max Planck Institute for Intelligent Systems, 70569 Stuttgart, Germany
[*] corresponding author email: sina.mayr@psi.ch

Soft x-rays allow for an element-specific analysis of materials, providing information on both their magnetic and chemical states - and this even with high spatial resolutions when x-ray microscopy is applied. Especially photon-in photon-out measurements in x-ray transmission geometry give access to the full sample structure, while also supporting the application of magnetic fields and electrical excitations to the sample [1]. However, the low absorption lengths for soft x-rays exclude the study of bulk samples or of thin films grown on bulk substrates, limiting the investigation of e.g. epitaxial materials.
Here, we present an approach where we employ xenon (Xe) plasma focused ion beam (PFIB) milling to obtain soft x-ray transparent windows out of bulk samples [2]. The use of a fast Xe PFIB simplifies such window fabrication when compared to a conventional Ga FIB (see e.g. [3]). Our method allows for the milling of thin windows (several 100 nm thick) with areas of the order of 100 µm × 100 µm into bulk substrates (Fig. 1). In addition, we present a way to empirically determine the transmissivity of such windows during the fabrication process by correlating their transparencies for electrons (Fig. 2a) to that of soft x-rays (Fig. 2b). Our thinning approach can be applied to a variety of different sample systems and substrates that are otherwise not accessible for soft x-ray transmission measurements.

[1] P. Willmott; *Introduction to Synchrotron Radiation: Techniques and Applications;* Wiley (**2019**).
[2] S. Mayr et al.; *Xenon Plasma Focused Ion Beam Milling for Obtaining Soft X-ray Transparent Samples*; Crystals 11 (**2021**), 546.
[3] J. Förster et al.; *Direct observation of coherent magnons with suboptical wavelengths in a single-crystalline ferrimagnetic insulator;* Physical Review B 100 (**2019**), 214416.

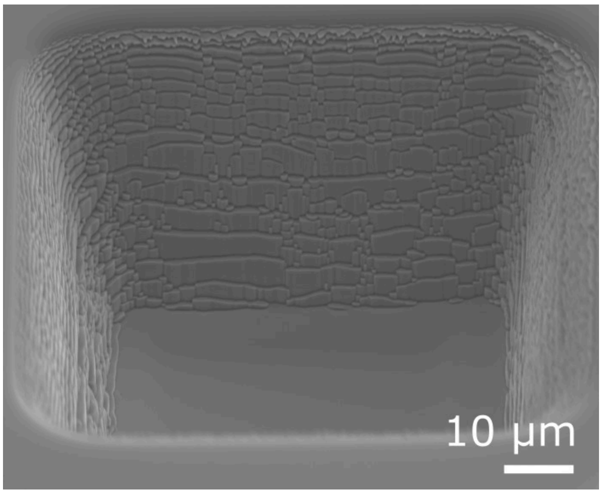

Fig. 1: SEM image of a window milled with a Xe PFIB into a $SrTiO_3$ (STO) substrate recorded at a tilt of 55° with respect to the surface normal.

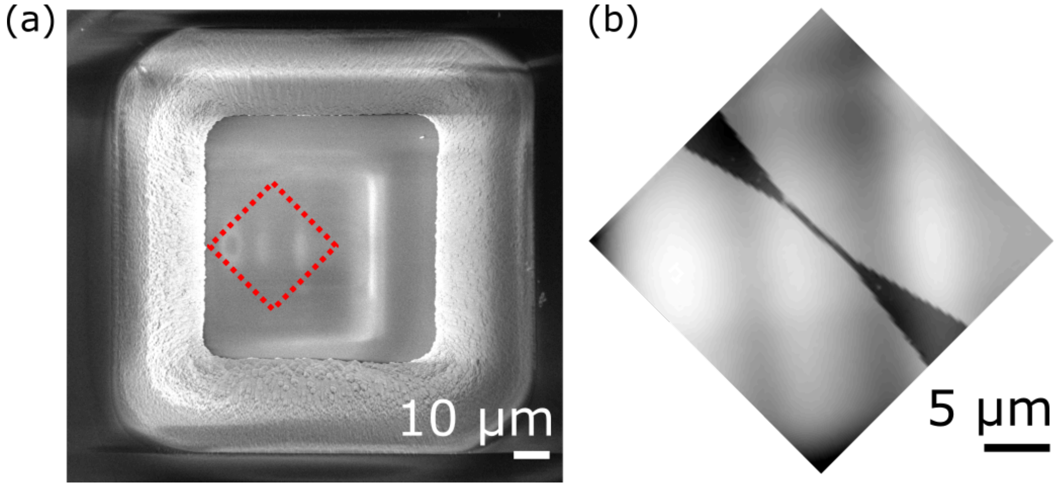

Fig. 2: Comparison of transmissivity between electrons and soft X-rays of a Ga-doped yttrium iron garnet (YIG) film grown on gadolinium gallium garnet (GGG). (**a**) Scanning electron micrograph of the full window. (**b**) Logarithmic x-ray transmittance of the detail region indicated by the dotted square taken by Scanning Transmission X-Ray Microscopy.

Using of light and heavy ion beams in modern FIBs

P. Mazarov[1*], F. Meyer[1], T. Richter[1], W. Pilz[1,2], L. Bischoff[2], N. Klingner[2], G. Hlawacek[2]

[1] Raith GmbH, Konrad Adenauer Allee 8 44263 Dortmund, Germany
[2] Helmholtz-Zentrum Dresden-Rossendorf, Institute of Ion Beam Physics and Materials Research, Bautzner Landstraße 400, 01328 Dresden, Germany

[*] Corresponding author email: Paul.Mazarov@raith.de

The incident ion defines the interaction mechanism with the sample surface caused by the energy deposition and thus has significant consequences on resulting nanostructures [1]. Therefore, we have extended the FIB technology towards the stable delivery of multiple ion species by liquid metal alloy ion sources (LMAIS) [2]. These LMAIS provides single and multiple charged ion species of different masses. As an example we introduce the GaBiLi LMAIS [3]. Such "universal" source enables high resolution imaging with light Li ions and sample modification with Ga or heavy polyatomic Bi clusters, all coming from the same ion source. Light ions are of increasing interest due to the available high resolution in the nanometer range and their special chemical and physical behavior in the substrate. We compare helium and neon ion beams from a helium ion microscope with beams such as lithium, boron, and silicon, obtained from a mass-separated FIB using a LMAIS with respect to the imaging and milling resolution, as well as the current stability [4]. The bombardment of solids by poly-atomic (cluster) ions leads to nonlinear collision cascades in near-surface regions. In comparison with linear cascades by mono-atomic ions, much higher energy deposition occurs up to local surface melting [5]. Here, we also report the study on the sputter yield of Si under the bombardment by atomic Bi^+ and cluster Bi_n^+ (n = 2-4) ions with the same specific energy related to one incidence single atom [6].

[1] P. Mazarov, V. Dudnikov, A. Tolstoguzov, *Electrohydrodynamic emitters of ion beams*, Phys. Usp. 63 (2020) 1219.

[2] L. Bischoff, P. Mazarov, L. Bruchhaus, and J. Gierak, *Liquid Metal Alloy Ion Sources – An Alternative for Focused Ion Beam Technology*, Appl. Phys. Rev. 3 (2016) 021101.

[3] W. Pilz, N. Klingner, L. Bischoff, P. Mazarov, and S. Bauerdick, *Lithium ion beams from liquid metal alloy ion sources*, JVSTB 37(2), Mar/Apr (2019) 021802.

[4] N. Klingner, G. Hlawacek, P. Mazarov, W. Pilz, F. Meyer, L. Bischoff, *Imaging and Milling Resolution of Light Ion Beams from HIM and Liquid Metal Alloy Ion Source driven FIBs,* Beilstein J. Nanotechnol. 11 (2020) 1742.

[5] L. Bischoff, K.-H. Heinig, B. Schmidt, S. Facsko, and W. Pilz, *Self-organization of Ge nanopattern under erosion with heavy Bi monomer and cluster ions,* Nucl. Instr. Meth. B 272 (2012) 198.

[6] A. Tolstogouzov, P. Mazarov, A. Ieshkin, S.Belykh, N. Korobeishchikov, V. Pelenovich, D.J. Fu, *Sputtering of silicon by atomic and cluster bismuth ions: An influence of projectile nuclearity and specific kinetic energy on the sputter yield,* Vacuum 188 (2021) 110188.

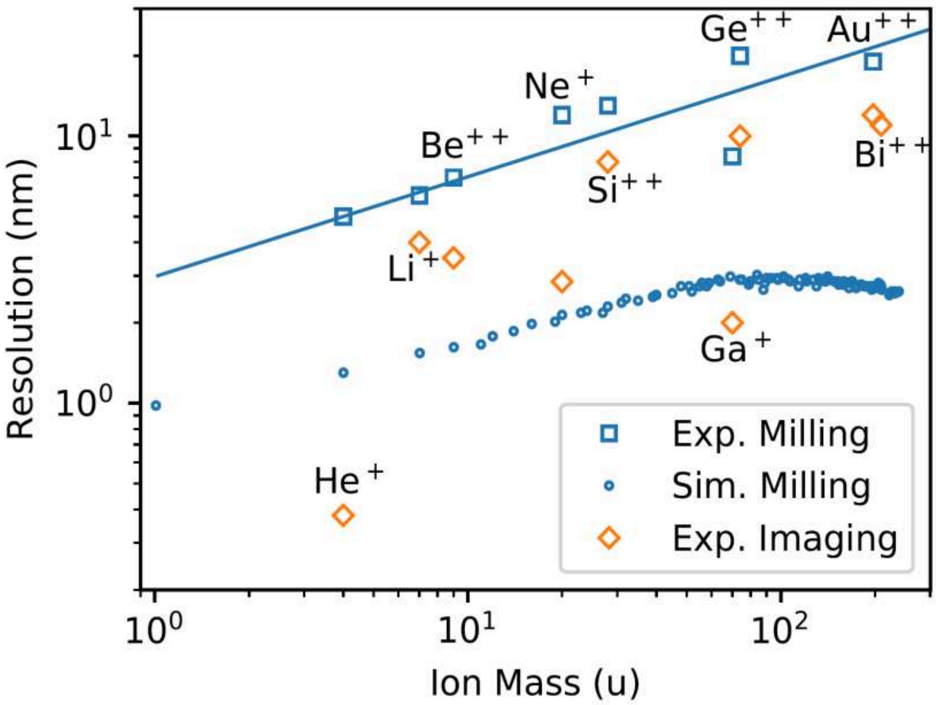

Fig. 1: Summary of the imaging resolution (80/20), experimentally achieved trench width, and simulated minimum milling width (FWHM) for FIBs working with different ion species and technologies depending on the ion mass.

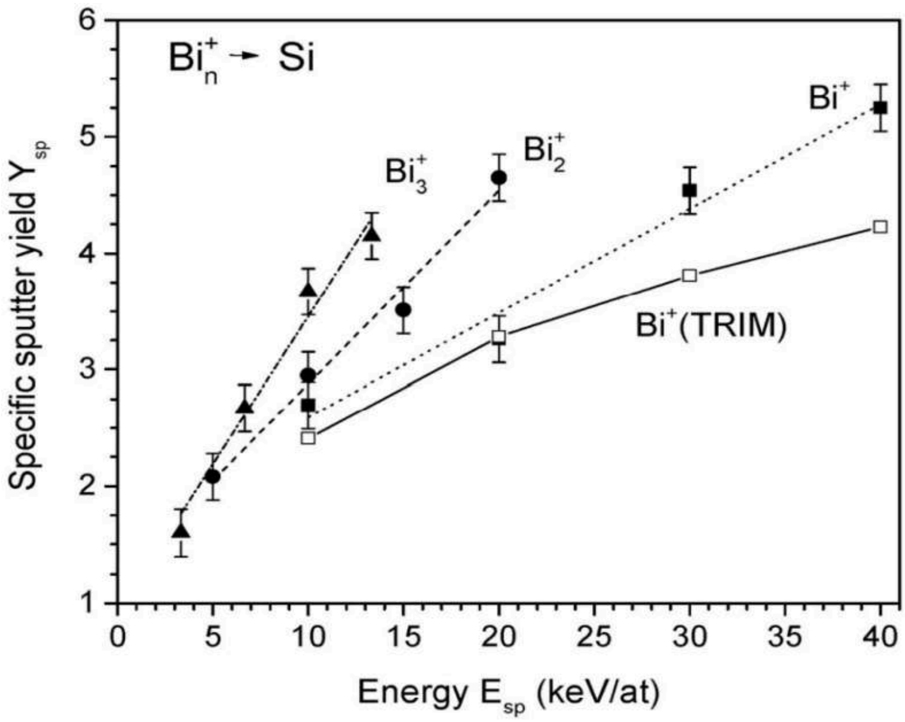

Fig. 2: Specific sputter yield of Si versus the specific energy of Bi_n^+ (n = 1–3) projectiles.

Fabrication of micro and nanostructures from crystals of topological insulators

K. Maćkosz[1, 2*], A. Szkudlarek[1], M. Gajewska[1], M. Sikora[1]

[1] AGH University of Science and Technology, Academic Centre for Materials and Nanotechnology, A. Mickiewicz Av. 30, 30-059 Kraków, Poland
[2] AGH University of Science and Technology, Faculty of Physics and Applied Computer Science, A. Mickiewicz Av. 30, 30-059 Kraków, Poland
[*] corresponding author email: mackosz@agh.edu.pl

Bismuth chalcogenides belong to the group of materials that can make future electronic devices far more powerful than today. These layered materials, especially Bi_2Te_3, exhibit excellent thermoelectric properties associated with good electronic and low thermal conductivity. Single crystals of selected bismuth chalcogenides reveal also the unique properties characteristic for Topological Insulators (TI), namely extraordinary robust electronic transport at the surface with a layer thickness of few nanometers and mostly insulating interior. Similar properties can be found in some semiconductors, but in TI the flow of electrons on the surface is not affected by impurities and dopants according to the theory, which makes TI particularly promising for use in magnetoelectrics and spintronics. However nanostructurization of those materials is still a challenging process, as the quality of the structure surface will affect the material behavior. Few approaches based on ion milling have taken up to now.

Recently a new Focused Ion Beam (FIB) solution that combines high throughput plasma focused ion beam milling with ultra-high resolution Scanning Electron Microscope (SEM) optics has been presented. Xe plasma FIB revile less implantation of xenon in comparison to gallium due to its chemical inertness, and due to low conductivity the samples electrical behavior remains unchanged. In a comparison to standard Ga^+ milling, Xe^+ plasma FIB, which is a new tool for nanostructure fabrication, could have a crucial advantage for materials with active surface states such as bismuth chalcogenides.

Our research is centered on systematic studies of defects induced in chalcogenides (Bi_2Se_3 and Bi_2Te_3) by the nanostructurization process with focused ion beams using Ga^+ and Xe^+ ions. The single crystals of those materials, synthesized using Bridgman method, were processed using Ga^+ and Xe^+ FIB. The fundamental goal of the study is to optimize the parameters of lithography processes (beam current, kinetic energy of ions, time of exposure, etc.) in order to keep the minimal desired size and shape of the nanostructures and preserve topological insulators properties by minimizing the damage in the surface states induced by the impinging ions.

Investigation of Boron Liquid Metal Alloy Ion Sources for Focused Ion Beam Applications

L. Bischoff[1*], N. Klingner[1], P. Mazarov[2], W. Pilz[1,2], and F. Meyer[2]

[1] Helmholtz-Zentrum Dresden-Rossendorf, Institute of Ion Beam Physics and Materials Research, Bautzner Landstrasse 400, 01328 Dresden, Germany
[2] Raith GmbH, Konrad-Adenauer-Allee 8, 44263 Dortmund, Germany
* corresponding author email : l.bischoff@hzdr.de

Focused Ion Beam (FIB) processing is established as a well-suited and promising technique in R&D in nearly all fields of nanotechnology for patterning and prototyping on the µm-scale and below. Liquid Metal Alloy Ion Sources (LMAIS) represent an alternative to expand the FIB application fields beside all other source concepts [1]. Due to the interest on light elements, especially boron, various alloys were investigated and characterized, see Tab 1. In this contribution we will describe $Co_{31}Nd_{64}B_5$ as the most promising alloy in more detail. The mass spectrum of such a source, obtained in a VELION FIB-SEM system (Raith GmbH) [2] is shown in Fig. 1. The source operation life time was longer than 600 µAh and a first imaging characterization showed a lateral resolution of (30 ± 5) nm so far, see Fig. 2. This LMAIS is suited for several mass-filtered FIB applications like implantation, high rate sputtering, surface patterning or ion lithography [3]. The switching between the certain ion species. B – very light, suitable for ion lithography or writing p-type doping. Co – medium mass for applications in the field of nano-magnetics or $CoSi_2$ for ion beam synthesis of conductive nano-structures on Si. Finally Nd as double charged heavy ion for ion sputtering. The change between ion species can be done in seconds and leads to remarkable expansion of the application spectrum of FIB technology.

[1] L. Bischoff, P. Mazarov, L. Bruchhaus, and J. Gierak, *Liquid Metal Alloy Ion Sources - An Alternative for Focused Ion Beam Technology*; Appl. Phys. Rev. 3 (**2016**) 021101.

[2] L. Bischoff, N. Klingner, P. Mazarov, W. Pilz, and F. Meyer, *Boron Liquid Metal Alloy Ion Sources for special FIB applications,* JVST B 38 (**2020**) 042801.

[3] L. Bruchhaus, P. Mazarov, L. Bischoff, J. Gierak, A. D. Wieck, and H. Hövel*, Comparison of Technologies for Nano Device Prototyping with a Special Focus on Ion Beams – A Review,*
Appl. Phys. Rev. 4 (**2017**), 011302.

Source material	T_{melt} (°C)	Emitter	Content of Boron
$Au_{77}Si_{18}B_5$	370	Ta, W	$^{11}B^+/Au^+$ < 10^{-5}
$Au_{70}Ge_{25}B_5$	370	Ta, W	$^{11}B^+/Au^+$ $6x10^{-4}$
$Au_{68}Ge_{22}Ni_5B_5$	370	Re	$^{11}B^+/Au^+$ $4x10^{-3}$
$Co_{31}Nd_{64}B_5$	650	Ta, Re, W	$^{11}B^+/Co^+$ 0.1
$Ni_{40}B_{60}$	1032	W	No B emission

Tab. 1: Source materials, melting temperature, emitter tip material and content of B in the beam.

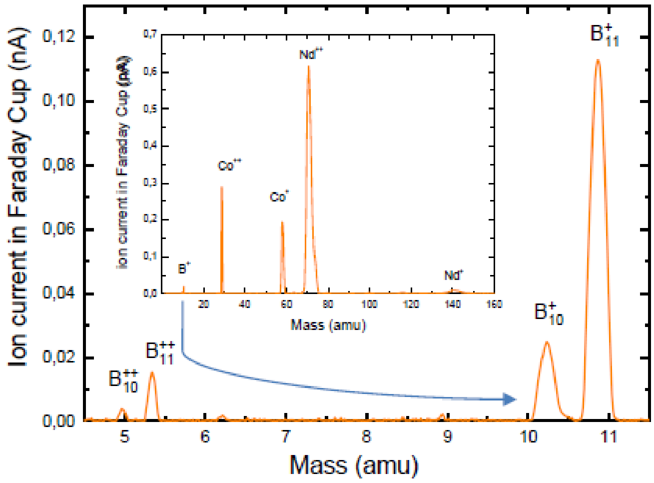

Fig.1: Mass spectrum of a $Co_{31}Nd_{64}B_5$ LMAIS obtained in the VELION system. The main part is shown in the inset as well as the evidence of the single and double charged well separated boron species.

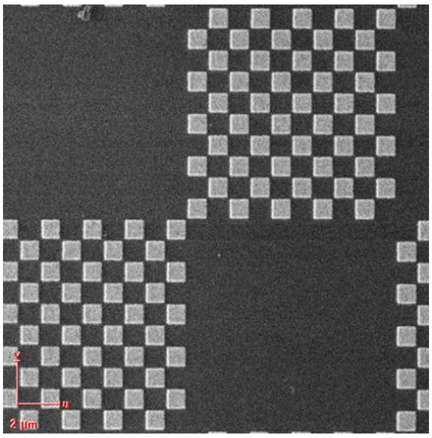

Fig. 2: Imaging of a Chessy-test structure with an ^{11}B FIB with 5 pA.

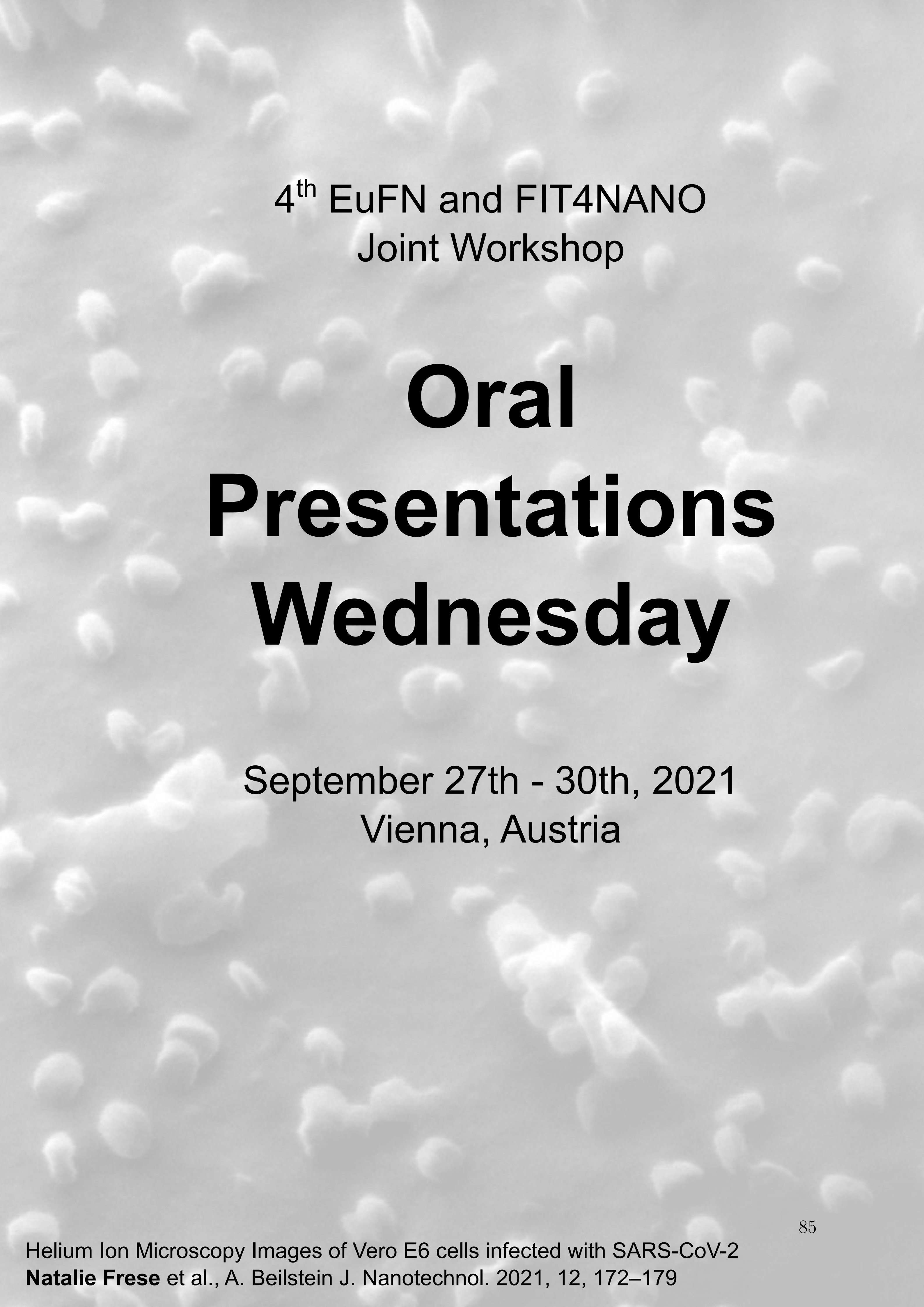

4th EuFN and FIT4NANO
Joint Workshop

Oral Presentations Wednesday

September 27th - 30th, 2021
Vienna, Austria

Helium Ion Microscopy Images of Vero E6 cells infected with SARS-CoV-2
Natalie Frese et al., A. Beilstein J. Nanotechnol. 2021, 12, 172–179

Ion Beam Based Fabrication of Nanoelectronic and Nanomechanical Devices

J. Llobet[1] and F. Perez-Murano [1*]

[1] Institute of Microelectronics of Barcelona (IMB-CNM, CSIC) . Carrer dels Til·lers, s/n, E-08193 Bellaterra, Spain.
[*] Corresponding author email: Francesc.Perez@csic.es

The fabrication technology of semiconductor-based devices has experienced a sustained exponential growth for more than 6 decades. Presently, the level of dimensional control and material composition is approaching the single atom accuracy. At short term, the next generations of semiconductor electronic devices will require improved fabrication methods, that could fulfill accuracy requirements but also capability for scaling up in view of practical applications. In this talk, we will present examples of explorative activities for the realization of nanoelectronics and nanomechanical devices, and we will discuss possible future lines for the application of focused ion beams in quantum technologies.

Focused Ga+ beam implantation of silicon is an efficient way for the prototyping of nanoelectronics and nanomechanical devices. The incorporation of Ga into a substrate induces chemical and structural changes, increasing the resistance to etching. As it is possible to implant very small volumes, structures with sub-10 nm accuracy can be created, as, for example, suspended silicon nanowires [1], single electron (hole) devices [2], and complex mechanical resonators [3] (Fig. 1).

The recently EU project IONS4SET [4] has explored a novel route for the large scale fabrication of single electron transistors based on silicon nanocrystals embedded in a silicon pillar [5]. The silicon nanocrystals are synthesized by silicon ion irradiation and annealing. Contacting the silicon pillars with enough accuracy has meant a major challenge, requiring new process development (Fig. 2).

At the final part of the talk, we will discuss opportunities for introducing focused ion-beams in the manufacturing of semiconductor spin qubits.

[1] J. Llobet et al; *Fabrication of functional electromechanical nanowire resonators by focused ion beam implantation;* J. of Micro/Nanolithography, MEMS, and MOEMS 14 (**2015**), 031207.
[2] J. Llobet et al. *Resonant tunnelling features in a suspended silicon nanowire single-hole transistor; Appl. Phys. Lett. 107 (**2015**), 223501.*
[3] V. Tzanov et al. *Multi-Frequency Resonance Behavior of a Si Fractal NEMS Resonator;* Nanomaterials 10 (**2020**), 811.
[4] www.IONS4SET.eu
[5] M-L Pourteau et al. *Sub-20 nm multilayer nanopillar patterning for hybrid SET/CMOS integration;* Micro and Nano Engineering 9 (**2020**) 100074

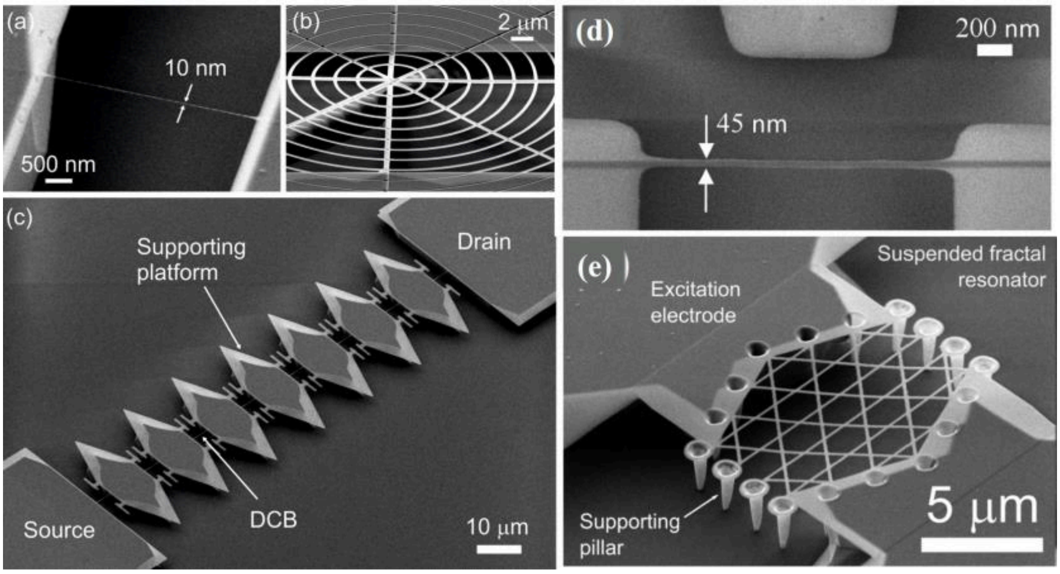

Fig. 1: SEM images of nanomechanical devices fabricated by focused Ga^{+} beam implantation of silicon (a): 10 nm wide suspended Si nanowires [1]; (b) and (c): Arrays of suspended Si nanowires [1]. (d): suspended Si nanowire with a side gate electrode that presents single electron behavior [2]; Fractal nanomechanical resonator [3]

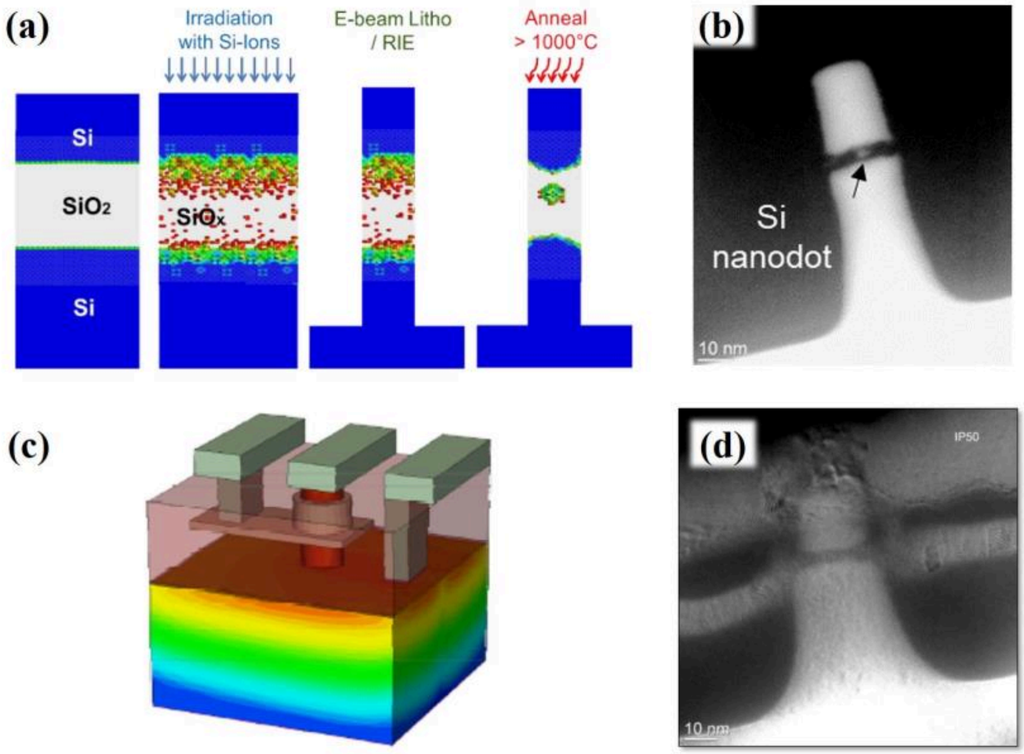

Fig. 2: Single electron transistor (SET) based on an embedded Si nanocrystal (Si-nc)(IONS4SET project [4]). (a): Simulations of the synthesis of the (Si-nc); (b): TEM image of a pillar with an embedded Si-nc; (c) Scheme of the electrical contacts to build up the SET; (d): TEM image of a contacted pillar

Challenges to TEM sample preparation of stacked Si/SiO_2/Si nanopillars for SETs using Focused Ion Beam

H.J. Engelmann[1*], L. Bischoff[1], R. Hübner[1], K.H. Heinig[1], G. Hlawacek[1], J. von Borany[1], M.L. Pourteau[2], G. Rademaker[2]

[1] Helmholtz-Zentrum Dresden-Rossendorf, Dresden, Germany, [2] CEA-Leti, Grenoble, France
[*] corresponding author email: h.engelmann@hzdr.de

Single Electron Transistors (SETs) open the way to semiconductor devices with extremely low power consumption. Quantum mechanical effects are used in such transistors: field-controlled tunneling of single electrons from a source to a drain via a quantum dot. SETs can be manufactured as thin Si pillars (source and drain) with a Si oxide layer in-between containing one Si quantum dot (Fig. 1). After SiO_x formation by ion beam mixing, a thermally activated phase separation including Ostwald ripening results in a self-organization of Si nanocrystals in the SiO_2 layer acting as Si quantum dots (Si NDs). For SET operation at room temperature, the diameter of the Si pillars needs to be < 12 nm, the Si ND diameter must be in the range of 2…3 nm and the distances between Si NDs and source/drain cannot be larger than 1.5 nm allowing quantum mechanical tunneling of the electrons.
Thus, Transmission Electron Microscopy (TEM) must be used for the structural characterization of these SETs. Si NDs inside the SiO_2 matrix can only be detected by using the Si plasmon loss in the energy-filtered TEM mode. TEM sample preparation is challenging because of the very small 3D structure of the pillars (Fig.2) and the need for very thin TEM lamellae (30…40 nm in thickness). The Focused Ion Beam (FIB) lift-out technique can be used to prepare such samples. Setting markers and gradual thinning of the lamella from both sides (with TEM inspection in between) is necessary.
Surprisingly, comprehensive TEM studies uncovered that the oxide layer of a Si/SiO_2/Si layer stack can become dramatically thinner in pillars fabricated from this stack by Reactive Ion Etching (RIE). The oxide layer thinning depends on the pillar diameter. For instance, an originally 8 nm thick SiO_2 layer is reduced to 2.6 nm in 15 nm diameter pillars. In order to prove that this oxide shrinkage is caused by RIE and not by sample preparation the most critical process in the FIB preparation - which is the electron-beam-assisted carbon-protection-layer deposition - was analyzed in detail: pillars were irradiated with different electron doses and then, the SiO_2 thickness was measured in the TEM. As can be seen in Fig. 3 there is a clear influence of the electron dose on the oxide thickness. This can be explained by charge accumulation in pillar Si caps (drain), followed by dielectric breakdowns through filament formation across the SiO_2 layer accompanied by Si oxide dissociation and oxygen emanation from the SiO_2 disc rim of the pillars. However, as can be seen in Fig. 3 the FIB-caused contribution to the oxide thickness reduction is only a small part. The main contribution comes from the pillar RIE process based on the same physical reason (charging of the pillar Si caps).

This work was supported by the European Union's H-2020 research project 'IONS4SET' under Grant Agreement No. 688072.

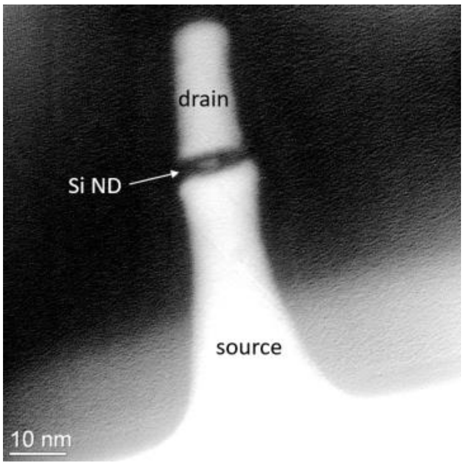

Fig. 1: SET pillar with one Si quantum dot (Si ND)
(EFTEM Si plasmon loss image)

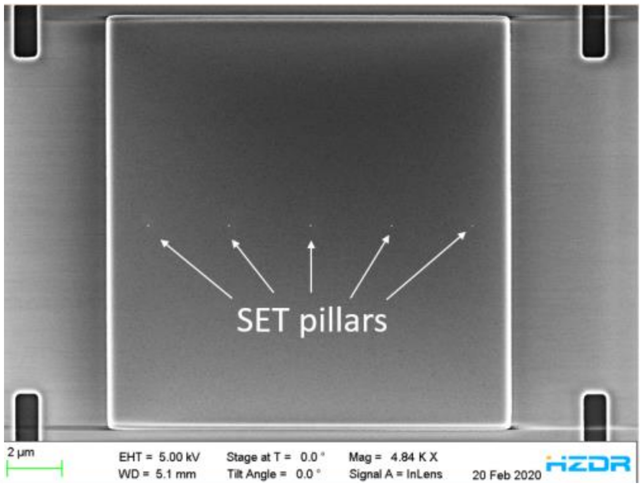

Fig. 2: SET pillar test structure (SEM image), pillar diameter left to right: 36/31/27/21/15 nm, as measured by TEM

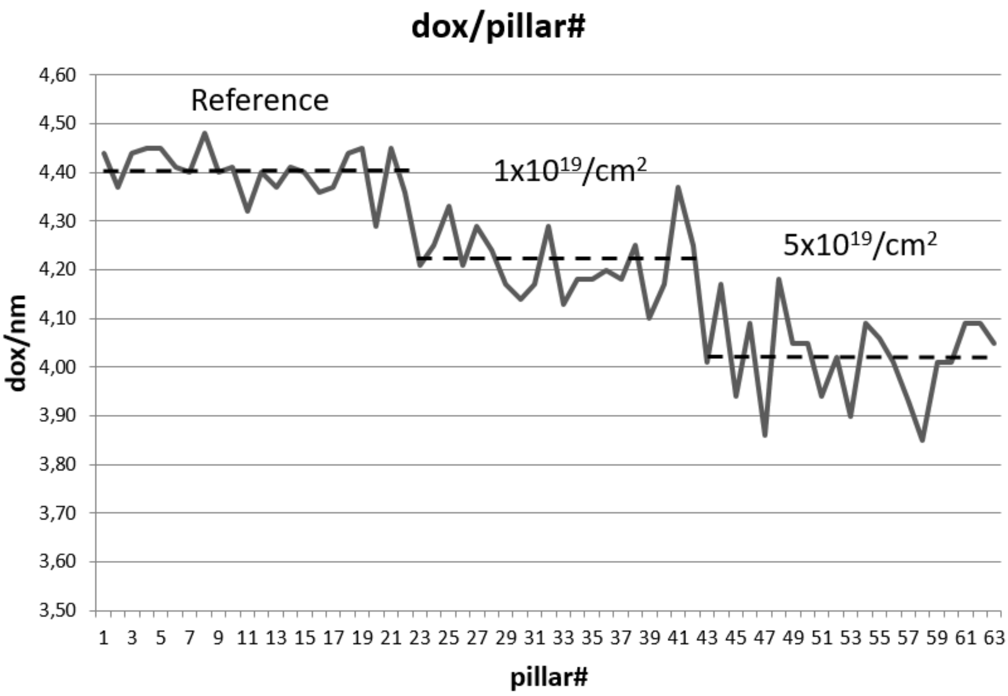

Fig. 3: plot of SET Si oxide thickness dox against pillar number after irradiation of SET pillars with different electron doses (accelerating voltage 800 V), reference: no extra irradiation

Advanced TEM Lamella Preparation in FIB-SEM by Taking Advantage of Innovative Lift-out Methods

Martin Sláma[1] *, Petr Klímek[1], Andrey Denisyuk[1], Jiří Dluhoš[1]

[1] TESCAN ORSAY HOLDING, 623 00, Libušina třída 21, Brno, Czech Republic
[*] corresponding author email: martin.slama@tescan.com

The success of transmission electron microscopy (TEM) analysis depends heavily on the quality of the sample preparation. And sample preparation requirements become more stringent when atomic resolution is needed or when material features are smaller or more complex. Using FIB to prepare samples for TEM provides the best method for achieving the required thin lamella and ensuring uniform quality. Today's novel materials, however, require more advanced sample preparation methods to assure that sample features can be observed with the desired level of detail.

For these novel materials, sample thickness is not the only parameter that must be considered. FIB-SEM instruments allow site-specific sample preparation by combining several techniques that help to locate the feature of interest on the sample or determine the orientation of a structure. More detailed analyses, such as chemical analysis or analysis of the sample's crystallographic orientation, can be done to locate area of interest. These traditional FIB-SEM methods help to not only distinguish the area more precisely, but also can reveal optimal sample orientation for the plane from which the lamella is to be prepared. This correlative approach also can be combined with more dedicated techniques, for example TOF-SIMS analysis which can play a key role in identifying trace concentrations of a particular element. In some cases, the samples will require that the lamella be prepared from a specific geometry, which necessitates the use of a lift-out technique **that allows a high degree of freedom to orientate the sample with respect to the milling and polishing ion beam**.

Innovative lift-out methods allow analysis of samples from a specific geometry that is different from the analyzed plane in FIB-SEM view. These innovative lift-out methods provide the possibility to rotate the lamella after extraction from the bulk sample. This way, planar, inverted TEM samples can be prepared. Additionally, lamellae can be prepared without restriction to lamella rotation after lift-out and therefore almost any geometry can be applied. This post-liftout motion freedom can be beneficial for specific samples depending on their composition, for example, samples with inner structures that create excessive curtaining artifacts. By appropriately positioning the structures, the curtaining can be mitigated, and the TEM lamella quality will improve significantly.

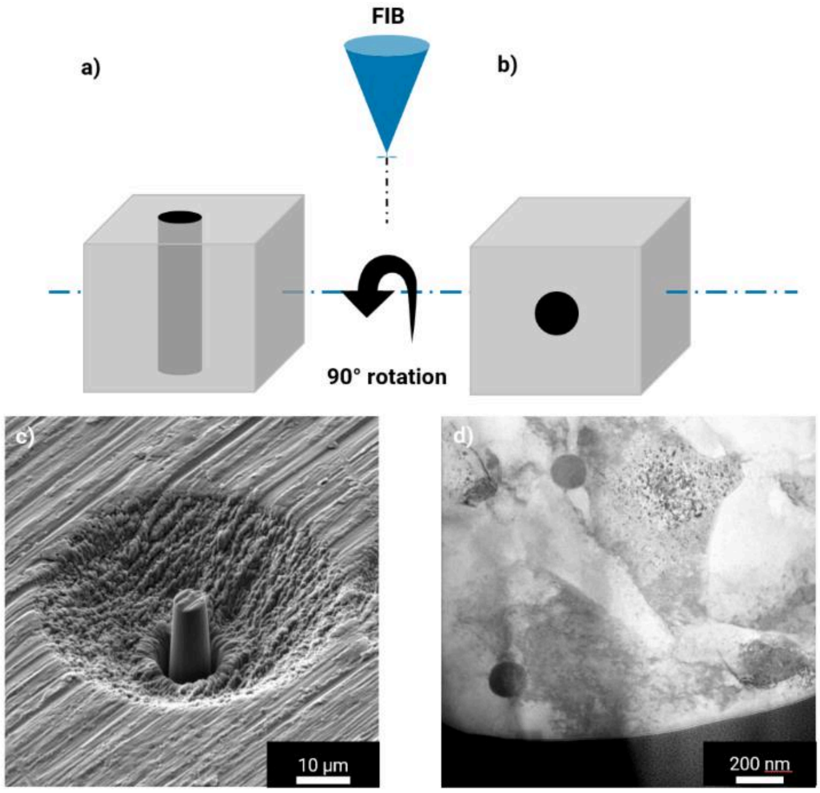

Fig. 1: Planar TEM lamella prepared from Al pillar. a) Schematic drawing of Al pillar in sample b); Schematic drawing of lamella orientation after applied post-liftout rotation; c) Overview SEM image of pillar before TEM sample preparation and d) STEM brightfield image from FIB-SEM detector of final lamella

3D Correlative Tomography and Microscopy

B. Winiarski[1,2*], G. Pyka[3], R. Geurts[4], C. Jiao[4], A. Brinek[1], A. Chirazi[5] and D. Lichau[5]

[1] Thermo Fisher Scientific, Vlastimila Pecha 12, Brno 627 00, Czech Republic
[2] Department of Material, The University of Manchester, M1 3BB, U.K.
[3] Université Catholique de Louvain, 1348 Louvain-la-Neuve, Belgium
[4] Thermo Fisher Scientific, Achtseweg Noord 5, 5651 GG Eindhoven, Netherlands
[5] Thermo Fisher Scientific, Impasse Rudolf Diesel, Bât A, F-33708 Mérignac, Bordeaux, France.
[*] corresponding author email: bartlomiej.winiarski@thermofisher.com

Current scientific and industrial research challenges span across different length scales and are driven by various physical and chemical phenomena. The dawn of two- and three-dimensional (2D and 3D) correlative microscopy and tomography (CMT) greatly advanced understanding phenomena in life and material sciences [1-6]. 2D/3D CMT for the same regions of interest and at different length scales allows spatial and temporal registration in two and three dimensions of many imaging modalities (e.g. in life sciences: visible light imaging, electron and cathodoluminescence imaging is often coregistrated; In materials sciences: x-ray computed tomography, electron and ion microscopy, EBSD, EDS, WDS analytics, Raman, AFM, SIMS, XPS, etc.)

CMT in materials [1-5] and life sciences [6] uses number of micro/nano x-ray CT scanners, optical microscopes, Ga^+ LMIS and Xe, Ar, O, N Plasma DualBeam and Laser Xe Plasma DualBeam microscopes (with analytics, e.g. EBSD, EDS, SIMS, etc.), TEM microscopes, nano CT in TEM and SEM, etc. There are two key factors that makes CMT approachable and successful for real world problems: (a) interrogation volumes and probe size (resolutions) of various techniques must overlap (Fig. 1), and (b) coordinate systems of samples and region of interest (RoI) are tracked and registered in 2D and 3D.

The advent of Xe Plasma FIBs allowed bridging the gap between macro- and nano-scale and accessing region of interest buried few hundreds of microns below the surface [1]. While commercially available femtosecond Laser Plasma FIB [4, 7, 8] with ease can access locations below 1 mm in a dozen of minutes [8] keeping the sub-nanometer imaging resolution of SEM column.

Typically, apparatuses are self-contained and have different requirement for sample preparation, size, fixture, handling and transferring etc., thus direct sample transfer between is very limited or entirely prohibited. While commercially available correlative microscopy transfer means are designed for 2D data acquisition, e.g. optical microscopy (OM) to SEM, SEM to Raman, etc. with extension to, somewhat 3D, superficial surface layers (dozens of microns) when using LMIS FIB-SEM. The first real 3D correlative tomography and microscopy purpose designed cross-platform (µCT ⇔ DualBeams) sample transfer and MapsTM-based correlation solution was recently proposed by Winiarski at al. [4] and is already adopted in academic and industrial environments.

In this contribution we focus on advancements of 3D correlative microscopy and workflows for materials science, e.i. in battery research, jet engines, additive manufacturing, polymer composites, and semiconductor industries. In the studies we use set of research instruments, HeliScan µCT, DualBeams and TEM microscopes and various cross-platform coordinates registration methods. The workflows we use achieve highest µCT resolution (< 400 nm) and allow real 3D correlative tomography and microscopy by accessing region of interest in any location of the specimen and collecting quantitative information using 3D-EBSD/EDS, etc. Our correlative hardware solution is supported by Maps-based [4] and Avizo-based workflows [1] and is compatible with the inert gas transfer hardware and the cryo stage.

[1] B Winiarski at al. Supplement of Microscopy and Microanalysis 152 (**2017**), p. S4-S9.
[2] B Winiarski at al. Microscopy and Microanalysis 23 (**S1/2017**), p. 342-343.
[3] TL Burnett et al. Scientific Reports 4 (**2014**), p. 4711.
[4] B Winiarski at al. Microscopy and Microanalysis 25(S2-**2019)**:870-871.
[5] R Moroni, et al. Scientific Reports 6 (**2016**), p. 30109.
[6] S Meschini. European journal of histochemistry (**2017**) EJH 61(s4):1
[7] SJ Randolph et al. Journal of Vacuum Science & Technology B36 (**2018**), p. 06JB01.
[8] B Winiarski & R Geurts. Wiley Analytical Science, Aug. (**2020**), https://analyticalscience.wiley.com/do/10.1002/was.00070019

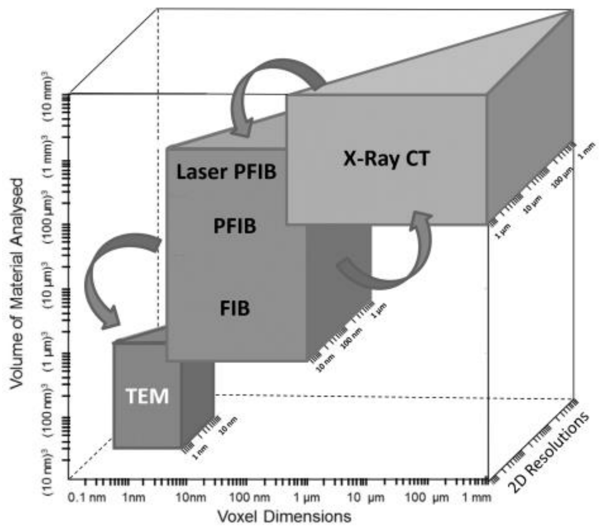

Fig. 1: Shows multi-scale and multi-modal imaging methods typically used in materials science. DualBeam platforms are used both for sample preparation for other systems and for the data collection, where arrows show possible sample transfers and systems stage coordinates co-registration.

Rapid prototyping of probes for surface enhanced Raman scattering (SERS) with focused ion beams

C. Simo[1], B. Schröppel[1], M. Fleischer[2], C. Burkhardt[1]

[1] NMI Natural and Medical Sciences Institute at the University of Tübingen, 72770 Reutlingen, Germany
[2] Institute for Applied Physics and Center LISA+, University of Tübingen, Germany
*corresponding author email: claus.burkhardt@nmi.de

Surface enhanced Raman scattering (SERS) allows the detection of analyte molecules in very low concentration with Raman spectroscopy. This effect was discovered and investigated more than 40 years ago and is still under development. A past [1] and recent [2] review give a good overview on theoretical and experimental results with SERS.

At NMI different projects are ongoing where we need reliable measurements of analytes from immune cell signals in the culture medium and from receptors of native and modified immune cells. Raman Spectroscopy with SERS will support this analysis.

In recent years we have developed a template stripping process to fabricate SERS substrates with defined nanopyramids, which were then tested for the detection of 4-MBA as shown in Fig. 1 and 2 [3,4]. To optimize the enhancement factor EF of these structures we vary the morphology by changing parameters of the fabrication process. Surface sensitive imaging of some substrates was performed with the Orion Nanofab Helium ion microscope (HIM).

For fast and reliable fabrication of substrates with different nano structures we use FIB milling in a Zeiss Crossbeam 550. With the FIB scan generator, arrays of pores were milled in a thin gold layer with a size of the milling field up to 200µm, 128 or 265 pixels and probe currents in the range between 1.5nA and 30nA. These pores work as SERS substrate or may be used as substrate for a template stripping process for fabrication of arrays of gold nano cones. In future we plan to use the HIM for additional nano structuring with the focused Helium ion beam.

[1] A. Campion and P. Kambhampati; Surface enhanced Raman scattering; Chemical Society Reviews, **1998**, 241

[2] J. Langer, D.J. de Aberasturi, J. Aizpurua et. al.; Present and Future of Surface Enhanced Raman Scattering; ACS Nano, **2020**, 28

[3] M. Martina, M. Fleischer, C.J. Burkhardt; Template stripping and bonding of smooth probes with nanoscale features for tip enhanced Raman spectroscopy; Microelectronic Engineering, **2017**, 31

[4] C. Simo, poster Microscopy Conference MC 2021 (online), 22.-26.8.2021

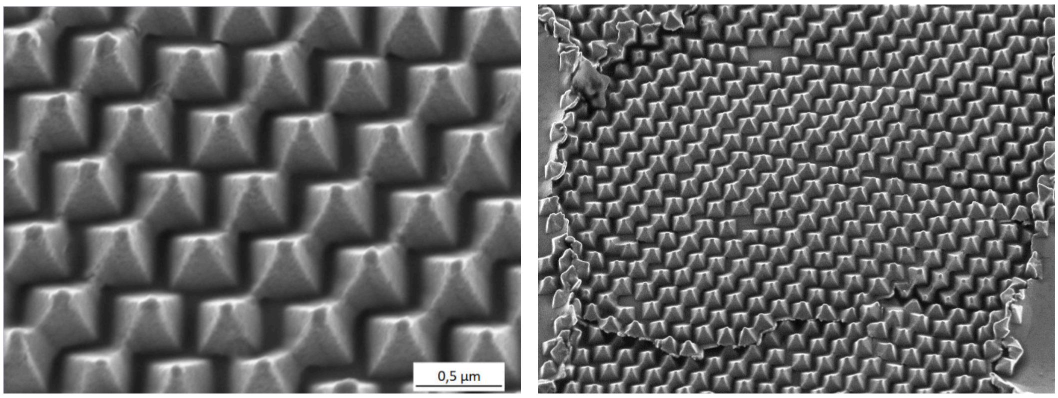

Fig. 1: Flexible SERS substrate with gold pyramids after measurement of 4-MBA as analyte

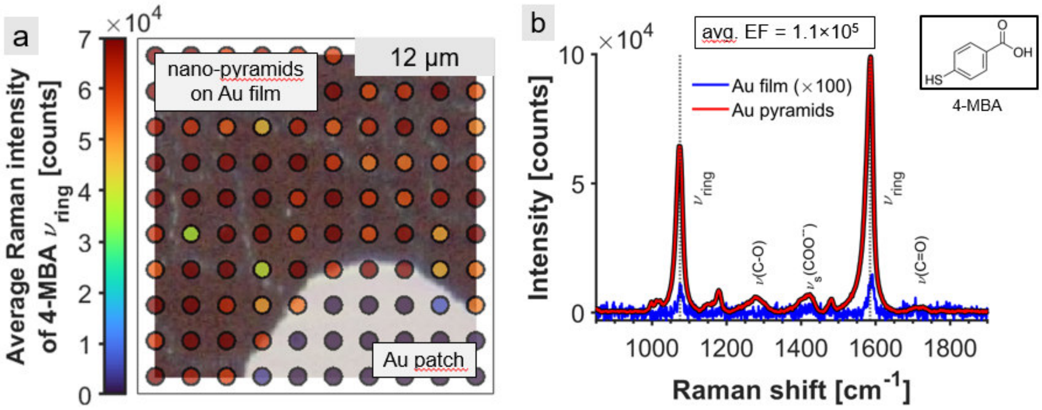

Fig. 2: Raman spectra at different spots after coating the substrate with 4-MBA. Excitation with 633nm HeNe Laser, power: 10mW. Measured enhancement factor EF > 10^4

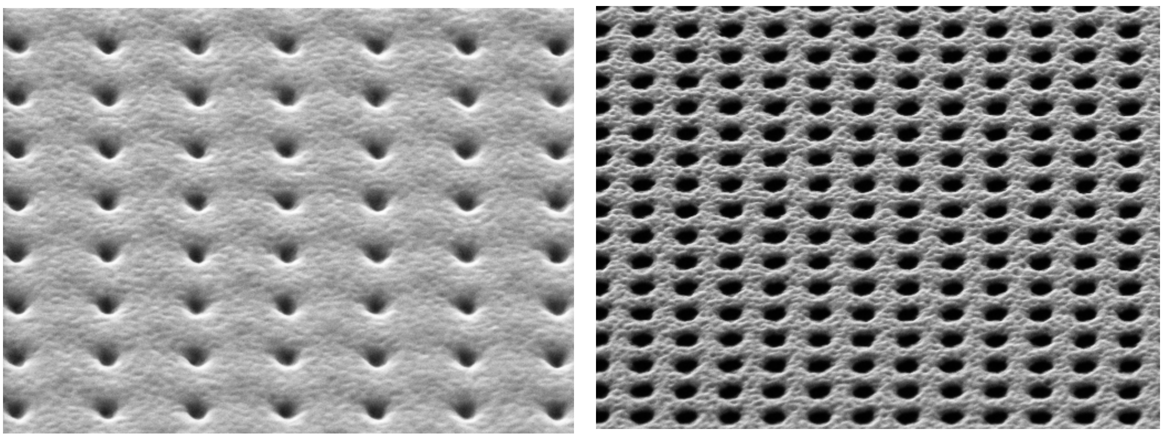

Fig. 3: Array of spots milled in gold with a Gallium FIB (Zeiss Capella; 30kV). Probe current 1,5nA (left) and 15nA (right), dwell time 1,64ms, Distance between pores: 800nm

Multimodal characterisation on FIB instruments combining nano-scale SIMS and SE imaging

T. Wirtz, O. De Castro, J.-N. Audinot, H. Hoang, A. Biesemeier

Advanced Instrumentation for Nano-Analytics (AINA), MRT Department, Luxembourg Institute of Science and Technology, 41 rue du Brill, L-4422 Belvaux, Luxembourg
* corresponding author email: tom.wirtz@list.lu

The structural characterisation and the chemical analysis at the nanometer scale are of highest relevance in a large variety of fields, ranging from the high-resolution imaging of dopant distributions in complex electronic devices to the generation of chemical maps of sub-cellular structures in biological samples to understand the underlying physiological processes. The following key characteristics are required and enabled in our instrument developments: (1) highest spatial resolution, (2) excellent chemical sensitivity, (3) high dynamic range and (4) isotopic selectivity.

Secondary Ion Mass Spectrometry (SIMS) is an extremely powerful technique for analyzing surfaces, owing to its ability to detect all elements from H to U and to differentiate between isotopes, its excellent sensitivity and its high dynamic range. SIMS analyses can be performed in different modes: acquisition of mass spectra, depth profiling, 2D and 3D chemical imaging. Adding SIMS capability to FIB instruments offers a number of interesting possibilities, including highly sensitive analytics, in-situ process control during patterning and milling, highest resolution SIMS imaging (~10 nm), and direct correlation of SIMS data with data obtained by other analytical or imaging techniques on the same instrument, such as high resolution secondary electron (SE) images or Energy-Dispersive X-Ray Spectroscopy (EDX) spectra.

In this global context, we developed a double focusing magnetic sector SIMS system equipped with a novel continuous focal plane detector. This SIMS system allows for the detection of all masses in parallel for each single pixel, resulting in acquisition times as low as 1 s to obtain a full mass spectrum or 2 min to obtain a 512 x 512 pixel SIMS image with highest signal-to-noise and excellent dynamic range.

This SIMS system has been installed on several multi-modal FIB platforms, including a Thermo Fisher DualBeam and a ZEISS ORION NanoFab Helium Ion Microscope. In addition, we developed dedicated FIB-SIMS platforms including the npSCOPE and, most recently, the SIMS:ZERO, which is a novel highest-resolution highest-sensitivity FIB-SIMS platform combining zeroK's high brightness LoTIS Cs^+ ion source and LIST's SIMS system.

Here, we will review the performance of the different instruments with a focus on new developments, showcase methodologies for high-resolution 3D chemical imaging, present a number of examples from various fields of applications (nanoparticles, battery materials, photovoltaics, micro-electronics, tissue and sub-cellular imaging in biology, geology,…) and give an outlook on new trends and prospects.

Development of an O-TOFSIMS integrated on a UHV FIB/SEM workstation: challenges and innovative approaches for in depth correlated nano-analyzes and high-resolution imaging

Jean Almoric[1,2,*], Alexandra Fraczkiewicz[1], Malik Durand[3], Anthony Seret[3], Alexis NICOLAY[3], Arnaud Houel[1], Anne Delobbe[1], Isabelle Berbezier[2] and Nathalie Bozzolo[3]

[1] Orsay Physics, Fuveau, France
[2] Institut Matériaux Microélectronique Nanoscience de Provence (IM2NP), Marseille, France
[3] MINES ParisTech - Centre de mise en forme des matériaux (CEMEF), Sophia-Antipolis, France
[*] jean.almoric@orsayphysics.com

Research and development in nano-characterization techniques, down to the nanoscale, is increasingly challenging for the interdisciplinary field of nanotechnologies (including, but not limited to, microelectronics, metallurgy, and biology.), for improving products performance, quality and reliability. The latest generation of Orsay Physics workstations combining a gallium Focused Ion Beam (FIB) with a Scanning Electron Microscope (SEM) reach a lateral ion beam resolution of 2.5nm [1], which simultaneously allow for nanoscale patterning [2], implantation [3], TEM lamella preparation, cross sectioning and tomography by FIB slicing. SIMS analysis, which offers high resolution chemical imaging, can be combined with more conventional secondary electron imaging. This technique provides an efficient detection of light elements and a reliable separation of isotopes.

In this study we report the benefits of a correlative approach combining multiple analytical and imaging tools (O-TOF SIMS, SEM, FIB and GIS) into the same versatile and customizable UHV “NanoSpace” platform. Chemical mapping with a high spatial resolution (<30nm) and a high mass resolution (FWHM 4500 on ^{28}Si) was made possible by pulsing the secondary ion beam instead of the primary one, as done in conventional TOF-SIMS. Transmission and mass resolution were increased by redesigning and optimizing the extraction of secondary ions of an O-TOF (from TOFWERK company), and compared to the original system from TOFWERK. Finally, we will show that ultra-small precipitates in a nickel-based superalloy (Fig. 1), that were not possible to characterise by SEM-EDX, were identified and visualised by the new UHV Nanospace platform. The key capabilities of O-TOF SIMS/SEM/FIB developed here including high detection efficiency for a wide z range, surface sensitivity and imaging with high spatial resolution, can address ideally the issues of nanomaterials in several areas.

[1] S. Guillous et al; Review of Scientific Instruments 87, 113901 (**2016**); http://dx.doi.org/10.1063/1.4966675
[2] A. Benkouider et al; Thin Solid Films (**2013**); http://dx.doi.org/10.1016/j.tsf.2013.02.119
[3] M. Lesik et al; Science 366, 1359-1362 (**2019**); https://doi.org/10. 5281/zenodo.3249952

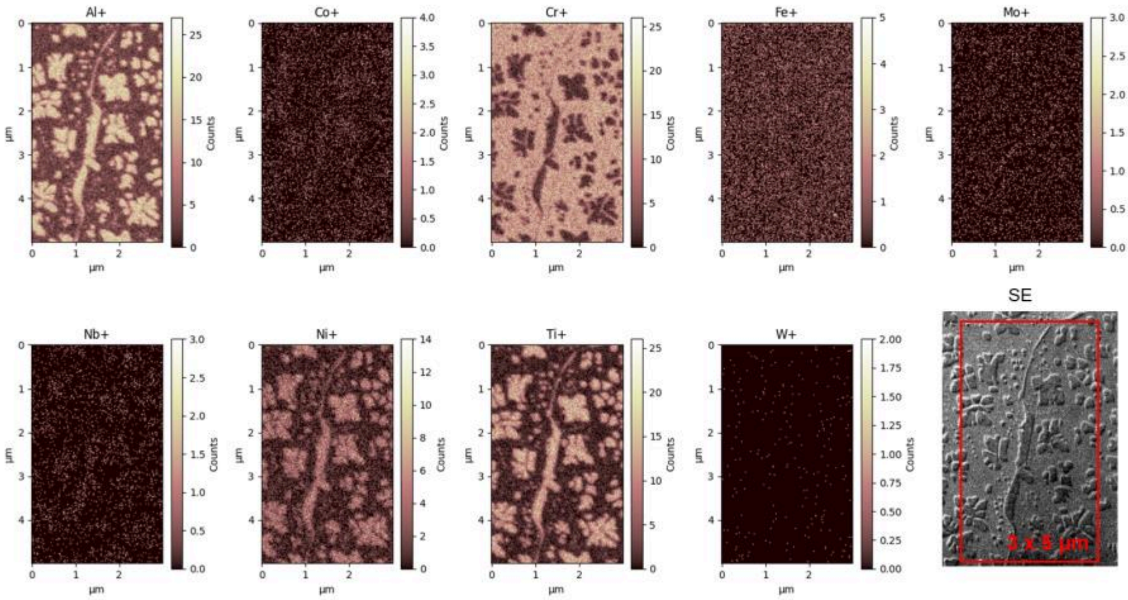

Fig. 1: Elemental maps obtained by O-TOFSIMS in the FIB/SEM UHV workstation on γ-γ' Ni based superalloy, revealing that the very fine (few tens of nm) precipitates are indeed consistent with γ'-Ni3(Al, Ti). FIB conditions were 30kV, 1pA and 50µs of pixel time. The total time of this FIB/SIMS analysis was 30 seconds. At bottom on the right the secondary electron image show in the red square the localization of the SIMS analyse.

Focused Electron Beam Induced Mass Spectrometry – new, versatile method of in-situ analysis of nanomaterials

J. Jurczyk[1,2], L.Pillatsch[3], L. Berger[4], A.Priebe[2], K. Madajska[5], Cz. Kapusta[2], I. B. Szymanska[5], J. Michler[1] and I. Utke[1*]

[1] Empa - Swiss Federal Laboratories for Materials Science and Technology, Laboratory for Mechanics of Materials and Nanostructures, Feuerwerkerstrasse 39, CH - 3602 Thun, Switzerland
[2] AGH University of Science and Technology Krakow, Faculty of Physics and Applied Computer Science, Al. Mickiewicza 30, 30-059 Kraków, Poland
[3] TOFWERK AG, Schorenstrasse 39, CH-3645 Thun, Switzerland
[4] Ecole Polytechnique Fédérale de Lausanne (EPFL), CH-1015 Lausanne, Switzerland
[5] Faculty of Chemistry, Nicolaus Copernicus University in Toruń, Gagarina 7, 87-100 Toruń, Poland
[*] corresponding author email: ivo.utke@empa.ch

Focused electron beam induced mass spectrometry (FEBiMS) is a novel analytical method, which allows for measurement of volatile ionic products of electron-induced dissociation of a compound, see figure 1a. It employs a focused electron beam (FEB) from a scanning electron microscope operated at high vacuum conditions > 10^{-6} mbar. So far, electron-induced reactions were investigated by mass spectrometry for gases or cryogenically condensed precursors in ultra-high vacuum [1]. The detection of volatile products during irradiation is important for nanostructuring methods like focused electron beam deposition (FEBID) [2] or ice lithography [3]. FEBiMS is a progression of the well-known FIB-SIMS method (focused ion beam - secondary ion mass spectrometry) – a powerful tool for nanocharacterization [4]. By using a time-of-flight (TOF) detector combined with a FEB, charged products of e-beam irradiation of three solid state compounds $Ru_3(CO)_{12}$, $Ag_2(\mu\text{-}O_2CC_2F_5)_2$, $Cu_2(\mu\text{-}O_2CC_2F_5)_4$ were obtained. The fragmentation of $W(CO)_6$ was monitored during FEBID, see figure 1b. The latter experiment was the first real-time detection of charged species desorbing from the surface during FEBID. We will present first experimental results and discuss advantages and challenges of FEBiMS as a novel characterization method.

[1] J.A. Spencer, S.G. Rosenberg, M. Barclay, Y.-C. Wu, L. McElwee-White, D. Howard Fairbrother, *Understanding the electron-stimulated surface reactions of organometallic complexes to enable design of precursors for electron beam-induced deposition*, Applied Physics A 117(4) (**2014**) 1631-1644.
[2] S. Barth, M. Huth, F. Jungwirth, *Precursors for direct-write nanofabrication with electrons*, Journal of Materials Chemistry C 8(45) (**2020**) 15884-15919.
[3] D. Zhao, A. Han, M. Qiu, *Ice lithography for 3D nanofabrication*, Science Bulletin 64(12) (**2019**) 865-871.
[4] J.A. Whitby, F. Östlund, P. Horvath, M. Gabureac, J.L. Riesterer, I. Utke, M. Hohl, L. Sedláček, J. Jiruše, V. Friedli, M. Bechelany, J. Michler, *High Spatial Resolution Time-of-Flight Secondary Ion Mass Spectrometry for the Masses: A Novel Orthogonal ToF FIB-SIMS Instrument with In Situ AFM*, Advances in Materials Science and Engineering 2012 (**2012**) 180437.

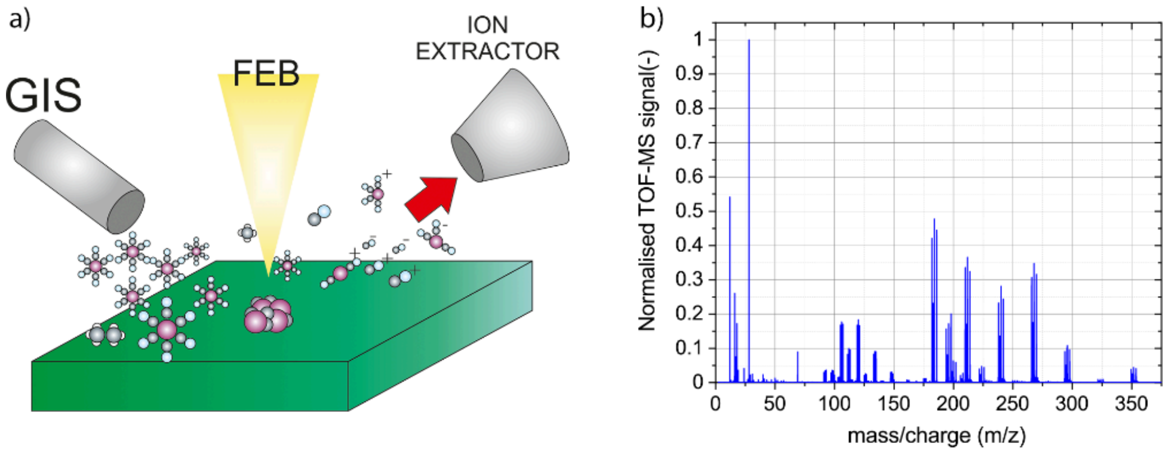

Fig. 1: a) Schematic representation of focused electron beam induced mass spectrometry (FEBiMS) during focused electron beam induced deposition (FEBID): gaseous precursor is delivered via gas injection system (GIS) over the substrate, where it adsorbs and is irradiated with electrons to yield a deposit on the surface. b) Volatile fragments are registered by the ion extractor giving the full-range mass spectrum via the time-of-flight mass spectrometer.

fibTOF: The use of secondary ion mass spectrometry capabilities for material characterization on a FIB-SEM microscope

Lex Pillatsch* and James Whitby

TOFWERK AG, Schorenstrasse 39, CH-3645, Thun, Switzerland
* corresponding author email: lex.pillatsch@tofwerk.com

High-end FIB-SEM dual beam microscopes are useful tools for surface characterization and structuring on the micro- and nanoscale. The FIB beam is used for precise milling of surface structures. Sputtered particles can be used to characterize the local composition of the sample.
The secondary ion mass spectrometry (SIMS) approach can achieve higher spatial resolutions than elemental detection techniques based on material-electron interactions. The scattering process of incident ions is less severe than for electrons. SIMS is useful when imaging light metals and halogens due to its high sensitivity to these elements. The fibTOF mass spectrometer developed by TOFWERK uses the time of flight principle to identify the mass of sputtered secondary ions (Figure 1). The incoming ions are extracted in a direction orthogonal to the initial flight path. This allows the use of a continuous FIB beam to sputter the surface which has advantages for the mass resolving power (and requires no modification to the microscope). The synchronization of the ion extraction with the scanning of the high brightness FIB beam leads to the elemental detection and imaging with a lateral resolution <50 nm and depth resolution <10 nm (depending on the FIB beam settings). The high sensitivity allows elemental concentrations at optimal analytical conditions down to a few ppm to be successfully detected.

In this presentation we will cover the design and the working principle of the fibTOF mass analyser in combination with a FIB-SEM microscope. The optimal analytical conditions for chemical mapping with either high lateral or depth resolution will be described. The ability of the instrument to measure thin layers and to detect buried interfaces will be demonstrated using the example of a multilayer AlGaAS/GaAs structure. The widespread use and strength of the fibTOF for representative applications such as light element detection (Li detection), metals, semiconductors and samples from life sciences will be discussed.

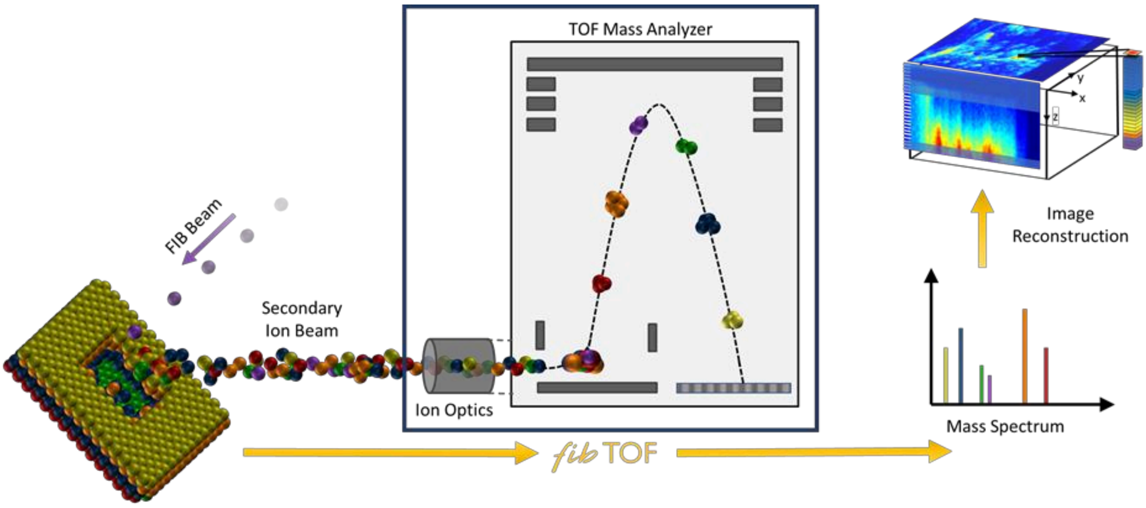

Figure 1: Schematic of FIB-SIMS operation using Tofwerk's fibTOF instrument

Review of fluorine gas-assisted FIB-TOF-SIMS for enhanced 3D chemical characterization of materials in nanoscale

Agnieszka Priebe[1,*], Jordi Sastre[2], Moritz Futscher[2], Jakub Jurczyk[1], Marcos Puydings[1], Laszlo Pethö[1], Emese Huszar[1], Tianle Xie[1], Ivo Utke[1], Yaroslav E. Romanyuk[2] and Johann Michler[1]

[1] Empa, Swiss Federal Laboratories for Materials Science and Technology, Laboratory for Mechanics of Materials and
Nanostructures, Feuerwerkerstrasse 39, CH-3602 Thun, Switzerland
[2] Empa, Swiss Federal Laboratories for Materials Science and Technology, Laboratory for Thin Films and Photovoltaics, Überlandstrasse 129, Dübendorf, CH-8600 Switzerland
[*] corresponding author email: agnieszka.priebe@empa.ch

The development of high-vacuum compatible time-of-flight secondary ion mass spectrometry (TOF-SIMS) detectors allows dual beam systems, consisting of focused ion beam and scanning electron microscopy (FIB/SEM), to be upgraded into chemical analysis instruments with lateral resolution <50 nm and depth resolution < 20 nm [1]. Furthermore, these detectors are compatible with *in situ* gas injection system (GIS), which enables for conducting gas-assisted TOF-SIMS measurements. Extensive studies on various inorganic materials (pure metals, alloys and complex multilayers) [2-6] show that delivering fluorine gas to a sample surface during simultaneous surface bombardment with Ga^+ primary ion beam can significantly enhance generation of secondary ions, leading to higher resolution of 2D chemical images and depth profiles. Furthermore, it was observed that fluorine has potential for separating mass interference during TOF-SIMS, which is one of the main drawbacks of this technique when no gas is provided. Initial studies indicate also fluorine-induced polarity inversion of generated secondary ions from negative to positive. This can allow complete direct chemical characterization of a sample to be assessed from exactly the same volume during a single measurement (without any gas, two separate measurements have to be performed on two different locations due to the destructive nature of TOF-SIMS). In this work, we present a review of our recent studies, in particular focusing on the application of fluorine-gas assisted TOF-SIMS for analyzing complex buried sublayers in thin films (Fig.1) and microbatteries. The presented methodology is expected to play an important role in the development of new materials based on nanostructures, validation of fabrication processes and potential failure analysis.

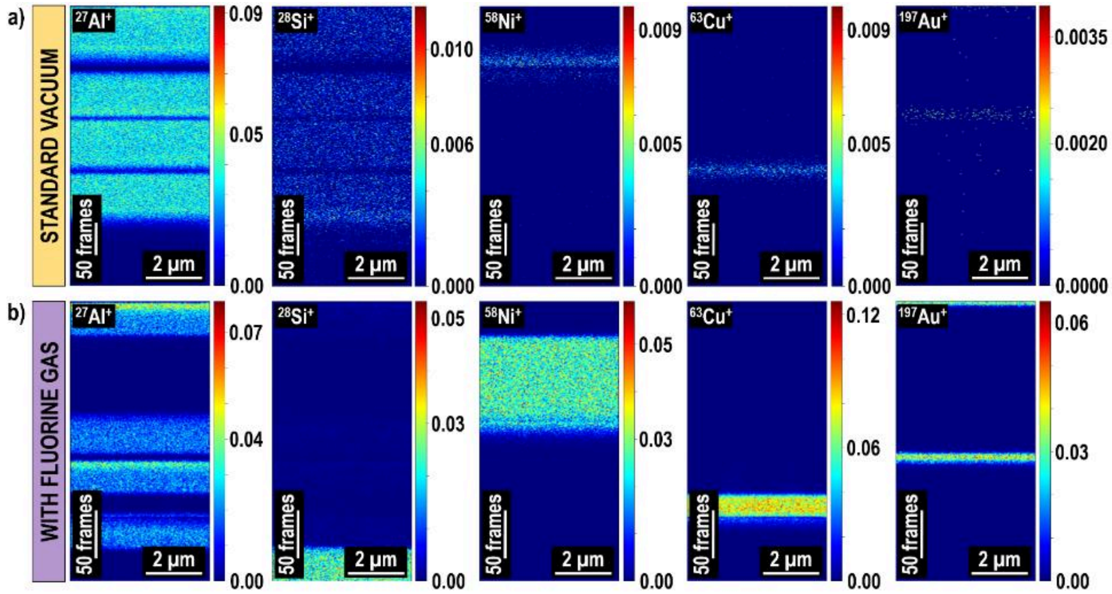

Fig. 1: 2D elemental images of the Al_2O_3/Ni/Al_2O_3/Au/Al_2O_3/Cu/Al_2O_3 multilayer. The signals of the most prominent isotopes are presented in *x-z* plane (i.e. in depth; integration in *y*-direction). The *z*-dimension is given as a number of frames, i.e. acquisition scans (1 frame = 10.24 s of the sputtering time). The color scale is given in counts per extraction. The TOF-SIMS results were obtained without (a) and with fluorine gas (b). Reprinted with permission from: A. Priebe et al., *High Sensitivity of Fluorine Gas-Assisted FIB-TOF-SIMS for Chemical Characterization of Buried Sublayers in Thin Films*, ACS Applied Materials & Interfaces (2021). Copyright © 2021 American Chemical Society.

[1] J. A. Whitby et al., *High Spatial Resolution Time-of-Flight Secondary Ion Mass Spectrometry for the Masses: A Novel Orthogonal ToF FIB-SIMS Instrument with In Situ AFM*, Advances in Materials Science and Engineering (2012), pp. 1-13

[2] A. Priebe et al., *Application of a gas-injection system during the FIB-TOF-SIMS analysis - influence of water and fluorine gases on secondary ion signals and sputtering rates,* Analytical Chemistry (**2019**), Vol. 91, pp. 11712 - 11722

[3] A. Priebe et at., *Fluorine gas coinjection as a solution for enhancing spatial resolution of time-of-flight secondary ion mass spectrometry and separating mass interference*, Analytical Chemistry (**2020**), Vol. 92, pp. 2121-2129

[4] A. Priebe et at., *Potential of gas-assisted time-of-flight secondary ion mass spectrometry for improving elemental characterization of complex metal-based systems*, Journal of Analytical Atomic Spectrometry (**2020**), Vol. 35, pp. 2997-3006

[5] A. Priebe et at., *High Sensitivity of Fluorine Gas-Assisted FIB-TOF-SIMS for Chemical Characterization of Buried Sublayers in Thin Films*, ACS Applied Materials & Interfaces (**2021**), Vol. 13, pp. 15890–15900

[6] J. Sastre et at., *Blocking Lithium Dendrite Growth in Solid-State Batteries with an Ultrathin Amorphous Li-La-Zr-O Solid Electrolyte*, chemrxiv (**2020**)

Challenges and benefits of fluorine gas coinjection during FIB-TOF-SIMS analysis

Krzysztof Wieczerzak*, Johann Michler

[1]Empa, Swiss Federal Laboratories for Materials Science and Technology, Laboratory for Mechanics of Materials and Nanostructures, CH-3602 Thun, Switzerland
* corresponding author email: krzysztof.wieczerzak@empa.ch

TOF-SIMS is a powerful analytical method, which provides elemental, chemical state, and molecular information from surfaces of organic and inorganic materials. The strength of this technique lies in its high detection sensitivity in the range of parts per million (ppm) or even parts per billion (ppb) as well as its capability of elemental identification of large areas in the hundreds of micrometers in size and small areas in the nanometric regime without any additional sample preparation. In this talk, we will discuss challenges and benefits of FIB-TOF-SIMS analysis enhanced by fluorine gas, delivered via gas injection system (GIS). All experiments in this work were performed using TOF-SIMS detector, which is an add-on to the commercial FIB/SEM instrument. We will present results on high purity 41 elements and on real-life multicomponent samples with heterogeneous microstructures. We will demonstrate that fluorine-assisted sputtering can be an attractive alternative for FIB-TOF-SIMS analysis under standard vacuum conditions due to meaningfully improved ionization probability of elements and reduced negative effect of preferential reoxidation in multicomponent samples.

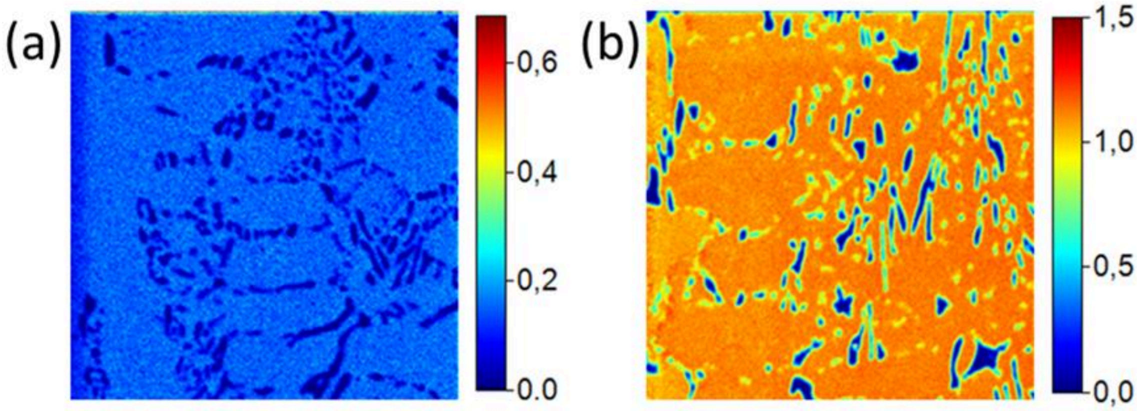

Fig. 1: The $^{58}Ni^{+}$ isotope distribution maps of the Ni-based hardfacing alloy, strengthened by M_7C_3 and MC carbides. (a) Maps collected under standard vacuum conditions and (b) with coinjection of XeF_2 precursor during FIB sputtering. SIMS analysis was done with a primary $^{69}Ga^{+}$ beam operating at 30 kV and 500 pA. Total sputtering time was 780 s. The FIB spot size (FWHM) was 16.1 nm, and pixel spacing was 58.5 nm. The ion signal on each map is averaged over 20 frames. A color scale next to the ion maps indicates TOF-SIMS signal (counts/pixel).

Defect Engineering, Ion Implantation and Nanofabrication using the Helium Ion Microscope

F. I. Allen[1,2,3*]

[1] Department of Materials Science and Engineering, UC Berkeley, CA 94720, USA
[2] California Institute for Quantitative Biosciences, UC Berkeley, CA 94720, USA
[3] National Center for Electron Microscopy, Molecular Foundry, LBNL, Berkeley, CA 94720, USA
[*] author email: francesallen@berkeley.edu

Since its commercialization in 2007, the Helium Ion Microscope (HIM) has emerged as a versatile platform for imaging [1], analysis [2], and materials modification [3], on length scales down to the sub-10-nm domain. This talk will give an overview of the broad scope of materials modification research enabled by the HIM, including site-selective and dose-controlled ion irradiation for defect engineering of material properties such as electrical conductivity and ferromagnetic behavior, ion implantation studies to elucidate the mechanisms of helium nanobubble growth and subsurface swelling, and direct-write nanofabrication using both focused ion beam milling and ion beam-induced deposition. Looking to the future, I will discuss the importance of in-situ methods to control the sample environment and probe the material response in real-time, as well as the key roles of correlative analysis, theory and simulations.

[1] M. Schmidt, J. M. Byrne, I. J. Maasilta; *Bio-imaging with the helium-ion microscope: A review*; Beilstein Journal of Nanotechnology 12 (**2021**), 1.

[2] T. Wirtz, O. De Castro, J.-N. Audinot, P. Philipp; *Imaging and Analytics on the Helium Ion Microscope;* Annual Review of Analytical Chemistry 12 (**2019**), 523.

[3] F. I. Allen; *A review of defect engineering, ion implantation, and nanofabrication using the helium ion microscope*; Beilstein Journal of Nanotechnology 12 (**2021**), 633.

Transformation of tin spheres into hollow cubes by He^+ irradiation

N. Klingner[1*], K.-H. Heinig[1], D. Tucholski[1], W. Möller[1], R. Hübner[1], L. Bischoff[1], G. Hlawacek[1], S. Facsko[1]

[1] Helmholtz-Center Dresden-Rossendorf, Dresden, Germany
[*] corresponding author email: n.klingner@hzdr.de

Broad ion irradiation of nanoobjects can considerably change their shape. Examples are ion-beam hammering [1], ion-induced shaping of buried particles [2], and ion-induced viscous flow of nanopillars [3]. Such shape changes are mainly driven by the kinetics of defects generated by binary collisions of ions and recoils. Here, we report a new kind of ion-induced structure evolution.

Sub-micrometer Sn spheres were irradiated with 30 keV He^+ ions in a Helium Ion Microscope (HIM). Above a He^+ fluence of ~10^{17}/cm², Sn extrusions appeared on the surface of the spheres and were imaged with the HIM. Initially, small, pyramid-like facetted extrusions form at the equator of the tin spheres (north pole pointing to the ion source). Later, each sphere becomes completely covered with tin and appears like a facetted single-crystalline cube. No Sn extrusions were observed for tin spheres with diameters smaller than ~100 nm. Transmission electron microscopy and Auger electron spectroscopy studies show that the single-crystalline tin spheres are covered with a few-nm-thick SnO skin and that the extrusions grow epitaxially on the exposed tin surface.

A model was developed which assumes that the He^+ ions generate ~70 Frenkel pairs per ion in the body-centered tetragonal lattice of tin. The implanted helium atoms, interstitials, and vacancies are confined by the SnO skin. Some He atoms will occupy vacancies which will partially inhibit their recombination with interstitials. This results in an increasing pressure of the “interstitial gas”. Furthermore, the He^+ ion irradiation will cause erosion of the SnO skin. The sputter coefficient increases with the angle of incidence, so that openings in the SnO skin will form in the equator regions first. The interstitials can now escape from the interior of the Sn sphere and form an epitaxial regular Sn lattice on the outside.

Computer simulations were performed based on this model. The Frenkel pair generation and the SnO skin sputtering are simulated with dynamical programs based on the Binary Collision Approximation TRI3DYN [4]. Reaction-diffusion dynamics as well as nucleation and extended defect growth were simulated with a 3D kinetic lattice Monte Carlo program [5] using an RGL-potential for tin. The simulation reproduces the experimentally observed formation of He-filled cavities driving the extrusions leading to cube formation.

[1] Snoeks et al., Nucl. Instr. Meth B 178 (2001) 62

[2] Schmidt et al., Nucl. Instr. Meth. B 267 (2009) 1345

[3] Xu et al., Semicond. Sci. Technol. 35 (2020) 15021

[4] Möller, Nucl. Instr. Meth. B 322 (2014) 23

[5] Strobel et al., Phys. Rev. B 64 (2001) 245422

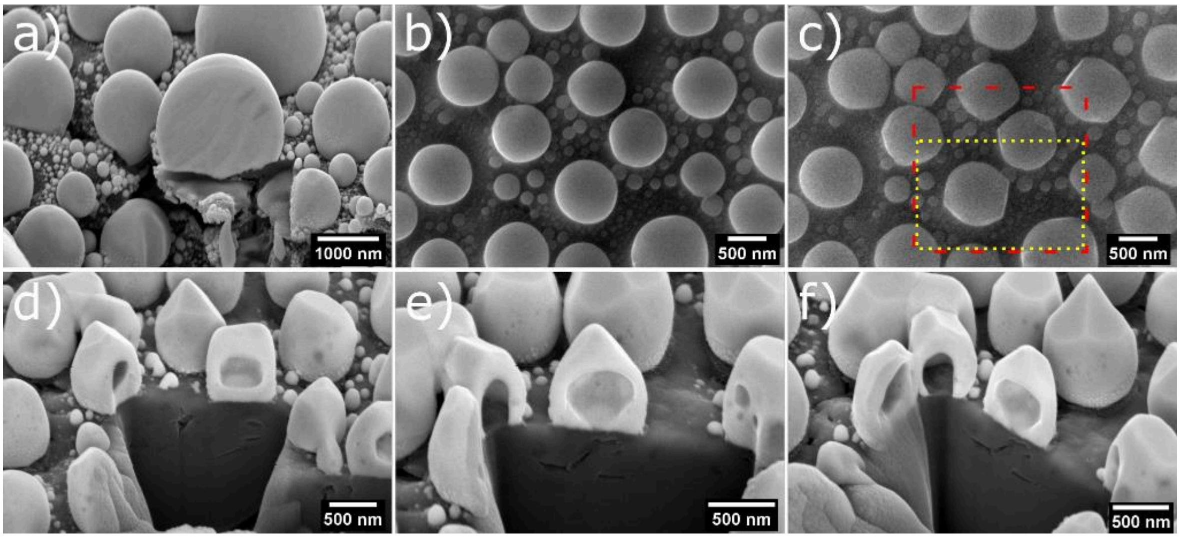

Figure 1: a) SEM image under 54° of an unirradiated tin sphere, cut with a gallium focused ion beam (FIB). b) to f) show the same area of the tin sample. b) HIM image before irradiation. c) HIM image after irradiation with visible protrusions. The yellow, dotted area is a guide to the eye for the gallium-FIB-sputtered region in d). The red, dashed area indicates the region of the sputtered area in e) and f). d) to f) SEM images under 54°of irradiated tin spheres with protrusions that have been opened by FIB sputtering. Hollow regions are visible that were probably filled with helium. The sample has been rotated clockwise in f) to image the inside of 3 opened tin objects.

How hot does it get? Heat-Generation under the He^{+}-Ion Beam and Implications for Imaging and Milling of Biological Objects

Matthias Schmidt*, Marc Tamisier, Chaturanga D. Bandara, Robin Dittrich and Hryhoriy Stryhanyuk

ProVIS - Centre for Chemical Microscopy, Dept. of Isotope Biogeochemistry, Helmholtz-Centre for Environmental Research, Leipzig, Germany
* corresponding author email: matthias.schmidt@ufz.de

During the past decade helium-ion microscopy (HIM) has been used successfully to study biological objects at high resolution [1]. A major advantage of HIM over scanning electron microscopy is that it is not a mere imaging technique but can on top of it be used as an ultra-fine nano-fabrication tool with low proximity effects. Studies of He^{+}-ion milling of biological objects comprise opening the mouth-cavity of a nematode [2], cross-sectioning a phage-infected *E.coli* [3], a bdelloplast [4] and a bacterium on a dragonfly-wing [5], to name some. In most of these studies, the ion-milled surfaces appear smooth with no particular contrast when imaged with the HIM after milling. This may be due to the decreased roughness of the milled surface or homogenisation due to mixing of atoms close to the surface such that neither topography nor materials contrast is gained. However, it is also very likely that significant thermal damage, e.g. degradation or melting, occurred during the milling process. Furthermore, in some delicate materials degradation under the beam occurs even during imaging as for instance shown on cellulose nano-fibrils which only stayed intact if the ion-doses did not exceed 0.9ions/nm^2 [6].

From a microscopist point-of-view it is of particular importance to estimate the sample temperature under the ion-beam and how it is influenced by instrument parameters like type of ion (e.g. He^{+} or Ne^{+}), ion-dose, beam current and pixel-spacing. A case study of heat damage in biological samples under ion beam probing was carried out by Wolff *et al.* who employed SRIM and COMSOL modelling [7].

In this work, we set out to determine parameter-sets that can serve as a starting point for ion-beam milling of biological objects. For that, well-defined patterns were milled into Field's alloy (also commercialised as Bolton 144), an eutectic mixture of In, Bi and Sn melting at 62°C, Fig.1(left). Subsequently, the patterns were imaged to determine whether the alloy melted or not such that a threshold temperature could be determined for this test-system, Fig. 1, left. In doing so, the most suitable combinations of dwell time and pixel-spacing were determined keeping ion dose and beam current fixed. The corresponding parameter-sets were determined for biological objects comprising insect wings, bacteria and microbial corrosion crusts. Fig. 1(right) shows lines milled into a dragonfly wing with Ne^{+}. Finally, steps towards the development of a simple and flexible mathematical model to estimate the sample temperature under the beam are presented.

[1] Schmidt, Byrne and Maasilta, *Bio-Imaging with the Helium-Ion Microscope*, Beilstein J. Nanotechnol. **(2021)**, 12, 1, DOI: 10.3762/bjnano.12.1

[2] Joens, Huynh, Kasuboski, Ferranti, Sigal, Zeitvogel, Obst, Burkhardt, Curran, Chalasani, Sern, Goetze and Fitzpatrick, *Helium ion Microscopy (HIM) for the imaging of biological samples at sub-nanometer resolution*, Sci. Rep. **(2013)** 3:3514, DOI: 10.1038/srep03514

[3} Leppänen, Sundberg, Laanto, de Freitas Almeira, Papponen, Maasilta, *Imaging Bacterial Colonies and Phage-Bacterium Interaction at Sub-Nanometer Resolution Using Helium-Ion Microscopy* **(2017)** 1, 1700070, DOI: 10.1002/adbi.201700070

[4] Said, Chatzinotas, Schmidt, *Have an Ion on it: The Life-Cycle of Bdellovibrio bacteriovorus Viewed by Helium-Ion Microscopy*, Adv. Biosyst. **(2019)** 3, 1800250, DOI: 10.1002/adbi.201800250

[5] Bandara dragonfly-wing *Resolving Bio-Nano Interactions of E.coli Bacteria-Dragonfly Wing Interface with Helium Ion and 3D-Structured Illumination Microscopy to Understand Bacterial Death on Nanotopography*, *ACS Biomater. Sci. Eng.* **(2020),** 6, 7, 3925–3932 DOI:10.1021/acsbiomaterials.9b01973

[6] Ketola, Leppnen, Turpeinen, Papponen, Strand, Sundberg, Arstila and Retulainen, *Cellulose nanofibrils prepared by gentle drying methods reveal the limits of helium ion microscopy imaging*, RSC Adv. **(2019)** 9, 15668, DOI: 10.1039/c9ra01447k

[7] Wolff, Klingner, Thompson, Zhou, Lin, Peng, Ramshaw and Xiao, *Modelling of focused ion beam induced increases in sample temperature: a case study of heat damage in biological samples* **(2018)** 272, 1, 47, DOI: 10.1111/jmi.12731

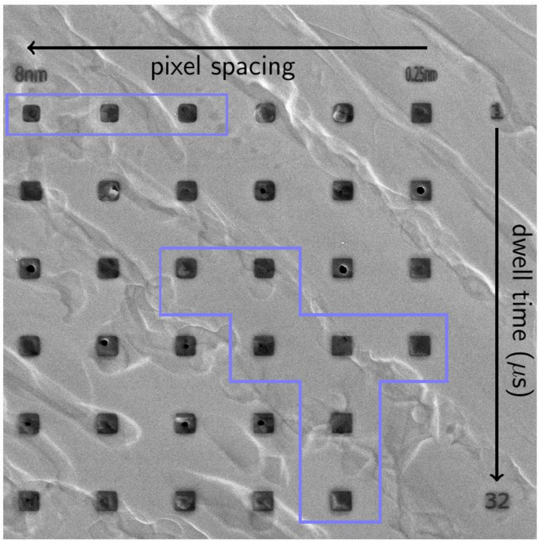

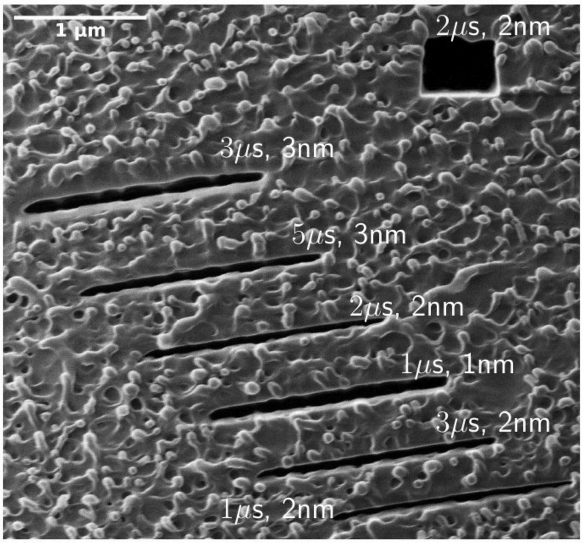

Fig. 1: Left : 25keV He^+-miling of 0.5x0.5µm^2 squares into Field's alloy. The milling was done at a constant ion-dose of 0.5nC/µm^2 with a beam current of 4.2pA. Patches in which the metal did not melt during the miling are framed in blue. **Right:** 25keV Ne^+-milling into a dragonfly wing using a beam current of 1.5pA. The lines are 1.5µm long and milled with an ion-dose of 1nC/µm. The labels indicate dwell time and pixel spacing during the milling, respectively. The rectangle was milled with the same beam current at a dwell time of 2µs and spacing of 2nm. The ion-dose for the rectangle was 1nC/µm^2.

Magneto-structural phase transition in $Fe_{60}V_{40}$ alloy thin films

Md. Shadab Anwar[1,3*], H. Cansever[1], B. Boehm[2], R.A. Gallardo[5], R. Heubner[1], U. Kentsch[1], S. Zhou[1], B. Eggert[4], H. Wende[4], K. Potzger[1], J. Fassbender[1], K. Lenz[1], J. Lindner[1], O. Hellwig[1,2] and R. Bali[1]

[1]Helmholtz-Zentrum Dresden-Rossendorf, Institute of Ion Beam Physics and Materials Research, Bautzner Landstraße , Dresden, Germany
[2]Technical University of Chemnitz, Germany
[3]Technical University of Dresden, Germany
[4]Faculty of Physics and Center for Nanointegration Duisburg-Essen (CENIDE), University of Duisburg-Essen, Lotharstr. Duisburg, Germany
[5]Departamento de Física, Universidad Técnica Federico Santa María, Valparaíso, Chile
*Corresponding Author: m.anwar@hzdr.de

Ferromagnetism can be induced in non-ferromagnetic precursor thin films such as B2 $Fe_{60}Al_{40}$ [1] and B2 $Fe_{50}Rh_{50}$ [2] through lattice disordering. The disordering can be induced using focused ion beams, such as in a He/Ne ion microscope, to produce ferromagnets of desired geometries at the nanoscale. Here we describe a magnetostructural transition in $Fe_{60}V_{40}$ thin films achieved via ion-irradiation. $Fe_{60}V_{40}$ thin films of thickness 40 nm were grown onto heated SiO_2/Si substrate using magnetron sputtering at optimum growth temperature of 573 K. We show that the as-grown films possess a saturation magnetization (M_S) of 17 kA/m and irradiation with 25 keV Ne^+ - ions at fluences of $\sim 5 \times 10^{15}$ ions/cm^2 leads to an increase of M_S to ~750 kA/m , as shown in Fig. 1. Observations using X-ray Diffraction as well as Transmission Electron Microscopy reveal a structural short-range order (SRO) in the as-grown films, that transforms to A2 phase (bcc) $Fe_{60}V_{40}$ with increasing Ne^+ - fluence. Above a threshold Ne^+ - fluence, the A2 region appears to nucleate at the film surface and with increasing fluence, it propagates deeper into the film. The transition has been tracked using Conversion Electron Mössbauer Spectroscopy as well as Ferromagnetic Resonance, to observe the variation of local magnetic ordering and dynamic behavior, respectively. These results form the basis for further investigations on nanomagnets embedded within $Fe_{60}V_{40}$ thin films through the application of focused ion beams.

Financial support by DFG grants BA 5656/1-2 and WE 2623/14-2 is acknowledged.

[1] Ehrler, J. *et al., New J. Phys.*, 22, 073004 (2020).
[2] Eggert, B. *et al., RSC Adv*.,10, 14386 (2020).

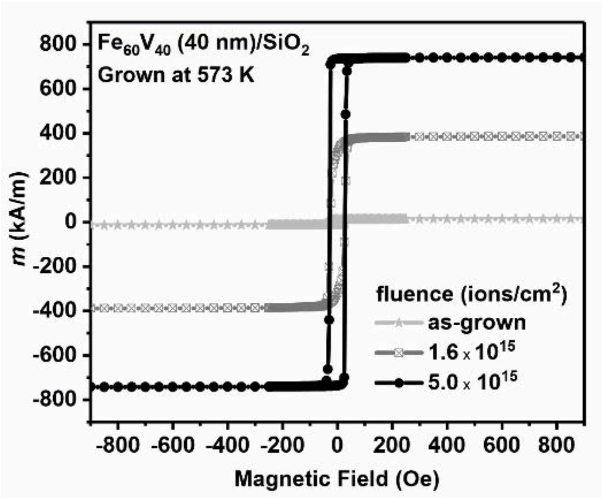

Fig. 1: The effect of 25 keV Ne^+ irradiation at various fluences, on the magnetization vs. field behaviour of $Fe_{60}V_{40}$ thin films.

Achieving Near "Damage-free" (S)TEM Sample Preparation by Low-energy Argon from Focused Multi-ion Plasma FIB

C. Jiao[1*] and D. Phifer[1]

[1] Thermo Fisher Scientific, Eindhoven, The Netherlands
[*] corresponding author email: Chengge.Jaio@thermofisher.com

With the introduction of multi-ions plasma ion beams to FIB-SEM, optimizing ion species for specific tasks is becoming common as our understanding grows from both experience and simulation data. For example, xenon ions have been providing advantages of high sputtering yield for large 3D-volume-data-acquisition, and correlated microscopy applications. Reactive oxygen ion beam processing has also been shown to dramatically improve milling quality for carbon-carbon bonding materials by smoothing the cut-face very effectively during sputtering. In this presentation, we explore the recent progress of low-energy-focused-argon ion beam provided by Helios 5 Hydra Plasma FIB for TEM specimen preparation. The plasma FIB argon ion beam can be used as low as 500 eV for specimen preparation, where ion interactions are closer to conditions needed for producing the lowest damage samples.

Ions species selection is critical for near "damage-free" TEM specimen preparation. With conventional gallium FIB, it is a challenge to make a TEM specimen without gallium implantation because gallium reacts with many materials (e.g., steel, aluminum alloy, GaN/AlGN etc). Xenon plasma FIB first opened an opportunity for "gallium-free" TEM specimen preparation with lower amorphous layer thickness. However, Xenon ions induce higher vacancy-density in target materials.

Experimentation with the Helios Hydra for making (S)TEM samples has confirmed that the focused argon ion beam is the most suitable ion species for damage-free TEM specimen preparation guided by the investigation of ion-solid interaction SRIM data [1].

With Plasma FIB argon ion energy at 500 eV, it is possible to approach "damage-free" TEM specimen preparation domain.

[1] C. Jiao, J. Graham, Xu Xu, T. Burnett, and B. van Leer. Low Energy 500 eV Focused Argon Ion Beam Provided by Multi-Ions Species Plasma FIB for Material Science Sample Preparations. Microsc.Microanal. 27 (Spupl 1). 2021

Mechanism-Based Design of Precursors for FEBID and FIBID

Jo-Chi Yu[1], Scott J. Matsuda,[1] Rachel M. Thorman,[2] Elif Bilgilisoy,[2] D. Howard Fairbrother[2] and Lisa McElwee-White[1,*]

[1] Department of Chemistry, University of Florida, Gainesville, Florida 32611-7200 USA
[2] Department of Chemistry, Johns Hopkins University, Baltimore, Maryland 21218-2685, USA
[*] corresponding author email: lmwhite@chem.ufl.edu

Focused electron beam-induced deposition (FEBID) and focused ion beam-induced deposition (FIBID) are direct write fabrication techniques that use focused beams of charged particles (electrons or ions) to create 3-D metal-containing nanostructures by decomposing organometallic precursors onto substrates in a low-pressure environment. For many applications, it is important to minimize contamination of these nanostructures by impurities from incomplete ligand dissociation and desorption. We use ultra high vacuum (UHV) surface science studies to obtain mechanistic information on electron- and ion-induced processes in organometallic precursor candidates [1, 2]. The results are used for the mechanism-based design of custom precursors for FEBID and FIBID [3, 4].

Differences in the results from FEBID and FIBID will be presented using examples taken from deposition of Ru, Pt and Fe-containing alloys. For example, electron irradiation of $Ru(CO)_4I_2$ yields RuI_2, while ion-induced fragmentation of the same precursor affords pure Ru (Fig. 1). These results suggest that for precursors that undergo incomplete ligand desorption during FEBID, a switch to FIBID could lead to high metal content deposits from the same precursor due to the balance between ion-induced deposition and preferential sputtering of impurity atoms during FIBID.

[1] R.M. Thorman, S.J. Matsuda, L. McElwee-White, D.H. Fairbrother, *Identifying and Rationalizing the Differing Surface Reactions of Low-Energy Electrons and Ions with an Organometallic Precursor*, J. Phys. Chem. Lett. 11 (**2020**) 2006.

[2] E. Bilgilisoy, R.M. Thorman, J.-C. Yu, T.B. Dunn, H. Marbach, L. McElwee-White, D.H. Fairbrother, *Surface Reactions of Low-Energy Argon Ions with Organometallic Precursors*, J. Phys. Chem. C 124 (**2020**) 24795.

[3] W.G. Carden, H. Lu, J.A. Spencer, D.H. Fairbrother, L. McElwee-White, *Mechanism-Based Design of Precursors for Focused Electron Beam-Induced Deposition*, MRS Commun. 8 (**2018**) 343.

[4] J.-C. Yu, M.K. Abdel-Rahman, D.H. Fairbrother, L. McElwee-White, *Charged Particle-Induced Surface Reactions of Organometallic Complexes as a Guide to Precursor Design for Electron and Ion Induced Deposition of Nanostructures*, (**2021**) submitted for publication.

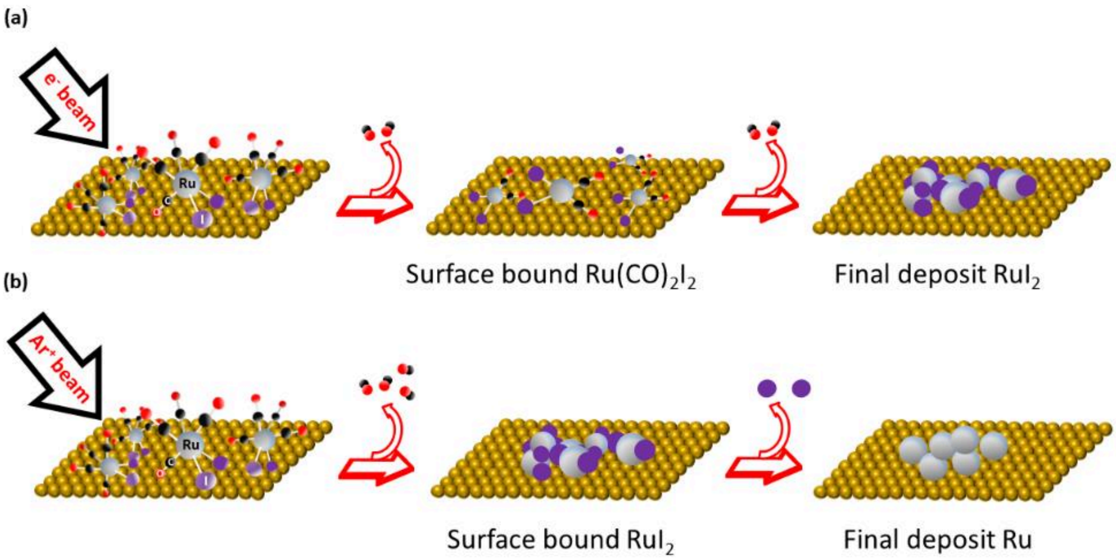

Fig. 1: Comparison of the electron and ion-stimulated surface reactions underlying (a) FEBID and (b) FIBID from $Ru(CO)_4I_2$, respectively. $Ru(CO)_4I_2$ gas phase molecules adsorb to the substrate surface and are exposed to (a) defocused primary electron energy source (500 eV) and (b) defocused Ar^+ ion source (860 V).

The Battle for the last few Nanometers - Refining 3D Nanoprinting of Closed Structures via FEBID

A. Weitzer [1], M. Huth [2], G. Kothleitner [1,3] and H. Plank* [1,3,4]

[1] Institute of Electron Microscopy and Nanoanalysis, Graz University of Technology, 8010 Graz, Austria
[2] Institute of Physics, Goethe University Frankfurt, 60323 Frankfurt am Main, Germany
[3] Graz Centre for Electron Microscopy, 8010 Graz, Austria
[4] Christian Doppler Laboratory - DEFINE, Graz University of Technology, 8010 Graz, Austria
* corresponding author email: harald.plank@felmi-zfe.at

Focused Electron Beam Induced Deposition (FEBID) is one of the few additive direct-write techniques capable of producing 3-dimensional objects on the nanoscale [1]. With feature sizes below 100 nm on a regular basis and below 20 nm under optimized conditions, it is a highly promising candidate for building even complex 3D nanostructures with high precision. The working principle uses the electron beam assisted, localized immobilization of surface adsorbed precursor molecules that are injected into the microscope vacuum chamber in a gaseous state. Thereby, the demands on substrate materials and surface morphologies are very low and together with a constantly growing range of precursor gases, 3D-FEBID evolved into a very powerful and flexible 3D nanoprinting technology. In the past, however, most fabricated 3D structures were meshed [2], meaning individual nanowires were connected at specific points in 3D space to form certain target structures. Recent progress focuses on the expansion from mesh-like towards closed structures, which would strongly enhance its design flexibility. The main challenge in this regard is non-uniform growth conditions due to local beam heating, which for closed objects depends on additional parameters that include the object's overall dimensions and individual XY pixel positions during growth (see Fig. 1). Moreover, complex electron trajectories in closed objects have to be considered, introducing additional proximity effects. To attend all these challenges, we combined 3D-FEBID experiments with finite element simulations and developed a python-based compensation tool. Effectively, the model slightly adapts the parameters at each XY position within individual single layers, according to implications by local beam heating and trajectories, which strongly increases spatial precision (Fig. 2a). This highly precise concept for the fabrication of fully or partially closed 3D objects crucially expands the design possibilities of FEBID-based 3D nanoprinting (Fig. 2b) for new applications in research and development.

[1] L. Hirt et al.; *Additive Manufacturing of Metal Structures at the Micrometer Scale.* Adv. Mater. 29 (**2017**) 1.

[2] R. Winkler et al.; *3D nanoprinting via focused electron beams*. J.Appl.Phys. 125 (**2019**), 210901

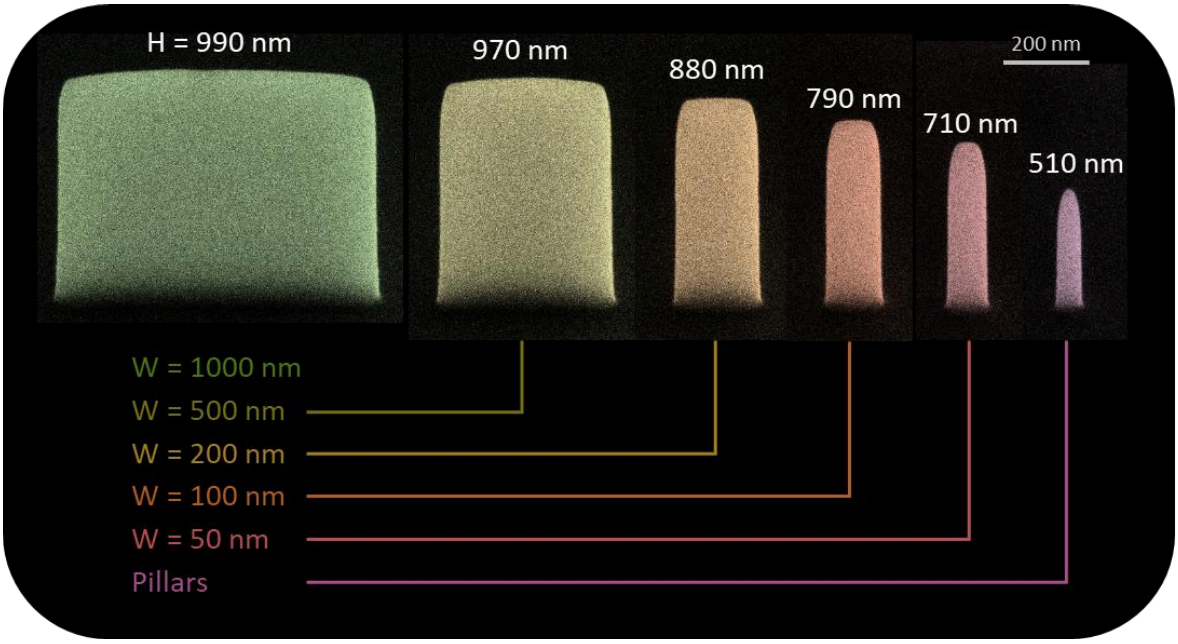

Fig. 1: Display of the different growth conditions for varying element dimensions on the example of vertical walls of different widths that were built with the same total radiation times of 2 s per XY pixel column from bottom to top.

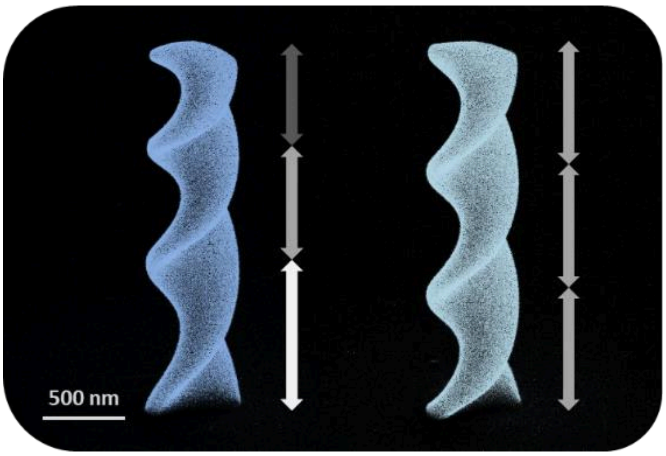

Fig. 2a: Comparison of uncompensated (left) and height compensated screws (right)

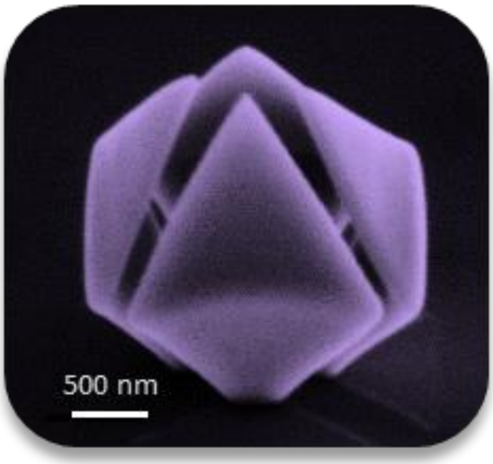

Fig. 2b: Advanced closed 3D Nanostructure

FEBID 3D-Nanoprinting at Low Substrate Temperatures: Pushing the Speed While Keeping the Quality

J. Hinum-Wagner[1], R. Winkler*[1], D. Kuhness [1] and H. Plank[1,2,3,*]

[1] Christian Doppler Laboratory - DEFINE, Graz University of Technology, 8010 Graz, Austria
[2] Institute of Electron Microscopy and Nanoanalysis, Graz University of Technology, 8010 Graz, Austria
[3] Graz Centre for Electron Microscopy, 8010 Graz, Austria

[*] corresponding author email: robert.winkler@felmi-zfe.at; harald.plank@felmi-zfe.at

Focused ion beam (FIB) processing techniques are of great importance in today´s nanofabrication. Beyond subtractive structuring, the typical availability of gas injection systems at related microscopes also enables additive manufacturing by focused particle beam induced deposition (FIBID/FEBID). Recent advances in this field have unlocked the precise fabrication of complex, freestanding 3D architectures at the nanoscale [1], elevating FIB / SEM dual beam microscopes to the status of true 3D nanoprinters. Although 3D-FIBID/FEBID is superior to other direct-write methods in many aspects [2] such as high flexibility in design, material and functionality, the low deposition speed inhibits large-scale production as needed for most industrial applications. The limiting factor for the growth rates is the availability of local precursor molecules. For 3D-FEBID growth, it was found that local heating by the electron beam itself can affect the precursors residence time at the growth front, which changes the effective coverage up to a point, where further growth becomes unstable [3]. Based on those insights, we here reverse the situation and lower the substrate temperature using a home-built Peltier cooling stage inside the FIB to study the impact on growth stability and fabrication precision. In detail, we use a challenging 3D multi-pod designs (Fig. 1) to investigate the growth dynamics (growth rates), wire dimensions, internal grain structure (transmission electron microscopy) and the influence of the support geometry in a temperature range from 5 °C to 30 °C. Results for the Pt-precursor used reveal that cooling the substrate increases the growth rates by a factor up to 5.6 (Fig. 2) without loss of 3D printing quality [4], hence paving the way for more efficient fabrication of high-fidelity 3D nanoarchitectures.

[1] R. Winkler, J.D. Fowlkes, P.D. Rack, H. Plank; *3D nanoprinting via focused electron beams*. J. Appl. Phys. 125 (**2019**), 210901.

[2] L. Hirt, A. Reiser, R. Spolenak, T. Zambelli; *Additive Manufacturing of Metal Structures at the Micrometer Scale.* Adv. Mater. 29 (**2017**) 1.

[3] E. Mutunga, R. Winkler, J. Sattelkow, P.D. Rack, H. Plank, J.D. Fowlkes; *Impact of Electron-Beam Heating during 3D Nanoprinting*. ACS Nano 13 (**2019**), 5198.

[4] J. Hinum-Wagner, D. Kuhness, G. Kothleitner, R. Winkler, H. Plank; *FEBID 3D-Nanoprinting at Low Substrate Temperatures: Pushing the Speed While Keeping the Quality;* Nanomaterials 11 (**2021**), 1527.

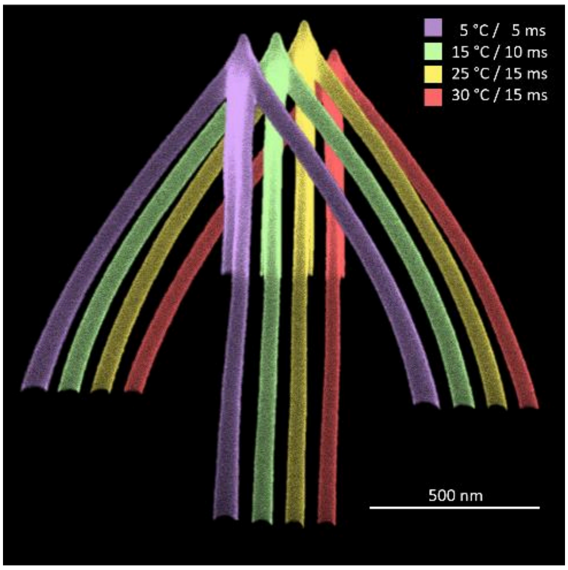

Fig. 1: Maintaining the shape quality during low temperature FEBID. Collage of FEBID-tetrapods of similar height fabricated at substrate temperatures of 5 °C, 15 °C, 25 °C, and 30 °C and pixel process times of 5, 10, 15, and 15 ms.

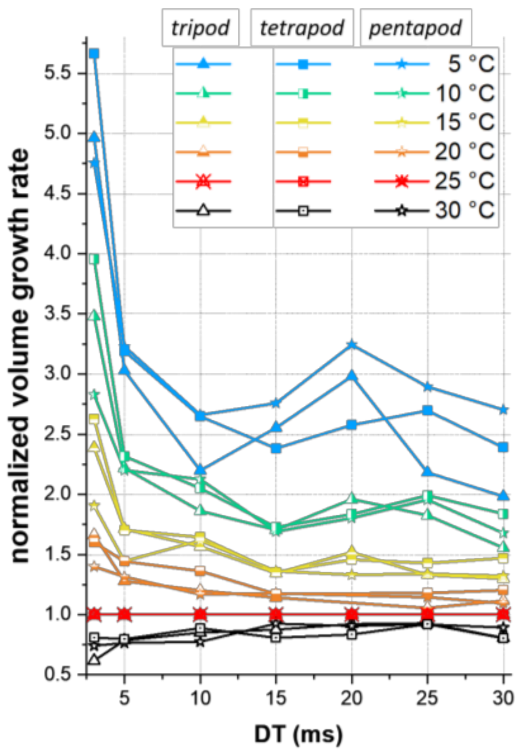

Fig. 2: Boosting the volume growth rates at low temperature FEBID. The plot shows dwell-time dependent volume growth rates for different substrate temperatures (see legend), normalized to 25 °C for tri-, tetra-, and pentapods (see symbols).

Compact Chiral Nano Helix Arrays as Femtomolar Biosensing Tool

M. Manoccio[1,*], M. Eposito[1], E. Primiceri[1], A. Leo[1], V. Tasco[1], M. Cuscunà[1], G. Gigli[1,2] and A. Passaseo[1]

[1] CNR NANOTEC Institute of Nanotechnology, Via Monteroni, 73100 Lecce, Italy
[2] Department of Mathematics and Physics Ennio De Giorgi, University of Salento, Via Arnesano, 73100 Lecce, Italy
*corresponding author email: mariachiara.manoccio@nanotec.cnr.it

Advanced nanofabrication technologies enabling the realization of even more complex structures allow to extend the nanophotonic application field towards new generation biosensors. In such a field, fast and real-time identification of biomarkers is highly demanded for rapid diagnosis with less-invasive methods by means of low-cost miniaturized and portable point of care devices. Here, we demonstrate advanced biosensing capabilities obtained through the compositional and shape-engineering of 3D chiral metamaterials realized with Focused Ion Beam Induced Deposition (FIBID) for the detection of small biomolecules at ultra-low concentrations.

We realized compact arrays of right-handed platinum nano-helices (the core of the device, Figure 1a) by means of FIBID technique. We engineered the growth parameters to build up these structures, evolving in the third dimension, with accurate shape, sizes and geometrical arrangement, in order to operate in the visible range[1]. The obtained intrinsically-chiral geometry generates a circular polarization dependent optical response from these structures, leading to a circular dichroism spectrum evolving as a function of surrounding medium changes, as in Figure 1b. Moreover, the differential nature of this response suppresses background interference effects [2], allowing to work even in optically dense environments like body fluids. The chiral nanostructures have been coated, by means of cyclic voltammetry, with a functional thin polymeric layer, required for subsequent antibody immobilization. The resulting metal-dielectric architecture enhances the chiroptical plasmonic properties of the chiral metamaterial in the far- and near-field, and offers a large surface to molecular immobilization[3]. By tracking the shift of the metamaterial CD spectrum, we recorded the detection of surface-specific binding events between the antibody and the Tar-DNA binding protein, TDP-43, a biomarker for early-stage detection of neurodegenerative diseases[4], at different molar concentration, from 1pM down to 10 fM, in aqueous solutions and in human serum (all the steps are schematically represented in Figure 1c). We believe that our finding provides new perspectives for novel diagnostic tools.

[1] Manoccio, M.; Esposito, M.; Passaseo, A.; Cuscunà, M.; Tasco, V. *Focused Ion Beam Processing for 3D Chiral Photonics Nanostructures*. Micromachines **2021**, 12 (1), 1–28.

[2] Jeong, H. H.; Mark, A. G.; Alarcón-Correa, M.; Kim, I.; Oswald, P.; Lee, T. C.; Fischer, P. *Dispersion and Shape Engineered Plasmonic Nanosensors*. Nat. Commun. **2016**, 7.

[4] M. Manoccio, M. Esposito, E. Primiceri, A. Leo, V. Tasco, M. Cuscunà, D. Zuev, Y. Sun, G. Maruccio, A. Romano, A. Quattrini, G. Gigli, A. Passaseo, *"Femtomolar Biodetection by a Compact Core–Shell 3D Chiral Metamaterial"*, *Nano Lett.* **2021**.

[4] Feneberg, E.; Gray, E.; Ansorge, O.; Talbot, K.; Turner, M. R. *Towards a TDP-43-Based Biomarker for ALS and FTLD*. Mol. Neurobiol. **2018**, 55 (10), 7789–7801.

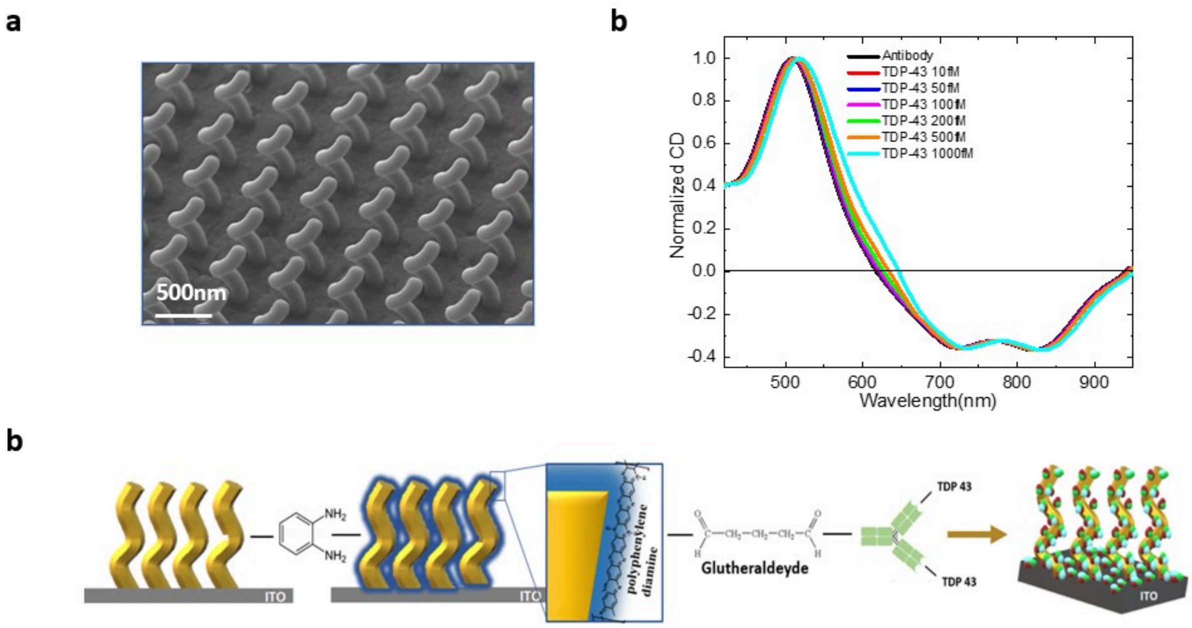

Figure 1. (a) SEM image of nano-helix array. (b) Surface-sensing detection of TDP-43. Normalized CD spectra acquired after the deposition of the antibody layer (used as spectral reference) and different concentrations of TDP-43 ranging from 10 fM to 1 pM. (c) Scheme of the sensing device and functionalization protocol. The core-shell architecture arises from covering the fabricated helix array with the P-oPD insulating polymer. Then, the antibody is immobilized onto the shell after crosslinking by gluthereldeyde. Finally, the target analyte, deposited on the sample surface, is recognized by the specific antibody sites.

Direct writing of chiral and nonlinear plasmonic devices

A. Tsarapkin[1,2*], V. Deinhart[1,2], E. Krauss[3], T. Feichtner[3,4] and K. Höflich[1,2]

[1] Ferdinand-Braun-Institut gGmbH, 12489 Berlin, Germany
[2] Helmholtz Zentrum Berlin, 14109 Berlin, Germany
[3] Physics Institute, University of Würzburg, 97074 Würzburg, Germany
[4] Department of Physics, Politecnico di Milano, 20133 Milano, Italy
[*] corresponding author email: aleksei.tsarapkin@FBH-Berlin.de

The miniaturization of electrical and optical devices over the last decades allowed many technological and economic advancements. With the help of novel techniques, such as direct electron beam writing and focused ion beam milling, it is now possible to achieve genuinely direct manufacturing down to the sub 20 nm scale in 3D.

In telecommunication and quantum optics, devices that permit control over the polarization of light is of crucial importance. Established devices are realized as bulky optical systems, however, we aim at designing a uniquely compact plasmonic converter and detector. The device is based on a vertically oriented gold double helix coupled to a planar two-wire transmission line as a plasmonic waveguide. Previously, the separate building blocks of the suggested system have been well studied. The single helix was shown to act as a sensitive detector of circularly polarized light [1], and the plasmonic waveguide exhibits modes with different effective group velocities depending on the incident polarization state [2]. One can utilize the latter fact to split modes spatially.

Using finite element method modelling, we calculated the extinction efficiency for different helical geometries (see Fig. 1a) and showed that varying helix radii and pitch finely tune resonant wavelengths. We obtained surface charge distributions on the double-helix, showing that both symmetric and antisymmetric modes can be excited (see Fig. 1b-d).

We will present the fabrication protocols that we have developed for both, helices (see Fig. 2a) and two-wire waveguides (see Fig. 2b). While the helices were directly written with a focused electron beam, the two-wire waveguides were cut from single-crystalline gold flakes by means of focused gallium-ion beam milling. We achieved high structuring resolution with both methods what will allow for efficient coupling to transform linear to circular polarization and to non-linearly convert frequency while retaining a device size of just a few microns.

[1] K. Höflich et al.; Resonant behavior of a single plasmonic helix; Optica 6 (**2019**), 1098.

[2] E. Krauss et al.; Reversible Mapping and Sorting the Spin of Photons on the Nanoscale: A Spin-Optical Nanodevice; Nano Lett. 19 (**2019**), 3364.

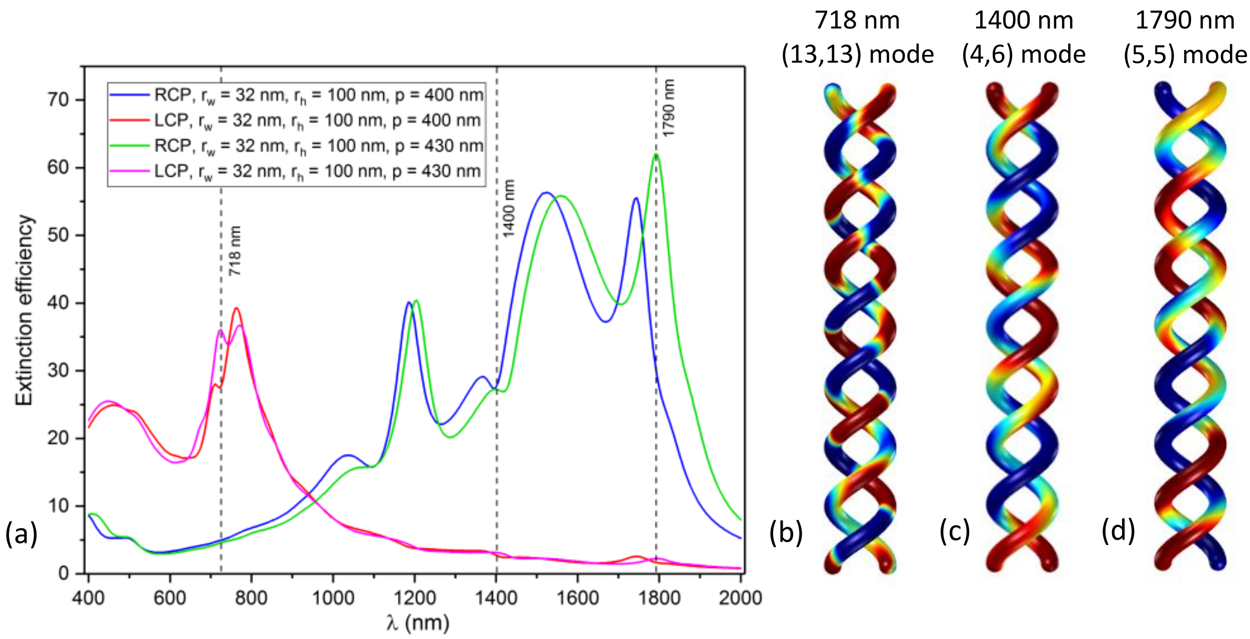

Fig. 1: (a) Extinction efficiency of 4 pitch double helices excited by both right (RCP) and left (LCP) circularly polarized light, r_w – wire radius, r_h – helix radius and p – helix pitch. RCP spectra of the helix with the higher pitch red shifts due to longer effective antennae length [1]. Surface charge distribution of the gold double helix (wire radius is 32 nm, helix radius 100 nm, helix pitch 430 nm, 4 pitches) shows excitation of a symmetric mode under incident LCP light at 718 nm, mode order is (13,13) (b), a mixed symmetric-antisymmetric mode under incident RCP light at 1400 nm, mode order is (4,6) (c) and an antisymmetric mode under incident RCP light at 1790 nm, mode order is (5,5) (d).

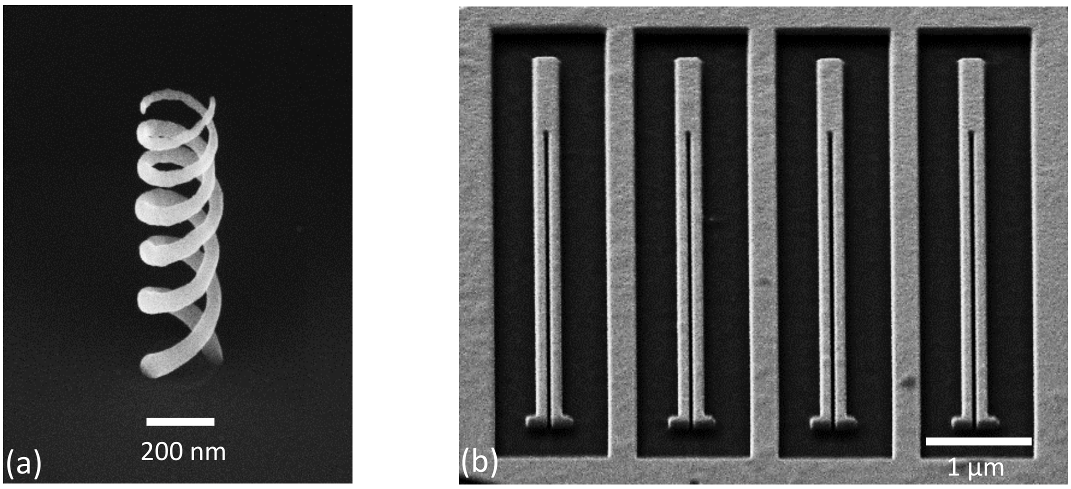

Fig. 2: (a) SEM image of a gold double helix with 3 turns. The image was taken for 45°. (b) SEM image of FIB milled two-wire transmission lines, width of the gaps does not exceed 25 nm. The image was taken for 54° tilt angle.

Adding the Design Possibility of Variable Diameters via Blurred Electron Beams during 3D Nanoprinting via FEBID

L. M. Seewald[1], R. Winkler [1], G. Kothleitner[2], H. Plank[1,2,3 *]

[1] Christian Doppler Laboratory – DEFINE, Graz University of Technology, 8010 Graz, Austria
[2] Graz Center of Electron Microscopy, 8010 Graz, Austria
[3] Institute of Electron Microscopy and Nanoanalysis, Graz University of Technology, 8010 Graz, Austria
[*] corresponding author email: harald.plank@flemi-zfe.at

Additive, direct-write fabrication via focused particle beams has evolved into a reliable 3D printing technology at the micro and nanoscale[1]. Similar to focused ion beam induced deposition (FIBID), the electron-based equivalent FEBID uses the nanoscale particle beam for highly localized immobilization of surface adsorbed precursor molecules. As the latter is injected by gas injection system, the demands on substrate material (vacuum and e-beam compatible) and surface morphology (accessible by the e-beam) are modest. Accurate control of the lateral beam movement enables highly localized deposition and thereby allows the fabrication of even complex 3D structures with nanoscale features down to the sub-20 nm range for freestanding features. While indispensable for certain purposes (e.g. 3D magnetic lattices[2] or nano-plasmonics [3]), the morphological delicacy of such structures can also result in low mechanical rigidity and limited thermal / electrical conductivities, narrowing the range of possible applications. Furthermore, it has recently been shown, that the overall 3D design is partly implying the finally arising branch diameters in an invariable way[4], which can limit the final functionality. Hence, it follows that a controlled diameter tunability is less optional but rather a prerequisite. Based on this motivation, we here introduce deliberate beam blurring as additional fabrication parameter and study its implications on 3D structures (Fig. 1). In addition, we observe and explain an increase in growth efficiencies by factors up to 5, driven by a shift in working regime conditions (Fig. 2a). At the same time, the highly unwanted proximal growth beneath intended 3D branches is strongly delayed, which increases the reliability of 3D-FEBID. By that, controlled on-purpose beam blurring expands the design flexibility of this technology (Fig. 2b) by means of tunable diameters for meshed objects at higher volume growth rates and reduced proximal growth.

[1] Winkler et al, J. Appl. Phys. 125 (**2019**) 210901

[2] Keller et al, Sci. Rep. 8 (**2018**) 6160

[3] Winkler et al, ACS Appl. Mater. Interfaces 9 (**2017**) 8233-8240

[4] Winkler et al, Addit. Manuf. 46 (**2021**) 102076

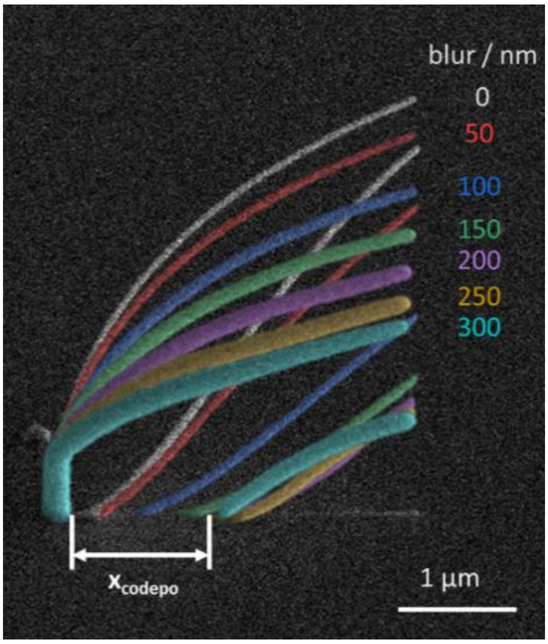

Fig. 1: Collage of 3D-FEBID "diving boards" illustrating the implications of a blurred electron beam. Branch dimensions can be tuned and segments exhibit less bending for increased blur (see legend), depicting improved growth stability. Additionally, unwanted proximal growth is strongly delayed, as indicated by the distance X_{codepo} and discussed in more detail in the contribution.

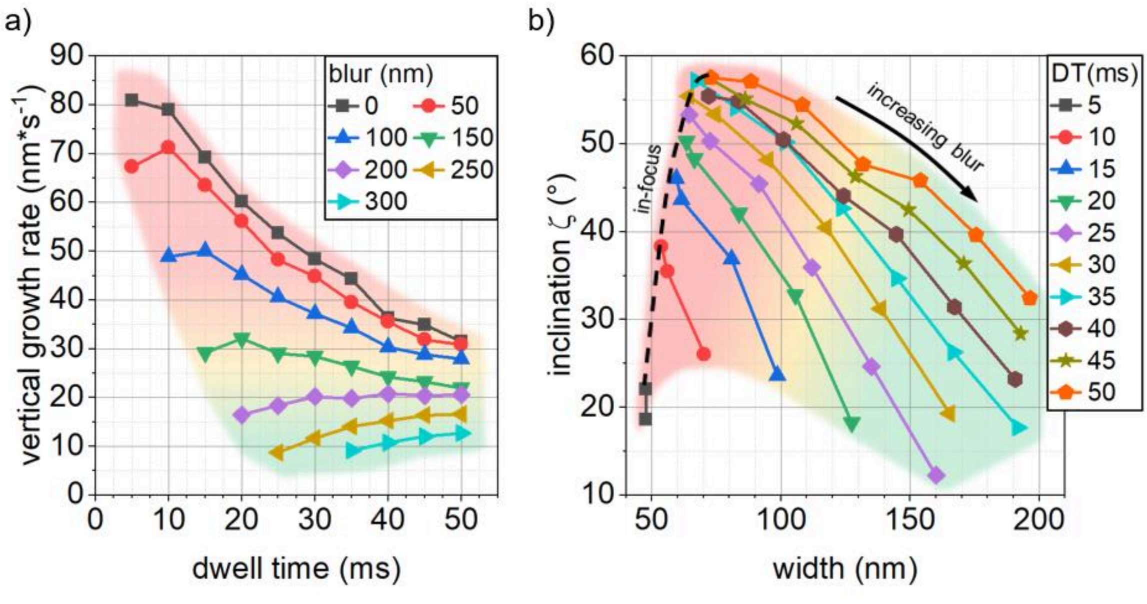

Fig. 2: a) Vertical growth rates as function of dwell time for differently blurred e-beams. With increasing beam blur the vertical growth rate changes its dwell time related behavior, indicating a shift in the working regime conditions. b) Added design flexibility to structural dimensions upon introducing a deliberately blurred beam. The dashed line illustrates the achievable inclination – width pairs for 3D branches at in-focus conditions.

4th EuFN and FIT4NANO
Joint Workshop

Poster Presentations

September 27th - 30th, 2021
Vienna, Austria

Helium Ion Microscopy Images of Aerosols trapped in filters
HZDR

Real time static SIMS Monitoring of Catalytic CO Oxidation to CO2 Over Platinum Surfaces

Marcel Janák[1], Antonín Jaroš[1], Dominik Hrůza[1], Miroslav Kolíbal[1,2] ,Tomáš Šikola[1,2], Petr Bábor[1,2*]

[1] Institute of Physical Engineering, Faculty of Mechanical Engineering, Brno University of Technology, Technická 2896/2, Brno, 616 69, Czech Republic
[2] CEITEC - Central European Institute of Technology, Brno University of Technology, Brno, 616 00, Czech Republic
[*] corresponding author email: baborpetr@gmail.com

Industrial development in recent decades has raised the importance of CO elimination from various gas product streams. Incomplete fossil fuel combustion in the production and transportation sector is the primary sources of atmospheric CO. Increased CO concentrations in living environments cause oxygen deprivation of the human body vital organs. CO molecules are also an unwanted byproduct of hydrogen production from natural gas or other carbon feedstocks (e.g., methanol). Excessive CO feeds to hydrogen fuel cells may cause decay in their electro-generation performance.

Platinum group metals (Ru, Rh, Pd, Ir, Pt) are the most widespread catalysts for CO oxidation by O2. The role of the catalyst is to increase the reaction rate by lowering activation barriers. Although the catalyst remains throughout the reaction unconsumed, structural changes like catalyst sintering, surface faceting, or surface poisoning in long-term runs lead to the catalytic activity lowering. Therefore, reaction mechanism and deactivation mechanism understanding is crucial for designing stable CO catalytic converters with high CO conversion rates.

Many conventional surface science techniques may be employed for heterogeneous catalysis research but not all of them offer sufficient chemical, spatial and temporal resolution. The selection of proper techniques is based on the research objectives. Our study's objective is the dynamics of catalytic CO oxidation over platinum polycrystalline microstructures at high vacuum pressures (1E-5 mbar). In-situ scanning electron microscopy (SEM) and in-situ static secondary ion mass spectrometry (SSIMS) were employed for the real-time observation of gas-phase- and temperature-induced processes on platinum surfaces. Elemental composition changes observed by in-situ SSIMS were compared with work function changes observed by in-situ SEM. Our research demonstrates the abilities of in-situ SSIMS as a powerful technique for the real-time chemical monitoring of surface composition in a flow reactor under fixed conditions. Spatio-temporal patterns of varying surface coverages were observed during distinct catalyst regimes in both instruments (see Figire 1 and Figure 2).

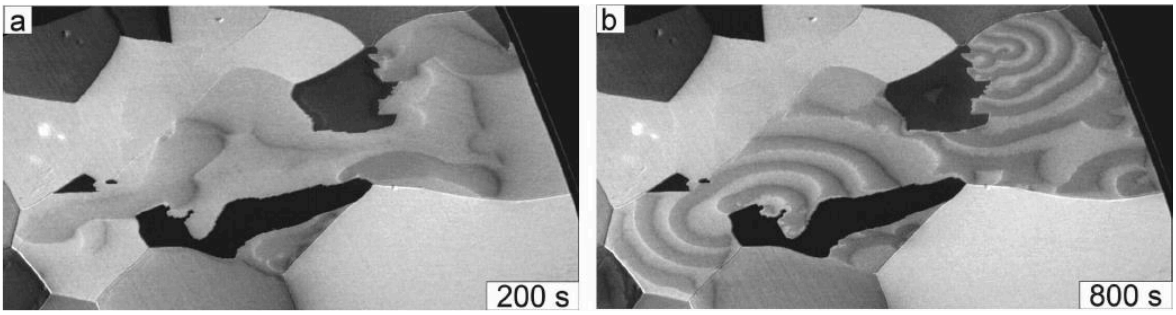

Figure 1: Temporal evolution of rotating spirals on Pt(4,1,10) surface at T = 170 °C observed by UHV-SEM TESCAN, pCO = 3.0 · 10−4 Pa, pO2 = 1.5 · 10−3 Pa. Bright areas are covered by CO; dark areas are covered by oxygen. The figure a) shows the evolution of the waves at the beginning of the experiment and formation of the spiral waves is on the figure b).

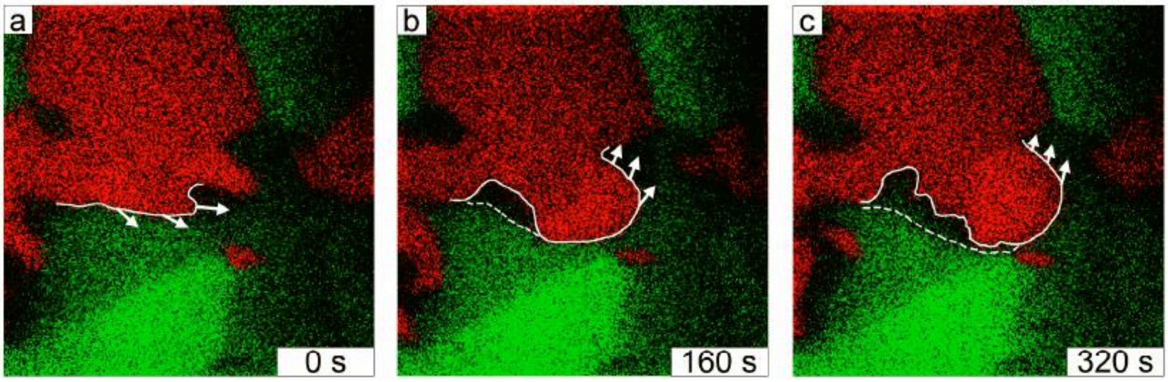

Fig. 2: Temporal evolution of patterns observed on an active Pt(4,1,10) grain at T = 170°C, p_{CO} = 3.0E-4 Pa, p_O = 1.5E-3 Pa measured by TOF-SIMS5 IONTOF on the same Pt grain line in the Figure 1. A full white line highlights the moving wavefront; white arrows indicate the direction in which the wave proceeds between frames; a dashed white line delimits the area without chemisorbed reactants.

Modifying Single-Layer and Bi-Layer Graphene using a Medium-Energy Electron Beam: A Raman Spectroscopy Study

J. Bonello Boissevain[1] , A. Agius Anastasi[1*]

[1] Department of Metallurgy and Materials Engineering, Faculty of Engineering, University of Malta, Msida, Malta
[*] corresponding author email: anthea.agius-anastasi@um.edu.mt

Exploring the influence of ion and electron beam interactions on graphene has paved the way towards modifying graphene's properties through defect engineering. This work focuses on introducing atomic defects in pristine chemical vapour deposited (CVD) single and bi-layer graphene (SLG and BLG) using both electron beam (EB) irradiation and oxidative etching. Raman spectroscopy was primarily used to characterise the graphene. Both EB irradiation and oxidative etching have been found to show a significant ability to modify the crystalline lattice of graphene by inducing boundary and vacancy-like defects and cause extensive blue-shifting in the primary D, G, and 2D peaks, respectively.

Using an electron beam at an accelerating voltage of 19.9 keV, CVD SLG deposited on silicon wafer was exposed to EB doses ranging from 22 to 278,000 $\mu C/cm^2$. This was followed by chemical etching using acidic potassium permanganate. A second layer of CVD SLG was then deposited on top of the modified graphene, hence creating a BLG stack. The same EB irradiation and chemical etching steps were repeated on the BLG. At every stage, Raman spectroscopy was used to understand the effect of electron bombardment on the crystalline quality of graphene. The Raman spectra for SLG and BLG graphene after EB bombardment, shown in Fig. 1, and a ratio between the D and D' peak intensities (I(D)/I(D')) of ~ 7 indicate that electron bombardment with a dose of 278,000 $\mu C/cm^2$ successfully induced vacancy-like defects [1].

Defect engineering graphene's properties using electron and ion bombardment has shown immense promise towards modifying graphene's properties for a wide range of applications, such as in filtration or desalination membranes [2].

[1] A. Eckmann, A. Felten, A. Mischenko, L. Britnell, R. Krupke, K. S. Novoselov and C. Casiraghi, "Probing the Nature of Defects in Graphene by Raman Spectroscopy," *Nano Letters,* vol. 12, no. 8, pp. 3925-3930, 2012.

[2] S. C. O'Hern, M. S. H. Boutilier, J.-C. Idrobo, Y. Song, J. Kong, T. Laoui, M. Atieh and R. Karnik, "Selective Ionic Transport through Tunable Subnanometer Pores in Single-Layer Graphene Membranes," *NanoLetters,* vol. 14, pp. 1234-1241, 2014.

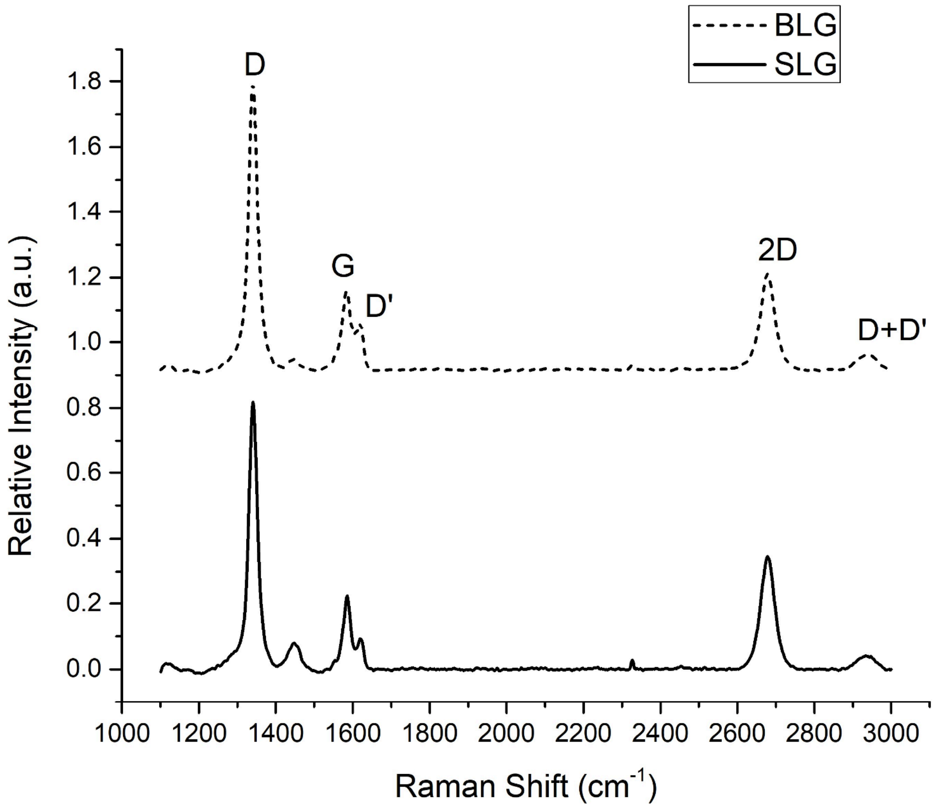

Fig. 1: Raman Spectra of SLG and BLG after electron bombardment at a dose of 278,000 μC/cm^2.

New volatile palladium(II) and nickel(II) perfluorinated amidine derivatives as potential precursor in FEBID/FIBID methods

A. Butrymowicz[1*] and I. B. Szymańska[1]

[1] Nicolaus Copernicus University, Faculty of Chemistry, Torun, Poland

[*] corresponding author email: aleksandra.butrymowicz@doktorant.umk.pl

Focused Electron/Ion Beam Induced Deposition (FEBID/FIBID) methods need enable to obtain 2D or 3D deposits, which are attractive due to the possibility of using them in nanoelectronics, biological diagnostics, and detection of substances using surface-enhanced Raman spectroscopy (SERS) [1]. These methods require metal coordination compounds that exhibit specific properties such as volatility, thermal stability, and sensitivity to electron or ion beams [2].

The synthesis of new, user-friendly perfluorinated palladium(II) and nickel(II) amidine derivatives with the general formula $[Pd_3((NH)_2CR_f)_6]$ and $[Ni_2(NH_2NHCR_f)_2(\mu{-}O_2CR_f)_4]$, where $R_f = CF_3$, C_2F_5 was developed. The composition and structure of the molecules were proposed on the basis of spectroscopy and elemental analysis. The compounds were studied by Thermal Analysis, Electron Impact Mass Spectrometry, Variable Temperature Infrared Spectroscopy – VT IR, and sublimation experiments to determine the volatility and the mechanism of their thermal decomposition. The data prove that palladium(II) complexes go into the gas phase without decomposition at 160°C, while in the case of nickel(II) compounds, sublimation temperature is lower, about 120°C. Based on the VT IR spectra analysis for $[Pd_3((NH)_2C_2F_5)_6]$, the presence of the complex in vapours was confirmed over the range 473−553 K. The EI MS and SEM/EDX studies were carried out to preliminary determine the interactions of the compounds with low and high energy electrons. In EI MS spectra molecular ion $[Pd_3((NH)_2CR_f))_6]^{+\bullet}$ and the following metallated fragments containing palladium: $[Pd_3((NH)_2CR_f)_5]^+$, $[Pd_3((NH)_2CR_f)_4]^+$, $[Pd_2((NH)_2CR_f)_4]^{+\bullet}$, $[Pd_2((NH)_2CR_f)_2]^{+\bullet}$, $[Pd((NH)_2CR_f)]^+$, $[Pd_3]^+$ were detected.

Acknowledgments

The A.B. wishes to acknowledge the Nicolaus Copernicus University for a grant: „Grants4NCUStudents" – IDUB project: 4101.00000070.

[1] P. Li, N. Liu, H. Yu, F. Wang, L. Liu, G. Lee, Y. Wang, W. J. Li; *Silver nanostructures synthesis via optically induced electrochemical deposition*; Sci. Rep. **(2016)**, 1–8.

[2] I. Utke, P. Swiderek, K. Höflich, K. Madajska, J. Jurczyk, P. Martinović, I. B. Szymańska; *Coordination and organometallic precursors of group 10 and 11: Focused electron beam induced deposition of metals and insight gained from chemical vapour deposition, atomic layer deposition, and fundamental surface and gas phase studies*; Coord Chem Rev. **(2021)**, 10.1016/j.ccr.2021.213851.

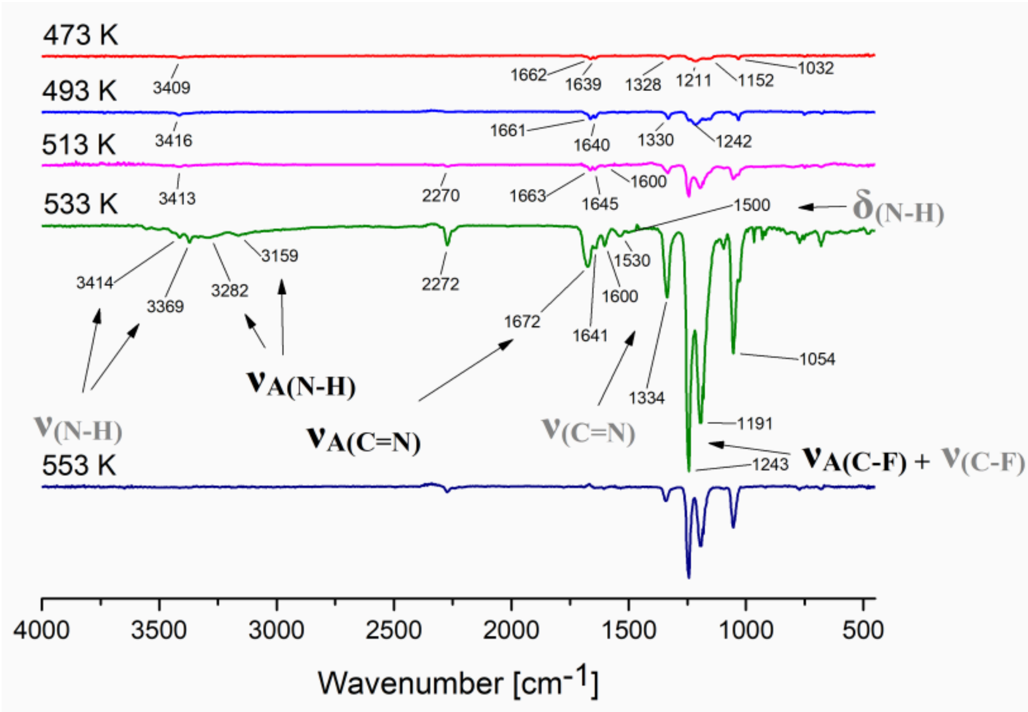

Fig. 1: VT IR spectra of $[Pd_3((NH)_2CC_2F_5)_6]$ in the temperature range 473–553 K, (labels: gray – bands characteristic for complex; black – bands typical for $NH_2(NH{=})CC_2F_5$).

Transport properties of systematically disordered Cr_2AlC films

J. S. Cabaço[1*], U. Kentsch[1], J. Lindner[1], J. Fassbender[1], C. Leyens[2,3], R. Bali[1], R. Boucher[2]

[1] Institute of Ion Beam Physics and Materials Research, Helmholtz-Zentrum Dresden-Rossendorf, Bautzner Landstraße 400, 01328 Dresden, Germany

[2] Institute for Materials Science, Technische Universität Dresden, Helmholtzstraße 7, 01069 Dresden, Germany

[3] Fraunhofer Institute for Material and Beam Technology IWS Dresden, Winterbergstraße 28, 01277 Dresden, Germany

* Corresponding author email: j.salgado-cabaco@hzdr.de

Nano-lamellar composite materials, known as MAX-phases, can possess a combination of ceramic and metallic properties. A prototype compound is Cr_2AlC, formed from a unit cell of Cr_2C sandwiched between atomic planes of Al, thereby imparting a good electrical conductivity, as well as mechanical stability, radiation and oxidation resistance [1, 2]. These properties rely on the lamellar structure of the compound, and systematic introduction of defects, such as displacing or doping atoms within the layers, has the potential to tune electron transport and modify magnetic properties. An ideal tool for defect implantation is ion-irradiation, available both in the form of a broad-beam for wafer-scale processing as well as focused ion-beams for device prototyping. Here we observe the modifications to the structural, transport and magnetic behavior of 500 nm thick Cr_2AlC after irradiation with Co^+ ions, and Ar^+ noble gas ions as control. The films were irradiated with 450 keV of Co^+ ions at fluences varying from 5×10^{12} to 5×10^{15} ions.cm^{-2}, and the control samples with 400 keV Ar^+ ions keeping the sample fluences. Structural analysis using XRD shows that ion-irradiation induces a suppression of the 0002 reflection, indicating a gradual decay of the nano-lamellar structure, see Fig. 1a. Increasing ion-fluence also leads to an increase of the saturation magnetization at 1.5 K, whereby both Ar^+ and Co^+ cause an increased magnetization, respectively to 150 and 190 kA.m^{-1}, for the highest fluences used. Large variations of the transport properties are observed (Fig. 1 b). Magnetoresistance (MR) in the non-irradiated sample shows a classical B^2 dependency, even up to high temperatures. At Co^+ fluences of 5×10^{13} ions.cm^{-2} the MR at 10 T shows a 2 orders of magnitude increase, up to 3% (10 T) at 100 K, see Fig. 1b. A similar effect also occurs for 5×10^{12} ions.cm^{-2} Ar^+ irradiated films, however with a smaller MR-increase. It appears that resistivity increases and the residual resistance ratio reduces with increasing fluence due to the introduction of disorder. These results show that ion irradiation induces significant changes in the transport properties of MAX phase materials, that will be further investigated. The systematic disordering of nano-laminated MAX phase films may therefore reveal interesting disorder and spin-related transport phenomena.

Funding by the Deutsche Forschungsgemeinschaft (DFG) - Project number 456078299 is acknowledged. Ion-irradiation has been performed at the Ion Beam Centre of the HZDR.

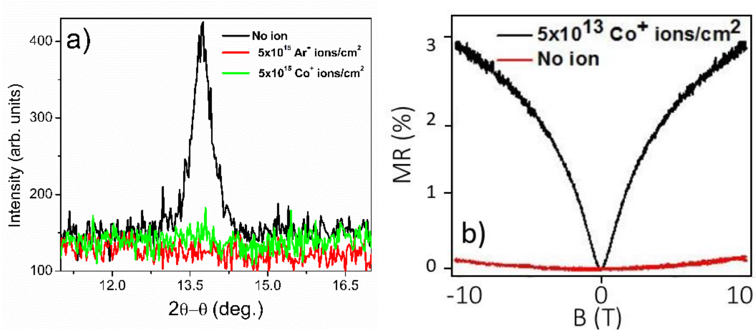

Fig.1: a) X-ray diffraction data for Cr_2AlC before and after irradiation with 5×10^{15} ions.cm^{-2} of Ar^+ and Co^+, measured at room-temperature, the peak suppression after implantation is evident. b) Magnetoresistance plot for no-ion and Co^+ implantation at 100 K and 5×10^{13} ions.cm^{-2}, a remarkable increase can be seen in the latter.

[1] A. S. Ingason, M. Dahlqvist, J. Rosen, Magnetic MAX phases from theory and experiments; a review; J. Phys.: Condens. Matter 28 (2016), 433003. [2] M. W. Barsoum, MAX Phases: Properties of Machinable Ternary Carbides and Nitrides; Weinheim: Willey-VCH (2013). [3] C. Wang, T. Yang, C. L. Tracy, C. Lu, H. Zhang, Y.-J. Hu, L. Wang, L. Qi, L. Gu, Q. Huang, J. Zhang, J. Wang, J. Xue, R. C. Ewing, Y. Wang, Disorder in $M_{n+1}AX_n$ phases at the atomic scale, Nature Communications 10, 622 (2019).

FIB-Fabricated Micro-Resonators

A. Estry[1*], C. Putzke[1] and P. Moll[1]

[1] Ecole Polytechnique Fédérale de Lausanne (EPFL), Institut des Matériaux, CH-1016 Lausanne, Switzerland
[*] corresponding author email: amelia.estry@epfl.ch

Elastic properties of materials are critical values which play a significant role both as a determinant for mechanical structures and as encoders for electronic behavior. Resonance-based techniques are probes of elasticity with exquisite sensitivity that require high geometric precision. We employ FIB microstructuring and deposition to fabricate cantilevers for the exploration of their mechanical and electronic properties as a function of temperature. The use of the FIB enables the study of quantum materials where clean room processes are unavailable. Furthermore, gas-assisted FIB induced deposition of metals, such as tungsten and platinum, have a unique microstructure that results in properties differing from their pure-metallic counterparts. Studies such as vibration of nanopillars[1,2] have been conducted to explore the mechanical properties of FEB and Ga-FIB deposits, while Xe-FIB deposits and the temperature response of these materials remain largely unexplored. We grow free-standing cantilevers of Xe-FIB deposits on thin Si_3N_4 membranes to probe their elasticities. As these deposits play a significant role for our micro-resonators fabricated from quantum materials, developing an understanding of their properties becomes increasingly critical.

[1] G. Arnold et. al.; *Tunable 3D Nanoresonators for Gas-Sensing Applications.* Adv. Funct. Mater. (**2018**).

[2] I. Utke, J. Michler,R. Winkler, H. Plank; *Mechanical Properties of 3D Nanostructures Obtained by Focused Electron/Ion Beam-Induced Deposition: A Review.* Micromachines. (**2020**), 397.

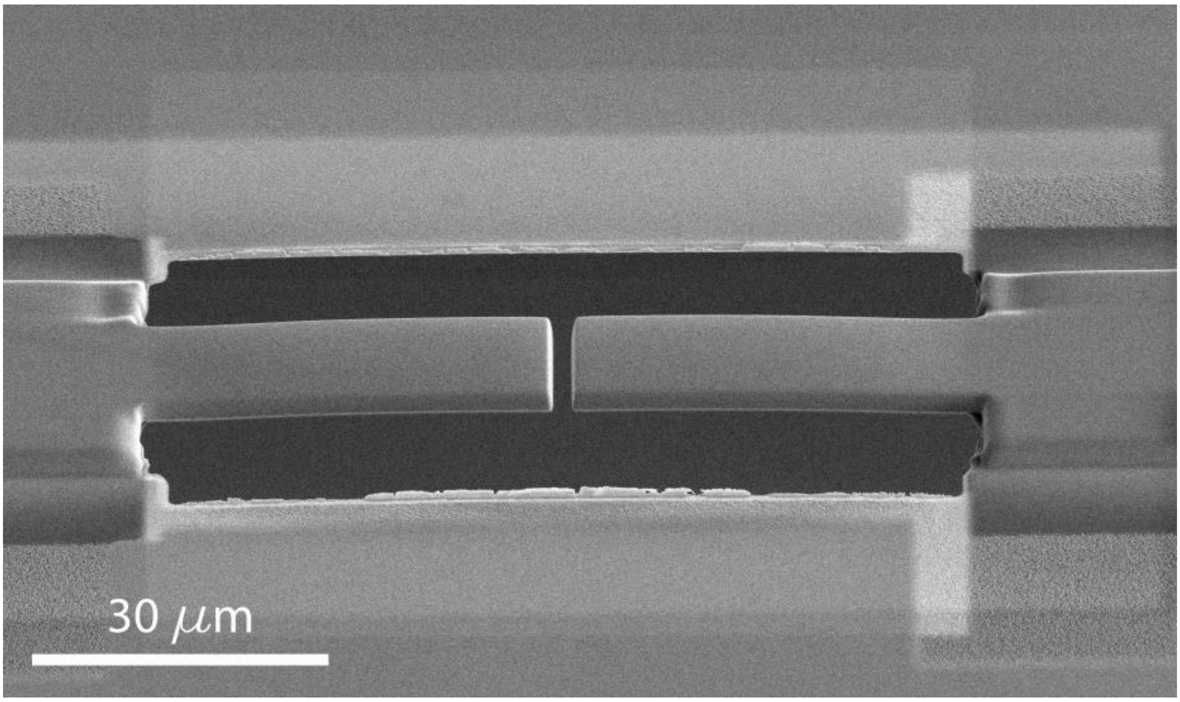

Fig. 1: Free-standing cantilever of FIB deposited tungsten fabricated on Si_3N_4 membrane.

Observing Carbon in Electron and Ion Beam deposition within FIB-SEM

Nicholas T.H. Farr,[1]* Gareth M. Hughes[2] and Cornelia Rodenburg[1]

[1] Department of Materials Science and Engineering, Sir Robert Hadfield Building, Mappin Street, University of Sheffield, Sheffield S1 3JD, UK
[2] Department of Materials, University of Oxford, Parks Road, Oxford OX1 3PH, UK;
* corresponding author email: n.t.farr@sheffield.ac.uk

Abstract: It is understood that carbon contamination present in scanning electron microscopes (SEM), Focused ion beam (FIB) systems and FIB-SEMs, can cause imaging artefacts which can influence the quality of TEM lamellae or structures fabricated within FIB-SEMs. The severity of such effects is contingent not only on the amount of carbon within a chamber but also its bonding state. Regardless of this, the presence of carbon and its bonding state is not routinely monitored within FIB-SEMs. In this presentation/study we confirmed that Secondary Electron Hyperspectral Imaging (SEHI) can be applied in different FIB-SEMs and used to monitor carbon built up/removal and bonding changes resulting from electron/ion beam exposure. In addition to the capacity to monitor, this presentation will also show the capability of Plasma FIB Xe exposure to remove unwanted carbon contamination from the surface of a Ti6246 alloy without the requirement of chemical surface treatments [1].

Results: Figure 1 displays the comparison of Highly oriented pyrolytic graphite (HOPG) secondary electron spectra (SES) collected in two separate Helios instruments. Here, the collection of SES from HOPG surfaces verifies SE peak positions, and acts as an initial calibration. From the collected SES, it is detected that both instruments expressed SE peak emissions at the same energy values. Two clear peaks were revealed by both instruments in the energy regions of 2–4.2 eV and 4.6–6 eV. Expected SE emission differences between the two SES plots appear in the peak intensities previously identified as sp2 and sp3 carbon bonding [2,3,4]. This initial baseline SES collected is useful not only to monitor carbon, but also to allow insights into the cleanliness of an SEM chamber and what forms of contaminant are present.

To gain a better understand of these two forms of carbon contamination, and the effect of sustained EBID (electron beam induced deposition) SES was collected from different areas of interest on an HOPG surface within the Helios DualBeam Plasma FIB. Figure 2A displays the resulting SES spectra from the various regions identified within Figure 2B. The three regions are termed EBID HOPG, HOPG and Aged HOPG. As the Figure 2B confirms, the EBID HOPG spectrum was taken from within a typical EBID window formed on a freshly exfoliated HOPG`s surface by scanning the area with the electron beam for 60 s. The HOPG spectrum was collected in a region outside this scan window. The Aged HOPG spectrum is taken from a grain that appears much brighter than most of the freshly exfoliated HOPG. Consequently, it is assumed that this is a grain of HOPG which had not been cleaved away entirely during the exfoliation procedure. All three regions showed peak emissions in the two ranges highlighted above in Figure 1, which is consistent with previous studies. EBID HOPG exhibited a larger emission for ACC build up than that of Aged HOPG and the exfoliated HOPG. Aged HOPG showed greater ACC than that of exfoliated HOPG, and also a greater sp3 peak than that of both the other regions.

From the SEHI stacks presented (Figure 2C) it is clear that a strong emission within the EBID window is present for sp2 and ACC. This finding further indicates that EBID can contribute to ACC deposition. Comparing Figure 2C SEHI stack to Figure 2D indicates that ACC has the capacity to prevent the emission of sp3 surface aged contamination by replacing it with ACC. Lastly from SEHI chemical mapping Figure 2E was produced via the uncovering of a component from NNMF in a range previous considered to be emissions resulting from the inclusion of oxygen containing functionalities [2]. The principal factor responsible for carbon surface evolution is the adsorption of water which significantly affects the properties of the surface. The emission signal displayed in the original CO/OH SEHI map (Figure 2E) was originally challenging to visualise therefore an enhanced brightness map was created and is given in Figure 2F. Here it is noticeable that oxidation of HOPG appears to be focused in regions of Aged HOPG and is covered in part by EBID contamination. These results highlights SES and SE chemical mapping abilities to observe and evaluate various forms of sample contamination within an SEM chamber from evidence taken from two different DualBeam SEM instruments. Results from the study also confirmed that SE chemical mapping has the capacity to chemically map surface contamination in both organic and non-organic material systems.

Utility Evaluation of GaN-tip Probes Fabricated in Focused Electron and Ion Beam Technology for Atomic Force Microscopy

Ewelina Gacka[1*], Piotr Kunicki[1], Paulina Łysik[1], Krzysztof Gajewski[1], Paulina Ciechanowicz[2,3], Dominik Badura[1], Bartosz Pruchnik[1], Damian Pucicki[1,2], Tito Busani[4], Teodor Gotszalk[1]

[1] Wrocław University of Science and Technology, Faculty of Microsystems Electronic and Photonic, Department of Nanometrology, Janiszewskiego 11/17, 50-372 Wrocław, Poland
[2] Łukasiewicz Research Network – PORT Polish Center for Technology Development, Stabłowicka 147, 54-066 Wrocław, Poland
[3] University of Wrocław, Faculty of Physics and Astronomy, Maxa Borna 9, 50-204 Wrocław, Poland
[4] University of New Mexico, Center for High Technology Materials, 1313 Goddard St SE, Albuquerque, NM 87106, United States of America
[*] corresponding author email: ewelina.gacka@pwr.edu.pl

Progress on the development of probes for scanning probe microscopy has been observed for years. Standard silicon cantilevers are commercially used and common in mass-production but do not satisfy all reliability criteria for measurements. Both cantilever tips and their conductive coating can degrade due to interaction with the investigated sample. For this reason, new conductive tip materials characterized by high hardness and good electrical properties are sought. Interesting to consider are AIII-BV materials, especially GaN. A scanning electron microscope (SEM) with focused ion beam (FIB), gas injection system and nanomanipulators can be used to fabricate such novel devices.

In this paper we report about GaN tip fabrication steps and verification of its properties and reliability in atomic force microscopy (AFM) and conductive atomic force microscopy (C-AFM) measurements. GaN microrod (MR) was used as tip. MRs were fabricated in the molecular beam epitaxy system in the vapour-liquid-solid growth mode at the PORT Polish Center for Technology Development [1]. The vertical growth of the columns was induced by As atoms. This resulted in columns with height and diameter of about 5.5 µm and 1 µm, respectively. GaN MR was transferred and welded on commercial silicon cantilever using focused electron beam induced deposition (FEBID) technology in SEM/FIB system – Fig. 1. To achieve nanometre resolution in AFM/C-AFM measurements, the tip was formed by FIB.

The mechanical parameters of the cantilever were determined by measuring the thermomechanical noise with a laser vibrometer. The utility of the tip was verified by C-AFM and long-time AFM measurements on the HOPG investigated sample in ambient conditions.

[1] P. Ciechanowicz, S. Gorantla, P. P. Michałowski, E. Zdanowicz, J. G. Rousset, D. Hlushchenko, K. Adamczyk, D. Majchrzak, R. Kudrawiec D. Hommel; *Arsenic-Induced Growth of Dodecagonal GaN Microrods with Stable a-Plane Walls*; Advanced Optical Materials 9 (2021), 2001348.

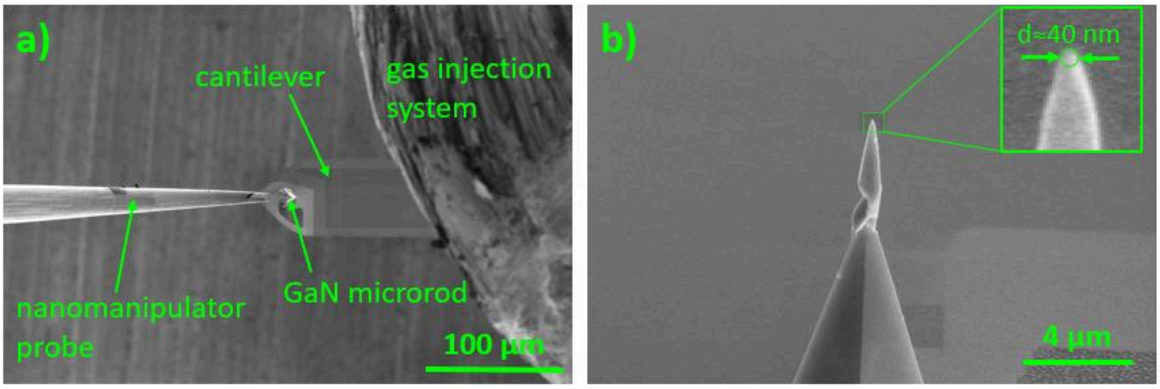

Fig. 1: SEM images of GaN tip deposition process: (a) GaN microrod welding process by FEBID method (nanomanipulator probe with GaN microrod at the end, Si commercial cantilever and $MeCpPtMe_3$ precursor gas injector system are indicated on the image), (b) GaN tip after FIB sharpening process (GaN tip curvature diameter is less than 40 nm).

FIT4NANO---Focused Ion Technology for functional nanomaterials

Gregor Hlawacek,[a] Maja Popovic,[b] Tom Wirtz,[c] Gerhard Hobler,[d] Katja Höflich,[e] Gemma Rius,[f] and Amy Gandy[g]

[a]Helmholtz-Zentrum Dresden-Rossendorf, 01328 Dresden, Germany
[b]"Vinča" Institute of Nuclear Sciences, Belgrade, Serbia
[c]Luxembourg Institute for Science and Technology, 4362 Esch-sur-Alzette, Luxemburg
[d]Technical University Vienna, 1040 Wien, Austria
[e]Ferdinand Braun Institute für Höchstfrequenz, 12489 Berlin , Germany
[f]IMB-CNM-CSIC Campus UAB, 08193 Bellaterra, Spain
[g]University of Sheffield, Sheffield, United Kingdom

g.hlawacek@hzdr.de

FIT4NANO[1] is a European COST[2] network of researchers with the aim to further develop focused ion beam (FIB) technology for the fabrication and characterization of functional nanomaterials. This will help to further strengthen Europe's leading role in the evolution of this enabling technology. FIBs are enabling research in numerous fields including semiconductor technology, quantum sensing and communication, development of devices based on 2D materials, photonic and phononic crystals, health and biology as well as raw materials, structural materials and space applications.

The Action comprises three groups of academic and industrial researchers. First, there is the group of developers of new focused ion beam sources, optics, detectors and spectrometers as well as add-ons for in-situ and in-operando experiments. The second and biggest group is applying FIBs to materials science, health and other research challenges, utilizing bleeding edge developments provided by group one. Both groups are supported by the third group that provides the software tools to understand and predict ion solid interaction effects at the nanoscale.

The instruments and methods developed by the Action are shared with stakeholders around the globe and a new FIB road-map will showcase current and future developments of this enabling technology for materials characterization and fabrication.

[1] https://www.fit4nano.eu.
[2] https:/www.cost.eu/actions/CA19140

Development and biological assessment in terms of cytotoxicity and hemolytic effect of hyaluronic acid (HA) based electrospun nanofibers

A.-T, Iacob[1*] and L. Profire[1]

[1] University of Medicine and Pharmacy "Grigore T. Popa" of Iași, University Street no 16, Romania

[*] Corresponding author email: andreea.panzariu@umfiasi.ro

Purpose: The aim of this paper is the formulation of novel electrospun nanofibers based on hyaluronic acid and polyethylene oxide (HA/PEO), incorporating different active substances (ASs) such as: propolis (P), insulin (I) and infusion of *Calendula officinalis flos (C*), as new dressing materials in the treatment of wounds. **Materials and methods**: The preparation of HA/PEO matrices was carried out in three stages: (i) the dissolving of HA and PEO in physiological brine by stirring at room temperature (ii) the ASs were added to the HA-PEO solution and stirred until a homogeneous mixture was obtained [1]; (iii) the electrospinning of the HA-PEO-ASs using a INOVENSO nanospinner [2]. Three nanofibrous matrices were developed: HA/PEO/P (A); HA/PEO/PI (B); HA/PEO-PC (C) as seen in the SEM micrographs represented in the **Fig. 1.** After the physical and chemical characterization, the developed nanofibers were subjected to the determination of the cytotoxicity by MTS assay (on normal dermal fibroblast cells) and the evaluation of hemolytic effect (based on human erythrocyte membrane stabilization assay) [2]. **Results:** All the developed formulations were not cytotoxic at concentrations up to 500 µg/mL and regarding the hemolytic effect, this was below 4%, which demonstrates a good bio-compatibility. **Conclusions:** After analyzing the data obtained, it was concluded that HA/PEO-PC nanofibers showed the most proper features, in terms of stimulating the normal fibroblasts' proliferation by 21%, at concentrations of 250 µg/mL and by 37% at 500 µg/mL, and also by the smallest hemolytic index of 2.8%. **Funding:** This work was supported by a grant of Romanian Ministry of Education and Research, CNCS-UEFISCDI, project number PN-III-P4-ID-PCE-2020-2687, within PNCDI IIII, contract no. 244/2021 and AUF-IFA 2019-2020 grant (contract no. 28/2019).

[1] O.M. Ionescu, A. Mignon, A.T. Iacob, N. Simionescu, L.G. Confederat, C. Tuchilus, L. Profire; *New Hyaluronic Acid/Polyethylene Oxide-based electrospun nanofibers: design, characterization and In Vitro biological evaluation*. Polymers (2021) 13, 129.

[2] J.J. Ahire, D.D. Robertson, A.J. Van Reenen, L.M.T. Dicks; *Polyethylene oxide (PEO)-hyaluronic acid (HA) nanofibers with kanamycin inhibits the growth of Listeria monocytogenes*. Biomed. Pharmacother. (2017) 86, 143–148.

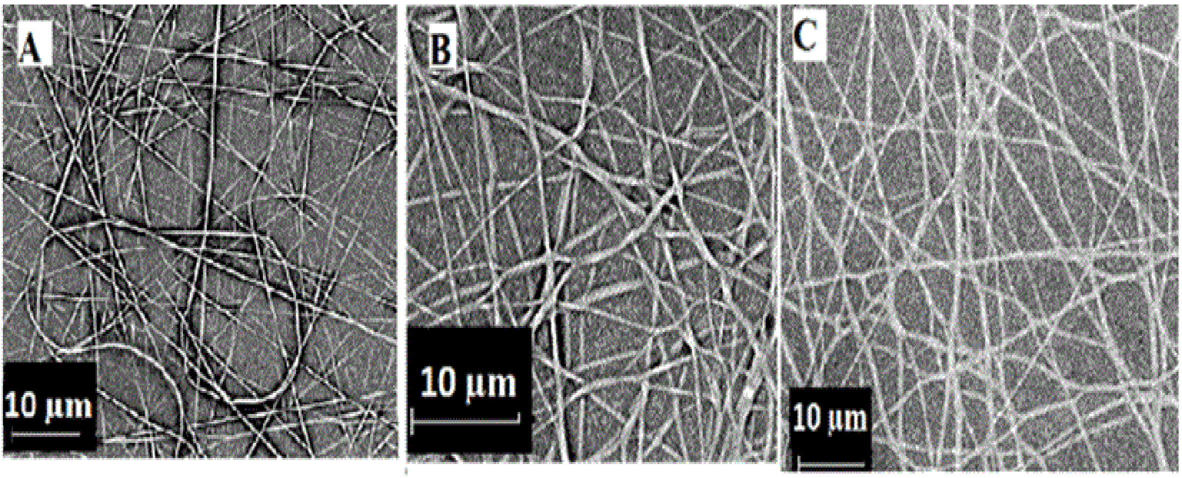

Fig. 1: SEM micrographs for HA/PEO/P (A); HA/PEO/PI (B); HA/PEO-PC (C)

Application of the FIB induced deposition method for the fabrication of AFM probe tips

A. Kolomiytsev*, O. Ilin and I. Panchenko

Southern Federal University, Institute of Nanotechnologies, Electronics and Equipment Engineering, Taganrog, Russia
* corresponding author email: askolomiytsev@sfedu.ru

One of the main problems in atomic force microscopy technology is the strong influence of the shape and radius of the tip curvature on the accuracy and resolution of research [1]. The application of the method of focused ion beam induced deposition of materials makes it possible to create probe tips of complex shapes for solving various nanometrology tasks. By combining the FIB local milling and FIB induced deposition methods [2], it is possible to achieve the formation of the tip of the probe with parameters unattainable using traditional microelectronics technologies.

In this work, the results of experimental studies on the formation of the tip of AFM probes by the method of local FIB-induced deposition of carbon and tungsten are presented. At the initial stage of work based on a standard tipless cantilever chip, a carbon tip with a height of 5 µm and a radius of curvature of the tip of 50 nm was fabricated (Fig. 1, a). In addition, the tip of the flared probe for the CD AFM technique was formed by FIB induced deposition (Fig. 1, b). FIB-fabricated probes were tested by examining AFM calibration gratings and compare the results of using commercial probes. Fig. 2 shows the profiles of the calibration grating measured by various probes. It is shown that the use of FIB fabricated probes can increase the accuracy of measuring the lateral dimensions of the structure by 33%. In addition, the FIB induced deposition method can be used to form the tip of aperture cantilevers for SNOMs with an aperture diameter of less than 100 nm [2].

Thus, the technology described in the work allows the formation of a special shape probe tips for ultra-precise nanometrology using the AFM, CD AFM, SNOM and many other scanning probe microscopy methods.

[1] A. Savenko, I. Yildiz, D.H. Petersen; *Ultra-high aspect ratio replaceable AFM tips using deformation-suppressed focused ion beam milling;* Nanotechnology 24 (2013), 465701.

[2] Yu. E. Vysokikh, T.V. Mikhailova; *Carbon tip aperture cantilevers: Fabrication & features in near-field magneto-optical imaging;* Journal of Magnetism and Magnetic Materials 529 (2021), 167837.

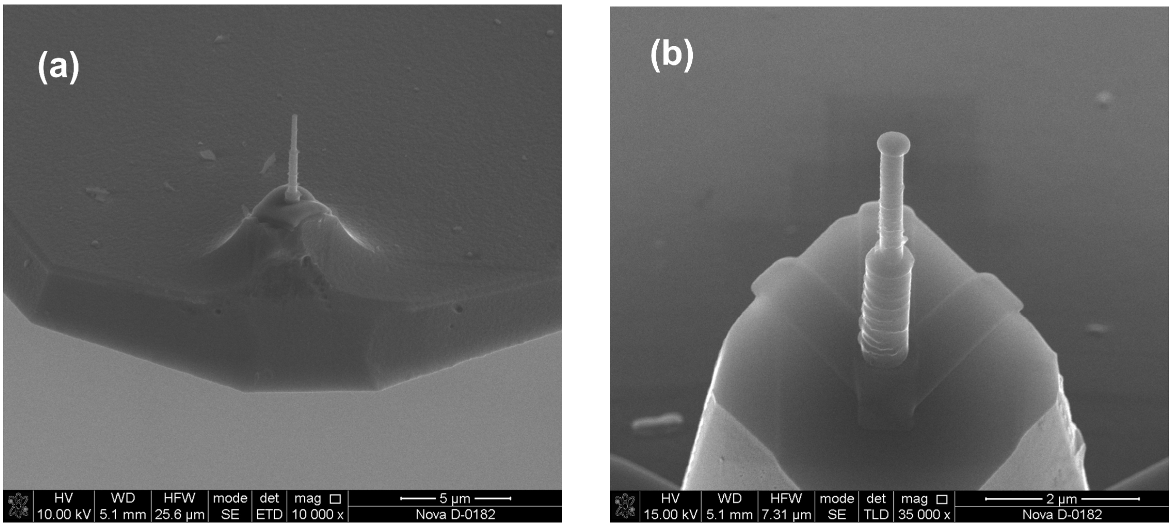

Fig. 1: SEM images of FIB-fabricated probes (a) – ultrahigh aspect ratio probe, (b) – CD AFM probe

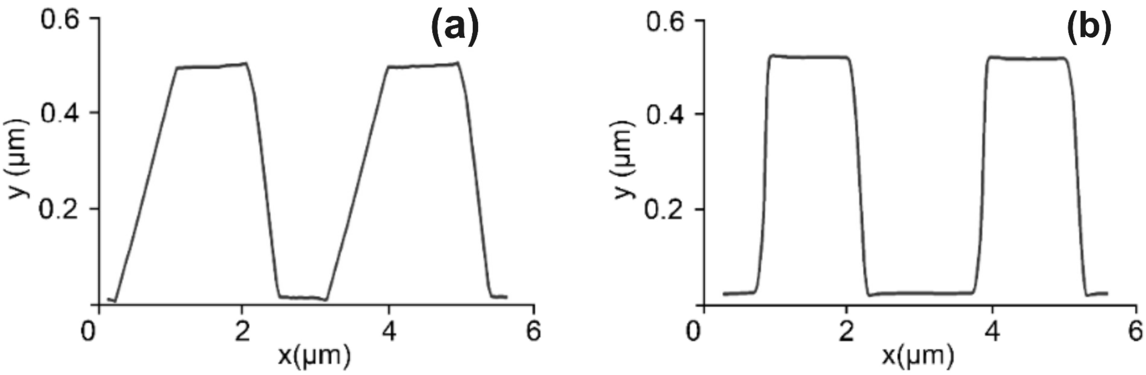

Fig. 2: Calibration grating profiles obtained with a commercial probe (a) and FIB fabricated probe (b)

Helium Ion Microscopy Patterning for Perpendicular Magnetic Anisotropy Thin Films

Jinu Kurian[1*], Aleena Joseph[1], Peter Dunne[1,4], Ciaran Fowley[2], Gregor Hlawacek[2], Salia Cherifi-Hertel[1], Gwenaël Atcheson[3], M Venkatesan[3], Serhii Sorokin[2], Bohdan Kundys[1], Michelangelo Romeo[1], Thomas M. Hermans[4], J. M. D. Coey[3], Bernard Doudin[1]

[1]Université de Strasbourg, CNRS, IPCMS UMR 7504, 23 rue du Loess, F-67034 Strasbourg, France.[2]Institute of Ion Beam Physics and Materials Research, Helmholtz-Zentrum Dresden - Rossendorf, Bautzner Landstraße 400, 01328 Dresden, Germany .[3]AMBER and School of Physics, Trinity College, Dublin 2, Ireland.
[4]Université de Strasbourg, CNRS, ISIS, 8 allée Gaspard Monge, 67000 Strasbourg, France.
* corresponding author email: jinu.kurian@ipcms.unistra.fr

We investigate helium ion (He^+) microscope irradiation of thin films heterostructures with perpendicular magnetic anisotropy (PMA). One key advance is the *in-situ* monitoring of the evolution of the out-of-plane magnetization under local ion irradiation using the anomalous Hall effect (Fig. 1a). Our result shows the resulting change in the Spin Orbit Torque (SOT) switching behavior on single and multi-repeat Co magnetic layer stacks (Fig. 2). The critical current required to switch the magnetic state ($\pm M_z$) depends on the saturation magnetization and magnetic anisotropy, which are interface dependent and can be tuned by He^+ irradiation [1]. The He^+ microscope allows both precise control of the anisotropy and <~10 nm spatial resolution, creating low-power switchable patterns without the need of lithography. We detail here how magnetic and current-driven switching can be compared and the switching power can be optimized.

[1] P. Dunne et. al., *Helium Ion Microscopy for Reduced Spin Orbit Torque Switching Currents,* Nano Lett. 20 (2020), 7036.

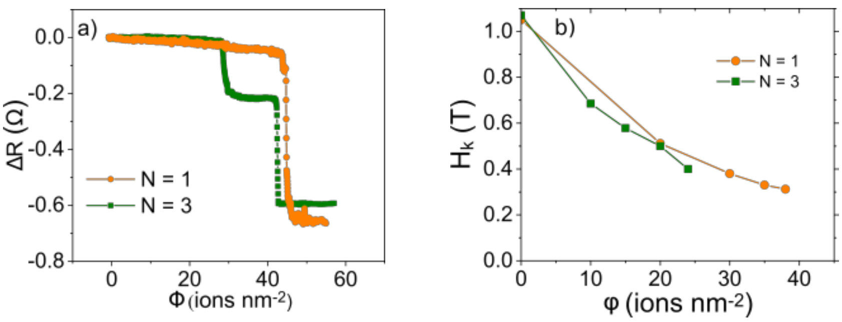

Fig.1: a) *In situ* evolution of anomalous Hall resistivity with irradiation dose b) *ex-situ* anisotropy field for specific irradiation doses.

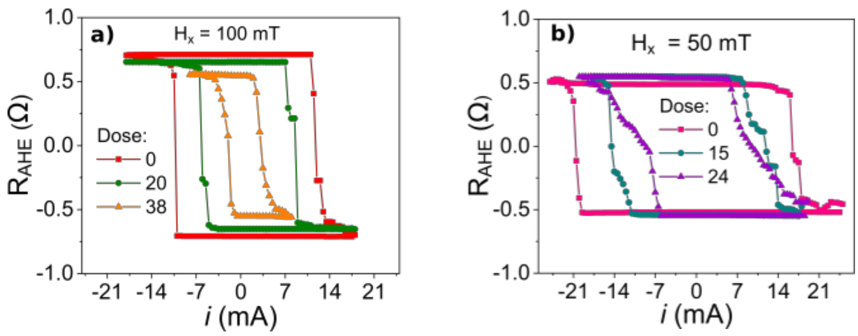

Fig.2: Current driven SOT switching of a) N=1 and b) N=3 repeat devices at selected irradiation doses.

The role of Americium-241 for the metal detection in solids, liquids and contamination using a portable spectrometer

C. Larosa[1*], A. Converti[1]

[1] University of Genoa, Department of Civil, Chemical and Environmental Engineering, Pole of Chemical Engineering, via Opera Pia 15, I-16145, Genoa, Italy

[*] corresponding author email: Claudio.Larosa@unige.it

The current demand for new portable devices from the citizen community has opened a new perspective of analysis in the fields of antiquity [1], relics [2], sedimentary of ferrous rocks, chemical pollution, and radioactive contaminants [3–5]. Based on these topics and interest the physical principle of XRF fluorescence [6] was applied to formulate a low-cost portable device, starting from an americium source, the same used for smoke detectors with radial dislocation (N=8), able to remove the last electron orbitals of shell elements at lower energies. The problem solving was applied to realize a portable spectrometer device with high sensibility vs. elements commonly analyzed in alloys or mixture using O-ring brass support, structured in order to generate photoelectrons, starting from Americium pieces on samples, suitable for generating signals. Furthermore, another aspect concerns the threshold limit value of detection, it was investigated in order to offer a significant highlight signal intensity output. The device was assembly from two modules: first of all. a low radioactive source with a radial dislocates on brass around a hole, second a detector, by using two electronic cards with an analogic multi-pins and a master USB connector. In the experimental section, two different hardware were compared in order to select the best choice that gives major stability at the lower current intensity and employing a minor number of electronic compounds. Data acquired from samples surface of mineral nature were acquired and elaborate with a freeware software of analysis in order to collect the element's signal and estimate their ratio. Device parts are innovative in the logical concept able to change and drive the sampling rate, the gain, and signal/noise ratio; the device is also able to detect elements near the Americium probe at a distance of~1-2 cm, tailored for small objects, potter fragments, oil painting, coins on the surface and from elements mixed in an alloy. The graph output shows elements from which is possible to measure the intensity and ratio between the elements. In conclusion, an innovative element s signals generate by Americium and analogic card configured with a USB master is proposed as a versatile system able to acquire signals without a pre-amplify system, operating on solids and liquids.

[1] K. F. Gebremariam, L. Kvittingen, F. G. Banica. Application of a portable XRF analyzer to investigate the medieval wall paintings of Yemrehanna Krestos Church Ethiopia; X-Ray Spectrom, 42, (**2013**), 462–469

[2] A. M. Markey, C. S. Clark, P. A. Succop, S. Roda; Determination of the feasibility of using a portable X-ray fluorescence (XRF) analyzer in the field for measurement of lead content of sieved soil; J. Environ Health, 70, 7, (**2008**) 24-30

[3] G. Buzanich, P. Wobrauschek, C. Streli, A. Markowicz, D. Wegrzynek, E. Chinea-Cano, M. Griesser and K. Uhlir PART II (Portable ART analyzer) –X-Ray Spectrom. 42, 462–469, (**2013**)

[4] P. Higueras, R. Oyarzun, J.M. Iraizoz, S. Lorenzo, J.M. Esbrí, A. Martínez-Coronado; Low-cost geochemical surveys for environmental studies in developing countries: Testing a field portable XRF instrument under quasi-realistic conditions; J. of Geochem. Explor. 113, **(2012**) 3-12,

[5] S. Clark, W. Menrath, M.Chen, S. Roda, P. Succop; Use of a field portable X-Ray fluorescence analyzer to determine the concentration of lead and other metals in soil samples Ann. Agric. Environ. Med. 6, (**1999**) 27–32.

[6] Z. W. Chen, W. M. Gibson, and H. Huang. High-Definition X-Ray Fluorescence: Applications Hindawi Publishing Corporation; X-Ray Optics and Instrumentation, ID 709692, 17 (**2008**)

Characterization of an ultracold Rb^+ focused ion beam

S. Xu, Y. Li and E. J. D. Vredenbregt*

Department of Applied Physics, Eindhoven University of Technology, P.O. Box 513, 5600 MB Eindhoven, the Netherlands

* corresponding author email: E.J.D.Vredenbregt@tue.nl

Focused Ion Beams are an important tool for the material science and semiconductor industry. Essential applications are editing circuits and repairing masks in the development phase, and failure analysis during wafer processing. Here a prototype FIB system is described that uses Rb^+ ions. The essential innovation is the use of a cold-atom ion source [1] based on photoionization of a laser-intensified and cooled atomic Rb^+ beam. The whole source is mounted onto a commercial FIB column and first beam profile and milling experiments have been performed [2-3].

Stable performance of the Rb^+ beam enabled beam profiling using a knife-edge method. Working at 8.5 keV and 6 pA, the beam was determined to have a d_{50} of 160 nm. After optimization, a d_{50} of a few nm and a predicted reduced brightness of near 1×10^6 A/(m^2·sr·eV) should be achievable, which is comparable with that of the commercial Ga^+ LMIS. Different energies and currents are also available with the beam.

Secondary electron yields for a variety of materials were determined (displayed in Fig. 1). The figure shows that, as a general trend, heavier atomic species produce fewer secondary electrons per ion.

Sputter yields of Rb^+ were determined by milling patterns on various samples. Fig. 2 shows the summary of measured yields. Here Ga^+ ions at 8.0 kV were applied for comparison. Overall, Rb^+ has a higher sputter yield compared to Ga^+ at similar beam energy, in some cases even larger than conventional 30 keV Ga^+. The results show that Rb^+ has promising prospects for nanomachining applications.

[1] J. J. McClelland *et al*; *Bright focused ion beam sources based on laser-cooled atoms*; Applied Physics Reviews 3 (**2016**), 011302

[2] G. ten Haaf; *Ultracold Rb Focused Ion Beam;* PhD thesis, Eindhoven University of Technology (**2017**)

[3] G. ten Haaf *et al*; *Measurements of the energy distribution of a high brightness rubidium ion beam;* Ultramicroscopy 190 (**2018**), 12

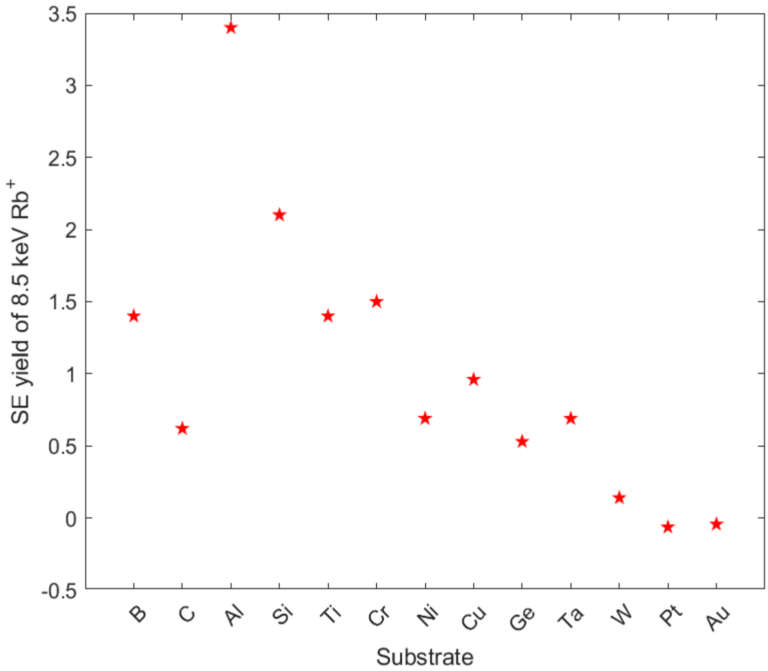

Fig. 1: Secondary electron yields of 8.5 keV Rb⁺ on various samples.

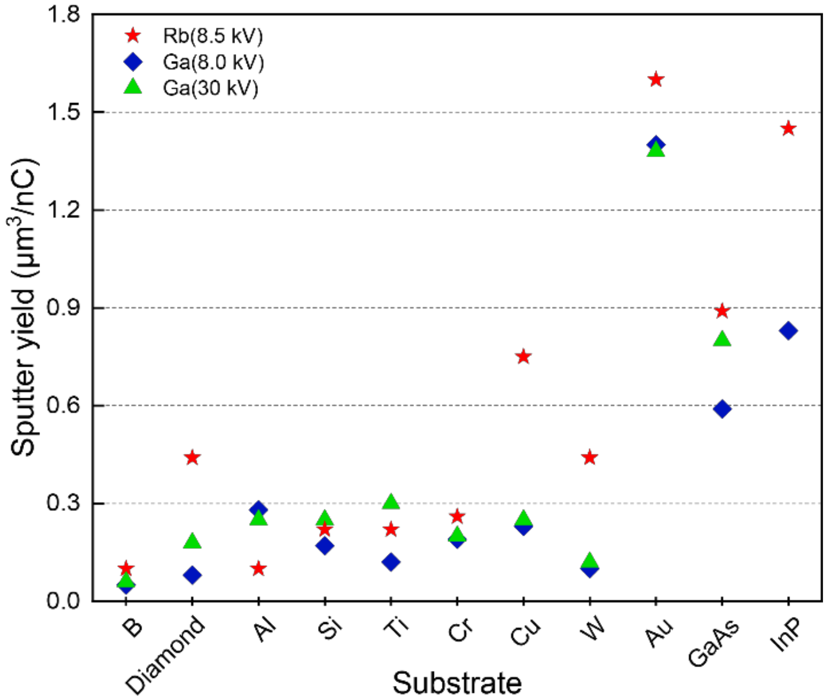

Fig. 2: Sputter yield measurements of Rb^+ and Ga^+ on various samples. The red markers represent Rb^+ at 8.5 kV, blue represent Ga^+ at 8.0 kV, and green ones are conventional Ga^+ beam energy respectively.

In-situ nanoindentation electron microscopy of the nanostructured semiconducting zincite thin-films

I. Panžić[1], V. Mandić[1*] and D. Kiener[2]

[1] Faculty of Chemical Engineering and Technology, Marulićev trg 20, 10000 Zagreb, Croatia
[2] Department of Materials Physics, Montanuniversität Leoben, Jahnstrasse 12, 8700 Leoben, Austria
[*] corresponding author email: vmandic@fkit.hr

ZnO is a semiconductor having large exciton binding energy, high electron mobility [1] and recently ability to prepare and describe its films in low-dimensional configurations. Desirable 1D configuration greatly facilitate boosting some of the materials physical properties such as efficiency of the charge transfer.

For synthesis purpose, physical deposition techniques are proven to be successful but many of them require demanding conditions. On the contrary, chemical processing such as chemical bath route enables the large-scale fabrication of well-aligned ZnO nanorods at mild temperatures [2]. For characterization purpose, conventional methods fail to provide a full understanding of the investigated material, thereof it was elucidated that more detailed insight in mechanical characteristics (hardness and elastic modulus) is highly desirable, particularly in the nanoscale regime, where nanoindentation method was shown to be a flexible and useful tool [3].

Here we prepared 1D nanostructured zincite thin-films and combine investigation of their hardness and elastic modulus as well as fracture toughness with advanced imaging techniques. For characterization we focus on the in-situ micromechanical experiments with advanced nanoindentation techniques (at elevated temperatures) in the scanning and transmission electron microscopy (SEM/TEM). The course of characterization was assisted by focused ion beam (FIB) based material structuring and digital image correlation techniques to observe, describe and understand occurrence of local deformations and generally microstructural evolution.

We were able to conduct a miniaturized fracture testing within the SEM and TEM apparatus. Results were utilized to qualify and quantify the materials resistance to mechanical failure such as undesirable cracking events. The mitigation of such events should enable major development role of the nanoscale optoelectronic devices.

[1] A. Janotti, C. G. Van De Walle, Reports Prog. Phys. 72 (2009) 126501.

[2] L. Schmidt-Mende, J. L. MacManus-Driscoll, Materials today 10 (2007) 40.

[3] X.Y. Tao, X.D. Li, Nano Lett. 8 (2008) 505.

Measuring slice thickness stability during a high resolution FIB-SEM serial-sectioning tomography

V. Ondračka[1], J. Dluhoš[2*], K. Rosíková[1], M. Joens[3], P. Matějíček[1]

[1] TESCAN Brno s.r.o., Libušina třída 816/1, Brno-Kohoutovice, 623 00, Czech Republic
[2] TESCAN ORSAY HOLDING a.s., Libušina třída 863/21, Brno-Kohoutovice, 623 00, Czech Republic
[3] TESCAN USA, Inc., 765 Commonwealth Drive, Suite 101 Warrendale, PA 15086, USA
[*] Corresponding author email: jiri.dluhos@tescan.com

The voxel size is of great importance when reconstructing sample volume data gathered during a FIB-SEM serial-sectioning tomography acquisition. While the X and Y voxel sizes are validated through careful SEM calibration during the microscope setup, the actual Z voxel size depends on the volume slicing procedure. Since the drift before the slicing is being compensated by a FIB drift correction, the drift during the slicing is relatively unknown. Therefore, the slice thickness is affected by stage stability, sample thermal drift, stage movement precision, and drift correction algorithm precision.

This study evaluated the FIB image drift measurements and compared it with actual slice thickness, measured as a shift per slice on the SEM image of known "ruler" structures proposed by Jones, Mingard, and Cox [1]. The surface structure was prepared on the top of a standalone silicon mask that was then transferred and attached to the sample surface, see Figure 1. A FIB-SEM tomography process of 330 slices was performed on TESCAN AMBER, Ga^+ based FIB-SEM. The nominal slice thickness was set to 5 nm; a low current FIB preset was used for slicing. FIB drift correction was applied before each slice. The cross-section image was captured by an SEM at 2 keV with 5 nm pixel size. The time per slice was 1 minute.

The resulting slice thickness was calculated from the sub-pixel structure change detection and is shown in Figure 2. The mean value achieved was 4.9 nm with a standard deviation of 0.72 nm over the 310 slices. The first 20 slices were excluded from the statistics as the lower thickness was caused by imprecise user positioning of the sliced volume. Furthermore, the FIB drift correction data was analyzed in Figure 3. Although an almost constant drift in the slicing direction was present during the process, it was not significantly contributing to the slice thickness error. Without the FIB drift compensation, this drift would have caused a systematic increase in the actual slice thickness of about 2.3 nm on average. Note that the sample was not rested in the microscope chamber but rather analyzed immediately after being placed inside. Apart from the errors of the measuring technique itself, the random FIB drift during the slicing and the precision of the drift correction is suspected to be the main contribution of the variation in slice thickness, leading to the found 0.72 nm standard deviation in slice thickness.

[1] H.G. Jones, K.P. Mingard, D.C. Cox; *Investigation of slice thickness and shape milled by a focused ion beam for three-dimensional reconstruction of microstructures;* Ultramicroscopy 139 (**2014**), pp. 20-28.

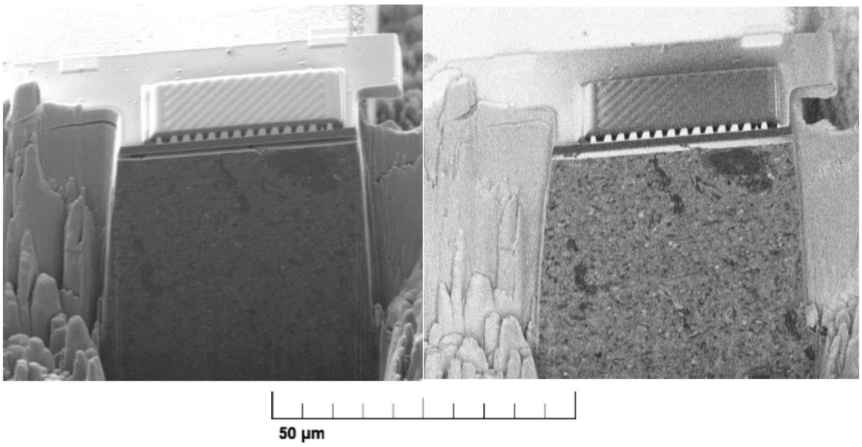

Fig 1: The surface „Cox-Jones“ ruler structure on top of a silicon mask and the imaged cross-section, captured using E-T and BSE detectors

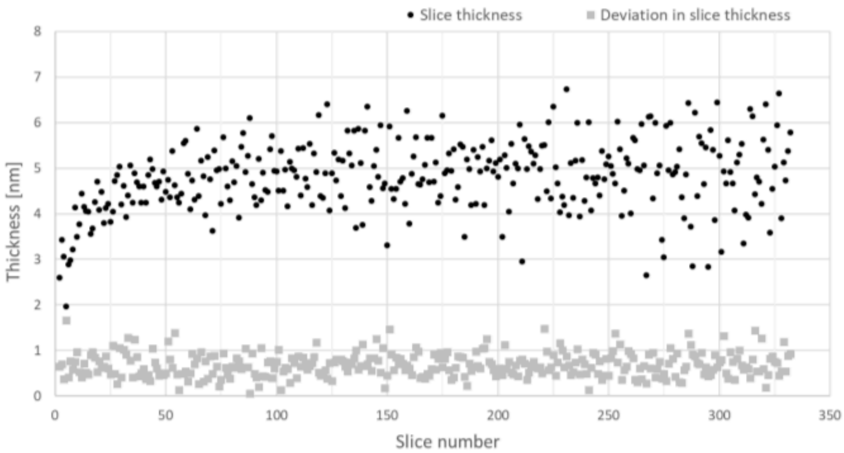

Fig 2: Slice thickness progression during a tomography run.

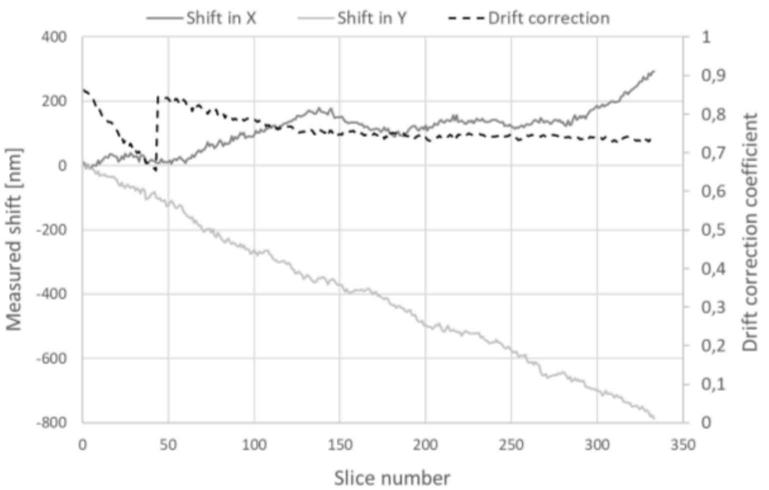

Fig 3: Measured shift by FIB drift correction mark correlation.

FIB-SEM on Polyolefins: Influence of Different Ion Beam Conditions

M. Paśniewski[1,2*], A.-J. Bons[1], N. Schryvers[2]
[1] ExxonMobil Chemical Europe Inc., European Technology Center, Machelen, Belgium
[2] EMAT, University of Antwerp, Belgium
[*] maciej.pasniewski@exxonmobil.com

Polyolefins such as polyethylene, polypropylene and associated rubber compounds are produced at a scale of 10^{10} kg per year globally. They play a crucial role in improving the daily life of billions of people by providing low-cost, light-weight, strong and effective food packaging, hygiene products, household objects, car parts, etc. New technologies provide stronger materials allowing down-gauging and light-weighting, thus reducing carbon footprint and waste. The development of new materials with improved properties is guided by an in-depth understanding of the microstructure of the materials, at a molecular and supra-molecular scale.

Focused Ion Beam - Scanning Electron Microscopy (FIB-SEM) can be used is an important tool for in-depth analysis of the microstructure at the nanoscale; it can also be used to prepare cross-sections with nanometer precision for other characterization techniques, such as Transmission Electron Microscopy (TEM) or Atomic Force Microscopy (AFM).

Interaction of matter with ions brings concerns regarding the nature of the newly created surfaces and how representative they are of the bulk phase, especially for such beam-sensitive materials as polyolefins. Initial analyses with AFM and Time of Flight-Secondary Ion Mass Spectrometer (ToF-SIMS) performed on FIB'd surfaces show significant alteration on the new surface. This project aims to assess the nature and extent of the surface damage, the fundamental processes involved and ways to minimize the damage.

The ongoing study includes preparation of cross sections in polyethylene (PE) under different incident angles and ion beam conditions, trying to assess the extent of the damage to the microstructure and possible ion implantation. Another study on polypropylene (PP) with five different focused ion beams (Ga, Ar, N_2, O_2 and Xe) with varying energies is ongoing. The prepared structures will be studied by ToF-SIMS to analyze the molecular structure (atoms and molecule fragments) and by TEM to analyze the extent of damage and ion implantation. New experiments on PP, PE and poly(methyl methacrylate) (PMMA) are planned.

Building a better understanding of ion beam–polyolefin interaction will provide confidence in our results and allow us to study the materials with electron microscopy more accurately. This will enable us to perform experiments more effectively, speeding up knowledge build and shortening the development cycle of new materials.

Ultrafast growth of cobalt nanostructures using Cryo-FIBID: application to electrical contacts on graphene, magnetism, and hard masking

A. Salvador-Porroche[1,2], S. Sangiao[1,2] C. Magén[1,2], M. Barrado[1,2], P. Philipp[3], D. Belotcerkovtceva[4], M. Venkata Kamalakar[4], P. Cea[1,2] and J. M. De Teresa [1,2*]

[1] Instituto de Nanociencia y Materiales de Aragón (INMA), Universidad de Zaragoza-CSIC, 50009 Zaragoza, Spain
[2] Laboratorio de Microscopías Avanzadas (LMA), Universidad de Zaragoza, 50018 Zaragoza, Spain
[3] Advanced Instrumentation for Ion Nano-Analytics (AINA), MRT Department, Luxemburg Institute of Science and Technology (LIST), L-4422 Belvaux, Luxembourg
[4] Department of Physics and Astronomy, Uppsala University, Box 516, SE-75120 Uppsala, Sweden
[*] corresponding author email: deteresa@unizar.es

Focused ion beam induced deposition under cryogenic conditions, also named Cryo-FIBID, is a powerful technique which has been, in the last few years, applied to grow metallic nanostructures. For instance, W-C metallic deposits and Pt-C quasi-metallic deposits were fabricated with an enhancement of the growth speed up to three and two orders of magnitude, respectively, if compared to standard FIBID processing carried out at room temperature[1,2]. In the present contribution, we will discuss the results obtained using the $Co_2(CO)_8$ precursor for the growth of cobalt nanostructures. This process mainly consists in the condensation of a 30 nm-thick precursor condensed layer on a Si or Si/O_2 substrate held at -100°C, its irradiation with a Ga^+ focused ion beam with a wanted pattern and substrate heating up to 30°C. We obtain Co-based deposits using very low charge doses, resulting in a process much faster than room temperature processing[3]. This single-step charge-based nanopatterning gives rise to the possibility of growing cobalt nanostructures in very large areas and exhibit sub-100 nm lateral resolution. The fabricated Co Cryo-FIBID nanostructures show metallic behavior with an electrical resistivity of 200 μΩ·cm and present ferromagnetic properties with a magnetization of 400 emu/cm^3. As a proof of concept, as shown in Fig. 1, electrical contacts onto graphene ribbons were grown by Cryo-FIBID, opening the route for a broad application of this technology to any 2D material. Moreover, this nanolithography process leads to suitable deposits for hard masking, demonstrating its structural functionality.

[1] R. Córdoba, P. Orús, S. Strohauer, T.E. Torres, J.M. De Teresa; Scientific Reports (**2019**), 14076.

[2] A. Salvador-Porroche, S. Sangiao, P. Philipp, P. Cea, J.M De Teresa; Nanomaterials (**2020**), 1906.

[3] C. Sanz-Martín, C. Magén, J.M. De Teresa; Nanomaterials (**2019**), 1715.

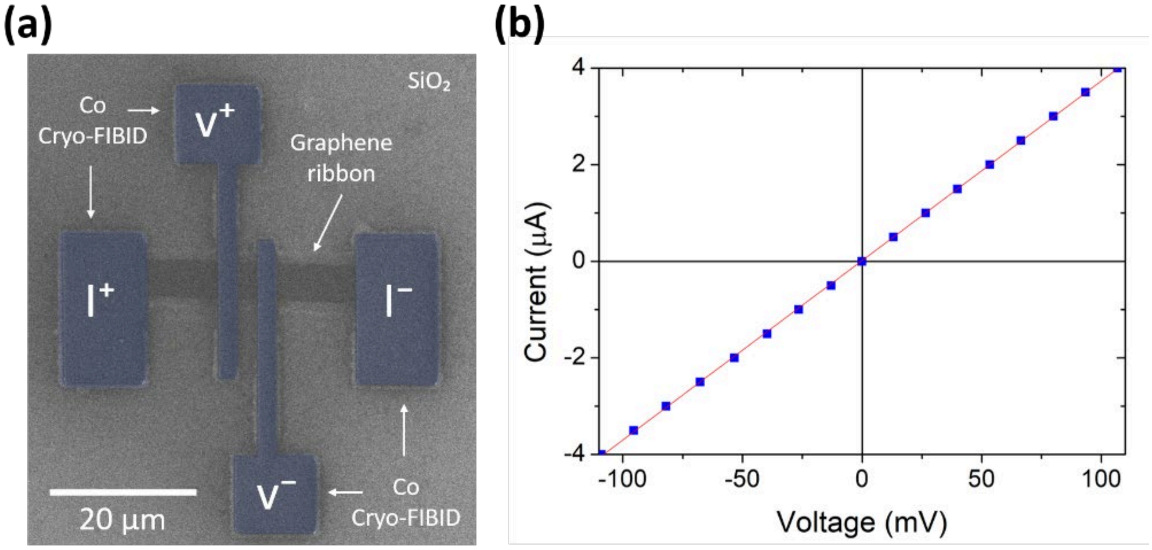

Fig. 1: (a) Artificially coloured SEM micrograph of the measured graphene sheet with the four electrical contacts grown by Co Cryo-FIBID technique. (b) Voltage-current dependence of the graphene ribbon indicating an electrical resistance of 27 kΩ.

Advances in Low-Strain FIB Microstructures

C. Putzke[1]* and P.J.W. Moll[1]

[1] Ecole Polytechnique Fédérale de Lausanne (EPFL), Institut des Matériaux, CH-1016 Lausanne, Switzerland

[*] corresponding author email: Carsten.Putzke@epfl.ch

Avoiding strain in micrometer sized objects is a key challenge when studying quantum materials on the micron scale. In particular, differential thermal contraction between the sample and its substrate can lead to uniaxial or bi-axial strain that is reflected in changes in the electronic correlations[1]. Further, too large strain eventually leads to fractures in the samples. Overcoming these issues allows for the study of electronic properties in unperturbed electronic structures over a wider temperature range.

In this work we will present a way to minimize these difficulties by using thin silicon-nitride membranes. We demonstrate the successful reduction of strain by means of magnetic quantum oscillation measurements in the topological semi-metal NbAs.

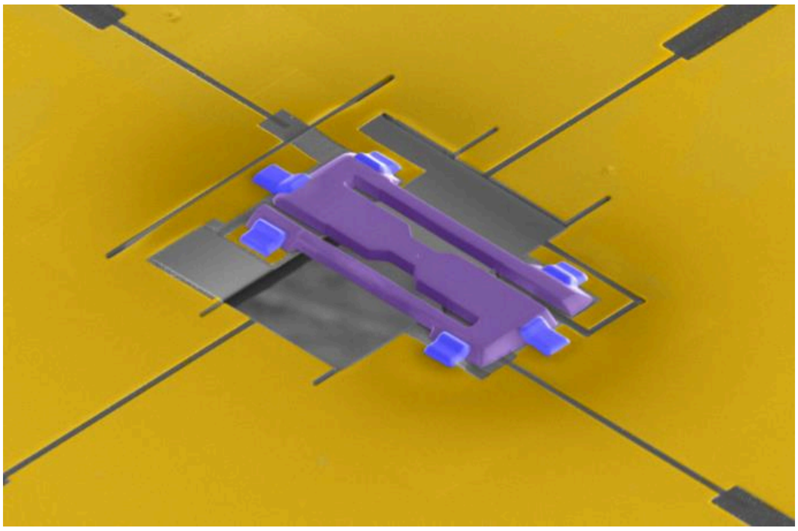

NbAs microstrucutre on silicon-nitride membrane for low strain electrical transport measurements at low strain.

[1] M.D. Bachmann, et al. Science 366, 221

Atmospheric Pressure Plasma Treatment of Polymer Thin Films and Polymer Nano- and Microfiber Membranes

E. Frau[1], V. Sanchez[1], L. Castro Nicolli[1], and S. Schintke[1*]

[1] Laboratory of Applied NanoSciences (COMATEC-LANS), Department of Industrial Technologies, Haute Ecole d'Ingénierie et de Gestion du Canton de Vaud, HEIG-VD, HES-SO // University of Applied Sciences and Arts Western Switzerland, CH-1401 Yverdon-les-Bains, Switzerland
[*] corresponding author email: silvia.schintke@heig-vd.ch

Understanding ion interactions on advanced materials is one of the goals of the Cost Action FIT4NANO in order to benefit of the possibilities of local surface modifications on nano- and microstructured thin film surfaces, as well as on nano- and microfibers. While deep knowledge has been gained on nanostructure generation by ions on metals and semiconductors over the last decades, in particular for highly advanced nano- and microelectronics fabrication processes, the understanding of ion interaction and surface structuring on polymers and polymer fiber materials is still in its infancy. Studies by atmospheric pressure plasma treatment (APT) on such materials are thus aimed to bridge the gap.

We have investigated the effect of atmospheric pressure plasma treatment (APT) on the surface structure of polymer thin films and on polymer fiber membranes. Polyvinylidene fluorid (PVDF) thin films were fabricated by semi-automated blade coating, PVDF fiber membranes were manufactured by electrospinning. PVDF samples were then treated using industrial APT sources, and low-pressure plasma treatment (LPT) in comparison. Surface structure, roughness, and wetting behavior of the thin films and membranes were analyzed by atomic force microscopy, optical microscopy, and water contact angle measurements. We present and discuss the observed effects and surface modifications as a function of atmospheric pressure plasma treatment parameters.

This work has been financially supported by HES-SO, project MIMATEC, grant IA-EXT20-102.

On-chip, geometry-induced strain in strongly correlated mesoscale structured materials

Kent. R. Shirer[1,2*], Javier Landaeta[2], Eric D. Bauer[3], Filip Ronning[3], Elena Hassinger[2], Andrew P. Mackenzie[2], Philip J. W. Moll[1]

[1] Institute of Materials, École Polytechnique Fédérale de Lausanne (EPFL), 1015 Lausanne, Switzerland
[2] Max Planck Institute for Chemical Physics of Solids, 01187 Dresden, Germany
[3] Los Alamos National Laboratory, Los Alamos, New Mexico 87545, USA
[*] kent.shirer@epfl.ch

Uniaxially stressed crystals experience a modification to their lattice constants. This modification can provide powerful insight into their electronic and magnetic structure and even induce new material phases. Furthermore, the effects of uniaxial stress often differ qualitatively from those of hydrostatic stress. $YBa_2Cu_3O_{6.67}$, a high temperature superconductor, has its critical temperature enhanced by hydrostatic stress but suppressed by in-plane uniaxial stress. [1]

Currently, the methods to apply a uniform uniaxial stress to materials rely on macroscopic single crystals or growing thin films on a substrate with a lattice constant mismatch. [1] [2] For transport devices in the mesoscopic regime, uniaxial stress provides a desirable parameter for tuning single-material domains. [3]

Here, we demonstrate how a focused ion beam can be used to geometrically induce uniaxial strain in a mesoscale transport device of $CeRhIn_5$, a strongly correlated antiferromagnet. [4] We show that the antiferromagnetic transition temperature can be tuned through strain by modifying the device geometry. Furthermore, superconductivity appears at high strains. These results suggest that geometry-induced strain could be utilized in both on-chip applications and fundamental research for devices at the mesoscale.

[1] M. Ikhlas, K. R. Shirer, P.-Y. Yang, A. P. Mackenzie, S. Nakatsuji and C. W. Hicks, "A tunable stress dilatometer and measurement of the thermal expansion under uniaxial stress of Mn3Sn," *Applied Physics Letters,* vol. 117, p. 233502, 12 2020.

[2] J. P. Ruf, H. Paik, N. J. Schreiber, H. P. Nair, L. Miao, J. K. Kawasaki, J. N. Nelson, B. D. Faeth, Y. Lee, B. H. Goodge, B. Pamuk, C. J. Fennie, L. F. Kourkoutis, D. G. Schlom and K. M. Shen, "Strain-stabilized superconductivity," *Nature Communications,* vol. 12, 1 2021.

[3] M. D. Bachmann, G. M. Ferguson, F. Theuss, T. Meng, C. Putzke, T. Helm, K. R. Shirer, Y.-S. Li, K. A. Modic, M. Nicklas, M. König, D. Low, S. Ghosh, A. P. Mackenzie, F. Arnold, E. Hassinger, R. D. McDonald, L. E. Winter, E. D. Bauer, F. Ronning, B. J. Ramshaw, K. C. Nowack and P. J. W. Moll, "Spatial control of heavy-fermion superconductivity in CeIrIn5," *Science,* vol. 366, p. 221–226, 10 2019.

[4] F. Ronning, T. Helm, K. R. Shirer, M. D. Bachmann, L. Balicas, M. K. Chan, B. J. Ramshaw, R. D. McDonald, F. F. Balakirev, M. Jaime, E. D. Bauer and P. J. W. Moll, "Electronic in-plane symmetry breaking at field-tuned quantum criticality in CeRhIn5," *Nature,* vol. 548, p. 313–317, 8 2017.

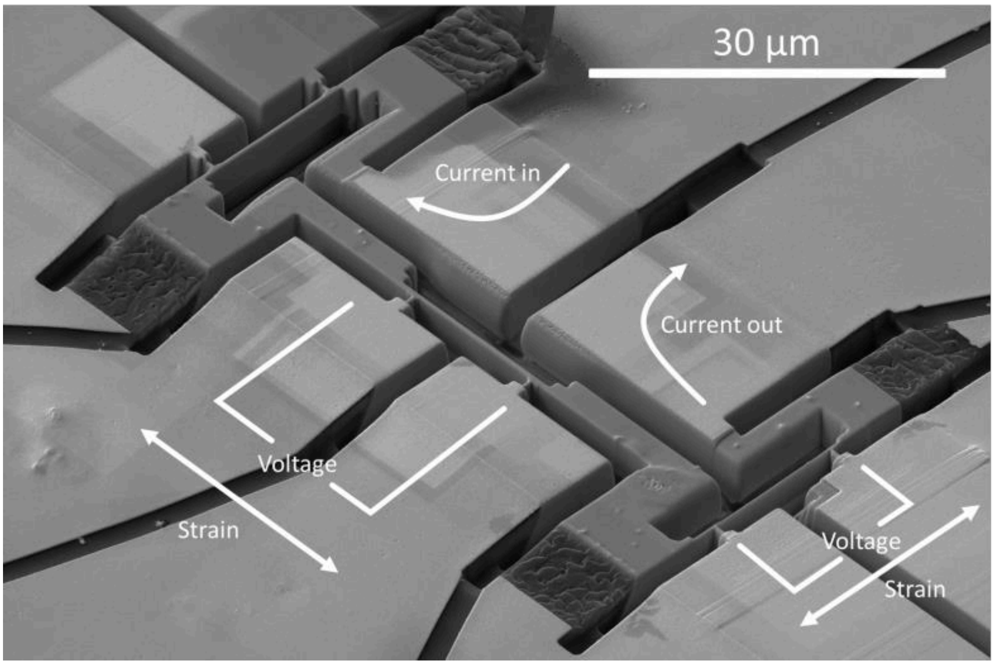

Fig. 1: A SEM image of a $CeRhIn_5$ meso-scale transport device for measurements of resistivity anisotropy on uniaxially strained bars. The four-point resistance bars are aligned along the tetragonal [100] (middle bar of the device) and [001] (upper left and lower right in the image) axes. The extreme aspect ratio of the bars, approximately 300 nm in width, 3 µm high, and 13 µm long, along with the bar's comparatively thick ends, generate a large uniaxial strain in the region between the voltage contacts.

Tungsten based SQUID Nanofabrication by Means of Focused Ion Beam Induced Deposition

F. Sigloch[a,*], P. Orús[a], S. Sangiao[a], and J. M. De Teresa[a,b]

[a]Instituto de Nanociencia y Materiales de Aragon (INMA), Universidad de Zaragoza-CSIC, 50009 Zaragoza, Spain
[b]Laboratorio de Microscropías Avanzadas (LMA), Universidad de Zaragoza-CSIC, 50018 Zaragoza, Spain

[*]Corresponding author email: fsigloch@unizar.es

Scanning Probe Microscopy (SPM) has become a standard tool in solid state physics to map the topographic, magnetic, electrostatic or thermal structure of a given surface with astonishing resolution. The experiments are carried out with simple probes, *e.g.* a sharp conducting, insulating or magnet tip.
In the present contribution we will discuss the capability of Focused Ion Beam Induced Deposition (FIBID) to allow the nanofabrication of arbitrary metallic and superconducting structures on SPM cantilevers. Therefore a Ga^+ ion beam is used to directly write a Superconducting Quantum Interference Device (SQUID) from a $W(CO)_6$ precursor gas. The resulting structure is a W-C compound which can be either metallic or superconducting, depending on the process parameters [1]. The present work deals with the fabrication, characterization and optimization of said nanoSQUIDs. In a first step the process parameters are optimized on a Si/SiO_2 chip. We report the successful deposition of Dayem-Bridge- (DB-) SQUIDs down to 100 nm $\times$ 100 nm (fig. 1). In a next step the electric and magnetic properties are characterized and the process parameters adapted to optimize the response of the SQUID to an external magnetic field. First electric characterizations as a proof of concept of DB-SQUIDs were performed showing strong influence of parasitic capacitances (fig. 2). Currently the suppression of these effects by means of a resistive shunt are investigated [2]. In parallel the obtained knowledge is used to deposit the nanoSQUIDs on SPM cantilevers The cantilevers are prepatterned with electric contacts to read out the SQUID and provided by IBM Zürich (fig. 3).

[1] J. De Teresa, P. Orus, et al.; *Comparison between Focused Electron/Ion Beam-Induced Deposition at Room Temperature and under Cryogenic Conditions*; Micromachines 10 (2019), 799.

[2] M. J. Martínez-Pérez and D. Koelle; *NanoSQUIDs: Basics & recent advances*; Physical Sciences Reviews 2.8 (2017).

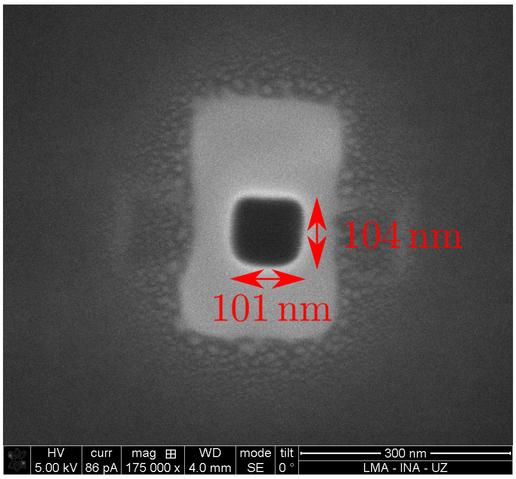

Fig 1: SEM image of a DB-SQUID. The DBs are 50 nm in width.

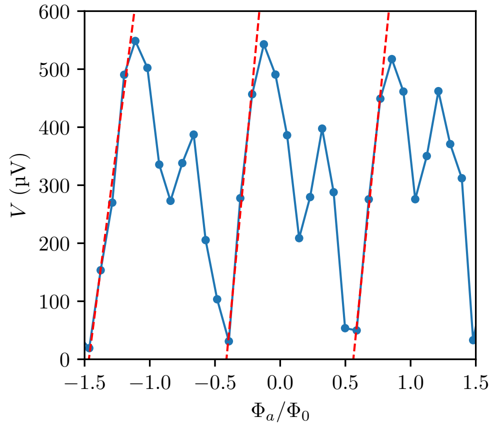

Fig 2: Voltage response of a SQUID to the flux of an external magnetic field passing through the SQUID loop.

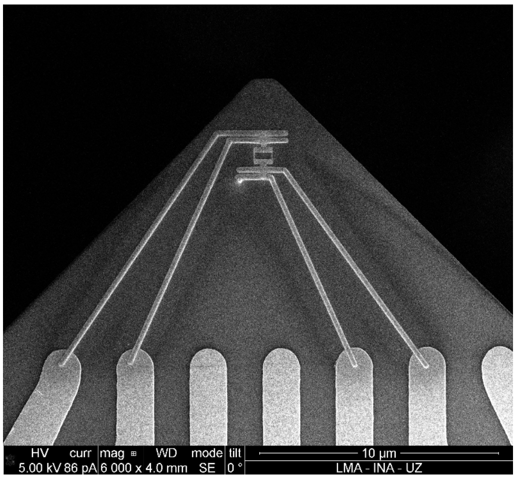

Fig 3: SEM image of a SQUID deposited onto an SPM cantilever.

Ion-beam sputtered ferroelectric ZrO_2 thin films

J. P. B. Silva[1*], F.G. Figueiras[2], R.F. Negrea[3], M.C. Istrate[3], S. Dutta[4], H. Aramberri[4], J. Íñiguez[4,5], C. Ghica[3], K.C. Sekhar[6], A.L. Kholkin[7]

[1]Centre of Physics of University of Minho and Porto (CF-UM-UP), Campus de Gualtar, 4710-057 Braga, Portugal
[2]IFIMUP & Department of Physics and Astronomy, Sciences Faculty, University of Porto, R. Campo Alegre 687, 4169-007 Porto, Portugal
[3]National Institute of Materials Physics, 105 bis Atomistilor, 077125 Magurele, Romania
[4]Materials Research and Technology Department, Luxembourg Institute of Science and Technology (LIST), 5 Av. des Hauts-Fourneaux, L-4362, Esch/Alzette, Luxemburg
[5]Department of Physics and Materials Science, University of Luxembourg, Rue du Brill 41, L-4422 Belvaux, Luxembourg
[6]Department of Physics, School of Basic and Applied Science, Central University of Tamil Nadu, Thiruvarur-610 101, India
[7]Department of Physics, CICECO-Aveiro Institute of Materials, University of Aveiro, 3810-193 Aveiro, Portugal

[*] corresponding author email: josesilva@fisica.uminho.pt

Zirconia and hafnia based thin films have attracted considerable attention in the last decade due to the existence of a ferroelectric behavior at the nanoscale, which can enable the downscaling of the next-generation of non-volatile memory devices [1]. The present work combines experimental structural studies with density-functional theory (DFT) calculations to disclose a novel rhombohedral R3m phase in epitaxially-strained (111)-oriented ZrO_2 thin films grown by ion-beam sputtering deposition technique on (111)-Nb:$SrTiO_3$ substrates. Comprehensive local and macroscopic ferroelectric characterization reveals that these ZrO_2 films display a switchable ferroelectric polarization reaching 20.2 µC/cm2 with a coercive field of 1.5 MV/cm, as shown in Fig. 1. Interestingly, the studied films show a ferroelectric behavior per se, i.e. a technological advantage over the previously studied conventional orthorhombic ZrO2 films where a wake-up cycle process is usually needed to induce ferroelectricity [2].

[1] X. Yan, Z. Xiao, C. Lu, Appl. Phys. Lett. 2020, 116, 013506.
[2] A. Chouprik, M. Spiridonov, S. Zarubin, R. Kirtaev, V. Mikheev, Y. Lebedinskii, S. Zakharchenko, D. Negrov, ACS Appl. Electron. Mater. 2019, 1, 275-287.

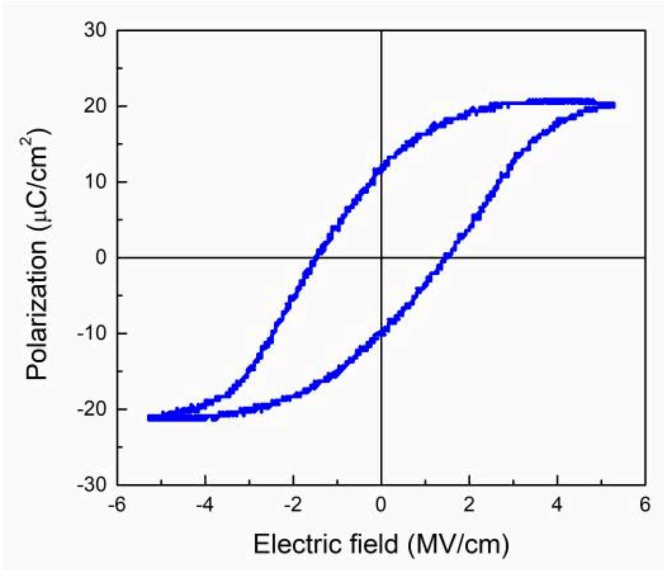

Figure 1. Polarizaion-Electric field (P-E) loops of the Nb:$SrTiO_3$/ZrO_2/Au capacitor.

Combining nanometrology and nanomanufacturing using a Nanofabrication Machine (NFM-100)

J. Stauffenberg[1*], I. Ortlepp[1], M. Holz[2], D. Dontsov[3], S. Hesse[4], I. Rangelow[5] and E. Manske[1]

[1] Technische Universität Ilmenau, Production and Precision Measurement Technology, 98693 Ilmenau, Germany
[2] nano analytik GmbH, 98693 Ilmenau, Germany
[3] SIOS Meßtechnik GmbH, 98693 Ilmenau, Germany
[4] IMMS GmbH, 98693 Ilmenau, Germany
[5] Technische Universität Ilmenau, Nanoscale Systems Group, 98693 Ilmenau, Germany

[*] corresponding author email: jaqueline.stauffenberg@tu-ilmenau.de

Current trends in micro- and nanotechnology show, it is of crucial importance to overcome the limitations of nanofabrication below 20 nm. In addition, it is becoming increasingly important to manufacture nanostructures over large areas with high precision. In this contribution the focus lies on a new Nano Fabrication Machine 100 (NFM-100) with a positioning range up to Ø 100 mm with an integrated atomic force microscope, which can be used especially for Field-Emission-Scanning-Probe Lithography (FESPL). Since several years the Group for Production and Precision Measurement Technology has already gained experience into nanopositioning and -metrology, which is shown with the development of the Nanopositioning and -measuring Machine 200 (NPMM-200) and the Nanomeasuring Machine (NMM-1) [1]. Based on many years of testing and developing these machines, the NFM-100 was developed especially for high precision and high dynamic planar nanopositioning. The NFM-100 uses a planar air bearing system. The table of the machine is driven by three voice-coil drives arranged at 120° to each other in the plane, which work in a closed loop with three fiber-coupled laser interferometers and thus enable positioning with sub-nanometre accuracy. Currently, the NFM-100 is equipped with a tip-based measuring system, which uses self-actuated and self-sensing microcantilevers, which are detecting the deflection of the beam at the clamping point through a piezoresistive measuring Wheatstone bridge. Additionally, the oscillation is realized through a thermomechanical actuator, which is based on the bimorph effect.
To overcome the limitations of nanomanufacturing, the combination of the NFM-100 and the AFM-/FESPL-System offer the possibility to fabricate and to measure structures in a range up to Ø 100 mm with high resolution and precision down to single nanometre range immediately one after the other without any sensor/tool change. While the movement in x- and y-direction is done by the NFM-100, the

AFM-/FESPL-System is only performing the movement in z-direction. As a result, the microcantilever is in a fixed position in x- and y- direction, while the sample to be analysed is moved by the NFM-100. As an example, the following figures shows a line scan with a length of 50 mm (Fig.1) and a section of around 200 µm (Fig.2).

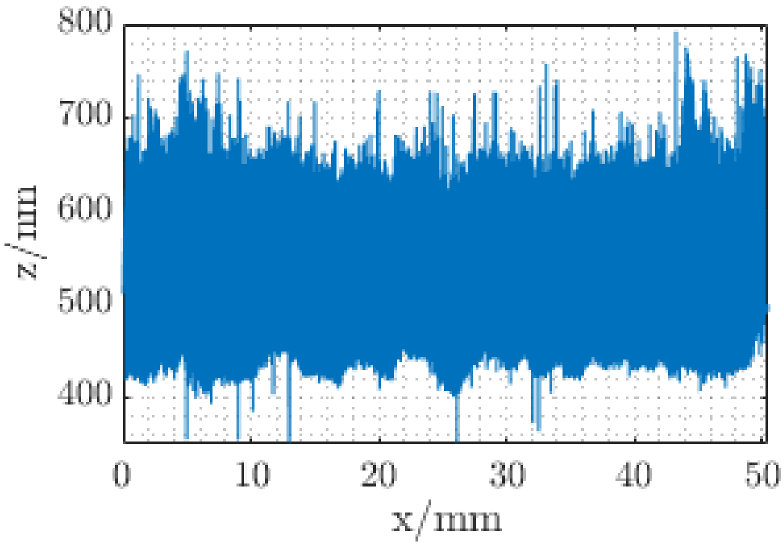

Fig.1: Linescan of a periodic step sample with a total length of 50 mm [2]

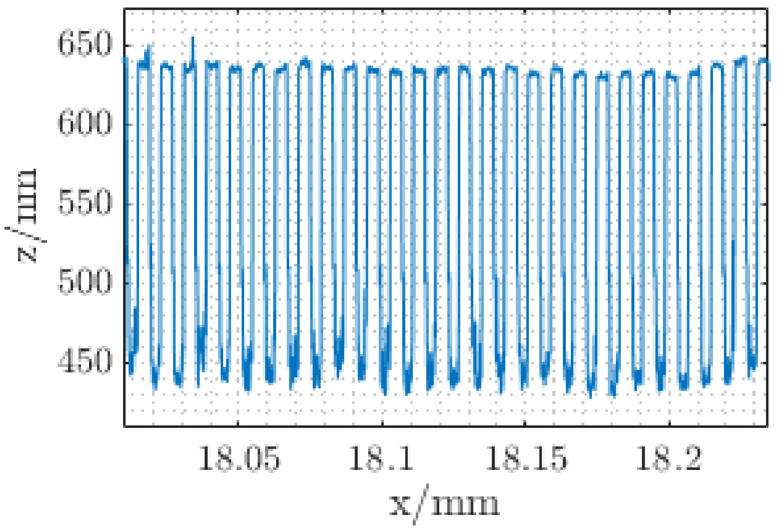

Fig.2: Section of the linescan (Fig.1) of a periodic step sample of 200 µm [2]

[1] E Manske et al. Progress of nanopositioning and nanomeasuring machines for cross scale measurement with sub-nanometre precision. 2020 *Meas. Sci. Technol.* **31** 085005

[2] J Stauffenberg et al. Nanopositioning and fabrication using the Nano Fabrication Machine with a positioning range up to Ø 100 mm. Proc. SPIE 11610, Novel Patterning Technologies 2021, 1161016; doi:10.1117/12.2583703

Removal of graphene and SiO_2 by water-assisted Focused-Electron-Beam-Induced Etching

Aleksandra Szkudlarek[1*], Jan M. Michalik[2], Inés Serrano-Esparza[3], Zdeněk Nováček[4,5], Veronika Novotná[4], Piotr Ozga[6], Czesław Kapusta[2], José María De Teresa[3,7]

[1]AGH University of Science and Technology Academic Centre for Materials and Nanotechnology, av. A. Mickiewicza 30, 30-059 Krakow, Poland

[2]AGH University of Science and Technology, Department of Solid State Physics, Faculty of Physics and Applied Computer Science, av. A. Mickiewicza 30, 30-059 Krakow, Poland

[3]Instituto de Nanociencia y Materiales de Aragón (INMA), Universidad de Zaragoza-CSIC, E-50009 Zaragoza, Spain

[4]NenoVision s.r.o. Purkyňova 649/127, 612 00 Brno

[5]Institute of Metallurgy and Materials Science, Polish Academy of Sciences, 25 Reymonta Street, 30-059 Kraków, Poland

[6]Institute of Physical Engineering, Faculty of Mechanical Engineering, Brno University of Technology,

Technická 2, 616 69 Brno, Czech Republic

[7]Laboratorio de Microscopías Avanzadas (LMA), Universidad de Zaragoza, E-50018 Zaragoza, Spain

[*] corresponding author email: aleszkud@agh.edu.pl

Graphene is one of the most extensively studied 2D materials, exhibiting extraordinary mechanical and electronic properties. Although many years have passed since the material was discovered, the patterning of single layers of graphene is still challenging using a standard resist and electron beam lithography. Recently, it has been shown that it is possible to directly etch graphene with water using Focused-Electron-Beam-Induced-Etching (FEBIE), with a spatial resolution of ten nanometers [1]. Nanopatterning graphene with such a method in one single step and without the use of a mask nor resist is a very appealing approach. However, in applying this process, we have found significant morphological changes induced on the SiO_2 substrate even at the low values of electron dose < $8nC/(\mu m)^2$. We conclude that the local substrate etching can be controlled to a certain extent through the tuning of beam parameters such as dwell time and dose.

[1] B. Sommer, J. Sonntag, A. Ganczarczyk, D. Braam, G. Prinz, A. Lorke, M. Geller, *Sci. Rep.* **2015**, *5*.

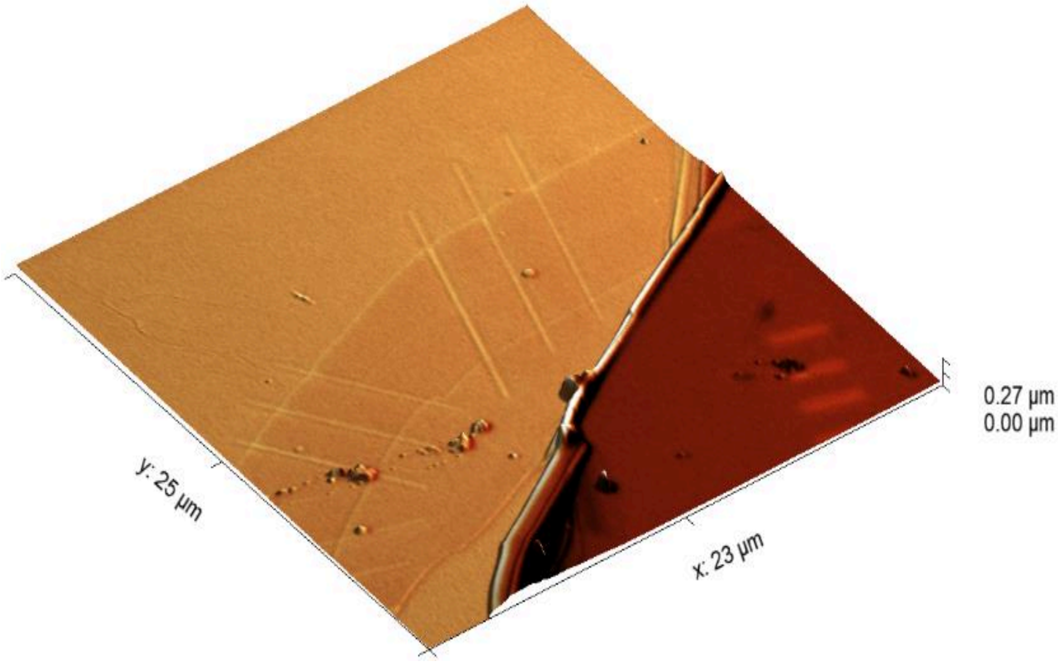

Fig. 1: Correlative Probe and Electron Microscopy of the etched patterns in graphene and morphological changes induced in SiO_2 substrate.

FIB preparation of thin metallic glassy films for *in-situ* thermal TEM examination

J. Turczyński[1*], B. Kurowska[1], W. Zajkowska[1], R. Sobierajski[1], J. Antonowicz[2] and S. Kret[1]

[1] Institute of Physics Polish Academy of Sciences, Al. Lotników 32/46, 02-668 Warsaw, Poland
[2] Faculty of Physics, Warsaw University of Technology, ul. Koszykowa 75, 00-662 Warsaw, Poland
[*] corresponding author email: turczynski@ifpan.edu.pl

Despite the commonness of the crystallization process, the dynamics of this phenomena has not been thoroughly researched yet. However, developing research methods, including *in-situ* observation of thermal crystallization process by TEM examination, allow to broaden the knowledge on this subject. Nevertheless, conducting such experiment requires sophisticated preparation combining both classical (mechanical) and FIB methods.

The thin (ca. 60 µm) strips of metallic glass $Pd_{82}Si_{18}$ were produced using the melt-spinning method. First step of the sample preparation was to achieve the thickness which enables electrons to penetrate material (< 100 nm), what was realized by classical method. Strips of $Pd_{82}Si_{18}$ alloy were initially cut and thinned using various tools like wire saw, grinder-polisher Buehler EcoMet 250 with diamond abrasive films and Dimpler Gatan 656. Subsequently, Precision Ion Polishing System (PIPS) Gatan 691 enabled to obtain a perforation in the sample (diameter ca. dozens of µm) with several nanometers thin area on the edge due to gentle argon ions etching. As-received sample and Protochips Fusion Thermal E-chip (Fig. 1a.) were inserted into Helios NanoLab 600 SEM equipped with FIB and Omniprobe. Rectangular piece (ca. 10 µm x 18 µm) was cut from thin etched film using gallium ions (Fig 1b.) and mounted to Ombiprobe needle (Fig. 1c.). Subsequently, obtained transparent foil was transferred onto the e-chip in such a way to cover a circular aperture (Fig. 1d.). Finally, the glassy film was attached using ionic platinum (Fig 1e,f.). The sample prepared this way allows for simultaneous *in-situ* heating during TEM imaging of the ongoing temperature-induced crystallization process.

This work has been supported by the National Science Centre Poland, through project No: 2017/27/B/ST3/02860

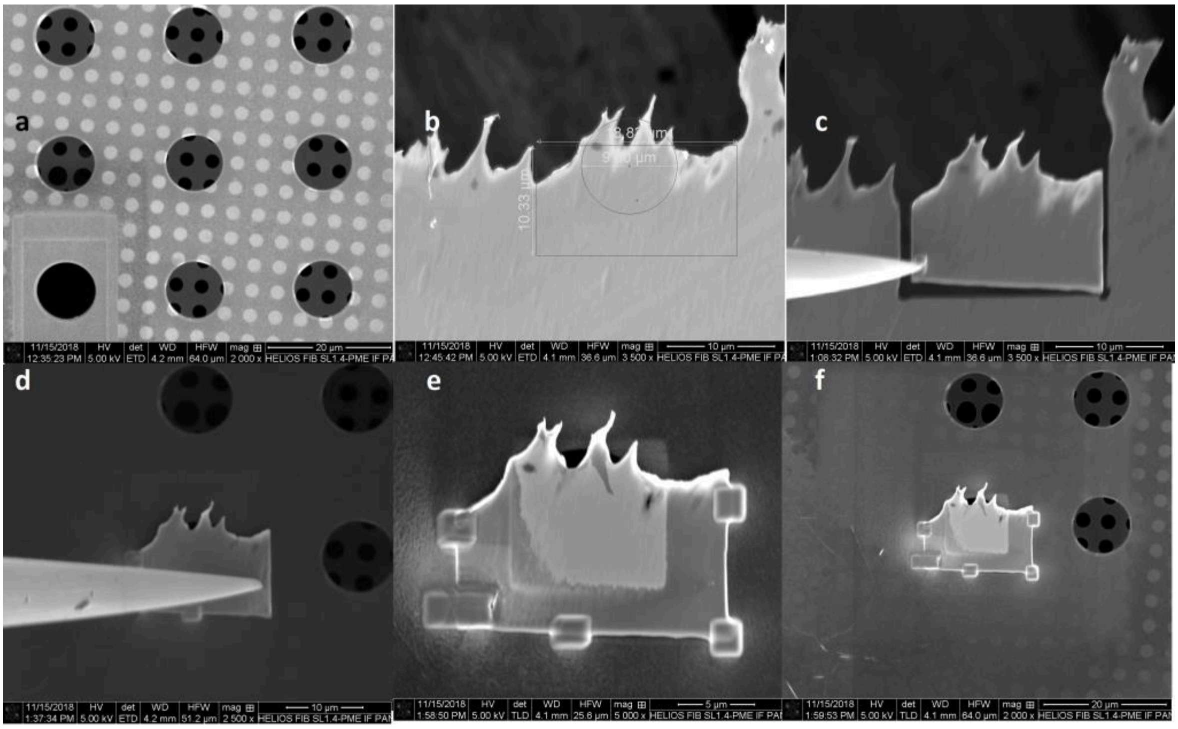

Fig. 1. The consecutive steps of cutting, transferring using Omniprobe and attaching to the e-chip of a thin metallic glass $Pd_{82}Si_{18}$ foil.

Engineering the Strain-sensitive Superconductivity of $CeIrIn_5$ with FIB

M. R. van Delft[1*], M. D. Bachmann[2], C. Putzke[1], C. Guo[1], J. A. W. Straquadine[1] and Philip J. W. Moll[1]
[1] Laboratory of Quantum Materials (QMAT), Institute of Materials (IMX), École Polytechnique Fédérale de Lausanne (EPFL), 1015 Lausanne, Switzerland
[2] Department of Applied Physics and Geballe Laboratory for Advanced Materials, Stanford University, Stanford, CA, USA

[*] corresponding author email: maarten.vandelft@epfl.ch

The ability to locally manipulate properties of materials, such as the superconducting critical temperature (T_c), has powerful device applications. The heavy fermion superconductor $CeIrIn_5$ has a T_c that can be modified via applied pressure [1] and it was recently shown that it can be manipulated in a strained FIB microstructure [2]. Here we build on this work and demonstrate a high level of local control over the T_c of $CeIrIn_5$, including the ability to suppress it down to zero kelvin.

The strain in our devices arises from a difference in thermal contraction between the substrate and the device, as illustrated in figure 1. Through a suitable choice of the substrate material, we can tailor our devices to experience either very little strain, or very strong strain. This strain is not uniform, but has a distribution depending on the geometry of the device. Using FIB, we can modify this geometry in order to prepare a device with a certain strain pattern suitable for our electrical measurements.

In order to predict the T_c distribution of a device, we simulate its strain using COMSOL Multiphysics. Figures 2a and b show an SEM image and simulated T_c map of one of our devices, respectively. This device is designed to exhibit a wide range of T_c values, allowing us test our model. As shown in figure 3, our simulations are in good agreement with experiment over the whole measured range. With this result in hand, we can reliably engineer the critical temperature of $CeIrIn_5$ to any value between zero and one kelvin.

[1] O. M. Dix *et al*. Anisotropic dependence of superconductivity on uniaxial pressure in $CeIrIn_5$. Phys. Rev. Lett. 102, 197001 (2009)

[2] M. D Bachmann *et al.* Spatial control of heavy-fermion superconductivity in $CeIrIn_5$. Science 366, 221–226 (2019).

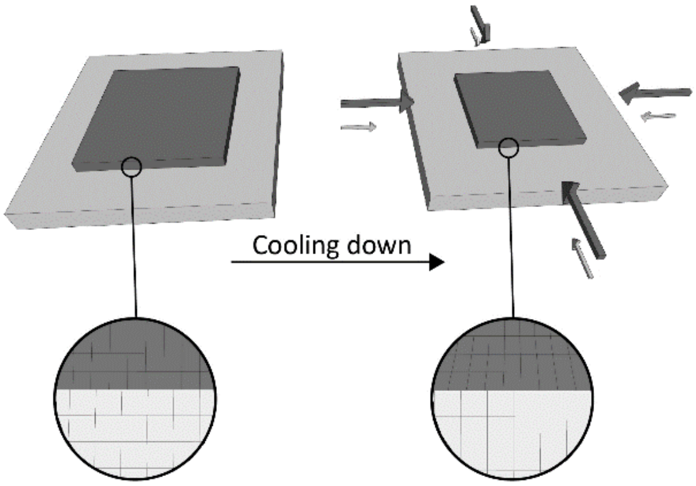

Fig. 1: Illustration of the mechanism leading to strain.

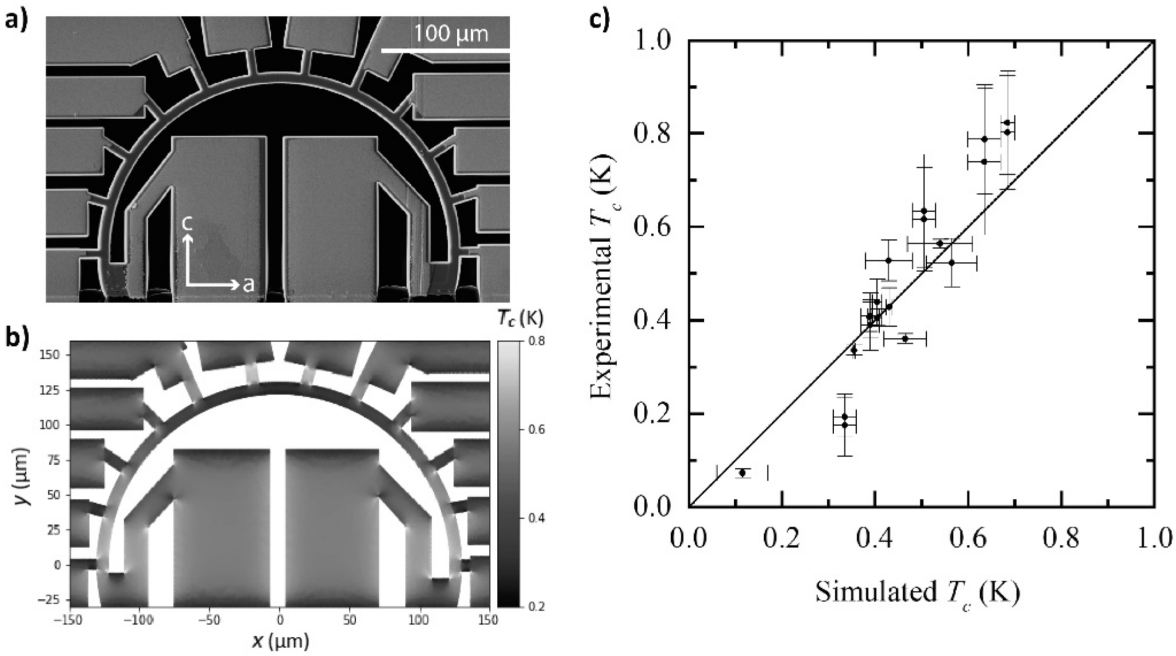

Fig. 2: **a)** SEM image of a circular device on a sapphire substrate, designed to exhibit a broad range of critical temperatures. **b)** Simulated critical temperature map of the device shown in **b**. **c)** Experimental versus simulated critical temperatures for several devices. The straight line indicates perfect agreement of simulation and experiment.

Complex artificial Features on a TEM grid fabricated with FIB Technology combined with Micromanipulation

K. Weinel[1*], R. Hesse[1], L. Agudo Jácome[1], I. Gonzalez-Martinez[2]

[1] Bundesanstalt für Materialforschung und -prüfung (BAM), Dept. Materials Engineering, Unter den Eichen 87, D-12205 Berlin, Germany

[2] IFW Dresden, Institute for complex materials, P.O. Box, D-01171 Dresden, Germany

[*] Corresponding author email: Kristina.weinel@bam.de

The phenomenon of expelling nanomaterial from microparticles under the influence of a convergent electron beam (CB) of a transmission electron microscope (TEM) is reviewed by I. Gonzalez-Martinez [1]. Converging the electron beam means a high amount of energy enters the microparticle at a very local place and interact with its atoms. Obviously, during this CB protocol, no imaging is possible, but after them, nanoparticles with different appearances are deposited next to the microparticle while its size is reduced.

We want to fill this blind spot in the observation as we want to help clarify the nature of the expelling phenomenon. One hypothesis is the so-called damage (of the microparticle) induced by an electric field (DIEF) and within this theory, the atoms are ionized and expelled in form of ionic waves.

To follow the paths of the expelled nanomaterial, we want to fabricate specimens with artificial features, as schematically exemplified in Fig. 1, using the focused ion beam (FIB) and micromanipulators, as experimental setups. As a first step towards the fabrication of such specimen, we make experimental feasibility studies. Bridges (gray regions in Fig. 1) are created by milling a commercially available electron transparent membrane (silicon oxide or carbon) on a Cu TEM grid. Platinum or carbon walls (blue features in Fig. 1) are built on top of those bridges and microparticles (yellow sphere in Fig. 1) of gold or other material are deposited in the center.

Fig. 2a) shows four square holes (black area) with residual silicon oxide membrane bridges (dark grey) between them with walls (light grey) on top. Figure 2b) shows a square hole (black) with bridges (white) on the right side on top of a carbon membrane (grey). There are still some obstacles in the manufacturing process which needs to be eliminated. For instance, the deposition process of the walls is not reliable as visible at the wall on top (in Fig. 2b)) where a hole arises instead of a wall. Nevertheless, the results are promising and further discussed in terms of the applicability for the DIEF experiment in the TEM.

[1] I. Gonzalez-Martinez, A. Bachmatiuk; *Electron-beam induced synthesis of nanostructures: A review*; Nanoscale (**2016**), 11340

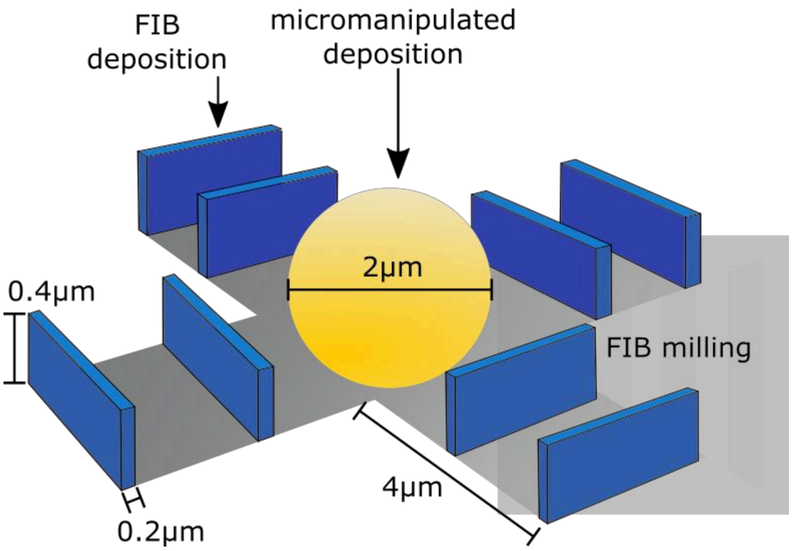

Figure 1: Sketch of one possible appearance of our specimen. The membrane bridges (grey) is worked out using FIB milling. The walls (blue) around the microparticle (yellow) are grown by FIB deposition while the particle in the center of the specimen is placed using micromanipulated deposition.

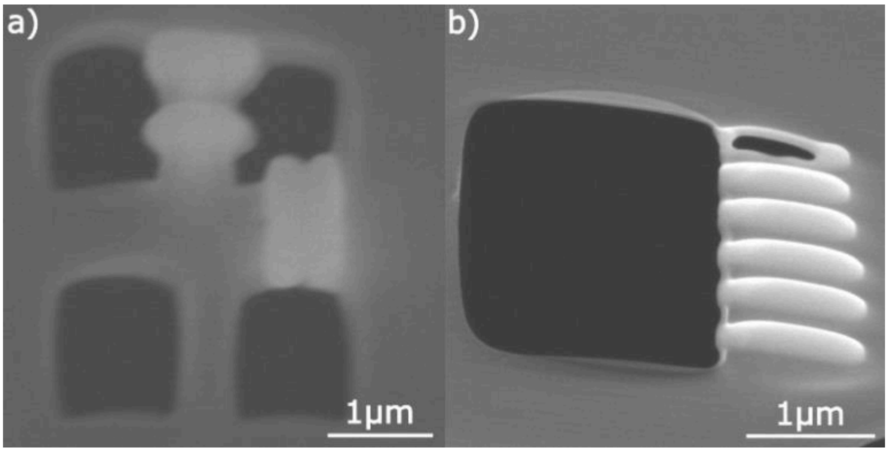

Figure 2: Scanning electron microscopy images are done with 20 kV, 5.7 nA. a) Milling of the square holes (black) was applied first on the silicon oxide membrane (dark grey) and afterwards growing of the walls (light grey was done. b) To start with growing walls (white) was tested on a carbon membrane (grey) and afterwards the square hole (black) was milled. From both images, it seemed to be a better choice to start with growing walls.

Contacting ZnO nanowires with platinum paths

W. Zajkowska[1*], B. Kurowska[1], J. Turczyński[1] , J. Polaczyński[2] and S. Kret[1]

[1] Institute of Physics Polish Academy of Sciences, Al. Lotników 32/46, 02-668 Warsaw, Poland
[2] International Research Centre MagTop, Institute of Physics, Polish Academy of Sciences, Al. Lotników 32/46, 02-668 Warsaw, Poland
[*] corresponding author email: zajkowska@ifpan.edu.pl

The interest in applications of nanoobjects in both science and technology is constantly growing, therefore there is a strong need to improve research methods in the nanoscale. The Authors aim is to conduct *in-situ* electrical 4-probe measurements of core-shell ZnO//Cr NWs by transmission electron microscopy (TEM) method using commercially available chips (Protochips).

ZnO NWs were grown by carbo-thermal method in a tube furnace at 940 °C for 15 min on sapphire (11-20) substrate. Vertically oriented NWs of ca. 40 µm length and ca. 100 nm width were covered by 20 nm chromium shell using magnetron sputtering Leica AC600 and transferred onto molybdenum thick holey carbon film TEM grid. Simultaneously, home-made chips for electrical measurements were prepared by electron-beam lithography on 500 µm thick Si (100) wafers covered with 300 nm of insulating SiO_2. The paths leading to the NW contact area were made by thermal evaporation of 10 nm Ti and 100 nm Au. (Fig. 1. a) Self-made chips are used for ex-situ testing and measurements.

NWs contacting process was conducted using FEI Helios NanoLab 600 SEM equipped with FIB and Omniprobe. The first stage of the process was to transfer single NW from the grid onto chip surface using Omniprobe needle (Fig. 1. b). The conduction properties of the tracks depend on the parameters of the FIB, in particular the voltage, current and ion or electron placement [1]. Processes were carried out involving the application of platinum paths in such a way that the NW was attached to the substrate while ensuring contact using ionic or electron platinum (Fig. 1. c). Optimization of the path production process is based on obtaining platinum contacts with the lowest possible resistance, what was checked in *ex-situ* determination of path resistance measurements. The ZnO//Cr//Pt cross-section will be examined using the FIB method.

[1]. R. Berthier, Development of characterization methods for in situ annealing and biasing of semiconductor devices in the TEM (2018)

This work has been supported by the National Science Centre Poland, through project No: 2019/35/B/ST5/03434 and by the Foundation for Polish Science through the IRA Programme co-financed by EU within SG OP.

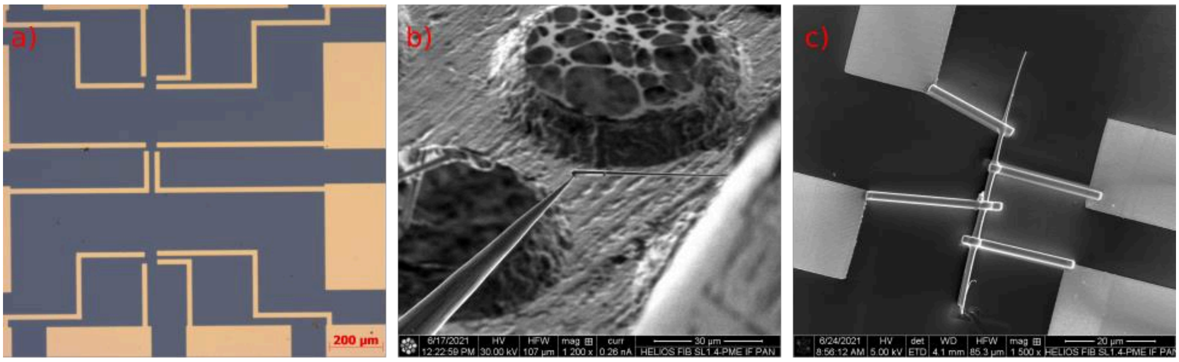

Fig. 1. Chip for measuring the quality of paths, made by electrolithography a), the process of NW transfer from the grid (visible in the background) to the chip. The NW is attached to the Omniprobe needle b), NW contacted to the chip paths (yellow areas in a)) by electron platinum c).

Focused Ion Beam-Based Microfabrication of Boron-Doped Diamond Single-Crystal Tip Cantilevers for Electrical and Mechanical Scanning Probe Microscopy

Ewelina Gacka[1*], Piotr Kunicki[1], Andrzej Sikora[1], Robert Bogdanowicz[2], Mateusz Ficek[2], Krzysztof Kwoka[1], Dominik Badura[1], Bartosz Pruchnik[1], Teodor Gotszalk[1], Ivo W. Rangelow[3],

[1] Wrocław University of Science and Technology, Faculty of Microsystems Electronic and Photonic Department of Nanometrology, 11/17 Janiszewskiego Street, 50-372 Wrocław, Poland
[2] Gdańsk University of Technology, Faculty of Electronics, Telecommunications and Informatics, Department of Metrology and Optoelectronics, 11/12 Gabriela Narutowicza Street, 80-233 Gdańsk, Poland
[3] Ilmenau University of Technology, Nanoskalige Systeme, Gustav-Kirchhoff-Str. 1, D-98684 Ilmenau, Germany
[*] corresponding author email: ewelina.gacka@pwe.edu.pl

Diamond is a wear resistant material due to the C-C bonds. It is characterised by low conductive properties that can be controlled by p-type doping with boron. For this reason it becomes a very attractive material for microelectronics applications, in particular as reliable probes for various types of scanning probe microscopy (SPM) when compared to commercial silicon cantilevers [1].

In this paper we report the application of single crystal boron-doped diamond (SC-BDD) particles as a tips for SPM. Diamond crystals were grown by the microwave plasma enhanced chemical vapour deposition method (Gdańsk University of Technology). Particles were transferred on the top of a commercial silicon cantilever using a nanomanipulation technique in the vacuum chamber of a scanning electron microscope with focused ion beam (FIB). Using the focused electron/ion beam induced deposition method, SC-BDD particles were welded to the cantilever. The conical shape was obtained during FIB milling process, as shown on Fig. 1a. Using thermomechanical noise recording, the mass change of the probe was monitored (Fig. 1b). The mass of the tip was determined to be 4.42 ng.

The goal of the investigation was to verify the wear resistance of diamond tips in mechanical and electrical measurements. During the durability tests, the tip passed a scanning length of 13.6 m in contact and lateral force microscopy modes with a 80 nN load force (Fig. 2). The probe radius was monitored by 3D tip reconstruction method.

[1] M. Hofmann, C. Lenk, T. Ivanov, I.W. Rangelow, A. Reum, A. Ahmad, M. Holz, E. Manske, Field emission from diamond nanotips for scanning probe lithography, J. Vac. Sci. Technol. B. 36 (2018) 06JL02.

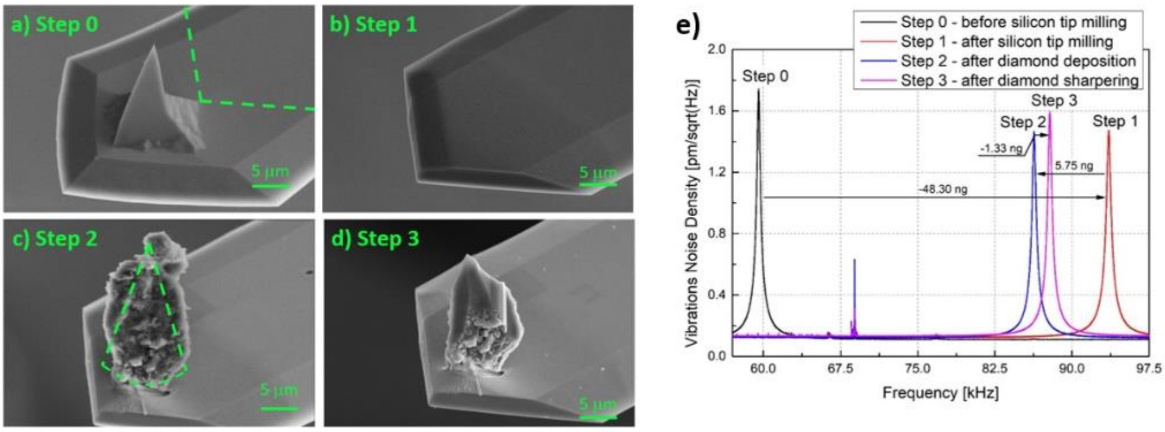

Fig. 1: Fabrication process of the microcantilever with the SC-BDD tip: (a) commercial AFM cantilever with a Si tip as a basic structure (dashed lines indicates the milled area of the cantilever), (b) step 1 – tipless cantilever after FIB milling, (d) step 2 – BDD particle welded on the cantilever (dashed lines indicates the cone-shape of tip after FIB milling), (e) step 3 – final FIB milling of the SC-BDD tip (e) thermomechanical noise and mass change determination recorded during fabrication of cantilever equipped with SC-BDD tip.

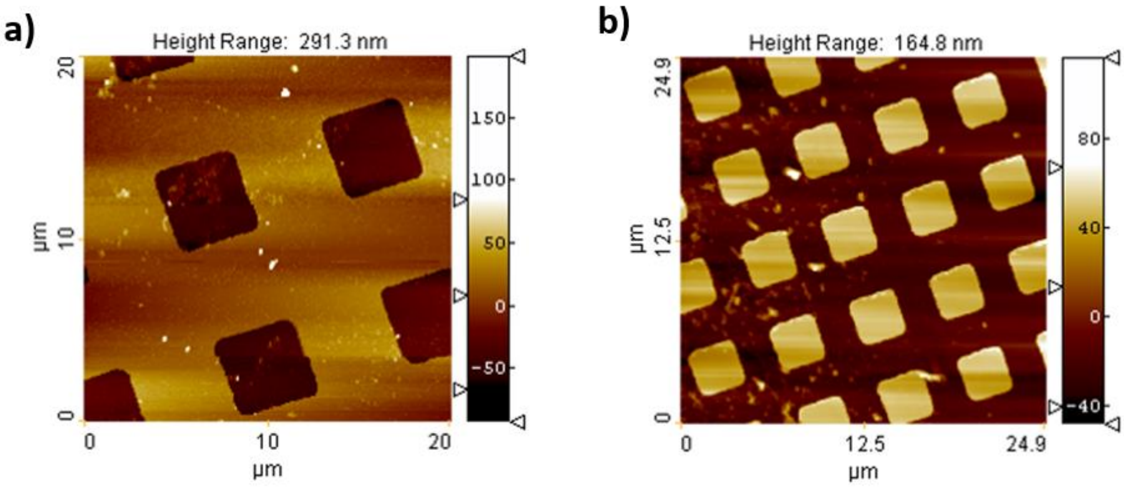

Fig. 2: Topography of patterned SiO_2/Au sample (a) at the beginning and (b) at the end of the experiment.